Comparative histopathological and transcriptomic evaluation of urologic cancer models

Simone de Brot

Dr. med. vet., DiplECVP

Thesis submitted to the University of Nottingham for the degree of Doctor of Philosophy

November 2019

Deleted: 1

Acknowledgments

First of all, THANK YOU, Nigel, for giving me the great opportunity to perform a PhD. What an absolutely positive experience it has been! You would be the reason to start a second PhD right now! Thank you so much for inspiring me for research, for your excellent support throughout my entire PhD time, for introducing me to so many prestiguous researchers and their teams, for trusting me when I came up with my own ideas, and for being a highly esteemed mentor and friend. I look very much forward to continuing our excellent teamwork in the field of cancer research. Working with you is a real pleasure.

David and Mark, thank you both for co-supervising my PhD. I have thoroughly enjoyed our constructive exchange of ideas and appreciated your guidance and support. David, your enthusiasm for research is contagious! Thank you for making sure I get infected with the research virus. We should definitely aim to continue trying to solve the mystery of these porcine renal droplets…! Thank you for being such a great person to work with.

I would like to thank all our collaborators for making this research study possible. My special thanks go to Prof Jenny Persson for providing the prostate cancer TMAs and completing the KDM staining, to Prof Lorraine Gudas for providing the TRACK mouse slides, to Dr Tim Scase for providing so many canine cancer tissues and to Dr Brian Robinson for sharing his expertise in human uropathology!

Thank you, Mandy, for being an amazing office buddy at the SVMS. I miss you and our coffee breaks, but am happy we are still in contact. As a team, we are now already raising a group of four juniors. Isn't this amazing…?!

Gary, thank you for giving me the chance to live and work in the UK for almost five years. I thoroughly enjoyed working for the SVMS Pathology and the entire school team. Thank you so much for making this period of my life a truly positive memory!

Sven, thank you for welcoming me in the ITPA team and for supporting my enthusiasm for research, including my PhD! I look forward to starting work in your research team and thank you for giving me the opportunity to join your group.

Gaby and Teresa, the best mum and mother-in-law, thank you so much for taking care of our boys while I was writing this thesis. You made it all possible. Thank you for supporting the ambitious idea of submitting my thesis not long after the birth of little Bernat. We did it…!

Llorenç, you are the person in my life who makes all my dreams come true. Thank you for being so supportive of all my (sometimes crazy, I know!) ideas. I am very lucky to have you by my side <3

To Jacob and Bernat who mean the world to me.

Table of Contents

Acknowledgments II
Table of Contents IV
List of abbreviations and acronyms VII
List of tables XIII
List of figures XVI
Abstract XX
1. Introduction 26
1.1 Bladder cancer (UC) in people and dogs 26
1.1.1 Epidemiology 26
1.1.2 Diagnosis 28
1.1.3 Tumor classification, grading and staging 34
1.1.4 Genetics 37
1.1.5 Prognosis 38
1.1.6 Therapy 39
1.1.7 Non-primate animal models for BC research 41
1.1.7.1 Rodents 41
1.1.7.2 Dogs 43
1.2 Prostate cancer (acinar adenocarcinoma and UC) in people and dogs 45
1.2.1 Epidemiology 45
1.2.2 Diagnosis 46
1.2.3 Tumor classification, grading and staging 49
1.2.4 Genetics 52
1.2.5 Prostate tumor tissue markers 53
1.2.5.1 p63 53
1.2.5.2 Uroplakin III 54
1.2.5.3 Lysine-specific demethylases 55
1.2.6 Prognosis 56
1.2.6.1 Overall prognosis 56
1.2.6.2 Prognostic factors 57
1.2.7 PC therapy 59
1.2.8 Non-primate animal models 62
1.2.8.1 Mice 62
1.2.8.2 Dogs 64
1.3. Kidney cancer (clear cell carcinoma) in people 65
1.3.1 Epidemiology 65
1.3.2 Diagnosis 66
1.3.3 Tumor classification, grading and staging 68

Deleted: IV
Deleted: VII
Deleted: XIII
Deleted: XVI
Deleted: XX
Deleted: 26
Deleted: 26
Deleted: 26
Deleted: 28
Deleted: 34
Deleted: 37
Deleted: 38
Deleted: 39
Deleted: 41
Deleted: 41
Deleted: 43
Deleted: 45
Deleted: 45
Deleted: 46
Deleted: 49
Deleted: 52
Deleted: 53
Deleted: 53
Deleted: 54
Deleted: 55
Deleted: 56
Deleted: 56
Deleted: 57
Deleted: 59
Deleted: 62
Deleted: 62
Deleted: 64
Deleted: 65
Deleted: 65
Deleted: 66
Deleted: 68

1.3.4 Genetics 69
1.3.5 Prognosis 70
1.3.6 Therapy 71
1.3.7 Animal models 72
2. Aims 74
3. STUDY 1. The dog as an animal model for bladder and urethral urothelial carcinoma: Comparative epidemiology and histology 76
3.1 Abstract 80
3.2 Introduction 81
3.3 Material and methods 82
3.4 Results 83
3.5 Discussion 86
4. STUDY 2. A fibromyxoid stromal response is associated with muscle invasion in canine urothelial carcinoma 99
4.1 Abstract 103
4.2 Introduction 103
4.3 Material and methods 106
4.4 Results 107
4.5 Discussion 109
5. STUDY 3. Transcriptome profile analysis of canine urothelial carcinoma by RNA-sequencing 119
5.1 Abstract 119
5.2 Introduction 120
5.3 Material and methods 122
5.4 Results 128
5.4.1 Differential gene expression 128
5.4.2 Alternative splicing analysis 131
5.5 Discussion 144
6. STUDY 4. Histopathological and immunohistochemical (p63 and Uroplakin III) study of canine benign and malignant prostate tissue 155
6.1 Abstract 155
6.2 Introduction 156
6.3 Material and methods 159
6.4 Results 161
6.5 Discussion 164
7 STUDY 5. Expression of KDM7A and KDM5B in human prostate carcinoma 179
7.1 Abstract 180
7.2 Introduction 181
7.3 Material and methods 183

Deleted: 69
Deleted: 70
Deleted: 71
Deleted: 72
Deleted: 74
Deleted: 76
Deleted: 80
Deleted: 81
Deleted: 82
Deleted: 83
Deleted: 86
Deleted: 99
Deleted: 103
Deleted: 103
Deleted: 106
Deleted: 107
Deleted: 109
Deleted: 119
Deleted: 119
Deleted: 120
Deleted: 122
Deleted: 128
Deleted: 128
Deleted: 131
Deleted: 144
Deleted: 154
Deleted: 154
Deleted: 155
Deleted: 158
Deleted: 160
Deleted: 162
Deleted: 174
Deleted: 174
Deleted: 175
Deleted: 177

7.4 Results 185
7.4.1 KDM7A 185
7.4.2 KDM5B 219
7.5 Discussion 244
8. STUDY 6. Histopathology and expression of RBP4 and MYC in TRACK (transgenic model of cancer of the kidney) mice 251
8.1. Abstract 251
8.2 Introduction 253
8.3 Material and methods 255
8.4 Results 258
8.4.1 Histology 258
8.4.2 Immunohistochemistry 269
8.4.2.1 RBP4 269
8.4.2.2 MYC 271
8.5 Discussion 275
9. Conclusions 282
10. Publications and presentations 289
11. References 293
12. Appendix 342

Deleted: 179
Deleted: 179
Deleted: 213
Deleted: 238
Deleted: 245
Deleted: 245
Deleted: 246
Deleted: 249
Deleted: 251
Deleted: 251
Deleted: 262
Deleted: 262
Deleted: 264
Deleted: 268
Deleted: 275
Deleted: 281
Deleted: 285
Deleted: 333

List of abbreviations and acronyms

A3SS	Alternative 3’ splice site
A5SS	Alternative 5’ splice site
ACIN1	Apoptotic chromatin condensation inducer 1
AD	Androgen deprivation
AJCC	American Joint Committee on Cancer
ALKBH	AlkB homolog
APAF1	Apoptotic peptidase activating factor 1
APC	Adenomatous polyposis coli
AQP1	Aquaporin 1
AR	Androgen receptor
ARID1A	AT-rich interaction domain 1A
AS	Alternative splicing
ATM	Ataxia telangiectasia mutated
AWERB	Animal welfare and ethical review body
BAP-1	BRCA1 associated protein 1
BAX	BCL2 associated X
BBN	N-butyl-N-(4-hydroxybutyl)nitrosamine
BC	Bladder cancer
BCG	Bacillus Calmette-Guérin
BPH	Benign prostatic hyperplasia
BRCA1/2	Breast cancer 1/2
BT	Brachytherapy
CTSE	Cathepsin E
CAV1	Caveolin 1
CCND1/3	Cyclin D1/D3
CcRCC	Clear cell renal cell carcinoma
CDH1	Cadherin 1
CDK3	Cyclin dependent kinase 3
CEACAM6	Carcinoembryonic antigen related cell adhesion molecule 6
CFA	Canis familiaris

CI	Confidence interval
CLDN3	Claudin 3
^{60}Co	Cobalt-60
COL6A3	Collagen type VI alpha 3 chain
COX	Cyclooxygenase
CPSE	Canine prostatic specific esterase
CSS	Cancer-specific survival
CTNNB1	Catenin beta 1
CT	Computed tomography
CTU	Computed tomography urography
CYR61	Cysteine-rich angiogenic inducer 61
DD3	Differential display code 3
DDR1	Discoidin domain receptor tyrosine kinase 1
DEG	Differentially expressed gene
DPC	Dog prostate cancer
dPSI	Difference of percent spliced in
DRE	Digital rectal examination
EAU	European Association of Urology
EBRT	External beam radiation therapy
EBRT+BT	External beam radiation therapy plus brachytherapy
EGFR	Epidermal growth factor receptor
EORTC	European Organization for Research and Treatment of Cancer
ERBB	Erythroblastic oncogene B
ETS	E twenty-six
F11R	F11 receptor
FANT	N-(4-5-nitro-2-furyl2-thiazolyl)-formamide
FDR	False discovery rate
FFPE	Formalin-fixed paraffin-embedded
FGFR3	Fibroblast growth factor receptor 3
FHL1	Four and a half LIM domain
FISH	Fluorescence *in situ* hybridization
FOSB	FBJ murine osteosarcoma viral oncogene homolog B

GEM	Genetically engineered mouse
GS	Gleason score
GWAS	Genome wide association studies
HDAC1	Histone deacetylase 1
HE	Hematoxylin and eosin
HER2	Human epidermal growth factor receptor 2
HIF	Hypoxia-inducible factor
HOXB13	Homeobox B13
HPA	Human Protein Atlas
HPF	High power field
HRAS	Harvey rat sarcoma viral oncogene homolog
IARC	International Agency for Research on Cancer
ICI	Immune checkpoint inhibitors
IHC	Immunohistochemistry
ISUP	International Society of Urological Pathology
JARID1B	Jumonji ATrich interactive domain 1B
JHDM1D	JmjC domain-containing histone demethylation protein 1D
KAT7	Lysine acetyltransferase 7
KDM	Lysine (K)-specific demethylase
KEGG	Kyoto encyclopedia of genes and genomes
KMT2D	Histone-lysine N-methyltransferase 2D
KRT14	Keratin 14
LHRH	Luteinizing hormone–releasing hormone
LY6E	Lymphocyte antigen 6 family member E
MDM2	Mouse double minute 2 homolog
MEN1	Multiple endocrine neoplasia type 1
MiRNA	MicroRNA
MMP9	Matrix metallopeptidase 9
MNU	N-methyl-N-nitrosourea
MpMRI	Multiparametric magnetic resonance imaging
MRI	Magnetic resonance imaging
MTNR1A	Melatonin receptor 1A

MXE	Mutually exclusive exon
NA	Not applicable
NICE	National Institute for Health and Care Excellence
NKX3.1	NK3 homeobox 1
NOXA1	NADPH oxidase activator 1
NSS	Nephron-sparing surgery
OR	Odds ratio
OS	Overall survival
PBRM1	Polybromo 1
PC	Prostate cancer
PCa	Prostate carcinoma
PCA3	Prostate cancer antigen 3
PGlC	Prostate glandular carcinoma
PHI	Prostate health index
PIK3CA	Phosphatidylinositol-4,5-bisphosphate 3-kinase catalytic subunit alpha
PIN	Prostatic intraepithelial neoplasia
PITX2	Paired-like homeodomain 2
PKN1	Protein kinase N1
PLIN2	Perilipin 2
PN	Partial nephrectomy
PPARG	Peroxisome proliferator-activated receptor gamma
PSA	Prostate-specific antigen
PSI	Percent spliced in
PSMA	Prostate-specific membrane antigen
PTEN	Phosphatase and tensin homolog
PXN	Paxillin
RASA3	RAS p21 protein activator 3
RB	Retinoblastoma
RBP4	Retinol-binding protein 4
RCC	Renal cell carcinoma
RI	Retained intron

RIN	RNA integrity number
RN	Radical nephrectomy
RNA	Ribonucleic acid
RNAseq	RNA sequencing
RP	Radical prostatectomy
RRM2	Ribonucleotide reductase regulatory subunit M2
SCC	Squamous cell carcinoma
SD	Standard deviation
SE	Skipped exon
SEM	Standard error of the mean
SERPINE2	Serpin family E member 2
SETD2	SET domain containing 2
SLIT2	Slit guidance ligand 2
SNP	Single nucleotide polymorphism
SRPX	Sushi repeat containing protein X-linked
SVIL	Supervillin
SVMS	School of Veterinary Medicine and Science
Tag	Simian Virus 40 T antigen
TATE	Tumor-associated tissue eosinophilia
TCF7L2	Transcription factor 7 like 2
TLS	Tertiary lymphoid structures
TNM	Tumor/Node/Metastasis
TBX2	T-Box 2
TE	Tumor enucleation
TKI	Tyrosine kinase inhibitor
TMA	Tissue microarray
TP53	Tumor protein 53
TPCN2	Two pore segment channel 2
TRACK	Transgenic mouse model of kidney cancer
TRAMP	Transgenic adenocarcinoma of the mouse prostate
TRUS	Transrectal ultrasound
TUR	Transurethral resection

TURBT	Transurethral resection of a bladder tumor
UC	Urothelial carcinoma
UP	Uroplakin
US	Ultrasonography
USA	United States of America
V-BTA	Veterinary bladder tumor antigen test
VEGF	Vascular endothelial growth factor
VHL	Von Hippel-Lindau
VIM	Vimentin
WHO	World Health Organization
WHWT	West Highland White terrier
WT	Wild type
ZEB1/2	Zinc finger E-box binding homeobox ½

List of tables

Table 1.1. WHO international histological classification of canine and human urothelial (urinary bladder) tumors. 33

Table 1.2. Pathological staging of canine and human urinary BC. 36

Table 3.1. Risk factors for UC in the studied dog population. 94

Table 3.2. Comparison of epidemiological factors of canine and human UC. 96

Table 3.3. Comparison of gross and histopathological features of canine and human UC. 98

Table 5.1. Case information of the 9 dogs which were selected for RNAseq. 124

Table 5.2. Summary of the AS analysis of 3 paired cases of canine UC, indicating the results for each subtype of AS in a separate column. 135

Table 5.3. Fourteen different genes with significant AS events (SE, MXE or RI) with reported relevance in human bladder and non-BC are listed. 137

Table 5.4. Relevance in BC and other cancer, and associated KEGG pathways are summarized for n=14 different genes with significant AS events in the present study (Summary of Table 8.3). 142

Table 5.5. Identified cancer-specific KEGG pathways and relevant genes in the AS analysis of 3 paired canine UC cases. 143

Table 6.1. P63 IHC staining of non-neoplastic canine prostate tissue. 172

Table 6.2. Combined p63 and UroplakinIII immunohistochemical staining of 38 canine prostate carcinomas. 173

Table 7.1. Block 1. Semi-quantitative assessment of cytoplasmic and nuclear KDM7A staining of PCa (primary tumor and metastases) and benign prostate tissue, as indicated per individual tissue core. 183

Table 7.2. TMA block 1. Overview of the semi-quantitative assessment of cytoplasmic and nuclear KDM7A staining of benign prostate and malignant primary and metastatic PCa, as indicated per tissue. 185

Table 7.3. Block 1. Mean values of the semi-quantitative assessment of KDM7A staining of PCa (primary tumor and metastases) and normal prostate, as indicated per tissue. 186

Table 7.4. Block 1. Mean values of the semi-quantitative assessment of cytoplasmic and nuclear KDM7A staining of PCa (primary tumor and metastases) and normal prostate, as indicated per tissue group. 187

Table 7.5. Block 2. Semi-quantitative assessment of cytoplasmic and nuclear KDM7A staining of PCa and benign prostate tissue, as indicated per individual tissue core. 194

Table 7.6. Block 2. Overview of the semi-quantitative assessment of cytoplasmic and nuclear KDM7A staining of malignant and benign prostate tissue, as indicated per tissue group. 196

Table 7.7. Block 2. Mean values of the semi-quantitative assessment of cytoplasmic and nuclear KDM7A staining of PCa and benign prostate tissue, as indicated per tissue group. 197

Table 7.8. Block 3. Semi-quantitative assessment of cytoplasmic and nuclear KDM7A staining of PCa and benign prostate tissue, as indicated per individual tissue core. 203

Table 7.9. Block 3. Overview of the semi-quantitative assessment of cytoplasmic and nuclear KDM7A staining of malignant and benign prostate tissue, as indicated per tissue group. 205

Table 7.10. Block 3. Mean values of the semi-quantitative assessment of cytoplasmic and nuclear KDM7A staining of PCa and benign prostate tissue, as indicated per tissue group. 206

Table 7.11. Summary of KDM7A staining of benign and malignant prostate tissue. 211

Table 7.12. Block 1. Semi-quantitative assessment of cytoplasmic and nuclear KDM5B staining of PCa (primary tumor and metastases) and benign prostate tissue, as indicated per individual tissue core. 216

Table 7.13. Block 1. Overview of the semi-quantitative assessment of cytoplasmic and nuclear KDM5B staining of normal prostate and malignant primary and metastatic PCa, as indicated per tissue. 218

Table 7.14. Block 1. Mean values of the semi-quantitative assessment of KDM5B staining of PCa (primary tumor and metastases) and normal prostate, as indicated per tissue. 219
Table 7.15. Block 1. Mean values of the semi-quantitative assessment of cytoplasmic and nuclear KDM7A staining of PCa (primary tumor and metastases) and normal prostate, as indicated per tissue group. 220
Table 7.16. Block 2. Semi-quantitative assessment of cytoplasmic and nuclear KDM5B staining of organ-confined PCa and benign prostate tissue, as indicated per individual tissue core. 226
Table 7.17. Block 2. Overview of the semi-quantitative assessment of cytoplasmic and nuclear KDM5B staining of benign prostate and organ-confined PCa, as indicated per tissue. 228
Table 7.18. Block 2. Mean values of the semi-quantitative assessment of KDM5B staining of PCa (primary tumor and metastases) and normal prostate, as indicated per tissue. 228
Table 7.19. Block 3. Semi-quantitative assessment of cytoplasmic and nuclear KDM5B staining of organ-confined PCa and benign prostate tissue, as indicated per individual tissue core. 232
Table 7.20. Block 3. Overview of the semi-quantitative assessment of cytoplasmic and nuclear KDM5B staining of benign prostate and organ-confined PCa, as indicated per tissue. 234
Table 7.21. Block 3. Mean values of the semi-quantitative assessment of KDM5B staining of PCa (primary tumor and metastases) and benign prostate, as indicated per tissue. 234
Table 7.22. Summary of KDM5B staining of benign and malignant prostate tissue. 235
Table 8.1. Histopathological scoring system kidney. 250
Table 8.2. Histopathological evaluation of the kidney. 253
Table 8.3. Summary of the renal histopathological findings. 256
Table 8.4. Histopathological evaluation of the liver. 257
Table 8.5. The results of the RBP4 IHC staining of the kidney. 262
Table 8.6. The results of the MYC IHC staining of all examined tissues. 265

List of figures

Figure 1.1. UC in the urinary bladder of an elderly female neutered pet dog. 45
Figure 3.1. The effect of sex, neutering, age, and dog breed on cancer incidence. 90
Figure 3.2. Microphotograph of UC in the urinary bladder of two dogs. 91
Figure 3.3. Microphotograph of two rare tumor variants in two dogs. 91
Figure 3.4. Microphotograph of UC with different histological growth patterns in the urinary bladder of two dogs. 92
Figure 3.5. Microphotograph of UC with different cellular features in the urinary bladder of four dogs. 92
Figure 4.1. Muscle-invasive UC in the urinary bladder of a 7-year-old neutered male crossbreed dog. 115
Figure 4.2. Muscle-invasive UC in the urinary bladder of a 7-year-old neutered male crossbreed dog. 116
Figure 4.3. UC in the urethra of a 12-year-old male curly-coated retriever. 117
Figure 4.4. Non-muscle invasive UC in the urinary bladder of a 6-year-old giant schnauzer. 117
Figure 4.5. Muscle-invasive UC in the urinary bladder of a 5-year-old female Labrador retriever. 118
Figure 5.1. Case 33. Screenshot of a digital histology slide containing fragments of non-neoplastic canine urinary bladder tissue. 126
Figure 5.2. Case 26. Screenshot of a digital histology slide containing fragments of a urinary bladder UC. 126
Figure 5.3. Illustration of the different types of alternative splicing events, which were assessed in the present study. 128
Figure 5.4. Heat map constructed by hierarchical clustering analysis of paired samples of n=3 dogs with canine UC. 129
Figure 5.5. Heat map constructed by unsupervised hierarchical clustering analysis of paired (n=3) (N: normal; T: tumor) and non-paired (n=6) tumor samples of n=9 dogs with canine UC. 130

Figure 6.1. Poorly differentiated, UPIII negative prostate carcinoma of a 9-year-old male surgically neutered Labrador retriever. HE. Bar indicates 500 µm. 171

Figure 6.2. Higher magnification of Figure 6.1. Bar indicates 50 µm. 171

Figure 6.3. Same case as shown in Figure 6.1 and 6.2, depicting an area with a different, predominantly sarcomatous growth pattern. HE. Bar indicates 50 µm. 172

Figure 6.4. Poorly differentiated (suspected glandular), UPIII negative prostate carcinoma of an adult giant schnauzer. Neoplastic cells appear anaplastic and a highly infiltrative growth is evident. HE. Bar indicates 100 µm. 172

Figure 6.5. Higher magnification of Figure 6.4. Bar indicates 50 µm. 173

Figure 6.6. Poorly differentiated (suspected urothelial) carcinoma of a 10-year-old male surgically neutered Labrador retriever. Extensive tumor necrosis is present. HE. Bar indicates 100 µm. 173

Figure 6.7. Higher magnification of figure 6.6, indicating the highly invasive tumor growth. HE. Bar indicates 50 µm. 174

Figure 6.8. P63 IHC of a UC in the prostate of a 9-year-old male neutered Labrador retriever. 169

Figure 6.9. P63 IHC of a UC in the prostate of a 11-year-old male neutered Welsh corgi. 169

Figure 6.10. P63 IHC of a normal prostate gland from a 9-year-old intact German shepherd x Rottweiler crossbreed dog. 170

Figure 6.11. P63 IHC of a premature prostate gland from a 8-week-old intact Cavalier King Charles spaniel. 170

Figure 6.12. UPIII IHC of three different prostate UC with variably intense, multifocal, apical membranous staining of neoplastic cells. 171

Figure 7.1. Case 107-8. 189

Figure 7.2. Case 165-1. 189

Figure 7.3. Case 125-10. 189

Figure 7.4. Case 125-7. 190

Figure 7.5. Case 165-1. 190

Figure 7.6. Case 125-2. 190

Deleted: 1

Deleted: 2

Deleted: 3

Deleted: 4

Deleted: 5

Figure 7.7. Normal myocardium. 190
Figure 7.8. Case 125-15. 191
Figure 7.9. Case 224-4. 191
Figure 7.10. Case 251-12. 191
Figure 7.11. Case 850. 199
Figure 7.12. Case 335. 199
Figure 7.13. Case 1013. 199
Figure 7.14. Case 623. 200
Figure 7.15. Case 850. 200
Figure 7.16. Case 1056. 207
Figure 7.17. Case 1085. 207
Figure 7.18. Case 1070. 207
Figure 7.19. Case 1105. 208
Figure 7.20. Case 1093. 208
Figure 7.21. Case 165-1. 221
Figure 7.22. Case 125-7. 221
Figure 7.23. Case 125-2. 221
Figure 7.24. Case 115-6. 221
Figure 7.25. Case 107-2. 222
Figure 7.26. Case 105-4. 222
Figure 7.27. Case 165-1. 222
Figure 7.28. Case 115-6. 222
Figure 7.29. Case 165-4. 223
Figure 7.30. Normal myocardium. 223
Figure 7.31. Case 224-4. 223
Figure 7.32. Case 125-11. 223
Figure 7.33. Case 251-12. 224
Figure 7.34. Case 224-4. Normal bone. 224
Figure 7.35. Case 335. 230
Figure 7.36. Case 291. 230
Figure 7.37. Case 441. 230
Figure 7.38. Case 1015. 237

Figure 7.39. Case 1068. 237
Figure 7.40. Case 1086. 237
Figure 7.41. Case 1021. 237
Figure 8.1A. Case 1α43-344 15-317 P2. 259
Figure 8.1B. Closer view of Figure 8.1A. 259
Figure 8.2. Case 1α43-342 15-317 P3. 259
Figure 8.3A. Case 1α43 335 15-261 P3. 260
Figure 8.3B. Closer view of Figure 8.3A. 260
Figure 8.4. Case 1α43-343 15-317 P2. 260
Figure 8.5. Case 43x-1-24 15-261 P5. 261
Figure 8.6. Case 1α43-342 15-317 P1. 261
Figure 8.7. Case 43x-1-23 15-261 P1. 261
Figure 8.8A. Case 43-348 RBP4 15-331 P4. 263
Figure 8.8B. Closer view of Figure 8.8A. 263
Figure 8.9A. Case WT♂ 8m-2 MYC 15-331 P3. 266
Figure 8.9B. Closer view of Figure 8.9A. 266
Figure 8.10. Case 43-350 MYC 15-331 P3. 266
Figure 8.11. Case 43-350 MYC 15-331 P3. 267
Figure 8.12A. Case 43-349 MYC 15-331 P3. 267
Figure 8.12B. Closer view of Figure 8.12A. 267

Abstract

Background: Urological cancers are common malignancies in people, with prostate, kidney and urinary bladder cancer accounting for three of the top ten most prevalent cancers worldwide. Despite ongoing efforts to improve therapeutic options, the prognosis for patients with advanced, metastatic urological cancers remains poor. As such, continued investigation into the development of novel therapeutic strategies, including the discovery of new anti-cancer drug targets, is urgently needed. To achieve this ambitious goal, it is essential to have relevant and suitable pre-clinical disease models readily available. For urological cancer, rodent models are well established and remain highly valuable. In contrast, non-rodent animal models, including pet dogs, which spontaneously develop urological cancer with striking molecular and morphological resemblance to the same disease in people, are currently underexploited.

This study aims to assess the dog as a potential animal model for urinary bladder and prostate cancers, and to investigate kidney cancer based on a transgenic mouse model of kidney cancer (TRACK). Specifically, this dissertation is structured as chapters presenting studies defined by the following aims:

i) Pathological and molecular characterization of the canine urothelial carcinoma (UC) model
ii) Pathological and molecular characterization of the canine prostate carcinoma (PCa) model
iii) Pathological and immunohistochemical evaluation of novel potential therapeutic targets in human PCa specimens
iv) Pathological and molecular investigation of mechanistic contributors to kidney clear cell cancer

Methods:

To address these aims the following analyses were completed.

Canine UC (STUDIES 1 to 3): Spontaneous, untreated canine primary urinary bladder and urethral UC (n=381) were epidemiologically and histologically

assessed. The following information was available: age at the time of first tumor diagnosis, sex, neutering status, and dog breed. Histological assessment included: histomorphological tumor classification based on the current 2016 WHO system, subgross (papillary vs non-papillary) growth, muscle invasion, tumor stroma, necrosis, and inflammation. In addition, 9 cases (n=3 paired non-tumor and tumor specimen, and n=6 non-paired tumor samples) were analyzed for the presence of different gene expression and alternative splicing (AS) by RNAseq.

Canine PCa (STUDY 4): Spontaneous, untreated canine primary prostate carcinomas (n=41) were histologically and immunohistochemically (p63, Uroplakin III) assessed and compared to n=61 benign (n=17 normal adult, n=15 hyperplasia, n=16 atrophy, n=14 normal premature) canine prostates. The available case information was the same as indicated for canine UC.

Lysine demethylase (KDM) expression in human PCa (STUDY 5): The expression of the androgen receptor coregulators, lysine demethylase 5B (KDM5B) and 7A (KDM7A), were assessed using immunohistochemistry (IHC) analysis of three tissue microarrays (TMA) containing a total of n=312 cores collected from n=62 benign and n=62 patient-matched malignant [n=15 metastatic prostate carcinoma (PCa); n=47 organ-confined PCa].

TRACK mice (STUDY 6): FFPE tissues (heart, lung, spleen, liver, pancreas, kidney, small intestine, testis, skeletal muscle) from n=66 mice, including 44 TRACK [hypoxia-inducible factor (HIF)-1α overexpressing] and 22 control [n=5 HIF-2α overexpressing and n=17 wild type (WT)] mice were histomorphologically assessed. Three TRACK and two WT mice were further evaluated for the expression of RBP4 and MYC by IHC

Results:

Canine UC: The mean age of dogs diagnosed with UC was 10.22 years (range 4-15 years), which is equivalent to 60-70 human years. A high correlation of UC diagnosis with female sex (odds ratio [OR] 3.51; 95% confidence interval [CI] 2.57-4.79; p<0.001), surgical neutering (OR 4.57; 95%CI 1.87-11.12; p<0.001), and breed (OR 15.11 for Scottish terriers; 95%CI 8.99-25.41; p<0.001) was observed. Primary tumors were staged as T1 (38%), T2a (28%), T2b (13%), and

T3 (22%). Non-papillary tumor growth was strongly associated with muscle invasion (OR 31.00; p<0.001). Conventional, not further classifiable infiltrating UC was the most common type of tumor (90%), followed by UC with divergent, squamous and/or glandular differentiation (6%). When comparing human and canine UC, the two most striking common features included high sex predilection and histological tumor appearance.

In 103 of 381 (27%) of canine UC cases, the tumor stroma was fibromyxoid, which was strongly associated with invasive growth of muscle (p<0.0001). Peritumoral and intratumoral inflammation was present in 308 of 345 (89%) and 287 of 381 (75%) of cases, respectively, and was mostly mild and lymphoplasmacytic. One hundred and fifteen of the 381 (30%) cases showed a variable eosinophilic inflammation, and 58 of 381 (15%) presented with formations of one or several lymphoid follicles. Twenty-four percent (91 of 381) of cases had tumor necrosis, which was typically mild. In 83 of 91 (91%) of cases, the necrosis was comedo-like. Moderate to severe tumor necrosis was associated with the presence of moderate to predominant fibromyxoid tumor stroma (p<0.02).

No significant differently expressed genes were found when canine UC and histopathologically non-malignant bladder mucosa were compared. In contrast, AS was common. Many of the identified altered genes (*SVIL, PXN, KAT7, ACIN1, TPCN2, SLIT2, MTNR1A, DDR1, APAF1, PKN1, F11R, TCF7L2, ALKBH, COL6A3*) and KEGG (Kyoto Encyclopedia of Genes and Genomes) pathways (focal adhesion, pathways in cancer, PI3K-Akt signaling among others) have been found to be relevant in human bladder cancer (BC). Finally, human BC, as well as acute myeloid leukemia and thyroid cancer pathways were shown to be enriched pathways in the assessed canine UC with differential AS.

Canine PCa: Based on histomorphology and Uroplakin III (UPIII) IHC, canine PCa were classified as UC (25/41; 61%), prostate glandular carcinoma (PGlC) (7/41; 17%) and anaplastic carcinoma (9/41; 22%). Most PCa contained either scattered p63 positive cells (21/39, 54%) or were p63 negative (14/39, 36%). The remaining 4 cases (10%), characterized by squamous (n=2) or low-grade,

urothelial differentiation (n=2), were strongly p63 positive. In non-neoplastic prostate tissue, nuclear staining for p63 was detected in basal and urothelial cells. The expression of UPIII was absent, weak, moderate or strong in 20/39 (51%), 13/39 (33%), 4/39 (10%) and 2/39 (5%) PCa, respectively and present in <10% of neoplastic cells in most (74%) cases. In non-neoplastic tissue, UPIII expression was limited to prostatic urethra and ducts.

KDM5B and KDM7A expression in human PCa: The lysine (K)-specific demethylase KDM7A was expressed in the majority of benign (60-89%) and malignant (70-100%) prostate tissues. KDM7A expression was higher in organ-confined PCa compared to benign prostate tissue ($p<0.05$). PCa metastases had a highly variable level of expression depending on the site of tumor spread, ranging from 0% (kidney) to 100% (adrenal, liver, testis) of cases, with intermediate values of 67-88% in bone, lymph node and lung. Cytoplasmic expression was reduced in renal ($p<0.05$) and bone ($p<0.001$) metastases compared to the primary tumor. Staining intensity was weak in the majority of benign (50-100%) and malignant (61-100%) samples. Nuclear expression was higher than cytoplasmic staining in organ-confined PCa ($p<0.001$) and benign ($p<0.05$) prostate tissue, which was vice versa in metastatic PCa. Distinct and strong cytoplasmic staining of prostate basal cells was observed in 28-88% (benign) and 0-58% (malignant) of cases. The lysine (K)-specific demethylase KDM5B was expressed in all assessed benign and malignant tissue cores. Cytoplasmic staining was strong in 82-91% of benign, 78-91% of organ-confined PCa, and 100% of metastatic PCa, with the exception of bone metastases, which had strong staining in 61% of cases. Nuclear staining intensity was strong in most benign (62-89%) as well as malignant (77-80%) tissues, with significantly decreased nuclear expression in bone metastases compared to benign prostate tissue ($p<0.001$).

TRACK mouse model of ccRCC: All TRACK mice presented with moderate to severe vacuolar tubular changes in the kidney, with presence of tubular dysplasia in 5/44 (11%) cases. A mild, chronic interstitial inflammation was seen

in 41/44 (93%) of HIF-1α mice, in none of the HIF-2α mice and in 5/17 (29%) of WT. Lesions compatible with chronic renal infarctions were seen in 6/44 (14%) HIF-1α mice, and in none of the control animals. Features of renal tubular regeneration was limited to 31/44 (70%) HIF-1α mice. A mild, chronic inflammatory response in the liver was present in 7/24 (29%) of HIF-1α mice, but none of the WT. RBP4 was expressed in the renal proximal tubular and glomerular parietal epithelial cells of 3/3 (100%) TRACK mice and remained undetectable in WT. Moderate to strong expression of MYC was seen in the renal tubules of TRACK and WT animals.

Conclusions: The results obtained show canine UC closely resembles the same disease in men on a histomorphological as well as molecular level, supporting the dog as an animal model for this malignancy. In canine UC, fibromyxoid tumor stroma is common and represents a strong indicator for muscle-invasive tumor growth, presumably indicative of poor prognosis. Canine PCa is characterized by a poor histomorphological differentiation. In most cases, the cell of origin remains uncertain, and either a glandular (acinar or neuroendocrine), ductal or urethral origin is possible. The dog has the potential to represent a valuable animal model for a highly aggressive form of PCa, including castration-resistant cancer.

Two potential PCa-relevant therapeutic targets, KDM5B and KDM7A were analyzed. Both proteins are expressed in benign and malignant human prostate tissue. In addition, KDM7A may have relevance as a prostate basal cell marker, whereas KDM5B may have as not yet discovered non-chromatin linked role.

The TRACK mouse model successfully develops pre-neoplastic and early neoplastic renal changes with comparable histomorphology as seen in spontaneous ccRCC, confirming its suitability as animal model for early stages of kidney cancer. In addition to premalignant renal lesions, TRACK mice show mild degenerative and inflammatory changes in the kidney and the liver and features of renal tubular regeneration, with an uncertain significance for oncogenesis. RBP4 is a promising potential cancer-specific marker for clear cell renal cell carcinoma.

Collectively these studies support the use of comparative models to advance understanding of oncogenic mechanisms.

1. Introduction

The present work is a comparative, morphological and molecular pathological study of urological cancers. More specifically, pet dogs with spontaneous lower urinary tract and prostate cancer were investigated as a non-primate animal model for UC of the urinary bladder and for prostate carcinoma, respectively. For that purpose, representative tissues collected from over 480 dogs were assessed by histopathology, IHC, and 9 were analyzed by RNA-sequencing. Furthermore, a transgenic mouse model of kidney cancer (TRACK) was evaluated histologically, including the immunohistochemical expression of two cancer-relevant markers. This thesis includes six different works, two of which have already been published in scientific peer-reviewed journals.

1.1 Bladder cancer (UC) in people and dogs

1.1.1 Epidemiology

BC is a common malignant disease and mostly, over 90%, consists of UC. BC is the ninth most frequent cancer worldwide in people, the 7th most common in men and the 17th most common in women (Antoni et al., 2017; Burger et al., 2013). BC comprises approximately 2% of all cancers, with about 330,000 new BC cases each year globally (Andreassen et al., 2016). In Europe, 19 and 4 out of 100,000 men and women, respectively will be diagnosed with BC (Alfred Witjes et al., 2017; Ferlay et al., 2013). The highest incidence rates are observed in highly developed countries (Europe and Northern America), where BC is the fourth and ninth most common cancer in men and women, respectively (Antoni et al., 2017; Burger et al., 2013). Europe has among the highest incidence rates of BC in the world, being highest in Southern Europe (Antoni et al., 2017). In less developed regions, the majority of BC is suspected to be caused by infection with *Schistosoma haematobium* (Antoni et al., 2017). Currently, there is a trend for decline in incidence and mortality in European men, which is likely due to less tobacco smoking and industrial solvent exposures, which are the main risk factor of BC. Mortality is decreasing in European women, but

incidence is increasing for reasons that are uncertain (Antoni et al., 2017). BC predominantly affects elderly patients with the median ages of initial diagnosis being 69 and 71 years in men and women, respectively. BC is rare in patients under 40 years of age (Williamson et al., 2013). BC has a strong male predominance, 75% of all BC cases occur in men (Antoni et al., 2017; Burger et al., 2013). The lower BC incidence in women is likely due to historically lower smoking prevalence and less occupational exposures to carcinogens (Burger et al., 2013). Contrary to the incidence rate, the mortality rate is higher in women than in men, the reasons for this phenomenon are still unknown (Burger et al., 2013). Possible reasons are being explored, including unequal access to health care, delays in diagnosis and treatment, environmental exposure to carcinogens, and anatomic and hormonal factors (Burger et al., 2013). BC incidence and survival vary among ethnic groups (Yee et al., 2011). Incidence rates are higher in Caucasians compared to people of African ethnicity. African Americans are however associated with higher-stage disease at initial presentation and reduced survival (Lee et al., 2006; Yee et al., 2011). Even if age, tumor stage and grade are adjusted, the difference in survival persists between white and black Americans (Yee et al., 2011). So far, the more aggressive form of BC in Africans could not be demonstrated to be caused by clear genetic differences, and the differences in survival are not fully explained by different disease presentation and quality of treatment (Yee et al., 2011).

In dogs, BC has a similar incidence rate as seen in humans, comprising 1-2% of all canine cancers (Knapp et al., 2014; Meuten and Meuten 2016; Mutsaers et al., 2003; Norris et al., 1992). Tens of thousands of dogs are affected by BC every year worldwide (Fulkerson and Knapp, 2015). As in people, UC is by far the most common type of canine BC, accounting for over 90% of all BC cases (Knapp et al., 2014; Norris et al., 1992; Patrick et al., 2006). In dogs, as in people, BC incidence increases with age, and mainly affects older animals, with reported mean ages of 9 to 11 years (approximately over 60 equivalent human years)(Knapp et al., 2000; Mutsaers et al., 2003; Norris et al., 1992). Contrary to the situation in people, canine UC has a strong female predominance, with reported female/male ratios of 1.7 to 1.95:1 (Knapp et al., 2014). Reasons for

the observed sex predisposition have not been determined in the dog. Obviously, occupational risk factors and smoking does not apply to dogs, even though an association with second-hand smoke cannot totally be excluded. In dogs, certain breeds are at high risk to develop BC. Scottish terriers have an up to 20-fold increased risk to develop BC compared to mixed breed dogs (Fulkerson and Knapp, 2015; Mutsaers et al., 2003). The cause of this breed-associated risk is not known yet, but very likely represents a genetic predisposition to BC. In contrast to people, canine UC is usually diagnosed late in the course of disease when a bladder mass is already palpable or visible by radiography or ultrasound.

1.1.2 Diagnosis

The presence of blood in the urine (hematuria) is the most common presenting symptom of BC in people and dogs and should be followed by further examination, including cystoscopy, urinary cytology, and imaging of the urinary tract (Alfred Witjes et al., 2017; Urquidi et al., 2016; Zhang et al., 2016). Specific urinary markers are not recommended for BC diagnosis at present (Alfred Witjes et al., 2017). After cystoscopy, cytology and imaging, the next step is an examination of the urinary tract under anesthesia and transurethral resection, followed by histopathological examination and staging of the tumor (Alfred Witjes et al., 2017).

Dogs with suspected BC are usually evaluated by physical examination, hematology and serum biochemistry, urinalysis, thoracic radiography, abdominal ultrasonography, and urinary tract imaging (Fulkerson and Knapp, 2015). In both dogs and people, definitive diagnosis of BC requires histopathologic examination of a tumor biopsy, which can be obtained by cystoscopy, surgery (cystotomy), or traumatic catheterization (Alfred Witjes et al., 2017; Borjesson et al., 1999; Cannon and Allstadt, 2015; Fulkerson and Knapp, 2015).

Urinalysis

The two most common urine-based tests are urine cytology and fluorescence *in situ* hybridization (FISH) assay (Caraway and Katz, 2010; Gopalakrishna et al., 2017; Gopalakrishna et al., 2016; He et al., 2016). Urine cytology is a widely used and well-established diagnostic test since decades (Caraway and Katz, 2010; He et al., 2016). It is a quick, non-invasive and relatively inexpensive screening tool for BC (Zhang et al., 2016). Even though this test is useful to diagnose high-grade tumors, it is however often not sensitive enough for low-grade BC (He et al., 2016; Zhang et al., 2016). Another limitation of urine cytology includes a large inter- and intra-observer variability. Cytology has a low sensitivity (38-51%), but is very specific (94-98% specificity), especially for high-grade disease (He et al., 2016). The FISH test UroVysion® (Abbott Molecular Inc, Des Plaines, Illinois, USA) is able to detect urothelial cancer cells in the urine and can be performed on urinary cytology preparations. This assay is able to identify specific chromosomal abnormalities in urine epithelial cells (Caraway and Katz, 2010). The FISH assay has a higher sensitivity than conventional cytology, and is ideally used as an additional test. It should be noted, however, that similar to conventional cytology, FISH has a lower sensitivity for detecting low-grade UC compared to high-grade UC (Caraway and Katz, 2010). Although FISH results are determined independent of cytology, they should be correlated with cytological findings. In addition to urine cytology and FISH assays, current research has focused on developing non-invasive methods for early detection of tumor associated antigens (tumor markers) shed in the urine (Beukers et al., 2017; Urquidi et al., 2016). The development of accurate tests for the non-invasive detection of UC continues to be a challenge, and urine markers with high specificity and sensitivity are not yet available.

Dogs with UC typically present with abnormal urinalysis, including hematuria, pyuria, proteinuria and/or bacteriuria (Borjesson et al., 1999; Meuten and Meuten 2016; Norris et al., 1992). These urine abnormalities are however non-specific and also seen in non-neoplastic conditions, such as urinary tract

infections or kidney disease (Borjesson et al., 1999). As in people, urine cytology has a low to moderate sensitivity, especially for lower grade tumors. In a study with over 90 dogs, only 30% of dogs with UC had malignant cells detected in the urine (Norris et al., 1992). On the other hand, evaluation of cytology samples can be misleading in cases of urinary tract infections when bladder epithelial cells may mimic a neoplastic population (Cannon and Allstadt, 2015). Comparable to the human bladder tumor antigen (BTA) test, a urine antigen test for canine UC, the Veterinary Bladder Tumor Antigen Test V-BTA [Alidex Inc (subsidiary of Polymedco Inc), Redmond,
Washington, USA] has been reported to be highly sensitive (80-90% sensitivity), but its low specificity limits its diagnostic value (Henry et al., 2003b). This canine test has been developed based on high molecular weight glycoproteins, which are detected in the urine of people with UC.

Imaging

The initial evaluation of a patient with clinically suspected BC is not uniform: some institutions perform imaging prior to cystoscopy, whereas others start with cystoscopy (Verma et al., 2012). Cystoscopy and imaging modalities are complementary. Computed tomography urography (CTU), unenhanced or contrast-enhanced, is routinely used to detect and stage BC. Magnetic resonance imaging (MRI) is an alternative to CTU, particularly in patients with contraindications to contrast media, but is generally considered inferior to CTU for BC detection (Kassouf et al., 2016; Niederhauser et al., 2013; Qu et al., 2011; Verma et al., 2012). The accuracy of CTU for BC detection varies, with sensitivity and specificity of 59-93% and 89-99% respectively, while MRI has a sensitivity of 80-88% with a comparable specificity of 95-99% (Knox et al., 2008; Niederhauser et al., 2013; Qu et al., 2011). CTU or MRI cannot replace diagnostic cystoscopy due to their limited ability to detect and differentiate flat bladder lesions (Verma et al., 2012). Ultrasonography (US) is another imaging modality, which is more cost-effective than CTU and MRI and lacks ionizing radiation, but tends to have a lower sensitivity (less than 70%)(Kassouf et al., 2016; Knox et al., 2008).

In dogs, ultrasonography is commonly used as an initial imaging modality, because it is a non-invasive, widely available technique that does not require anesthesia (Lee et al., 2016) (Hanazono et al., 2014). US is rather reliable to diagnose muscle-invasive BC, but has limited abilities to detect non-muscle-invasive tumors (Hanazono et al., 2014). Poor prognostic indicators include bladder wall involvement, heterogeneous tumor mass and trigone location (Hanazono et al., 2014). For canine BC staging, radiographs of the thorax and abdomen are common practice and recommended (Biller et al., 2016). As in people, CTU and MRI are superior to ultrasonography and radiography for both BC detection and staging, but are still not routinely used in dogs due to limited availability and increased costs (Lee et al., 2016).

Cystoscopy

Subtle bladder pathologies cannot be detected by imaging techniques. Therefore, BC detection and staging requires endoscopic examination (cystoscopy), which is the gold standard for detecting BC. It has a sensitivity and specificity of approximately 95% (Gopalakrishna et al., 2017; Kolodziej et al., 2016). The sensitivity of cystoscopy can further be increased by using fluorescence light (Isfoss, 2011; Lerner et al., 2012). Cystoscopy is however invasive, uncomfortable and expensive and has only limited ability to detect occult microscopic disease or the presence of tumors in atypical locations (Beukers et al., 2017; Kolodziej et al., 2016). Only 58-68% of small or flat tumors are detected by cystoscopy (Kolodziej et al., 2016). Cystoscopy is also not able to grade cancer or to assess tumor infiltration. This technique is therefore recommend to be used in combination with imaging modalities, including CTU, MRI and US.

In dogs, cystoscopy can be an invaluable additional test to routine diagnostic procedures of the lower urinary tract, primarily due to its feasible costs and the availability of equipment in most veterinary practices (Messer et al., 2005). This technique is primarily used for obtaining UC tissue for histopathological examination in order to confirm a diagnosis of UC (Fulkerson and Knapp, 2015).

Tumor samples obtained by cystoscopy are known to be of better diagnostic quality in female dogs (96% success rate) compared to male dogs (65% success rate) (Childress et al., 2011). This is mainly due to their anatomical differences, which also require the use of different equipment (Messer et al., 2005). Cystoscopy can be difficult or even impossible to perform in small dogs. If a biopsy sample cannot be obtained by cystoscopy, cystotomy is often the preferred alternative (Childress et al., 2011).

Biopsy

Biopsy refers to the histopathological examination of tumor tissue, which is required to confirm the diagnosis of UC. Furthermore, histological examination allows subtyping of UC, based on well-defined microscopic features, which are described in the WHO/International Society of Urological Pathology (ISUP) Consensus Classification of 2016 (Humphrey et al., 2016) (Table 1.1). Histological UC variants are reported to be associated with different prognosis and therapeutic response (Xylinas et al., 2013). When comparing different studies, there is however a large variation (7-81%) in the reported frequencies of the different histological variants. This may potentially be explained by differences in tumor stages at the time of histopathological diagnosis and lack of consistency regarding sampling techniques and pathological interpretation (Xylinas et al., 2013). In general, patients with variant UC histology have a higher risk of disease recurrence and cancer-specific mortality compared to pure UC patients (Black et al., 2009; Chalasani et al., 2009; Xylinas et al., 2013).

Canine UC is well characterized histologically with comparable microscopic morphology as described in people (Patrick et al., 2006). The histological classification of canine UC is therefore recommended to be done following closely the human classification system (WHO/ISUP Consensus Classification 2016) (Humphrey et al., 2016). The most up to date classification system for canine UC is based on the WHO Histological Classification of Tumors of the Urinary System of Domestic Animals, which has been updated in 2004 (Meuten 2004). At present, however, this or other tumor classification systems are not

consistently being used when diagnosing UC in dogs (Patrick et al., 2006). Given the different histopathological classifications used in published studies, the reported incidence of histological UC variants varies therefore widely (Patrick et al., 2006).

Species	Canine	Human
Reference	WHO International Classification of Tumors of Domestic Animals (Urinary System) (Meuten 2004)	WHO Classification of Tumors of the Urothelial Tract (Humphrey et al., 2016)
Histological tumor classification	Urinary bladder tumors **Epithelial Tumors** - Papilloma - Adenoma - Carcinoma - Transitional cell carcinoma (UC) ▪ Papillary and infiltrating ▪ Papillary and noninfiltrating ▪ Nonpapillary and infiltrating ▪ Nonpapillary and noninfiltrating (carcinoma in situ) - Squamous cell carcinoma - Adenocarcinoma - Undifferentiated carcinoma	Urothelial tract **Urothelial tumors** - Non-invasive urothelial neoplasms - UC in situ - Non-invasive papillary UC, low-grade - Non-invasive papillary UC, high-grade - PUNLMP - Urothelial papilloma - Inverted urothelial papilloma - Urothelial proliferation of uncertain malignant potential - Urothelial dysplasia - Invasive UC - Nested - Microcystic - Micropapillary - Lymphoepithelioma-like - Plasmacytoid/signet ring cell/diffuse - Sarcomatoid - Giant cell - Poorly differentiated - Lipid-rich - Clear cell

Table 1.1. WHO international histological classification of canine and human urothelial (urinary bladder) tumors.

Abbreviations: PUNLMP: Papillary urothelial neoplasm of low malignant potential; UC: Urothelial carcinoma; WHO: World Health Organization

1.1.3 Tumor classification, grading and staging

UC can be subdivided by grade, stage, and histological subtype (Cheng et al., 2009; Hansel et al., 2013). Current staging systems are provided by the 2009 WHO Tumor/Node/Metastasis (TNM) classification and The American Joint Committee on Cancer (AJCC) (8th edition, 2017) (https://cancerstaging.org/, accessed 20 November 2019) (Table 1.2). The recommended staging systems categorize UC based on the presence and invasive growth of the primary tumor (T), involvement of lymph nodes (N) and presence of distant metastatic spread (M) (Bostrom et al., 2010; Humphrey et al., 2016). Gross and histopathologic staging of UC is crucial in regard to patient prognosis and treatment decision. Pathologic staging assesses the presence or absence of invasive tumor growth and, in the case of invasive tumors, the extent of invasion into the bladder wall and adjacent tissues (Bostrom et al., 2010; Hansel et al., 2013). Progressive invasion into the bladder wall increases with tumor stage, and can involve the lamina propria (pT1), superficial (pT2a) or deep muscle layer (pT2b), perivesical fat either microscopically (pT3a) or macroscopically (pT3b), and adjacent tissues (pT4a) or the pelvic/abdominal wall (pT4b) (Hansel et al., 2013). In addition to tumor invasion, vascular invasion also needs to be assessed due to its importance as prognostic marker. The current recommendation is to report vascular invasion, preferably with the support of IHC (Hansel et al., 2013). The 2009 TNM staging system categorizes lymph nodal status based on the number and size of positive lymph nodes (N0: No lymph node metastasis; N1: metastasis in a single lymph node <2cm; N2: metastasis in a single lymph node of 2-5cm, or multiple lymph nodes <5cm; N3: metastasis in a lymph node >5cm) (Humphrey et al., 2016). Additional factors, such as the largest dimension of metastasis, extranodal extension, and anatomic location of positive nodes, may also be important (Cheng et al., 2009). The presence of distant metastasis should always be indicated as absent (M0) or present (M1). If primary tumor, lymph nodes or distant metastasis cannot be assessed, it is recommended to indicate this as TX, NX or MX respectively. UC can be histologically graded as either low- or high-grade tumors (Grignon, 2009). Grading has prognostic importance in pT1 tumors, which can be either low- or high-grade. Most pT2

and higher stage tumors are however high grade, which makes histologic grading as an independent prognostic marker questionable. In addition to grading and staging, UC can histologically be sub-typed into conventional UC or UC variants (Amin, 2009; Humphrey et al., 2016; Xylinas et al., 2013; Zhai et al., 2007). UC has a tendency for divergent cell differentiation with the most common being squamous followed by glandular. Divergent differentiation frequently parallels high grade and high stage UC and should therefore be indicated when diagnosing UC.

Canine UC can be graded and staged based on WHO guidelines for human UC, which were reported to be readily applicable for dog tumors (Meuten and Meuten 2016; Patrick et al., 2006). For diagnostic purposes, the human TNM classification scheme has been adapted and simplified for canine UC (Meuten and Meuten, 2016; Owen 1980) (Table 1.2). Excluding carcinoma *in situ*, primary tumors can be divided into three different stages: T1 (superficial papillary tumor), T2 (tumor invading the bladder wall) and T3 (tumor invading adjacent organs). Lymph node involvement is limited to two N stages: N1 (regional lymph node involved) and N2 (regional and juxta-regional lymph node involved). The presence of metastasis is recommended to be indicated as in the human TNM system: M0 (no evidence of metastasis) or M1 (distant metastasis present). UC is divided into a low and high grade variant. Low grade UC is characterized by orderly arranged cells, with mild to moderate cellular and nuclear abnormalities and lack of invasion, whereas high grade UC presents with disordered cells, marked cellular and nuclear abnormalities, numerous mitoses and invasive growth. It is important to be aware that, in contrast to people, the vast majority of UC are high-grade in dogs (Meuten and Meuten 2016; Mutsaers et al., 2003). Histological grading is therefore unlikely to provide additional prognostic information for most of the canine UC cases. Comparable to the situation in people, canine UC has the tendency to show divergent differentiation. For diagnostic purposes, histological sub-classification of canine UC into conventional and UC variants is however not yet

done routinely. Therefore, only little is known about the different types of histomorphological UC variants and their frequencies in dogs.

Species	Canine	Human
Reference	WHO TNM Classification of Tumors in Domestic Animals (Owen 1980)	AJCC 8th edition, 2017 (https://cancerstaging.org/)
Tumor staging	**Primary tumor (T)** Tis Carcinoma in situ T0 No evidence of primary tumor T1 Superficial papillary tumor T2 Tumor invading the bladder wall T3 Tumor invading neighboring organs **Regional lymph nodes (N)** N0 No regional lymph node involved N1 Regional lymph node involved N2 Regional lymph node and juxtaregional lymph node involved **Distant metastasis (M)** M0 No evidence of metastasis M1 Distant metastasis present	**Primary tumor (T)** TX Primary tumor cannot be assessed T0 No evidence of primary tumor Ta Non-invasive papillary carcinoma Tis Carcinoma in situ: 'flat tumor' T1 Tumor invades subepithelial connective tissue T2 Tumor invades muscularis propria - pT2a Tumor invades superficial muscularis propria (inner half) - pT2b Tumor invades deep muscularis propria (outer half) T3 Tumor invades perivesical tissue - pT3a Microscopically - pT3b Macroscopically (extravesical mass) T4 Tumor invades any of the following: prostatic stroma,seminal vesicles, uterus, vagina, pelvic wall, abdominal wall - T4a Tumor invades prostatic stroma, uterus, vagina - T4b Tumor invades pelvic wall, abdominal wall **Regional lymph nodes (N)** NX Lymph nodes cannot be assessed N0 No lymph node metastasis N1 Single regional lymph node metastasis in the true pelvis N2 Multiple regional lymph node metastasis in the true pelvis N3 Lymph node metastasis to the common iliac lymph nodes **Distant metastasis (M)** M0 No distant metastasis M1 Distant metastasis

Table 1.2. Pathological staging of canine and human urinary bladder carcinoma. The canine staging system has been adapted and simplified. Abbreviations: AJCC: American Joint Committee on Cancer; TNM: Tumor/Node/Metastasis; WHO: World Health Organization

1.1.4 Genetics

Recent advances in technology have made it possible to capture genomic alterations in cancer. Whole genome sequencing studies of UC have revealed both well-characterized and novel genomic alterations (Cancer Genome Atlas Research, 2014; Ikeda et al., 2015; Iyer et al., 2013; Ross et al., 2014). Genetic alterations are common in BC, and may potentially serve as therapeutic targets. Significant recurrent genetic mutations are observed, including multiple genes involved in cell-cycle regulation (CCND1, MDM2, RB1, TP53), chromatin regulation (ARID1A, KDM6A), and kinase signaling pathways [ERBB2 (HER2/neu), ERBB3, FGFR3, PIK3CA](Cancer Genome Atlas Research, 2014; Ross et al., 2014). Chromatin regulatory genes are more frequently mutated in UC than in any other common cancers studied so far. In muscle-invasive UC, TP53 has been reported to be the most commonly mutated gene (59%), followed by MLL2 (KMT2D) (27%), ARID1A (25%) and KDM6A (24%) (Ikeda et al., 2015). The identification of mutated genes in UC is promising for developing molecular targeted therapy. One major limitation in the development of targeted therapy is however the fact that UC is genetically very heterogeneous (Ikeda et al., 2015; Iyer et al., 2013). In addition to potential therapeutic targets, mutated genes may also serve as molecular prognostic markers of UC. A variety of molecular markers have been found to be associated with tumor grade and stage (FGFR3, hyaluronate), risk of occurrence (CCND3, CyclinE, HRAS, p21, p27, p53, pRB), and disease progression (CEACAM6, CYR61, FHL1, FOSB, RRM2, SRPX)(Birkhahn et al., 2010; Cheng et al., 2011b; Lopez-Beltran et al., 2008; Mengual et al., 2009; Passerotti et al., 2011; Shariat et al., 2008). Overall, molecular grading and staging of UC is considered relevant in order to predict disease course and response to therapy (Cheng et al., 2011b).

Molecular studies of canine UC has been limited. Three highly recurrent numerical chromosomal aberrations were identified by Shapiro et al. (Shapiro et al., 2015): gain of dog chromosome (CFA) 13 and 36 and loss of CFA 19. A study of Dhawan et al. (Dhawan et al., 2015) has demonstrated considerable similarities between enrichment patterns of genes in canine and human

invasive UC. These included patterns mirroring basal (EGFR, JUN, MMP9) and luminal (ERBB2, ERBB3, PPARG, TBX2) subtypes, and enrichment for genes involved in p53 pathways (APC, BAX, CTNNB1, HDAC1, MDM2, NOXA1, PTEN) and epithelial mesenchymal transition markers (CDH1, CLDN3, VIM, ZEB1, ZEB2).

1.1.5 Prognosis

The prognosis of UC varies greatly between different tumor grades and stages. Non-muscle-invasive UC, which accounts for 70-80% of all UC in people, has a significantly better prognosis than muscle-invasive disease. Recurrence rates at one year for non-muscle-invasive UC range widely from 15 to 70% (Allard et al., 1998; Chamie et al., 2013; Kluth et al., 2013; Sylvester et al., 2006). The probability of progression from non-muscle-invasive to muscle-invasive UC ranges from 7 to 40% (Allard et al., 1998; Chamie et al., 2013; Sylvester et al., 2006). Some of the most significant clinical and pathologic prognostic factors for non-muscle-invasive UC include: Number of tumors (single or multiple), tumor size, prior recurrence rate, tumor stage and grade, presence of concurrent carcinoma *in situ* (Allard et al., 1998; Babjuk et al., 2013). Based on these prognostic factors, patients with non-muscle-invasive UC can be divided into three different risk groups. The groups are defined based on risk tables provided by the European Organization for Research and Treatment of Cancer (EORTC) (Babjuk et al., 2013). Patients with muscle-invasive UC generally have a poor prognosis. Even with aggressive surgery (radical cystectomy), UC recurs in about 30% of patients (Breau et al., 2014; Lehmann et al., 2009). Local recurrence occurs in 5-25% of patients, usually within 24 months after surgery. Distant metastasis is seen in 50-75% of patients, again depending on tumor stage and lymph nodal involvement (Alfred Witjes et al., 2017; Lehmann et al., 2009). Metastatic recurrence mostly occurs in lymph nodes, lungs, liver, and bone, again typically within 24 months (Alfred Witjes et al., 2017). Survival times of patients with UC vary depending on several factors, including geographic location, ethnicity, and tumor stage, among others (Richters et al., 2019). In Europe, the average five-year survival time was estimated to be

approximately 70% for patients, which were diagnosed with BC between 2000 and 2007 (Marcos-Gragera et al., 2015).

Dogs diagnosed with UC have generally a very poor prognosis, with a significantly reduced relative survival time compared to people with the same cancer (Fulkerson and Knapp, 2015; Knapp et al., 2013). Less than 20% of dogs survive for 1 year or more despite cancer treatment (Knapp et al., 2013; Norris et al., 1992). At the time of diagnosis, metastases are detected in 20% or more of dogs, and at the time of death, 50-60% of dogs have evidence of distant tumor spread (Knapp et al., 2013; Mutsaers et al., 2003). In addition, canine UC is difficult to remove surgically because of the common trigonal tumor location and the frequent urethral involvement. Complete cystectomy, which is a routine treatment in people, is only rarely attempted in dogs. Only very few reports are available in the scientific veterinary literature, including only very low numbers of dogs treated with complete cystectomy (Mutsaers et al., 2003; Saeki et al., 2015). Partial cystectomy is more commonly done in dogs, but local and distant tumor occurrence is very common in treated dogs. An overall median progression-free interval of 235 days has been reported for dogs, which underwent partial cystectomy, with a median survival time of less than one year (Marvel et al., 2017). The vast majority (up to 80%) of canine UC are reported to be muscle-invasive (tumor stage T2), which is associated with poor prognosis *per se* (Fulkerson and Knapp, 2015). Despite recent progress in the management of canine UC, this cancer is still not curable in most cases in dogs.

1.1.6 Therapy

Therapeutic management differs between non-muscle-invasive and muscle-invasive UC. Therapeutic approaches include surgery (transurethral resection (TUR), cystectomy), intravesical chemotherapy, intravesical immunotherapy and/or radiotherapy.

Non-muscle-invasive UC

For non-muscle-invasive cancer, TUR and intravesical chemotherapy and/or immunotherapy are the main treatment modality (Malmstrom et al., 2009; Tan et al., 2016). Intravesical chemotherapy serves to either prophylactically reduce the risk of UC recurrence or as an adjuvant treatment after TUR. Mitomycin C (MMC) is the most common form of chemotherapy used (Malmstrom et al., 2009; Sylvester et al., 2004; Tan et al., 2016). The purpose of intravesical chemotherapy is to destroy remaining circulating tumor cells within the bladder after transurethral resection (TUR) of a bladder tumor and small unidentified UC. Low risk non-muscle-invasive UC patients only require a single instillation of intravesical chemotherapy, whereas patients with intermediate risk of disease recurrence and progression need repeated treatment 3-4 weeks after TUR (Tan et al., 2016). Intermediate to high risk disease patients with non-muscle-invasive UC are recommended to be treated with intravesical immunotherapy >1 week after TUR. The most important immunotherapeutic agent against UC recurrences is bacillus Calmette-Guérin (BCG), which is an attenuated bacterial strain (Bohle et al., 2003; Han and Pan, 2006; Malmstrom et al., 2009). Although BCG is very effective, this treatment bears the risk of toxicity. Current EAU (European Association of Urology) as well as NICE (National Institute for Health and Care Excellence) guidelines recommend BCG therapy, but with certain caution and by following a defined schedule (Babjuk et al., 2017) (https://www.nice.org.uk/, accessed 1 November 2019).

Muscle-invasive UC

Radical cystectomy and lymph node dissection are the treatments of choice for muscle-invasive UC. Surgery alone is however considered insufficient due in part to micrometastases. Chemotherapy before cystectomy or full-dose radiation therapy is recommended in clinically fit patients (Lazaro et al., 2016; Park et al., 2016a). Recommended chemotherapy is a cisplatinum-based combination therapy. Bladder-sparing approaches are reasonable alternatives to cystectomy for patients who are unfit for surgery and those who wish to

avoid radical surgery. Options include TUR alone, TUR followed by radiotherapy alone, chemotherapy alone or combination of chemotherapy and radiotherapy (trimodality treatment) (Arcangeli et al., 2015; Lazaro et al., 2016).

In dogs, partial cystectomy and systemic chemotherapy is currently the standard of care for management of UC. Complete surgical tumor excision is often not feasible attributed to the trigonal location of most tumors, the frequent finding of metastases at the time of diagnosis, and the severe side effects (Arnold et al., 2011; Fulkerson and Knapp, 2015). Most dogs with UC are treated with chemotherapy, cyclooxygenase (COX) inhibitors, or combinations of these drugs (Knapp et al., 2013; Knapp et al., 2014). Cisplatin, carboplatin, doxorubicin, mitoxantrone, mitomycin C, and vinblastine-based chemotherapy protocols have been reported, but a standard of care chemotherapy protocol for treatment of canine UC has not been established (Henry et al., 2003b). Intravesical chemotherapy in dogs is rarely performed, even though limited studies report promising results of intravesical mitomycin C treatment (Abbo et al., 2010). Studies of radiation therapy for UC in dogs are rare and report variable success (Choy and Fidel, 2016; Fulkerson and Knapp, 2015; Poirier et al., 2004; Walker and Breider, 1987).

1.1.7 Non-primate animal models for BC research

1.1.7.1 Rodents

There are two categories of animal models, dividing them into autochthonous (spontaneous) and non-autochthonous (transplantable) models. Spontaneous models include carcinogen induced or genetically engineered models.

Carcinogen models

The administration of certain carcinogenic chemicals, such as BBN [N-butyl-N-(4-hydroxybutyl)nitrosamine], FANT [N-(4-5-nitro-2-furyl2-thiazolyl)-formamide], and MNU (N-methyl-N-nitrosourea), can lead to the development of UC in mice and rats (Crallan et al., 2006; Ding et al., 2014; Ringuette-Goulet et al., 2018). The carcinogenic substance is commonly given orally, whereas direct intravesical or subcutaneous applications are less frequently performed.

With some differences depending on the animal species, way of application and type and dosage of carcinogen, cancer is usually detected within several months (Kanemoto et al., 2016). BBN, which is present in tobacco smoke, is the most commonly used carcinogen due to its high predilection for the urinary bladder as well as a higher stability and safety in handling compared to other carcinogenic substances (Ding et al., 2014; He et al., 2012). When compared to spontaneous human UC, cancer induced by BBN in mice and rats has a similar histomorphological appearance and up to 20% of identical differentially expressed genes (Ding et al., 2014; Fantini et al., 2018; Lu et al., 2011; Palmeira et al., 2010; Vasconcelos-Nobrega et al., 2012). When comparing mice and rats, BBN-induced murine UC is often more aggressive with a more invasive growth and a higher mutagenic effect compared to rats which usually develop a superficial type of UC (He et al., 2012; Kanemoto et al., 2016). Finally, the rodent BBN cancer model is not only a powerful tool for studying the disease, but allows also identifying and testing potential therapeutics (John and Said, 2017).

Transplantable models

Depending on the origin of transplanted cells or tissues, this animal model is referred to as either syngeneic (rodent cells transplanted into immunocompetent rodent) or xenogeneic (human cells transplanted into immunocompromised mice), respectively (Talmadge et al., 2007). Most frequently, cancer cells are injected outside of the bladder, usually subcutaneously, representing a heterotopic transplantation. Orthotopic engraftments, i.e. cell implantation into the bladder lumen or wall, are more challenging and expensive to perform and to assess and are therefore much less commonly performed (Chan et al., 2009; Hadaschik et al., 2007; John and Said, 2017; Raven et al., 2018; Ringuette-Goulet et al., 2018; Zhang et al., 2015). One major disadvantage of heterotopic engraftments, however, is the lack of a bladder-specific microenvironment, which can have a significant effect on morphological and molecular tumor characteristics, metastatic potential and tumor response to drugs or other therapeutics. Being able to use and examine

human patient-derived cancer cells is one of the major advantage of xenogeneic models. In order to avoid immune rejection, this model however requires immunodeficient mice, which does not allow evaluations of any immune responses.

Transgenic models

Transgenic mice are genetically engineered animals (GEM), which either lack (tumor-suppressing) or carry additional (tumor-promoting) genes (John and Said, 2017). Ideally, the gene of interest can selectively be switched on and off in a specific location (spatially), i.e. within the bladder, as well as for a limited time (temporarily). For that purpose, promoters, which control the expression of the gene of interest, have been developed. The Uroplakin II promoter is one of the most commonly used promoter in BC GEM models (John and Said, 2017; Lin et al., 1995). Transgenic models enable the study of certain genes. In BC, H-RAS, p53, RB, PTEN, fibroblast growth factor receptor are some of the most frequently mutated and best studied genes (Apolo et al., 2009; John and Said, 2017; Kobayashi et al., 2015; Wang et al., 2017a). Compared to other types of cancer, transgenic models however are not very commonly used. Bladder tissue-specific gene expression as well as the development of a malignant tumor phenotype has been shown to be challenging. Most GEM models of BC display non-invasive tumors, whereas the majority of GEM models fail to develop invasive growth or metastasis (Kobayashi et al., 2015).

1.1.7.2 Dogs

Laboratory animals

Compared to rodents, dogs are infrequently used as experimental animals for BC, mostly due to ethical constraints as well as increased time and costs of each experiment. Dogs have been shown to develop UC upon application of carcinogenic substances, including BBN (Okajima et al., 1981). Furthermore, in relatively few studies, potential therapeutics for UC have been tested in dogs (Lu et al., 2011). In a cohort of laboratory Beagle dogs, UC occurred in 3.8% of dogs which were used for a low-dose, whole-body, ^{60}Co gamma radiation study

(Nikula et al., 1989). Surprisingly, the UC was considered a spontaneous disease in these dogs, unrelated with the radiation treatment. This conclusion may however be interpreted with caution and an association between cancer development and the performed radiation experiment is possible. More common than testing in laboratory dogs, potential biomarkers and therapeutics for UC have been evaluated in pet dogs (Allstadt et al., 2015; Henry et al., 2003a; Szigetvari et al., 2018).

Pet dogs

Spontaneous, naturally-occurring UC is common in pet dogs, providing a unique opportunity to use canines as animal models for human UC (Fulkerson et al., 2017). Most canine UC are highly malignant, characterized by invasive growth and frequent metastasis, comparable to muscle-invasive UC in men. Human and canine UC share many features, including histomorphological and molecular tumor characteristics, sites of metastasis, and response to therapy (de Brot et al., 2018; Dhawan et al., 2015; Knapp et al., 2016; Sommer et al., 2018). Studying the development of UC and testing therapeutics in dogs with UC may provide the chance to gain knowledge in both human and veterinary medicine with benefits for both affected people and dogs. Nevertheless, this animal model is still underexploited and deserves to receive more attention. The great advantages, such as the spontaneous occurrence of cancer in an immune-competent large animal with exposure to the same environmental factors like people, are well worth to invest in the associated increased ethical issues and costs of this animal model.

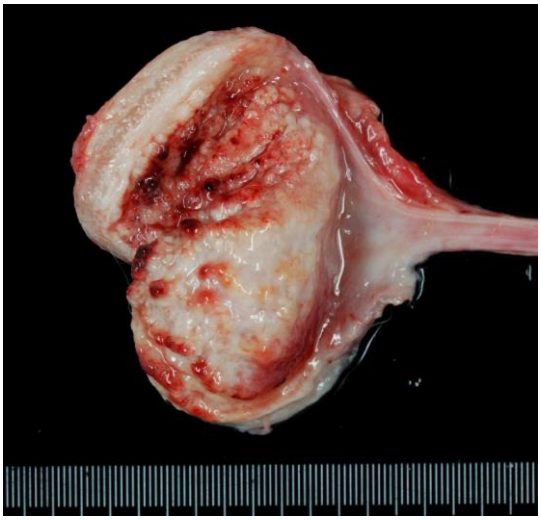


Figure 1.1. UC in the urinary bladder of an elderly female neutered pet dog. Note that the bladder has been incised for a better visualization of the mucosal neoplastic growth. The ruler indicates millimeter.

1.2 Prostate cancer (acinar adenocarcinoma and UC) in people and dogs

1.2.1 Epidemiology

Prostate cancer (PC) is the second most common cancer in men globally, with highest incidence rates in elderly men of developed countries, with a predisposition for African-Americans (Bray et al., 2018; Rebbeck et al., 2013). In 2018, over 1.2 Mio. new cases were registered worldwide, accounting for more than 350,000 deaths (Rawla, 2019). Incidence rates, which are highly variably between different countries, are highest in the USA and continue to increase worldwide (Quinn and Babb, 2002). Differences in disease detection methods, therapeutic approaches and genetics have been proposed to explain the high variability in tumor incidence between the different geographic locations. In contrast to incidence rates, mortality rates are less variable, but still differ significantly between different geographical areas. In the more developed countries, age-adjusted mortality rates have a tendency to decline, whereas mortality is increasing in less developed countries (Rawla, 2019; Sharma, 2019). There is still very poor knowledge regarding the etiology of PC.

Positive family history, age as well as a fat-rich diet however have been demonstrated to be risk factors (Abdel-Rahman, 2019; Cheng et al., 2019; Narita et al., 2019; Pienta and Esper, 1993). Certain gene mutations, including BRCA1/2 as well as HOXB13 are associated with increased risk of PC, confirming a genetic predisposition (Giri et al., 2018).

It has long been believed that PC is limited to men and very few animal species, including lions and dogs. Spontaneous canine PC is uncommon, with a prevalence of less than 1% (Bell et al., 1991; Teske et al., 2002). Elderly dogs are at highest risk to be diagnosed with PC, with a mean age of 9 to 10 years (corresponding to 65-75 human years) (Teske et al., 2002). Even though any dog breed may be affected, some breeds, including the Bouvier des Flandres, seem to be more prone to develop the disease (Teske et al., 2002). Surgically neutered, i.e. bilateral orchiectomized, dogs are more likely to be affected compared to sexually intact dogs (Bryan et al., 2007; Obradovich et al., 1987; Teske et al., 2002). The role of testicular as well as non-testicular androgens in the oncogenesis of canine PC remains however uncertain. At the time of diagnosis, canine PC is already at an advanced stage of disease in most if not all dogs, often with metastatic spread to lymph nodes or distant organs. Consequently, the prognosis is poor for most affected dogs, and curative treatment is not available up to present.

1.2.2 Diagnosis

In men, the diagnosis of PC is commonly made based on a transrectal ultrasound (TRUS)-guided prostate biopsy, following increased levels of serum prostate-specific antigen (PSA) and/or an abnormal digital rectal examination (DRE) (Futterer et al., 2015).

PSA

PSA has been a routinely used, well-established marker for prostatic disease in men since decades (Wang 1979, Stamey 1987, Altwein 1999). Regular measuring of PSA in the serum offers a highly valuable tool to detect PC at an

early stage and is recommended as a screening method by the European Association of Urology as well as the American Urological Association (Gandaglia et al., 2019). In order to prevent cancer overdiagnosis, overtreatment and unnecessary biopsies, PSA screening needs to be performed in a structured manner and in the context of clinical features, including age of the patient, family history and findings based on prostate palpation and imaging. The recommended interval of PSA testing is two years for men at increased risk and up to 8 years in low-risk patients (Gandaglia et al., 2019). In patients with a life expectancy of 10 years or less, PSA screening is not recommended as these men are unlikely to benefit from an early diagnosis (Mottet et al., 2017).

Biopsy

As a standard procedure, prostate biopsy is performed with the aid of TRUS. From apex to base of the gland, between 10 and 12 random core biopsies should be sampled (Eichler et al., 2006; Hara et al., 2008). If areas of cancer are suspected based on digital rectal examination or TRUS, cores of these areas are obtained as well. Each biopsy needs individual reporting, including its location and ISUP 2005 tumor grade. For overall tumor grading, the new ISUP 2014/WHO 2016 grading system, using five groups of tumor, is recommended to be applied, in combination with a conventional Gleason score (Epstein et al., 2017; Offermann et al., 2019; Pierorazio et al., 2013). If the biopsy is negative, a re-biopsy should be performed if certain histopathological or clinical findings, such as rising PSA levels, presence of atypical glands, suspicious DRE, are observed (Mottet et al., 2017).

Imaging

Multiparametric magnetic resonance imaging (mpMRI) is a relatively recent new approach in the diagnostic work-up of PC and is proposed to be performed as a follow-up test, after initial prostate biopsies have been taken (Futterer et al., 2015; Gandaglia et al., 2019; Gandaglia et al., 2016). Compared to ultrasound-guided random biopsy sampling, mpMRI is more sensitive and may

be used for additional targeted biopsy sampling. In particular, mpMRI is strongly recommended before repeating a biopsy (Stabile et al., 2019). As a standalone test, in a biopsy-naïve population, mpMRI is currently not recommended. Another advantage of mpMRI are the lower chances to detect clinically non-relevant cancer, hereby reducing the risk of over diagnosis as well as unnecessary biopsies. Four sequences should be included in mpMRI, i.e. T1-weighted images, T2-weighted images, diffusion- weighted images and dynamic contrast- enhanced imaging, and the MRI findings should be interpreted and reported in a standardized way (Stabile et al., 2019). Currently, the Prostate Imaging Reporting and Data System (PI-RADS) v2, which was developed in 2014, is recommended to be used for the interpretation of mpMRI images (Weinreb et al., 2016).

Biomarkers

Even though serum PSA is a useful and widely used biomarker for PC, elevated values are not specific for PC and do not allow any differentiation between indolent and aggressive cancer. In order to prevent over diagnosis and overtreatment, there is an urgent need for more highly sensitive and specific biomarkers. These may be measured in either serum or urine of PC-suspected men and are recommended to be used as additional tests alongside total blood PSA screening (Tan et al., 2019; Vedder et al., 2014). Prostate cancer antigen 3 (PCA3), also known as differential display code 3 (DD3) is a non-coding, prostate-specific mRNA, which has been shown to be overexpressed in PC tissue and which can be measured in the urine. This marker has been shown to be useful for the reduction of unnecessary biopsies. The sensitivity and specificity of this biomarker has been interpreted as acceptable (Cui et al., 2016; Tan et al., 2019). Another two markers, which aid in reducing the number of avoidable biopsies and which are measured in the serum include the prostate health index (PHI) and a four kallikrein (4k) panel (Vickers et al., 2010). The PHI consists of a formula which contains total, free and precursor PSA. The 4k panel includes total, free, and intact PSA and kallikrein-related peptidase 2. Both markers aid in differentiating indolent from clinically significant PC, with

a comparable, overall good, performance (Carlsson et al., 2013; Nordstrom et al., 2015).

In dogs, the diagnosis of PC is usually suspected based on clinical signs, digital rectal examination, imaging and analysis of urine and prostatic fluid, and is confirmed by biopsy (Alonge et al., 2018b). In contrast to men, the serum marker PSA does not appear to be a reliable diagnostic tool in dogs because it typically fails to increase or remains undetected in the serum of dogs with PC (Alonge et al., 2018b; Bell et al., 1995). Biopsy is required in order to establish a final diagnosis and can be performed percutaneously or excisionally. Under sedation or anesthesia, percutaneous sampling can be performed perineal or transabdominal, with or without the aid of US. An excisional biopsy is collected during surgery, which requires full anesthesia. For the visual examination of the gland, x-ray and US are the most commonly applied imaging modalities. Even though US is more sensitive for detecting prostate disease, x-ray allows to check for metastasis at the same time.

In contrast to the situation in men, the potential of PSA as biomarker remains controversial in dogs. Serum PSA could not yet be demonstrated to significantly increase in dogs with PC or other pathologies of this gland (Bell 1995). More recently, another serum marker, canine prostatic specific esterase (CPSE), has been proposed in order to screen dogs with suspected prostate disease. Similar to PSA of men, CPSE has enzymatic activity and is known to be the most abundant and specific androgen-dependent protein of prostatic secretion in dogs (Chapdelaine et al., 1984a; Frenette et al., 1987). Even though CPSE may be a suitable marker for prostate pathologies, it lacks specificity for PC (Alonge et al., 2018b). To date, a serum marker with comparable sensitivity and specificity as PSA in men has not yet been identified in dogs.

1.2.3 Tumor classification, grading and staging

Tumor classification

Prostate tumors are highly heterogeneous on a morphological as well as molecular level. Based on the WHO tumor classification system, PC is

subclassified based on its histomorphology (Humphrey et al., 2016). The system includes six larger groups of prostate tumors, i.e. epithelial, neuroendocrine, mesenchymal, hematolymphoid, miscellaneous and metastatic tumors. The different prostate tumor subtypes do not only vary in their morphological appearance, but are also characterized by distinct molecular pathologies and clinical features (Inamura, 2018). Based on either specific gene fusions or mutations, the Cancer Genome Atlas research network divides primary PC into seven different molecularly distinct subtypes. The most common known molecular pathologies in PC include fusions involving androgen-regulated genes and E twenty-six (ETS) transcription factor family members. Based on the presence or absence of ETS rearrangements, tumors are defined as ETS positive or ETS negative, respectively (Inamura, 2018; Tomlins et al., 2009). Once the clinical significance of the molecular tumor subclasses is better understood, this tumor subdivision may be valuable for a better prognostic prediction and personalized therapies (Barbieri and Tomlins, 2014).

Grading

Since the first description in 1966 by Donald Gleason (Gleason, 1966), the Gleason grading system has been used ever since and still represents a valuable prognostic tool for PC (Shah, 2009). This system includes five different grades, which are based on the subgross histomorphological appearance of the examined tumor tissue. The morphology becomes more complex with higher Gleason grade. Furthermore, tumors are given a Gleason score, which is defined by the most prevalent (primary) and the second most prevalent pattern. On several occasions, the ISUP has amended the Gleason grading system. The most recent changes were introduced by the ISUP in 2014, proposing to use five Gleason grade groups instead of Gleason scores 2-10 (Epstein et al., 2016). Further amendments include the division of tumors with Gleason score 7 into two different grades and the assignment of separate grades for Gleason score 8 and score 9-10 tumors. ISUP recommends to report both grade using the new Grade Groups 1-5, as well as the Gleason score.

Staging

Tumor stage refers to the anatomical extension and distribution of neoplastic tissue, which is relevant for both prognosis and therapy. Clinical stage describes the extent of cancer at the time of diagnosis and is based on patient history, physical examination, and imaging techniques. Originally, DRE has been performed to clinically stage PC. More recently, mpMRI has been proposed as an additional method for tumor staging because of its higher sensitivity and reduced interobserver variability (Draulans et al., 2019). Pathological stage is based on histopathological findings of radical prostatectomy tissues. Both clinical and pathological stage use a so-called TNM classification, which includes the description of the extent of the primary tumor (T category), involvement of regional lymph nodes (N category), and spread (or metastasis) to distant sites (M category) (Humphrey et al., 2016). In a next step, the T, N, and M categories are then combined, corresponding to a stage group (I to IV). Typically, stage I tumors are confined to the organ of origin, and stage IV tumors have evidence of distant metastasis.

Based on the WHO Histological Tumor Classification of Domestic Animals, prostate carcinoma is further classified as adenocarcinoma or poorly differentiated carcinoma (Owen 1980). In dogs, PC is however characterized by a heterogeneous histomorphological appearance, and two or more types of histological differentiation within the same tumor section are common. Glandular, urothelial and squamous morphologies are most frequently observed (Cornell et al., 2000). So far, molecular subtypes of PC have not been well defined in dogs. When grading canine PC, the Gleason grading system, which was last modified in 2005, may be applied since growth patterns are comparable between the two species (Palmieri and Grieco, 2015). Comparable to human PC, two or more different growth patterns are frequent. In a study assessing 45 canine PC, cribriform, solid and small acinar/ductal were the most commonly observed primary, secondary, and tertiary patterns, respectively (Palmieri and Grieco, 2015). In dogs, the highest Gleason score (GS10) is most common, whereas GS 7 is most frequent in men. The higher score in canine

tumors most likely corresponds to advanced stage of the disease, which is often detected late in dogs. For tumor staging, thoracic and abdominal imaging (US or x-ray) should be performed. In addition, CT or MRI scans may be performed in order to screen for metastatic bone lesions.

1.2.4 Genetics

It is well known that PC has a strong heritable component, possibly the highest of any type of cancer (Hjelmborg et al., 2014; Lynch et al., 2016). Men with a positive family history are at a two to four-fold increased risk to develop this malignancy, with the highest risk for relatives of early-onset cases and those with more than one affected family member. Familial PC is however very heterogeneous on a genetic level, making it difficult to identify relevant genetic abnormalities. Despite many available genome wide association studies (GWAS), there is still relatively little known about the genetic pathologies, which contribute to the high heritability of PC. Almost one third of the familial relative risk of PC can be explained by 167 known common genetic variants, i.e. single nucleotide polymorphisms (SNPs). They include SNPs with effect on the oncogene MYC or PSA genes, among others. Even though the individual SNP is only associated with a small risk for PC, their effect on cancer risk is multiplicative and therefore highly significant. Higher risk variants such as mutations in the tumor suppressor genes HOXB13 and BRCA1/2 are much less common, accounting for approximately 6% of familial PC risk (Devitt and Dreicer, 2019; Giri and Beebe-Dimmer, 2016). BRCA mutations have been demonstrated to be associated with early onset of disease as well as with worse prognosis. Men at increased risk are therefore recommended to be tested for the presence of BRCA1/2 and HOXB13 mutations, and the test result may have an influence on the screening methods, prognosis and the choice of therapy (Devitt and Dreicer, 2019; Walsh, 2017). PC also harbors genomic abnormalities, which are highly specific to the disease, such as androgen receptor (AR) gene alterations. Lesions in the AR gene are however restricted to castration-resistant PC, most likely as a consequence of the therapy.

In dogs, PC can affect any breed even though some breeds, including the Bouvier des Flandres, appear to be at increased risk (Bryan et al., 2007; Teske et al., 2002). This association with some specific breeds may possibly represent a genetic predisposition for canine PC. To date, there is only limited knowledge about the genetics of canine PC. Comparable to human PC, downregulation of NKX3.1 and upregulation of MYC is also observed in dog PC (Fonseca-Alves et al., 2018a). In contrast to human PC, hypermethylation of NKX3.1 could not be detected, and the mechanism of reduced genetic expression remains unknown in dogs. Furthermore, the genetic profile of canine and human PC share similarities, including reduced expressions of well-known tumor suppressor genes, such as ATM, BRCA1, CDH1, MEN1, PTEN and TP53 (Laufer-Amorim et al., 2019; Rivera-Calderon et al., 2016). Based on reduced levels of PTEN, p53, and AR, combined with an increased expression of MDM2, canine PC may resemble castration-resistant PC in men (Rivera-Calderon et al., 2016).

1.2.5 Prostate tumor tissue markers

Tumor markers can provide a valuable prognostic or diagnostic tool and their expression in tissue is most commonly assessed by IHC.

As previously mentioned in the section about biomarkers, PSA is not suitable as serum marker for prostate disease in dogs. In canine being and malignant prostate tissue, PSA was however reported to be expressed (Lai 2008, Bell 1995). In normal canine glands, acinar, urethral as well as ductal cells showed immunohistochemical PSA staining. In the present study, PSA expression was not assessed. The following more detailed description is limited to a few selected tumor markers, which have been used in the present studies of prostate glandular and urethral cancers.

1.2.5.1 p63

P63, a member of the p53 family, is expressed in two isoforms, TAp63 and ΔNp63 (also known as p40), with opposing tumor suppressor and oncogenic functions. In prostate tissue, p63 is used as a diagnostic marker. It is primarily

a marker for basal cells, and is routinely used for the diagnosis of prostate adenocarcinoma (Brimo and Epstein, 2012; Dabir et al., 2012; Epstein et al., 2014; Signoretti et al., 2000). In the normal prostate gland, acini are lined by a continuous basal cell layer. This layer is however lost during carcinogenesis, and carcinoma typically lacks p63 expression. In the healthy prostate, luminal glandular cells lack p63 expression. In most prostate carcinomas, the expression of p63 is either absent or restricted to a low number of neoplastic cells (Kunju et al., 2006). One rare subtype of prostate adenocarcinoma with p63 expression of luminal cells has however been described (Giannico et al., 2013). The prognostic significance of p63 expressing prostate adenocarcinomas remains however unknown (Giannico et al., 2013). Furthermore, p63 is also used as urothelial marker, and has been proposed to be valuable for differentiating poorly differentiated glandular prostatic from urothelial carcinoma (Alshenawy and Saied, 2015; Chuang et al., 2007; Kunju et al., 2006; Oh et al., 2016).

In contrast to the human prostate, the normal canine gland is characterized by a discontinuous basal cell layer, with fewer basal cells than in men (Leav et al., 2001; Romanucci et al., 2016). Therefore, the discontinuity of the basal cell layer is not a diagnostic criteria for cancer, and basal cell markers are not routinely used for PC diagnosis in dogs. Comparable to the normal human prostate, luminal glandular cells lack p63 expression. As in men, most PC of dogs are characterized by absent or rare expression of p63 (Della Salda et al., 2019; Fonseca-Alves et al., 2018b; Romanucci et al., 2016). Similar to human PC, a rare subtype of p63 positive luminal PC has been described (Fonseca-Alves et al., 2018b; Romanucci et al., 2016). So far, studies investigating the role of p63 as urothelial marker are lacking in dogs.

1.2.5.2 Uroplakin III

Uroplakins (UP) are expressed in terminally differentiated urothelial lining (umbrella) cells and include four different types, namely UPIa, UPIb, UPII and UPIII. In the prostate, UPs are expressed in the urothelium of the urethra and

proximal ducts. UPIII, a highly specific but only moderately sensitive marker for urothelial differentiation, may be used as a diagnostic marker in cases of prostate adenocarcinoma where UC is a differential diagnosis (Hameed and Humphrey, 2005; Kaufmann et al., 2000; Mhawech et al., 2002). Sensitivities are reported to range between 50 and 60%, and tend to be lower in metastatic compared to primary UC (Kaufmann et al., 2000). UPIII has been shown to have potential as prognostic marker in UC of the bladder. Reduced UPIII expression was demonstrated to be associated with lymphovascular invasion, pathologic stage, and grade (Matsumoto et al., 2008). The suitability of UPIII as prognostic marker of prostate UC still needs to be investigated.

In dogs, UPIII has a similar specificity and sensitivity as urothelial marker compared to men. Canine studies reporting the expression of UPIII are however largely restricted to the assessment of urinary bladder tissue, and UPIII expression in canine prostate tissue has only extremely rarely been analyzed (Ramos-Vara et al., 2003). Furthermore, studies, which describe the combination of p63 and UPIII expression in the canine prostate, appear to be lacking.

1.2.5.3 Lysine-specific demethylases

KDM7A

Lysine-specific demethylase 7A (KDM7A), also known as JHDM1D (JmjC domain-containing histone demethylation protein 1D), modifies the level of methylation in histone, thereby regulating gene expression on an epigenetic level (Osawa et al., 2011; Park et al., 2016b). KDM7A has been shown to act as tumor suppressor by down-regulating angiogenesis in different types of cancer. As a co-regulator of AR, the expression level of KDM7A plays a role in PC. The level of KDM7A expression is regulated by the level of tumor-suppressing miR137 (Nilsson et al., 2015). In androgen responsive PC cells, miR137 is increased by androgen. This is in contrast to androgen-independent PC, where miR137 expression is reduced or absent. Consequently, epigenetic silencing of

miR137 may be important in promoting androgen signaling during prostate carcinogenesis and progression

KDM5B

Lysine-specific demethylase 5B (KDM5B), also known as JARID1B (jumonji ATrich interactive domain 1B) or PLU-1, is another member of the JHDMs subfamily. KDM5B was shown to be up-regulated in PC and to act as oncogene by promoting the activation of androgen receptor target genes, similarly to KDM7A (Han et al., 2017; Xiang et al., 2007). The expression of KDM5B is repressed by both miR137 (Nilsson et al., 2015) and miR-29a, potentially offering a therapeutic target for PC (Li et al., 2015a). Indeed, the expression of miR-29s has been shown to be reduced in different cancers (Li et al., 2015a).

In canine tissue, the expression of lysine-specific demethylases have not yet been assessed and their role in benign or malignant dog prostate is unknown.

1.2.6 Prognosis

1.2.6.1 Overall prognosis

Clinically, PC is a very heterogeneous disease with a highly variable prognosis. Mortality rates differ significantly between the different geographic areas, presumably due to genetic and environmental factors (Bray et al., 2018; Ferlay et al., 2019; Taitt, 2018). Furthermore, depending on Gleason tumor grade, mortality rates vary, with a range between 5 (grade 2-6) and 38% (grade 9) (Brockman et al., 2015). Globally, PC has the fifth highest cancer mortality rate, which is 6.7%. In many developed countries, mortality rates are decreasing, most likely due to earlier diagnosis because of screening and improved therapeutic options (Bray et al., 2018). This is in contrast to other geographic areas where mortality rates continue to increase. In localized PC, recurrence rates after radical prostatectomies range between 20 and 40% and are defined as increased levels of PSA, consistent with a biochemical recurrence. Variables, which have an effect on the recurrence rate include preoperative PSA level, Gleason grade, positive surgical margins, lymph node involvement and

extraglandular cancer growth (Tourinho-Barbosa et al., 2018). Overall survival is high (up to 100%) for organ-confined cancer cases, but can be as low as 30% five years after diagnosis if the tumor has spread to distant organs (Taitt, 2018). Among other factors, such as tumor grade and stage, the survival rate is dependent on the therapeutic approach. Following radical prostatectomy, which is a common treatment for PC with curative intent, the 10-year overall survival is between 72 and 86% (Hackman et al., 2019).

PC in dogs is associated with a very poor prognosis due to high tumor grade and stage at the time of diagnosis. Highly invasive tumor growth and widespread metastasis are common (Cornell et al., 2000). No screening test is currently routinely performed in dogs, and a reliable and specific marker for subclinical PC is not available. Therapy for canine PC is only palliative as no curative treatment seems to work for affected dogs (Leroy and Northrup, 2009). Survival times for dogs with clinical signs are very short, in most cases ranging between few weeks to some months (Cornell et al., 2000; Sorenmo et al., 2004).

1.2.6.2 Prognostic factors

Histopathology

When PC tissue is assessed, either core biopsies or prostatectomy specimens, certain prognostic factors are recommended to be reported, including histological type, proportion of tissue affected by cancer and tumor grade (Humphrey et al., 2016). In addition, TNM stage, surgical margins, tumor size and lymphovascular space invasion are further prognostic features of prostatectomized tissues. Gleason grade, which is predictive for tumor progression and mortality, is the most important tissue-based prognostic factor and is highly relevant for the choice of therapy. A Gleason score of 4+3 is associated with a 5-fold increased risk to die from PC compared to a score of 3+4 or ≤6 (Bill-Axelson et al., 2018). PC-related death is 10 times more likely in men with PC of a score of 8 or 9, compared to a Gleason score of ≤6. With the purpose to estimate the prognosis, several nomograms based on a range of

clinical as well as pathological prognostic variables have been developed (Stephenson et al., 2006). Furthermore, risk groups, based on clinical and pathological factors, have been defined with the aim to facilitate treatment choice. The American Joint Committee on Cancer (https://cancerstaging.org/, accessed 20 November 2019) differentiates between cancer stage groups . The risk is estimated to be very high for locally advanced and metastatic groups. For localized disease, the risk ranges from very low to high, depending on tumor stage, Gleason score and PSA level (Humphrey et al., 2016). After grade, tumor stage is the most important prognostic factor for recurrence and mortality due to PC. Organ-confined cancer (pT2) needs to be differentiated from PC with extraprostatic extension (pT3), which has a higher risk of recurrence after prostatectomy (Carver et al., 2006).

Biomarkers

In addition to tumor histomorphology, molecular biomarkers could reveal valuable prognostic information, which is crucial when choosing the most appropriate treatment. Identifying a suitable robust biomarker has been shown to be a challenging task. Markers for cellular proliferation (e.g. Ki67), assessed by IHC, are suitable for predicting tumor growth and progression (Carneiro et al., 2018; Hammarsten et al., 2019; Richardsen et al., 2017). Loss of tumor suppressor genes, such as PTEN (phosphatase and tensin homolog) is a further valuable prognostic marker, which is associated with PC progression and death (Alford et al., 2017; Bismar et al., 2018; Carneiro et al., 2018). The proto-oncogene MYC has prognostic potential on a genetic level, but with conflicting results on a protein level (Carneiro et al., 2018; Pettersson et al., 2018). On an epigenetic level, hypermethylation of selected promoters, such as PITX2 (paired-like homeodomain 2), has been well-documented and shown to be effective as biomarker (Jiang et al., 2019). Increased methylation is associated with higher risk of PC recurrence. Despite the detection of several potentially promising biomarkers, as described above, it is crucial to be aware that none of these markers have been fully validated. Their suitability in clinical practice remains therefore uncertain and requires further investigation. Finally, the

expression of a collection rather than individual genes and proteins may serve as prognostic marker. Such transcript signatures have potential as biomarkers, but need further careful validation before their implication in practice (Klein et al., 2014; Walker et al., 2017).

Considering that PC in dogs is usually a high grade and high stage tumor at the time of diagnosis, histopathological examination is unlikely to provide any additional prognostic information. When graded by the modified Gleason system, most if not all canine PC have the highest Gleason score of 10 at the time of diagnosis (Palmieri and Grieco, 2015). The expression of certain human PC molecular biomarkers has been confirmed in canine PC tissue, including decreased levels of PTEN and increased expression of MYC (Fonseca-Alves et al., 2018a; Fonseca-Alves et al., 2013; Rivera-Calderon et al., 2016). Some of these markers are valuable in order to differentiate benign from cancerous prostate tissue. Their prognostic significance, however, has only rarely been investigated.

1.2.7 PC therapy

Active Surveillance

Considering the negative consequences of cancer overtreatment, low-risk patients with localized PC and a life expectancy of at least 10 years may be closely monitored instead of being immediately treated with curative intent. These patients are regularly assessed following a predefined surveillance program, including screening via DRE, imaging, re-biopsy and PSA levels. Treatment is only considered once certain thresholds are reached, which is a change of tumor grade in the re-biopsies in most of the cases (Tosoian et al., 2015). Since only low-risk patients should be selected for this treatment modality, cancer-specific survival (CSS) is expectably very high in patients under active surveillance, often reaching 100%. CSS and overall survival does not differ between men immediately treated and on active surveillance (Tosoian et al., 2015). Overall, active surveillance is a feasible alternative to curative treatment in low-risk patients. It is noteworthy though that upgrading of

Gleason grade occurs relatively common, i.e. in almost 50% of patients, during the time of surveillance and may have therapeutic and prognostic consequences (Verep et al., 2019).

Radical prostatectomy (RP)

Removing the entire prostate (except capsule) is currently a standard procedure for curative treatment of localized PC. This surgery can be done in either an open way, by laparoscopy or with the help of a robot. Oncological, urinary function and sexual function outcomes do not significantly differ between the three different approaches. In patients with localized PC, cancer mortality does not significantly differ between active surveillance, RP and radiotherapy (Guo et al., 2019; Hamdy et al., 2016). In high or medium-risk patients, it is recommended to dissect pelvic lymph nodes during RP surgery (Mottet et al., 2017). Despite its relevance for tumor staging, a convincing therapeutic effect of a lymph node dissection has not been demonstrated (Fossati et al., 2017). Unfortunately, post-operative incontinence and erectile dysfunction are common problems following RP (Parker et al., 2011). Robot-assisted prostatectomy has been shown to have higher rates of sexual potency compared to open RP (Nyberg et al., 2018). The rate of urinary incontinence however does not seem to significantly differ between the different surgical methods.

Radiotherapy

For treating PC, primarily medium or high-risk localized disease, there are two main modalities of radiotherapy, external beam radiation therapy (EBRT) and EBRT plus brachytherapy (EBRT + BT). In EBRT, high-energy X-ray beams are directed to the prostate from outside, which has been shown to be effective when treating localized PC (Dearnaley et al., 2014; Zietman et al., 2005). Improved techniques, i.e. conformal radiotherapy, allow the use of higher doses without significantly increasing associated morbidities. For conformal radiotherapy, a 3-dimensional image of the tumor is being created in order to target the cancer as precise as possible, while sparing the surrounding non-

cancerous tissue. Brachytherapy (BT), also known as internal radiation, refers to radiation within the prostate by placing radioisotopes into the glandular tissue. This method allows increasing overall radiation dose, while minimizing radiation dose to normal tissues (Chen, 2019). In medium and high-risk localized PC, patients treated with EBRT + BT have improved survival compared to EBRT alone (Amini et al., 2016).

Hormonal treatment

For androgen deprivation (AD), the level of testosterone can be reduced by either limiting its production via castration or by blocking its action via blocking androgen receptors. At present, chemical castration, using luteinizing hormone–releasing hormone (LHRH) is the preferred option over surgical castration via orchiectomy (Pagliarulo et al., 2012). Long acting LHRH agonists are most commonly used. AD therapy is well accepted for metastatic PC, but remains controversial for organ-confined disease. Indeed, hormonal therapy is known to be associated with certain morbidities, including cardiovascular (myocardial infarct), metabolic (diabetes), and skeletal complications (osteoporosis) (Keating et al., 2013). AD therapy may also be applied in combination with radiotherapy, which is linked to a lower mortality rate compared to AD therapy alone in locally advanced PC (Warde et al., 2011; Widmark et al., 2009). In low-risk PC however, AD in combination with radiotherapy is not recommended due to the lack of convincing beneficial therapeutic effect. Similarly, the combination of AD with surgical therapy, i.e. radical prostatectomy, fails to provide convincing evidence for any therapeutic benefits (Pagliarulo et al., 2012).

In dogs, PC therapy is primarily limited to palliative treatment. Radiotherapy, surgery and chemotherapy have all failed to cure the disease in dogs (Cunto et al., 2019). In dogs with localized disease, prostatectomy may be attempted, but the therapeutic benefit is questionable (Cunto et al., 2019; Leroy and Northrup, 2009). Surgical therapy is so far not well accepted by surgeons and dog owners due to i) the overall poor prognosis of PC in dogs, ii) the significant

postoperative morbidity, and iii) its expected poor therapeutic effect. Furthermore, hormonal treatment, i.e. surgical castration is also not a feasible option for affected dogs as it does not improve the prognosis since canine PC is usually androgen-insensitive. Finally, active surveillance is not feasible for dogs with PC due to the commonly aggressive behavior of PC in affected animals.

1.2.8 Non-primate animal models

1.2.8.1 Mice

Transgenic Adenocarcinoma of the mouse prostate (TRAMP)

More than two decades ago, a genetically engineered mouse model was created, which is characterized by the directed expression of the ectopic oncogene Simian Virus 40 T antigen (Tag) in prostatic tissue, consequently causing prostate-specific inactivation of p53 and Rb tumor suppressor activity (Gelman, 2016; Gingrich and Greenberg, 1996; Kido et al., 2019). By the age of 24-30 weeks, all TRAMP mice develop PC. With resemblance to human PC, this model is able to produce progressive PC, ranging from prostatic intraepithelial neoplasia (PIN) to invasive adenocarcinoma. TRAMP mice are also suitable for investigating metastatic PC as well as androgen independence. These animals develop metastasis at a high frequency, most commonly with spread to lymph nodes and lung (Gingrich and Greenberg, 1996). In castrated animals, PC is less well differentiated and has a higher rate of metastasis compared to non-castrated mice. Interestingly, androgen-independent tumors have a high tendency to show a neuroendocrine differentiation. This finding does not match with spontaneous human PC where neuroendocrine differentiation is rare. Overall, this animal model is considered appropriate to study the pathobiology of tumor initiation and progression as well as the effect of certain therapeutics (Kaplan-Lefko et al., 2003).

Loss of PTEN

Phosphatase and tensin homolog deleted on chromosome ten (PTEN) is a tumor suppressor gene, which is frequently lost in many types of cancer,

including PC (Cuzick et al., 2013; Wang et al., 1998). Homozygous deletion of PTEN leads to embryonic death in mice. For the development of neoplastic prostate changes, this model consequently requires PTEN heterozygous animals, or alternatively, prostate-specific PTEN knockout (Jiao et al., 2007). Depending on the mouse strain and type of targeted vector, this model varies in its tumor phenotype, including infiltrative growth, the development of metastasis as well as neuroendocrine differentiation after castration (Grabowska et al., 2014). Furthermore, many PTEN loss models have been generated, which include the deletion of additional (often tumor suppressor) genes. Either in combination with other genes or isolated, loss of PTEN mouse models have one major limitation, which is the lack of two highly relevant features for aggressive human PC, which include castration-resistant PC and the development of bone metastases.

Overexpression of MYC

MYC is a oncogenic transcription factor, which is overexpressed in a variety of tumors, including PC (Gurel et al., 2008). In PC, the overexpression of MYC occurs as an early event and is present in more than 75% of PIN (Gurel et al., 2008; Kim et al., 2012). In addition, higher tumor stage tends to go along with higher MYC expression. Based on different promoters, there are two types of murine MYC models, namely Hi-MYC and Lo-MYC. MYC model mice develop PIN in their first 4 weeks of life, with progression to adenocarcinoma at the age of 6 to 12 months in all animals (Ellwood-Yen et al., 2003; Iwata et al., 2010). In contrast to the models based on overexpression of Tag (e.g. TRAMP), PC induced by overexpression of MYC do not show a neuroendocrine differentiation (Koh et al., 2010). MYC-based mouse models have also shown that the expression of the tumor suppressor NKX3.1 is negatively regulated by MYC (Ellwood-Yen et al., 2003; Iwata et al., 2010). Finally, it is important to be aware of the two main limitations of this model, which are the lack of metastasis and failure to produce castration-resistant cancer (Grabowska et al., 2014). Combined with other genetic alterations, e.g. loss of PTEN or p53, this model is however valuable to study PC (Kim et al., 2012).

1.2.8.2 Dogs

Laboratory dogs

In 2012, an orthotopic dog PC (DPC)-1 model was established, which was based on the successful tumor development after orthotopic DPC-1 cell implantation in one dog in 2001 (Anidjar et al., 2012; Anidjar et al., 2001). The DPC-1 cells originally came from a PC which occurred in a 11-year-old male entire Doberman pinscher. This model reliably produces high-grade prostate carcinomas with predominantly micropapillary and cribriform histological patterns. Tumor metastasis are seen in lymph nodes, lung, and less commonly in pelvic bone. DPC-1 cells do express AR, are however insensitive to androgens in vitro (Anidjar et al., 2012). This model may therefore be valuable for studying castration-resistant PC in men.

Another orthotopic canine PC model using cultured canine Ace-1 PC cells was developed in 2013 (Keller et al., 2013). The Ace-1 cell has its origin in a PC from a castrated 8-year-old Labrador retriever. Similar to the DPC-1 model, this model is able to produce tumor metastasis, which occurs in half of the dogs, with spread to lymph nodes and the lung. Another advantage of this model is the histological resemblance to human PC. In contrast to the DPC-1 cells, however, it is important to know that the Ace-1 cells are AR negative, which may be interpreted as a limitation of the model.

Pet dogs

Even though not as common as in men, dogs develop spontaneous PC (Bell et al., 1991; Cornell et al., 2000; Lai et al., 2008a; Teske et al., 2002). Canine PC is a highly aggressive disease with a highly invasive growth as well as a high rate of metastasis to lymph nodes, visceral organs as well as bone. Once diagnosed with PC, the prognosis for the affected dogs is very poor and no curative therapy is currently available. Interestingly, PC in dogs has a tendency to affect castrated dogs, possibly resembling castration-resistant PC in men (Bell et al., 1991; Teske et al., 2002). This disease is not limited to a specific breed and can occur in any size and type of dog. Canine PC shares clinical as well as pathological features with human disease, which supports the dog as animal

model for human PC (Sun et al., 2017). Elderly dogs of 9 to 10 years of age (corresponding to approximately 65-75 years in men) are most commonly affected. Bone metastasis is frequent, and follows a similar distribution pattern as seen in men. Like in affected men, spread to axial sites is two to three times more common than to appendicular skeleton (Cornell et al., 2000). Histologically, canine PC has frequently a heterogeneous appearance, often with two or more types of differentiation in the same tissue section (Cornell et al., 2000). Either in combination or alone, glandular, urothelial, and squamous are the most common morphologies. Considering that canine PC also occurs in surgically castrated dogs, this cancer is interpreted to be androgen-insensitive. This is confirmed by the fact that most PC in dogs lack the expression of AR (Leav et al., 2001). This finding may be interpreted as a limitation of the canine model for the study of the more common, androgen-sensitive type of PC in men. On the other hand, this model may be a valuable, underexploited large animal model for the highly malignant hormone-refractory PC in men.

1.3. Kidney cancer (clear cell carcinoma) in people

1.3.1 Epidemiology

Kidney cancer ranks 12th in global cancer incidence. Renal cell carcinoma (RCC) accounts for approximately 90% of all kidney cancers, and 75% of RCC consist of the subtype clear cell renal cell carcinoma (ccRCC). Until recently, tumor incidence has been increasing, with highest rates in developed countries, including USA and Europe. Since 2012, incidence appears to remain stable. Mortality rates vary between geographic areas, with a tendency to decrease in Western countries (Saad et al., 2019). This tumor has a strong male predominance, has a tendency to occur in Caucasians more than Africans, and most commonly affects the elderly (Feng et al., 2019). For yet uncertain reasons, African-American patients have an increasingly higher incidence rate and poorer overall survival compared to Caucasians (Chow et al., 2013; Lin et al., 2015b). Interestingly, African countries have the lowest incidence rates, but African Americans are especially prone to develop the disease (Chow and Devesa, 2008; Ljungberg et al., 2011). This racial disparity may be explained by

differences in cancer screening and diagnostics, genetic background as well as environment and lifestyle. In addition to race, certain risk factors for RCC have been identified and include obesity, smoking, hypertension and certain genetic mutations (Al-Bayati et al., 2019; Chow and Devesa, 2008; Chow et al., 2000; Hidayat et al., 2017; Hunt et al., 2005; Ljungberg et al., 2011; Macleod et al., 2013; Nam et al., 2019). The association of smoking and the development of RCC is dose-dependent (Hunt et al., 2005). Patients who have been smoking for at least 20 years have a 50% higher risk to suffer from RCC compared to non-smokers. The mechanism by which obesity causes RCC remains poorly understood. Differences in hormone levels, including sex steroids and insulin-like growth factor 1, may play an important role. Hypertension, even if present to only a mild extent, poses a significant risk factor for RCC, possibly via increased levels of angiogenic and other growth factors (Chow et al., 2000). The same is true for an increase in blood pressure over time, independent of the baseline levels. Even though obesity and hypertension may be linked to each other, both pathologies have been identified to be independent risk factors for RCC. Finally, exposure to the ubiquitously present chemical substance trichloroethylene is known to represent a significant risk for developing RCC (Buhagen et al., 2016; Rusyn et al., 2014; Scott and Jinot, 2011). The relative risk ranges between 1.3 and 1.6 depending on the severity of trichoethylene exposure. On the basis of the association between kidney cancer and trichoethylene, which is used as industrial solvent, this substance has been classified as carcinogenic by The International Agency for Research on Cancer (IARC) (Rusyn et al., 2014).

1.3.2 Diagnosis

The majority of RCC are characterized by a late onset of clinical symptoms, and are most commonly detected incidentally during abdominal imaging for other medical conditions, via ultrasound, CT or MRI (Rossi et al., 2018). In patients, where imaging reveals either suspicion of metastatic disease or only a small renal mass, a percutaneous kidney biopsy may be performed before any surgical treatment is attempted (Richard et al., 2015). Core biopsy, which is the

preferred method over fine needle aspiration, bears a low risk of morbidity. Most ccRCC are solitary tumors in the renal cortex, without significant predilection for the right or left kidney. The neoplasia is generally well demarcated, surrounded by a pseudocapsule. By the time patients experience clinical signs, such as hematuria or flank pain, RCC is often already at an advanced stage. Nevertheless, a screening program for ccRCC is currently not available and controversial (Rossi et al., 2018). Regular screening for the disease would allow detecting kidney cancer at an earlier stage, which is prognostically highly significant. When diagnosed at an early stage, RCC may be cured by surgery alone. However, the downside of a screening program include high costs and the potential to over diagnose and over treat slow growing RCC. Proposed screening methods include urine dipstick, biomarkers and imaging (Rossi et al., 2018). Screening for the presence of microscopic hematuria by urine dipstick is not well accepted due to the very low specificity of this test. Currently, urine or serum biomarkers have not yet been established and validated for routine diagnostic work, but several markers have been proposed to have potential as diagnostic tool in the future. Two promising urinary biomarkers with moderate to high specificity and sensitivity are aquaporin 1 (AQP1) and perilipin 2 (PLIN2) (Morrissey et al., 2015; Sreedharan et al., 2014). The use of imaging as a screening method may be feasible, and US has been proposed as the most appropriate imaging modality (Filipas et al., 2003; Mizuma et al., 2002; Rossi et al., 2018). Some of the main advantages of US are the non-invasive and inexpensive nature of this well-established method. The sensitivity of US however is clearly reduced compared to CT and MRI. Nevertheless, CT is not recommended as a screening method due to the high costs and the expected frequent finding of incidental renal or non-renal changes (Rossi et al., 2018; Wernli et al., 2013). Even though not yet established for the general population, a screening program for people with increased risk of RCC is recommended. In addition to the above mentioned risk factors, certain diseases, including van Hippel Lindau disease and end stage kidney disease are strongly associated with the development of RCC. Affected people

should be screened at regular intervals for early detection of RCC (Ljungberg et al., 2019).

1.3.3 Tumor classification, grading and staging

RCC consists of three main subtypes, including papillary, chromophobe and clear cell, based on histomorphological and molecular characteristics (Moch et al., 2016). The term clear cell derives from the histological tumor appearance of this RCC subtype and these tumors are the focus of the current study. The neoplastic cells tend to have a clear cytoplasm due to intracellular lipids and glycogen, which are dissolved by histological processing. Most common histological patterns of ccRCC include solid alveolar and acinar, sometimes with cyst formation.

Grading

Tumor grading is highly relevant for prognosis of RCC and other types of cancer and therefore crucial in the diagnostic workup. RCC, and specifically ccRCC, is graded based on the recently defined four-tiered WHO/ISUP grading system, which has replaced the previously used Fuhrman grading system (Delahunt et al., 2019; Humphrey et al., 2016; Samaratunga et al., 2014; Warren and Harrison, 2018). This grading system defines four grades based on certain nucleolar and other cellular histomorphological features, which are assessed in one high-power field with the highest degree of nucleolar prominence (Delahunt et al., 2011). Grades 1 to 3 are given depending on nucleolar prominence and eosinophilia, whereas tumors with presence of pleomorphic giant cells, sarcomatoid or rhabdoid morphologies correspond to grade 4. In comparison with the previously used Fuhrman grading system, the current WHO/ISUP system has a tendency of downgrading grade 2 to grade 1 tumors (Delahunt et al., 2019). Recently, it has been acknowledged that the presence and extent of tumor necrosis should be incorporated in the current grading system because of its prognostic significance in ccRCC (Delahunt et al., 2013a; Delahunt et al., 2019).

Staging

Similar to other cancers, tumor (TNM) staging is one of the most important prognostic factors (Humphrey et al., 2016; Warren and Harrison, 2018). Referring to the 2010 TNM staging system, the different stages are defined based on tumor size, presence and extent of invasive growth as well as the presence of metastasis. Tumor stages pT1a, pT1b and pT2a are defined by the tumor size, which is assessed macroscopically by measuring the largest tumor diameter (Warren and Harrison, 2018). If tumor invasion into perinephric fat or renal sinus tissue or vascular spaces is present, either grossly or microscopically, tumors are staged as pT3a. Once the inferior vena cava is involved, either below or above the diaphragm, tumor stages pT3b and pT3c are assigned, respectively. Finally, stage pT4 is given once tumor invades the ipsilateral adrenal gland. Regarding the involvement of regional lymph nodes, the TNM staging system includes only two categories, namely pN1 and pN0, for node-positive and node-negative tumors, respectively. Tumors are assigned pM1 as soon as metastatic spread beyond regional lymph nodes is observed.

1.3.4 Genetics

Even though most RCC occur spontaneously, approximately 3 to 5% of these tumors have been estimated to have an inherited genetic background. The von Hippel-Lindau (VHL) familial cancer syndrome is strongly associated with the development of ccRCC, which occurs in around 70% of VHL disease patients (Carlo et al., 2019; Nielsen et al., 2016). Compared to spontaneous tumors, ccRCC in people with VHL syndrome occurs at a much younger age. The VHL disease is characterized by an altered VHL tumor suppressor gene allele. Patients develop ccRCC once the second wild-type allele has undergone spontaneous mutation or is epigenetically downregulated. The same gene is also altered in the majority of spontaneous ccRCC, either by deletion, mutation or epigenetic mechanisms (Gnarra et al., 1994; Kaelin, 2007). Some studies report genetic VHL alterations in as many as 92% of ccRCC (Sato et al., 2013). The function of the gene product, the VHL protein, is to target hypoxia-inducible factor alpha (HIF-α) for degradation under normoxic conditions.

Therefore, genetic mutations leading to the inactivation or lack of the VHL protein causes an accumulation of HIF- α, which further activates a range of growth factors among other proteins. The association of HIF- α and related growth factors with ccRCC tumorigenesis is not clearly understood (Kaelin, 2007). It is most likely that angiogenic and mitogenic effects of the activated growth factors are mainly responsible for the neoplastic cellular transformation (D'Avella et al., 2018). Up to present, a convincing association between VHL status and clinical tumor behavior has not been identified. Apart from VHL gene, other common mutations in ccRCC affect chromatin-modifying and other genes, including BAP-1, PBRM1, SETD2, KMD5C and PIK3CA, which are present in up to 40% of ccRCC (D'Avella et al., 2018; Mitchell et al., 2018). The prognostic and therapeutic significance of these mutations are uncertain, but of great interest due to their potential use as future therapeutics.

1.3.5 Prognosis

Similar to other cancer types, the most important prognostic factor for ccRCC is tumor stage, followed by tumor grade, which includes features such as tumor necrosis, tumor size, and divergent (sarcomatoid/rhabdoid) differentiation (Humphrey et al., 2016). Furthermore, histological subtype as well as age at diagnosis are prognostically significant. Tumor size is negatively correlated with survival, and the risk of death increases continuously with increasing tumor size (Delahunt et al., 2002). RCC with either sarcomatoid or rhaboid differentiation is characterized by a more aggressive clinical behavior, with a 2-fold increased risk of extrarenal tumor growth and distant metastasis in RCC with partial rhabdoid features (Delahunt et al., 2013b; Gokden et al., 2000). Even though controversially discussed, there is convincing evidence that the presence of tumor necrosis in RCC is associated with poorer overall and cancer-specific survival rates as well as recurrence and progression free survival (Zhang et al., 2018a). Compared with papillary and chromophobe RCC, the clear cell subtype tends to have the worst prognosis (Cheville et al., 2003; Delahunt et al., 2013b). For patients with ccRCC, the 5-year CSS rate is less than 70%, whereas the two other RCC subtypes have CSS rates of 86-88% (Cheville et al., 2003). Younger

age at the time of diagnosis is associated with better overall survival (OS) and CSS compared to older age (Cai et al., 2012; Feng et al., 2019). Patients with localized RCC who are younger than 40 years have a 5-year CSS rate of 91% compared to 78% for patients over 40 years of age (Taccoen et al., 2007). When using 55 years as age threshold, the 5-year CSS is 89% and 76% for younger and older patients with RCC, respectively (Jung et al., 2009). Even though of great interest as a diagnostic and potentially therapeutic tool, prognostic biomarkers are currently not applied in clinical practice.

1.3.6 Therapy

Surgery

For localized disease, radical nephrectomy (RN) has long been regarded as the therapy of choice. More recently, however, nephron-sparing surgery (NSS), i.e. partial nephrectomy (PN) or tumor enucleation (TE), has gained attention and is the preferred treatment option for pT1 tumors (Li et al., 2014; Xu et al., 2019). By limiting the amount of resected renal tissue, kidney function may be preserved, which is highly relevant for overall prognosis. In TE, the tumor is excised bluntly, avoiding a visible margin. In contrast to what would be expected, positive margins are not more common in TE compared to RN. Likewise, survival and tumor recurrence rates do not differ significantly between the two methods when assessed in pT1 RCC. TE however has the great advantage of better protecting kidney function when compared to PN or RN. Nevertheless, for both localized as well as higher stage RCC, the therapeutic efficacy of NSS versus RN is however still controversial. In any case, even for RCC of stage 2 and higher, the benefits of preserving renal function when performing PN appear to be greater than the associated morbidity when compared to RN (Vilaseca et al., 2019). An alternative treatment method, which also preserves healthy renal tissue, is cryoablation or other ablation techniques (Hu et al., 2019; Neves et al., 2019). This non-surgical intervention works via freezing and removing neoplastic cells via percutaneous access. When compared with PN, the therapeutic efficacy of ablation treatments in localized tumors remains however controversial (Hu et al., 2019). Some studies

report comparable recurrence free survival rates for both treatment modalities, whereas others demonstrate an increase in cancer-specific mortality in pT1 tumors treated with cryoablation (Pecoraro et al., 2019; Thompson et al., 2015). Nevertheless, it is generally accepted that ablation therapy may be advantageous for patients with multifocal tumors who benefit from reducing surgical interventions.

Systemic (adjuvant and neoadjuvant) therapy

For localized or locally advanced RCC, perioperative systemic, i.e. adjuvant or neoadjuvant, treatment is controversial (Gul and Rini, 2019; Martinez Chanza et al., 2019). In this context, the main aim of an adjuvant therapy is to eradicate potentially non-detected micrometastases and therefore reducing the rate of tumor recurrence and tumor progression, whereas neoadjuvant treatment has the purpose to reduce tumor size before surgery in addition to eradicating micrometastases. Tyrosine kinase inhibitors (TKI), primarily the potent vascular endothelial growth factor (VEGF) inhibitor Sunitinib, and immune checkpoint inhibitors (ICI) are currently the main adjuvant therapeutics of interest for localized RCC (Martinez Chanza et al., 2019). Unfortunately, the results of trials testing their efficacy have mostly been disappointing, and their use remains controversial (Ghali et al., 2019). This is in contrast to rather promising treatment outcomes of ICI and TKI in metastatic RCC (Angulo and Shapiro, 2019; Motzer et al., 2009).

1.3.7 Animal models

With great effort, different ccRCC mouse models have been generated in the last two decades, but so far they all have certain limitations to reproduce the disease on a molecular as well as morphological level (Hou and Ji, 2018). Based on the knowledge that *VHL* gene mutations are frequent in both sporadic and familial ccRCC, the first mouse models were created by inactivating this gene (Gnarra et al., 1997). Isolated inactivation of *VHL* was however insufficient to produce neoplastic changes in the kidneys of heterozygous mice, whereas homozygous animals died already in utero (Gnarra et al., 1997; Haase et al.,

2001; Kleymenova et al., 2004). For this reason, several mouse models were generated by combining *VHL* with one or more other gene mutations, with some promising results. Successful neoplastic transformation of renal tubular cells was achieved in mouse models, which included the inactivation of one or more of the following genes, combined with inactivated *VHL*: *Bap-1*, *Cdkn2a*, *Kif3a*, *MYC*, *p53*, *Pbrm1*, and *Rb1* (Hou and Ji, 2018; Schmidt and Linehan, 2017). Unfortunately, none of these models is however able to produce renal tumors, which sufficiently, either morphologically or molecularly, resemble spontaneous human ccRCC. Reasons for failing to establish a reliable model remain uncertain. Considering the direct relationship between VHL and HIF, a mouse model named TRACK (transgenic cancer of the kidney) has been generated, which is characterized by a mutated, constitutively active *HIF-α*. This model seems to successfully produce certain (pre-)neoplastic features in the kidney, with histomorphological resemblance to human ccRCC. Similar to other ccRCC GEM models, however, the TRACK model appears to be unable to produce fully developed neoplastic disease with convincing resemblance to spontaneous ccRCC (Fu et al., 2011).

2. Aims

The aims of this work were defined separately for the different types of urological cancer, and are as follows:

Pathological and molecular characterization of the canine UC model

i) Identification of epidemiological risk factors for canine UC, in comparison with human disease
ii) Histological characterization and tumor classification of canine UC, based on the 2016 human WHO classification system
iii) Comparison of histological features of canine and human UC, with focus on tumor subtype, stroma, inflammation and necrosis
iv) Assessment of the global transcriptional profile of UC in Scottish and West Highland White terriers, in comparison with human disease
v) Evaluation of the dog as animal model for muscle-invasive BC in people

Pathological and molecular characterization of the canine PCa model

i) Identification of epidemiological risk factors for canine PC, in comparison with human disease
ii) Histological characterization and tumor classification of canine UC, based on the 2016 human WHO classification system
iii) Analysis of the IHC expression of p63 and Uroplakin III in canine PC, in comparison with non-neoplastic prostate tissue
iv) Evaluation of the dog as animal model for high grade PCa in men

Pathological and immunohistochemical evaluation of novel potential therapeutic targets in human PCa specimens

i) Analysis of the IHC expression of KDM7A and KDM5B in human PC

Pathological and molecular investigation of mechanistic contributors to kidney clear cell cancer

i) Histomorphological characterization of kidney and other tissue from TRACK mouse model

ii) Analysis of the immunohistochemical expression of MYC and RBP4 in kidney and other tissue from TRACK mice

iii) Evaluation of the TRACK mouse model for renal carcinoma in people

3. STUDY 1. The dog as an animal model for bladder and urethral urothelial carcinoma: Comparative epidemiology and histology

This study has been published in Oncology Letters in 2018, with the corresponding DOI: 10.3892/ol.2018.8837.

Copyright Declaration: This is an open access article distributed under the terms of the Creative Commons Attribution-NonCommercial-NoDerivs License, which permits use and distribution in any medium including dissertations, provided the original work is properly cited, the use is non-commercial and no modifications or adaptations are made.

Authors' contributions

List of authors (in order as in the published study):

Simone de Brot (SdB), Brian D. Robinson (BDR), Tim Scase (TS), Llorenç Grau-Roma (LGR), Eleanor Wilkinson (EW), Stephen A. Boorjian (SAB), David Gardner (DG), Nigel P. Mongan (NPM)

Contributions:

- SdB contributed to the acquisition and analysis of the epidemiological data (age at the time of tumor diagnosis, sex, neutering status, and dog breed), with support of EW, TS and DG.
- SdB performed the histological examinations (tumor diagnosis, tumor stage and histological subtype, tumor growth pattern, and characterization of main histological features), with support of LGR, BDR and TS.
- SdB performed the statistical analysis (using the software SPSS v.22.0), with support of EW and DG.
- SdB compared the canine data with data available from scientific human literature, with support of SAB, BDR and NPM.
- SdB wrote the manuscript, with support of NPM.

- All authors critically reviewed the manuscript. All authors read and approved the final manuscript.

Background to the published work

UC is one of the top ten most common cancers in people, with comparable incidence rates of approximately 2% of all cancers in both men and dogs (Andreassen et al., 2016; Antoni et al., 2017; Burger et al., 2013; Knapp et al., 2014; Mohammed et al., 2003; Norris et al., 1992). In a previous canine UC study, certain risk factors for developing UC have been identified, including advanced age, female sex, certain dog breeds (Knapp et al., 2014; Norris et al., 1992). These findings, however, primarily derive from one single study and therefore require interpretation with certain caution. More specifically, the relevant study had the following limitations: A relatively low number of studied dogs (n=115) were investigated, only dogs from North America were included, and the data may be outdated due to the sample collection, which was performed more than three decades ago (between 1980 and 1985). Up to date, similar studies, which investigate epidemiological risk factors of canine UC, with a fairly large number of studied dogs and a European residency, are lacking.

In addition to epidemiological features, the gross and histopathological characterization of UC is relevant for tumor diagnosis, prognosis, and therapy (Humphrey et al., 2016). Histologically, human UC is a well described. In contrast, the histological appearance of UC in dogs has only been described in a few studies, which often contain a relatively small number of assessed dogs and a limited range of assessed histological parameters (Patrick et al., 2006).

As it is true for many different cancers, the macroscopic tumor appearance is relevant for UC diagnosis and prognosis. In people, the majority of UC present as a papillary growth, whereas flat or endophytic UC are less common (Sciarra et al., 2004). For human UC, the subgross tumor growth pattern, i.e. papillary versus non-papillary, is known to be of prognostic relevance (Guo et al., 2016; Sciarra et al., 2004). Non-papillary UC has been shown to be associated with worse prognosis in people. Canine UC have been described to either present as papillary or flat tumors (Meuten and Meuten, 2016). Studies, which investigate the macroscopic tumor appearance and its potential prognostic relevance of UC are however lacking in dogs.

UC is well known to have a tendency to undergo divergent differentiation (Amin, 2009; Moch et al., 2016; Zhai et al., 2007). Based on the type and extent of non-urothelial histomorphology, UC are further classified as different variants. The distinction of these tumor subtypes is considered relevant due to their demonstrated differences in tumor prognosis and response to therapy. In dogs, divergent differentiation has been shown to occur (Patrick et al., 2006). However, only few variants of canine UC have been described and their prognostic relevance is uncertain.

For these reasons, the following study has been performed with the aim to better characterize histological and epidemiological features of canine UC. Furthermore, by comparing the canine tumor characteristics with already reported features of human UC, the potential of using the dog as animal model for human UC shall be evaluated. The following work represents one of the largest yet undertaken comparative UC study.

3.1 Abstract

Despite the recent approval of several new agents for patients with metastatic UC, survival in this setting remains poor. As such, continued investigation into novel therapeutic options remains warranted. Pre-clinical development of new treatments requires an animal model that accurately simulates the disease in people. The aim of this study is to evaluate the dog as an animal model for human UC. Two hundred and sixty cases of spontaneous, untreated canine primary urethral and urinary bladder UC were epidemiologically and histologically assessed and classified based on the current 2016 WHO tumor classification system. Canine data was compared with human data available from scientific literature. The mean age of dogs diagnosed with UC was 10.22 years (range 4-15 years), which is equivalent to 60-70 human years. We observed a high correlation of UC diagnosis with female sex (odds ratio [OR] 3.51; 95% confidence interval [CI] 2.57-4.79; p<0.001), surgical neutering (OR 4.57; 95%CI 1.87-11.12; p<0.001), and breed (OR 15.11 for Scottish terriers; 95%CI 8.99-25.41; p<0.001). Based on the 2016 WHO tumor, node and metastasis (TNM) staging system, the primary tumors were characterized as T1 (38%), T2a (28%), T2b (13%), and T3 (22%). Non-papillary, flat subgross tumor growth was strongly associated with muscle invasion (OR 31.00; p<0.001). Irrespective of subgross growth pattern, all assessable tumors were invading beyond the basement membrane compatible with infiltrating UC. Conventional, not further classifiable infiltrating UC was the most common type of tumor (90%), followed by UC with divergent, squamous and/or glandular differentiation (6%). Seven out of the 260 (2.8%) cases were classified as non-urothelial based on their histological morphology. These cases included five (2%) squamous cell carcinomas, one (0.4%) adenocarcinoma and one (0.4%) neuroendocrine tumor. The two most striking common features of canine and human UC included high sex predilection and histological tumor appearance. Our results support the suitability of the dog as animal model for UC and confirm that dogs also spontaneously develop rare UC subtypes and bladder tumors, including plasmacytoid UC and neuroendocrine tumor, which are herein described for the first time in a non-experimental animal species.

3.2 Introduction

BC is the ninth most common malignancy worldwide and the most common cancer involving the urinary system. BC comprises approximately 2% of all cancers, with about 330,000 new BC cases each year globally (Ferlay et al., 2015; Ferlay et al., 2013). The highest incidence rates are observed in highly developed countries, where BC is the fourth and 14th most common cancer in men and women, respectively (Ferlay et al., 2013). Despite ongoing effort to improve therapeutic options, there is still no curative therapy available for metastatic disease. The pre-clinical development of new treatments requires an animal model that accurately simulates the disease in people. Rodent animal models with experimentally induced BC have been shown to be valuable, but their translational relevance has been limited (Ding et al., 2014; John and Said, 2017; Kobayashi et al., 2015). Therefore, well characterized spontaneous BC in companion animals could represent a useful tool to advance the development of improved diagnostics and therapeutics. Indeed dogs develop spontaneous BC, more specifically UC (transitional cell carcinoma), with striking clinical, histopathological and molecular similarities compared to humans (Knapp et al., 2000). Furthermore, companion animals and their owners share the environment, including exposure to carcinogenic components. In addition, other advantages of using spontaneous urinary BC in pet dogs as an animal model for human UC are: (1) reduced use of research animals (2), the shorter lifespan of dogs, relative to people, makes time-efficient clinical studies possible and, (3) dogs show a similar response to therapy used to treat people (Abbo et al., 2010; Arnold et al., 2011; Choy and Fidel, 2016; Henry et al., 2003a; Knapp et al., 2016). Yet one limitation to the use of the dog in preclinical studies of BC has been access to robust clinical and pathologic datasets. For this reason, this study, which is one of the largest yet undertaken comparative study, aims to evaluate the dog as animal model for human UC by comparing the epidemiology and histology of n=260 canine urinary bladder and urethral UC to the data available in literature regarding their human counterpart.

3.3 Material and methods

The study was approved by the University of Nottingham Animal Welfare and Ethical Review Body (AWERB) and the School of Veterinary Medicine and Sciences ethics committees. Informed written consent was obtained from the dog owners upon sample submission. All patient data has been anonymized. The present retrospective study includes archived FFPE tissues from 260 dogs with primary urethral (n=61) or urinary bladder (n=199) carcinomas. All samples were taken from pet dogs living in the United Kingdom (UK) and were originally submitted for diagnostic purposes. Two hundred fifty-nine cases were provided by a private diagnostic pathology laboratory (Bridge Pathology Ltd Bristol, UK) which received the tissue samples between October 2008 and April 2015. One additional case of canine urinary bladder carcinoma which was submitted to the University Nottingham Veterinary Pathology Service in May 2016 was also included. Non-invasive urothelial lesions, including papillomas, were excluded from the study due to the low number of cases in the present dog population. Tissue of canine in situ UC was not available. From the originally retrieved n=265 cases of UC, two cases were excluded due to poor tissue section quality, another two cases due to lack of convincing neoplastic features, and one case due to lack of information about dog breed and age. The following case information was available: age at the time of first tumor diagnosis, sex, neutering status, and dog breed. All canine cases (n=93,862) submitted to the same laboratory within the same time period were used as control population. These control dogs were diagnosed with a wide range of neoplastic and non-neoplastic diseases in various organs and tissues, excluding carcinoma of the lower urinary tract. Hematoxylin and eosin (HE) stained tissue sections of all 260 cases were available which were digitalized (scanner 3DHISTECH Pannoramic 250 Flash III) and assessed using the software 3DHISTECH Case Viewer by a board-certified veterinary pathologist (SdB), with support of a certified human uropathologist (BR) and a second veterinary pathologist (LGR). All cases were histologically assessed for tumor stage and histological subtype, based on the WHO tumor classification system 2016 (Moch et al., 2016). Subgross tumor growth patterns were evaluated

histologically at a low magnification (1 and 2x). Epidemiological and pathological canine data was compared with data available from scientific human literature which was available on PubMed (https://www.ncbi.nlm.nih.gov/pubmed/) in April 2017. Cancer incidence was calculated in percentage (%) for each dog breed (n=60 different breeds). 100% cancer incidence was defined as the total number of dogs of the same breed in the control population. Breeds with incidence rates above average (>0.823%) and with a minimum of n=5 cancer cases were defined as risk breeds. Three different breeds (Scottish terrier, Shetland sheepdog and West Highland White terrier) fulfilled these criteria and were grouped together as 'risk breeds'. 'Non-risk dog breeds' were defined as all dog breeds, including cross breeds, excluding Scottish terriers, Shetland Sheepdogs, and West Highland White terriers. Odds ratios were calculated in order to quantify the risk of dog breed, sex, neutering status with the development of cancer, and in order to quantify the risk of non-papillary tumor growth with muscle-invasive tumor growth. An independent t-test was performed to compare the mean age of risk breeds versus non-risk breeds, of dogs with muscle-invasive versus non muscle-invasive tumor growth, and of dogs with papillary versus non-papillary tumor growth, respectively. Chi-square test was used to test for associations between tumor incidence and dog breed, sex, and neutering status, and to analyze the association of tumor invasive growth with tumor growth pattern, dog breed, and sex. Binary logistic regression analysis was performed in order to identify and weigh risk factors, including dog breed, sex, and neutering. $p<0.05$ was accepted as statistically significant. Statistical analyses were performed using SPSS v.22.0.

3.4 Results

A total of 260 dogs with spontaneous urinary bladder (199/260, 77%) and primary urethral (61/260, 23%) UC were included in this study. Tables 3.1 and 3.2 summarize the main canine epidemiological findings and compare them with the corresponding human data available in the literature.

The mean age of dogs diagnosed with UC was older compared to dogs without UC (10.21 [+/- 2.0, range 4-15] years vs 7.1 [+/- 3.6] (Mean +/- SD, p<0.001). Dog breeds with only 1 case of UC were excluded from any further analysis (leaving 66,317 cases; 222 (0.3%) with UC). In univariate analyses (odds ratio [95% confidence interval], p<0.001), female sex (OR, 3.51 [2.57-4.79]), neutering (OR, 4.57 [1.87-11.12]) and breed (OR 15.11 [8.97-25.41] for Scottish terriers, OR 6.82 [3.01-15.49] for Shetland sheepdogs, and OR 2.79 [1.80-4.35] for West Highland white terriers) were identified as significant predictors of UC (Table 3.1). All remained significant (p<0.001) in multivariate analyses (Table 3.1). In addition, when the three top risk breed dogs were grouped together, they were found to be diagnosed with UC at a significantly younger age (mean 112.14 months [9.35 years], SD 19.16) compared to the group containing 'non-risk dog breeds' (mean 124.69 months [10.39 years], SD 24.74) (p<0.001). This effect was most evident for female neutered Scottish terriers (Figure 3.1). 'Non-risk dog breeds' were defined as all dog breeds, including cross breeds, excluding Scottish terriers, Shetland Sheepdogs, and West Highland White terriers.

All cases were histologically assessed for tumor stage and histological subtype, based on the World Health Organization (WHO) tumor classification system 2016 (Humphrey et al., 2016; Moch et al., 2016). Tumor location, growth pattern and main histological features of the studied dogs are summarized in Table 3.3 together with the equivalent information extracted from the human literature.

Gross tumor location was available for 29/199 (15%) bladder and 10/61 (16%) urethral UC cases. The most common location within the bladder was the neck (14/29, 48%), followed by the trigone (9/29, 28%), cranial (3/29 10%), ventral (1/29, 4%) and dorsal (1/29, 4%) bladder. In 2/29 cases (7%), tumor growth was present in both bladder neck and cranial areas. The location of urethral UC was more common in the distal (8/10, 80%) than in the proximal (2/10, 20%) urethra.

The subgross tumor growth pattern could be assessed in 66/199 (33%) bladder UC cases, which were provided as full transmural tissue sections. Two different

types of subgross growth appearance were recognized, papillary and non-papillary (also referred to as flat). Papillary UC (Figure 3.2A) were equally as common (33/66, 50%) as flat (Figure 3.2B) (33/66, 50%) tumors, with identical female : male ratio of 1 : 1.57 in both growth patterns (21/33, 67% females, 12/33, 33% males). Irrespective of growth pattern, all UC were invading beyond the basement membrane, compatible with infiltrating UC based on the WHO 2016 tumor classification.

When applying the tumor, node and metastasis (TNM) staging system provided by the 2016 WHO classification system (Moch et al., 2016), tumor characterization was limited to the assessment of the primary tumor. Information about the involvement of lymph nodes and presence of distant metastatic spread was not available, which prevented the performance of an overall tumor staging. The extent of tumor infiltration into the bladder wall could be assessed in 64/199 (32%) bladder UC cases which were available as transmural tissue sections. Thirty-eight % (24/64) of cases were limited to the lamina propria mucosae (T1), 28% (18/64) invaded the superficial muscularis propria (T2a), and 13% (8/64) the deep muscularis propria (T2b). A substantial number (14/64, 22%) of UC cases invaded perivesicular tissue (T3). Muscle-invasive growth could be assessed in 76/199 (38%) bladder UC cases. More than two thirds (52/76, 68%) were muscle-invasive tumors, which is compatible with high tumor stage. The tumor growth pattern of muscle-invasive UC could be assessed in 41/52 (79%) cases, and it was more commonly flat (30/41, 73%) than papillary (11/41, 27%). This was in contrasts to the non-muscle-invasive UC, the vast majority of which (22/24, 92%) presented with a papillary growth, with only rare flat tumor growth (2/24, 8%). Non-papillary, flat tumor growth was statistically significantly strongly associated with tumor muscle invasion (OR 31.00, 95% CI 66.24-153.95).

Conventional, not further classifiable infiltrating UC was the most common type of tumor (234/260, 90%), followed by UC with divergent differentiation (15/260, 6%) (squamous [8/260, 3%], glandular [5/260, 2%] or both [2/260, 1%]), and squamous cell carcinoma (5/260, 2%). One case was identified to be a bladder adenocarcinoma (not otherwise specified). Two rare urinary tract

tumors, including primary urethral plasmacytoid UC and neuroendocrine bladder tumor, have been identified in one dog each (Figure 3.3). Eight of the 234 not further classifiable infiltrating UC cases presented with certain characteristic histological features within a low percentage (1 to 20%) of the studied tissue section, including micropapillary and microcystic growth (Figure 3.4), neuroendocrine differentiation as well as the presence of neoplastic cells with plasmacytoid, rhabdoid, signet-ring cell, lipid-rich or glycogen-rich appearance (Figure 3.5). Since the divergent differentiation was however only observed in a minor portion of the examined tumor tissue, these tumors were diagnosed as not further classifiable infiltrating UC and not as UC with divergent differentiation. The urethral plasmacytoid UC was found in a 9-year-old male neutered crossbreed dog with a history of dyschezia and prostate enlargement. The submitted and histologically examined tissue was limited to urethra. Prostate tissue was not available and no further information about the follow-up of this dog was given. The neuroendocrine bladder tumor was diagnosed in a 13-year-old female neutered 7kg crossbreed dog with reported weight loss since a few months and a history of polyuria and polydipsia, pollakisuria, hematuria, and increasing lethargy over a period of less than 2 months. The tumor was diagnosed based on cystoscopy and biopsy. Due to late tumor diagnosis with very advanced disease and poor prognosis, the dog's owner decided against surgery and chemotherapy and elected euthanasia 3 weeks after the tumor diagnosis was made. Consent for a full post-mortem examination was given and confirmed the primary bladder tumor with metastases in lung, medial iliac and sacral lymph nodes.

Finally, non-conventional UC was associated with muscle-invasive tumor growth ($p<0.001$), being compatible with higher tumor stage.

3.5 Discussion

The present study confirms the previously observed striking epidemiological and pathological similarities between canine and human UC (Knapp et al., 2000; Knapp et al., 2014). The number of comparative human and canine BC studies available in the literature is still very low, with the most relevant studies being

done in North America (Decker et al., 2015; Dhawan et al., 2015; Norris et al., 1992; Patrick et al., 2006; Shapiro et al., 2015; Valli et al., 1995). The present study is the largest study with comparative epidemiology and histology, which includes 260 cases. It demonstrates that similar to the situation in people, canine UC mainly affects elderly patients. The mean age of dogs diagnosed with UC was over 10 years, which is equivalent to approximately 60 to 70 human years (Patronek et al., 1997), compatible with the mean age of people diagnosed with UC. Both canine and human UC have a strong sex predilection. While men are at a three-fold higher risk to develop UC compared to women, the situation is exactly the opposite in dogs. Similar to the situation in people, the reason for the sex predisposition is unknown in dogs. Behavioral, anatomic, physiological and hormonal gender differences have been discussed, but remain speculative (Dietrich et al., 2011; Prizment et al., 2007). It is important to take into account that most of the dogs in the present study were surgically castrated which could potentially have contributed to the observed female predisposition for developing UC. Indeed, neutering appeared as a risk factor for UC for both female and male dogs in the present and previous studies (Knapp et al., 2000). Interestingly, a similar phenomenon can be seen in women with a history of bilateral oophorectomy, who have a higher risk to develop UC (Dietrich et al., 2011; Prizment et al., 2007). Given that castration causes a change in the level of sex hormones and their receptors, these proteins likely play a major role in the carcinogenesis of UC. Previous studies have shown that reduced androgen receptor and increased estrogen receptor-beta expression are associated with higher tumor stage and grade, respectively (Boorjian et al., 2004; Kauffman et al., 2013; Miyamoto et al., 2012; Shen et al., 2006; Tuygun et al., 2011).

Another remarkable feature of canine UC is its high predisposition for certain dog breeds (Knapp et al., 2014; Norris et al., 1992), which we could confirm in our study. Dogs of the same breed are genetically closely related and can be compared to related human families. The Scottish terrier has been previously shown to be the breed with the highest risk (up to over 20-fold) to develop UC (Knapp et al., 2014; Norris et al., 1992). Present results confirm this

observation, which raises high suspicion of a strong genetic component of UC in certain dog breeds. Interestingly, the three dog breeds with highest risk to develop UC were significantly younger at the time of tumor diagnosis, compared to other dog breeds. The age difference was just over one year, which would be equivalent to approximately 7 human years (Patronek et al., 1997).

Pathologically, canine and human UC are very similar, both grossly and histologically. UC affects most commonly the urinary bladder in both people and dogs and represents the most common (over 90%) type of BC in both species. The lateral and posterior wall are the most common sites of UC in people (Sciarra et al., 2004; Stephenson et al., 1990; Xiao and Rashid, 2015), whereas dogs in our and previous studies tend to have UC within the neck and trigone area (Fulkerson and Knapp, 2015; Knapp et al., 2000). Reasons for the difference in preferred bladder subsites of UC between men and dogs are not known, but they may be due to the different orientation of the bladder within the body, leading to different intravesical urine flow. The prognostic significance of the different tumor bladder subsites is reported with some conflicting results, but involvement of neck or trigone appears to be associated with higher tumor stage and worse prognosis in people (Stephenson et al., 1990; Xiao and Rashid, 2015). This could potentially explain the higher UC tumor stages in dogs compared to men.

The vast majority, between 80 and 90%, of human UC grow papillary (Sciarra et al., 2004). Non-papillary (flat or endophytic) growth is much less common in people. This is in contrast to the findings of the here studied canine tumors which presented with an equal number of papillary and flat tumors. Interestingly, non-papillary growth has been demonstrated to be associated with higher tumor grade, muscle invasion and poor prognosis in people (Guo et al., 2016; Sciarra et al., 2004). The studied canine data confirms this observation.

Histologically, the present study demonstrates that UC of people and dogs are strikingly similar and directly comparable. Non-conventional UC are less common in both species and most frequently comprise UC with divergent,

glandular and/or squamous, differentiation. Other UC subtypes are rare in both species, but important to recognize given their association with poor prognosis (Amin, 2009). In the studied canine population, one case of primary urethral plasmacytoid UC in a male neutered dog, and one case of neuroendocrine tumor in the bladder of a female neutered dog were identified. Both tumors were high grade with evidence of intravascular neoplastic growth in the plasmacytoid UC and widespread lymph node and distant metastases in the neuroendocrine tumor, respectively. Neither of these two tumor types have been described in any non-experimental animal species and are herein reported for the first time as spontaneous tumors in an animal species. Other histological features, including micropapillary and microcystic growth, and rhabdoid, signet-ring cell, lipid-rich and glycogen-rich appearance of neoplastic cells were observed in a small proportion of the herein studied canine cases. These histological tumor features are poorly described in animals, but are well known features of UC in people (Amin, 2009; Humphrey et al., 2016; Zhai et al., 2007). These results therefore further support the value and suitability of the dog as animal model for UC in people.

In conclusion, canine and human UC are epidemiologically and pathologically directly comparable, which promotes the dog as a valuable animal model. Canine UC has an extraordinarily high predisposition for certain genetically closely related dog breeds which suggests a strong genetic component which needs further investigation. Female surgically neutered dogs are at highest risk to develop UC which leads to the speculation that sex hormones are crucial in the carcinogenesis of UC. Given the typically high tumor grades in dogs, canine UC appears to mimic the malignant muscle-invasive form of UC in people which is known to lack a well-established animal model that is so urgently needed to discover new therapeutic options. Finally, rare urinary tract tumors, including plasmacytoid UC and neuroendocrine tumor, occur spontaneously in dogs and are herein described for the first time in a non-experimental animal species.

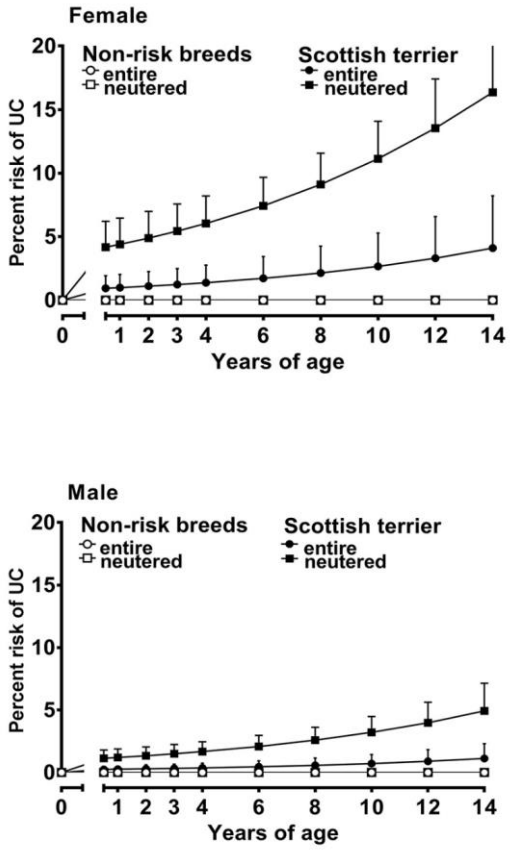


Figure 3.1. The effect of sex, neutering, age, and dog breed on cancer incidence. The risk of UC in Scottish terriers increases with age. This effect is strongest in female neutered dogs. Non-risk breeds are defined as all dog breeds, including cross breeds, excluding Scottish terriers, Shetland sheepdogs, and West Highland White terriers. Error bars indicate the standard errors of the mean (SEM).

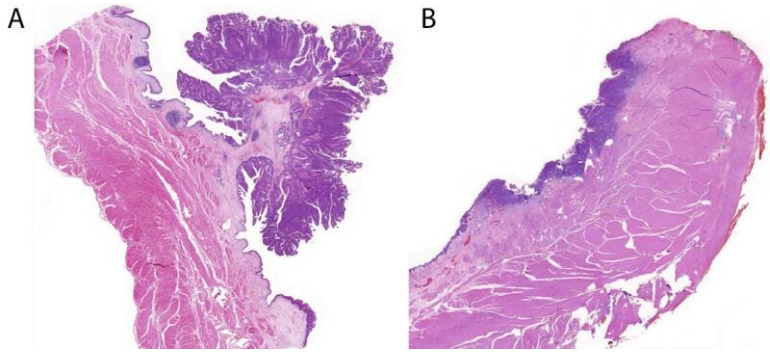


Figure 3.2. Microphotograph of UC in the urinary bladder of two dogs. Tumor growth is papillary in a 6-year-old female entire giant schnauzer (A) and flat in an 11-year-old male neutered Cavalier King Charles spaniel (B), respectively. Hematoxylin and eosin stain. Magnification x3 (A), x4 (B).

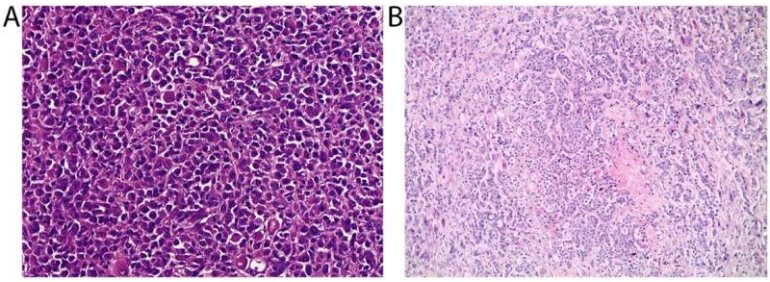


Figure 3.3. Microphotograph of two rare tumor variants in two dogs. A) Primary urethral plasmacytoid UC in a 9-year-old male neutered crossbreed dog. Round anaplastic cells grow in a sheet-like discohesive pattern. B) Neuroendocrine carcinoma in the urinary bladder of a 13-year-old female neutered crossbreed dog. Highly anaplastic cells form small cell nests and trabecules. Hematoxylin and eosin stain. x300 (A), x100 (B).

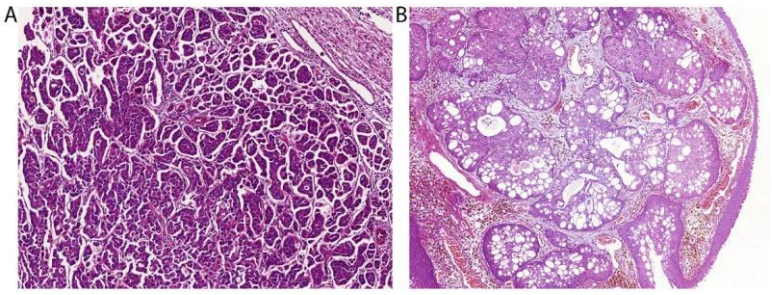


Figure 3.4. Microphotograph of UC with different histological growth patterns in the urinary bladder of two dogs. A) Micropapillary growth in a 10-year-old female neutered lurcher. B) Microcystic growth in a 12-year-old male neutered miniature pinscher. Hematoxylin and eosin stain. x100 (A), x50 (B).

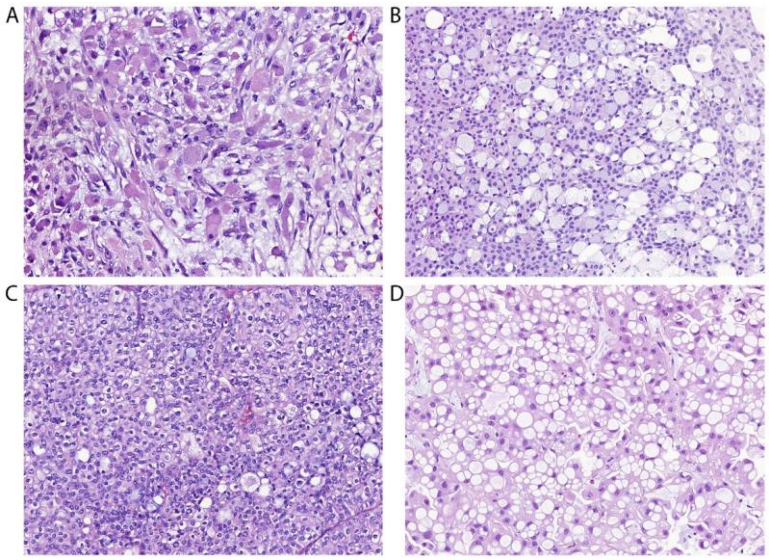


Figure 3.5. Microphotograph of UC with different cellular features in the urinary bladder of four dogs. A) Rhabdoid features in a 9-year-old female Labrador retriever; B) Presence of signet ring cells in a 12-year-old female neutered Labrador retriever; C) Glycogen rich areas in a 10-year-old male Jack

Russell terrier; D) Lipid rich areas in a 9-year-old female neutered West Highland White terrier. Hematoxylin and eosin stain. x300 (A), x200 (B-D).

	Absolute numbers	Prevalence (%)	Univariate OR	95% CI	P value	Multivariate OR	95% CI	P value
Female sex			**3.51**	2.57-4.79	<0.001	**2.92**	2.17-3.91	<0.001
With UC	170	77						
Without UC	31,243	48						
Neutering			**4.57**	1.87-11.12	<0.001	**3.75**	1.85-7.60	<0.001
With UC	166	75						
Without UC	37,054	88*						
Breed								
Scottish terrier			**15.11**	8.99-25.41	<0.001	**19.51**	11.48-33.16	<0.001
With UC	16	7						
Without UC	338	0.5						
Shetland sheepdog			**6.82**	3.01-15.49	<0.001	**12.33**	5.35-28.40	<0.001
With UC	6	3						
Without UC	268	0.4						
West Highland white terrier			**2.79**	1.80-4.35	<0.001	**3.30**	2.03-5.36	<0.001
With UC	22	10						
Without UC	2,504	4						

Table 3.1. Risk factors for UC in the studied dog population. Female sex, neutering and certain dog breeds were identified as risk factors by univariate and multivariate regression analysis.*Note that neutering status was unknown in 23,997 (36%) of cases

Abbreviations: CI: Confidence interval; OR: odds ratio; UC: urothelial carcinoma

	Canine UC (Present study)	Human UC (Literature)	Significance
Age	Mean: 10.22 years (equivalent to 60-70 human years)	Mean: 69-71 years (Madeb and Messing, 2004)	Mean age at UC diagnosis is comparable between people and dogs
Dog breed/ethnicity	Three breeds are highly predisposed to develop UC: 1) Scottish terrier (**OR 15.11**) 2) Shetland sheepdog (**OR 6.82**) 3) West Highland White terrier (**OR 2.79**)	White people are predisposed for UC (two fold risk) Black people are associated with higher-stage UC and reduced survival (Hankey and Myers, 1987; Lee et al., 2006; Yee et al., 2011)	Certain human ethnic groups and dog breeds have a high predisposition to develop UC Risk dog breeds with UC are significantly younger at the time of diagnosis compared to non-risk breed dogs with UC
Sex	<u>Incidence</u> Strong **female** predominance (**OR 3.51**) 195/260 (**75%**) females 65/260 (25%) males <u>Prognosis</u> Generally very poor (68% muscle-invasive at first tumor diagnosis)	<u>Incidence</u> Strong **male** predominance (75%) Ratio male : female = 3-4:1 <u>Prognosis</u> Women have poorer survival rate (56% 5-year survival) compared to men (68% 5-year survival) (Ferlay et al., 2015; Ferlay et al., 2013; Tracey et al., 2014)	In contrast to people, female dogs have an over three times higher risk to develop UC compared to males Female sex is associated with poor prognosis in both human and canine patients

Surgical castration (neutering)	<u>Females:</u> 149/195 (**77%**) neutered 3/195 (2%) entire 43/195 (22%) unknown <u>Males:</u> 41/65 (**63%**) neutered 4/65 (6%) entire 20/65 (31%) unknown <u>Control population:</u> 51,190/93,863 (55%) neutered 7,632/93,863 (8%) entire 35,041/93,863 (37%) unknown	Sex hormones and their receptors play a crucial role in UC development and progression Surgical castration in women increases the risk of developing UC (Dietrich et al., 2011; McGrath et al., 2006; Prizment et al., 2007)	Surgically neutered dogs have a four times higher risk to develop UC compared to entire dogs Surgical castration in women and female dogs is a risk factor for UC development Note: Surgical castration is a routine procedure in dogs (55% of our control dogs are neutered)

Table 3.2. Comparison of epidemiological factors of canine and human UC.

Abbreviations: OR: odds ratio; UC: urothelial carcinoma

	Canine UC (Present study)	Human UC (Literature)	Significance
Localization/subsite	191/260 **(74%) bladder** 61/260 (23%) urethra 8/260 (3%) bladder with extension into proximal urethra 14/29 **(48.28%) bladder neck,** 9/29 **(27.59%) trigone,** 3/29 (10.34%) cranial bladder/dome, 2/29 (6.90%) bifocal (bladder neck and cranial), 1/29 (3.45%) ventral bladder, 1/29 (3.45%) dorsal 8/10 **(80%) distal urethra** 2/10 (20%) proximal urethra	Bladder UC is more common than urethral UC (2% versus <1% of all malignancies) <u>Bladder</u> Bladder neck and trigone involvement is associated with higher tumor grade and worse prognosis <u>Urethra</u> Mostly proximal location in men and distal in women (Annan et al., 2017; Dayyani et al., 2014; Gakis et al., 2013; Kobayashi et al., 2014; Reis et al., 2011; Sciarra et al., 2004; Stephenson et al., 1990; Sui et al., 2017; Svatek et al., 2014; Swartz et al., 2006; Xiao and Rashid, 2015; Zhou et al., 2012)	UC is more common in urinary bladder than urethra in both people and dogs Bladder neck involvement is associated with poor prognosis Urethral UC is more common in distal portion in women and female dogs
Growth pattern	<u>Papillary</u> 33/66 (**50%**) T1 (n=22), T2a (n=9) <u>Non-papillary (flat)</u> 33/66 (**50%**) T1 (n=2), T2a (n=9), T2b (n=6), T3 (n=13) Non-papillary UC are over 30 times more likely to be muscle-invasive compared to papillary UC (**OR 31.00**)	Non-papillary UC are more likely to grow more invasive (74% muscle-invasive) compared to papillary UC (Guo et al., 2016; Kern, 1984; Sciarra et al., 2004; Terada, 2013)	Non-papillary growth is associated with higher tumor grade, muscle invasion and poor prognosis in both people and dogs

Muscle invasion	<u>Muscle-invasive</u> 52/76 (**68%**) - 30/52 (58%) non-papillary (flat) - 11/52 (21%) papillary - 11/52 (21%) unknown <u>Non-muscle-invasive</u> 24/76 (**32%**) - 22/24 (92%) papillary - 2/24 (8%) non-papillary (flat)	Women suffer from advanced tumor stages compared to men (Babjuk et al., 2013; Mungan et al., 2000; Tracey et al., 2014)	Tumor grade is typically higher in canine compared to human UC High grade, muscle-invasive UC is more common in female than in male in both human and canine patients
Tumor stage at first diagnosis	24/64 (38%) T1 18/64 (28%) T2a 8/64 (13%) T2b 14/64 (22%) T3	At the time of first tumor diagnosis, the majority (70-80%) of UC are non-invasive or early invasive (Amin and Tickoo, 2016; Babjuk et al., 2013; Ferlay et al., 2015)	At first tumor diagnosis, tumor stage is typically higher in canine compared to human UC
Tumor classification	234/260 **(90%) UC** 15/260 (6%) UC with divergent differentiation 5/260 (2%) SCC 1/260 (0.4%) adenocarcinoma 1/260 (0.4%) plasmacytoid UC 1/260 (0.4%) neuroendocrine tumor	90% UC 5% SCC and adenocarcinoma 5% other (Amin and Tickoo, 2016)	UC is the most common type of bladder cancer in both people and dogs with comparable frequencies Tumors with squamous or glandular differentiation are the second most common type of urothelial tumors in both people and dogs. Other variants of UC are rare in both species

Table 3.3. Comparison of gross and histopathological features of canine and human UC.

Abbreviations: OR: odds ratio; SCC: squamous cell carcinoma; UC: urothelial carcinoma

4. STUDY 2. A fibromyxoid stromal response is associated with muscle invasion in canine urothelial carcinoma

This study has been published in the Journal of Comparative Pathology in 2019, with the corresponding DOI: 10.1016/j.jcpa.2019.04.003.

Copyright declaration: As the author of this Elsevier article, you retain the right to include it in a thesis or dissertation, provided it is not published commercially. Permission is not required, but please ensure that you reference the journal as the original source. For more information on this and on your other retained rights, please visit: https://www.elsevier.com/about/our-business/policies/copyright#Author-rights

Authors' contributions

List of authors (in order as in the published study):

Simone de Brot (SdB), Llorenç Grau-Roma (LGR), Corazon Stirling-Stainsby (CSS), Martina Dettwiler (MD), Franco Guscetti (FC), Daniela Meier (DM), Tim Scase (TS), Brian D. Robinson (BDR), David Gardner (DG), Nigel P. Mongan (NPM)

Contributions:

- SdB contributed to the acquisition and analysis of the epidemiological data (age at the time of tumor diagnosis, sex, neutering status, and dog breed), with support of CSS, MD, FC, DM and TS.
- SdB performed the histological examinations (tumor diagnosis, invasive growth and histological tumor subtype, characterization of tumor inflammation, stroma and necrosis), with support of LGR, CSS, MD, FC, DM, BDR and TS.
- SdB performed the statistical analysis (using the software SPSS v.24.0), with support of CSS and DG.

- SdB compared the canine data with data available from scientific human literature, with support of CSS, BDR and NPM.
- SdB wrote the manuscript, with support of NPM.
- All authors critically reviewed the manuscript. All authors read and approved the final manuscript.

Background to the published work

Canine UC comprises approximately 2% of all cancers in dogs and is a well-known malignancy among veterinary practitioners and pathologists. The cytological and/or histological diagnosis is generally straightforward (Meuten and Meuten, 2016). This is essentially true for advanced tumors where histological features of malignancy are usually evident and for cancers with clinically confirmed location in the urinary bladder. The histopathological diagnosis is however more challenging in cases of low-grade UC, or when the neoplastic tissue samples have been collected from other organs than the bladder, including the prostate.

Reported histological description, including characteristic UC-specific features, primarily focus on cytomorphological parameters of the neoplastic cells. In contrast, histomorphology of tumor stroma, as well as other potentially relevant features for cancer diagnosis and prognosis, such as tumor necrosis and inflammation, are poorly described in dogs. Studies, which specifically describe tumor stroma of canine UC are rare. Most knowledge about UC stroma derives from published work dating back to 1995, which included 107 dogs with UC (Valli et al., 1995). In this study, the stroma was described to be of variable density, ranging from fine fibrovascular to desmoplastic. Furthermore, the same work pointed out that the stroma may potentially be important for prognosis even though this was only speculated. To date, a prognostic role for the tumor stroma was not demonstrated in canine UC.

Tumor inflammation, which is known to have prognostic relevance in cancer, including human UC (Hodgson et al., 2018; Mihatsch et al., 1979), has been poorly described in dogs. Knowledge about the quality and frequency of tumor inflammation in UC remains poor. The same work (Valli et al., 1995), also assessed the inflammatory component of canine UC. In Valli and colleagues' study, a lymphocytic, tumor-associated inflammatory response was reported to be common. In addition, there was speculation that a possible association between the quality and quantity of the tumor stroma and the inflammation

exists, potentially with prognostic relevance. So far, tumor inflammation could not be confirmed to have a prognostic value in canine UC.

The lack of knowledge about certain highly relevant tumor features, including stroma and inflammation, in canine UC motivated the following study. The following aims were defined: i) to histologically assess and characterize a large cohort of canine UCs, with emphasis on tumor stroma, inflammation and necrosis, and ii) to assess possible associations between these features and the available epidemiological data as well tumor invasive growth. The following work represents the largest reported canine comparative histological UC study.

4.1 Abstract

Canine UC is the most common type of cancer of the lower urinary tract and tends to affect elderly neutered female dogs, with a high predisposition for Scottish terriers. Tumor stroma, inflammation and necrosis are poorly characterized in canine UC and their role as prognostic factors is unknown. The aims of this study were to (1) assess histologically 381 canine UCs, with emphasis on myxoid tumor stroma, inflammation and necrosis, and (2) assess possible associations between these features and the available epidemiological data as well as bladder wall muscle invasion. In 103 of 381 (27%) of cases, the stroma was mixed collagenous and myxoid (fibromyxoid), which was strongly associated with invasive growth of muscle ($p < 0.0001$). Peritumoral and intratumoral inflammation was present in 308 of 345 (89%) and 287 of 381 (75%) of cases, respectively, and was mostly mild and lymphoplasmacytic. One hundred and fifteen of the 381 (30%) cases showed a variable eosinophilic inflammation, and 58 of 381 (15%) presented with formations of one or several lymphoid follicles. Twenty-four percent (91 of 381) of cases had tumor necrosis, which was typically mild. In 83 of 91 (91%) of cases, the necrosis was comedo-like. Moderate to severe tumor necrosis was associated with the presence of moderate to predominant fibromyxoid tumor stroma ($p < 0.02$). The results of this study indicate that fibromyxoid stroma is common in canine UC and is a strong indicator for invasive growth of muscle, which is consistent with a poor prognosis. Based on histomorphology, tumor necrosis in canine UC is best described as comedonecrosis.

4.2 Introduction

Urothelial (transitional cell) carcinoma is the most common cancer of the lower urinary tract in man and dogs (Dy et al., 2017; Knapp et al., 2014; Mutsaers et al., 2003; Norris et al., 1992). Canine UC most commonly affects elderly neutered female dogs, with a strong predisposition for Scottish terriers (de Brot et al., 2018; Knapp et al., 2014; Norris et al., 1992). At the time of diagnosis, affected dogs typically present with advanced disease and options for curative therapy are often limited (Abbo et al., 2010; Boria et al., 2005; Henry et al.,

2018). In order to improve therapy, and therefore the prognosis of UC affected dogs, a genetic and morphological tumor characterization, ideally on an individual basis, is crucial. When assessing the morphology of urothelial, or any other type of, tumors, features such as tumor stroma, inflammation and necrosis need to be included, due to their potential importance in tumor prognosis and response to therapy (Hodgson et al., 2018; Inoue et al., 2017; Samaratunga et al., 2005; Wang et al., 2015). In veterinary medicine, the stroma present in UC is characterized poorly, and is typically described as variably dense, fine fibrovascular to desmoplastic (Valli et al., 1995). In man, conventional UC is characterized by a desmoplastic tumor stroma (Samaratunga et al., 2005). Other, much less common stromal responses, reported only in people, include a myxoid and pseudosarcomatous reaction (Cox et al., 2009; Harik et al., 2006; Ro et al., 1993; Tavora and Epstein, 2009). Significant myxoid stroma can be seen in sarcomatoid UC, in UC with a pseudosarcomatous stromal response, and in rare cases of UC with abundant myxoid stroma (Mahadevia et al., 1989) (Cox et al., 2009; Ikegami et al., 2000; Sanfrancesco et al., 2016; Tavora and Epstein, 2009). A pseudosarcomatous stromal reaction is uncommon in the lower urinary tract and is characterized by the presence of plump, activated fibroblasts, associated with myxoid changes and increased cellularity (Mahadevia et al., 1989; Young et al., 1988). This type of stromal response has been reported in benign and malignant human urinary tract lesions, and occurs spontaneously, in response to trauma or tumor treatment, or in association with neoplasia (Ambrosini-Spaltro and Melissari, 2011; Harik et al., 2006; Hughes et al., 1991; Pearson et al., 1989; Vasilakaki et al., 2014).

Tumor inflammation is a well-known phenomenon, which has been studied extensively in various human tumors (Mantovani et al., 2008). In human UC, inflammation can play a prognostic role (Hodgson et al., 2018; Inoue et al., 2017; Offersen et al., 2002; Samaratunga et al., 2005). A mild, predominantly lymphoplasmacytic, intratumoral or peritumoral inflammation is a common finding in human and canine UC (Inoue et al., 2017; Mihatsch et al., 1979; Offersen et al., 2002; Samaratunga et al., 2005). The prognostic significance of

tumor inflammation in UC is controversial, but studies suggest that prominent inflammation is associated with better prognosis in people (Hodgson et al., 2018; Offersen et al., 2002). In this context, cancer-associated inflammation may be interpreted as evidence for antitumor immunity.

Tumor necrosis is widely accepted as a poor prognostic factor in various cancers. In general, tumor necrosis is understood to represent increased intratumoral hypoxia due to rapid cell turnover (Caruso et al., 2012; Hodgson et al., 2018). In human UC, the presence and extent of tumor necrosis has been shown to be associated with worse prognosis (Langner et al., 2006; Lee et al., 2007; Ord et al., 2007; Soave et al., 2015; Zigeuner et al., 2010). Where available, histological description of the necrosis in UC was consistent with coagulative necrosis (Langner et al., 2006; Ord et al., 2007; Zigeuner et al., 2010). One of these studies included a morphological variant of coagulative necrosis (i.e. comedo necrosis), in their histological assessment (Ord et al., 2007). By definition, comedo-type necrosis is characterized by the presence of well-circumscribed epithelial nests containing central necrotic material (Caruso et al., 2014).

In a previous study, we assessed epidemiologically and histologically 260 canine UCs (de Brot et al., 2018). In that population, elderly neutered female Scottish terriers were at highest risk for developing UC. The histological assessment included subgross tumor growth (papillary versus non-papillary), muscle-invasive growth and histological tumor classification. Tumor stroma, inflammation and necrosis were not specifically assessed.

Given the human literature and the lack of studies which characterize canine UC histologically, the aims of the present study were: (1) to histologically assess and characterize 381 canine UCs, with emphasis on myxoid tumor stroma, inflammation and necrosis, and (2) to assess possible associations between these features and the available epidemiological data as well as muscle invasion.

4.3 Material and methods

Samples

The present retrospective study includes archived formalin-fixed and paraffin wax-embedded tissues from 381 dogs with primary urinary bladder (n = 302), urethral (n = 77) or renal pelvic (n = 2) carcinomas, which were submitted between 1989 and 2016, to four different institutions located in the UK (n = 260; Bridge Pathology Ltd., Bristol, UK) and Switzerland (n = 121; University of Zurich; University of Bern; Zyto-Histo Diagnostics, Freienstein). The following case information was available: age at the time of tumor diagnosis, sex, neutering status and dog breed. No follow-up data were available.

Histology

HE-stained tissue sections from all 381 cases were available as both glass and digital (scanner 3DHISTECH Panoramic 250 Flash III; UK) or only glass (Switzerland) slides. The samples were assessed histologically by a board-certified veterinary pathologist (SdB), with support of a certified human uropathologist (BR) and five certified veterinary pathologists (LGR, MD, FG, DM and TS). All cases were classified for tumor subtype according to the WHO human tumor classification system (Humphrey et al., 2016). On all cases, semiquantitative assessment of peritumoral and intratumoral inflammation and tumor necrosis was performed as follows: 0, absent; 1, focal mild; 2, multifocal mild; 3, multifocal moderate; 4, multifocal severe or diffuse. The degree of severity was defined as follows (percentage of affected tissue per tissue section): for inflammation as mild, <10%; moderate, 10–30%; or severe, >30%; and for necrosis as mild, <5%; moderate, 5–20%; or severe, >20%.

Cases with peri- and/or intratumoral inflammation were assessed for the presence of lymphoid follicles (0, none; 1, 1 follicle; 2, 2–3 follicles; 3, >3 follicles), and number of eosinophils per 1 and 10 high power fields (HPF). For this purpose, HPFs with the highest number of eosinophils were selected. A HPF was defined as 0.237mm2 (×40 objective and ×10 ocular with field number 22) following the recommendations by Meuten et al. (Meuten et al., 2016). Cases with tumor necrosis were estimated for the presence of comedo-like necrosis,

and calculated as % of total necrosis (area percentage) (0, absent; 1, <10%; 2, 10–50%; 3, >50%). For all cases, a semiquantitative assessment of fibromyxoid tumor stroma was performed as follows: 0, absent; 1, focal mild; 2, multifocal mild; 3, multifocal moderate; 4, predominant. The degree of severity was defined as follows (percentage of fibromyxoid stroma within the total tumor stroma per tissue section): mild, <10%; moderate, 10–50%; predominant, >50%. Fibromyxoid stroma was defined as a variably dense mixed collagenous and myxoid stroma, irrespective of the extent and distribution of the two components. The fibromyxoid stroma was assessed on HE-stained tissue sections. In order to confirm both the myxoid and collagenous stromal component, serial sections from seven representative cases were stained with Alcian blue and Masson's trichrome stains. Cases with partial or full-thickness tunica muscularis (137 of 381) were assessed for muscle-invasive tumor growth. Muscle invasion was defined as tumor invasion into any level of the muscularis propria.

Statistics

Breed predisposition and the risk of the other available epidemiological factors were assessed statistically following previously reported criteria (de Brot et al., 2018). The Chi-square test was used to test for associations between tumor muscle invasion, tumor necrosis, fibromyxoid tumor stroma, peri- and intratumoral inflammation, and squamous and/or glandular differentiation of the tumor. P <0.05 was accepted as significant. Statistical analyses were performed using SPSS v.24.0 (IBM Corp., Armonk, New York, USA).

4.4 Results

In a previous study (de Brot et al., 2018), we reported the epidemiological data from 260 out of the current 381 cases. The additional cases (n = 121) included in the present study confirmed the previously reported predisposition for elderly neutered female Scottish terriers. Assessing all 381 cases, Scottish terriers were significantly younger (mean 9.04 + 1.7 years) at the time of tumor diagnosis, when compared with all other dog breeds grouped together (mean

10.27 + 2.2 years) ($p < 0.01$). The same effect was seen in male dogs (mean 9.78 + 2.4 years) when compared with female dogs (mean 10.32 + 2.1 years). A more detailed summary of the epidemiological data from the dogs included in the study is presented in Table 4.1.

Table 4.2 details the primary tumor location, tumor type and subtype, and muscle invasion of the studied cases. Urinary bladder was the primary tumor location in the majority (79%) of cases and UC was (88%) the most common type of tumor. Squamous differentiation, either partially in cases with UC (n = 22), or diffusely in cases with squamous cell carcinoma (SCC; n = 7), was present in 29 of 381 (8%) cases. Glandular differentiation was seen in 13 of 381 (3%) UCs and was diffuse in one case, the latter being consistent with primary bladder adenocarcinoma. Muscle invasion, defined as tumor invasion of any level of the tunica muscularis of the bladder or urethra, was common, and was present in two thirds of all assessable tumors.

Table 4.3 gives results for the presence of fibromyxoid stroma, inflammation and necrosis of all studied tumors. The tumor stroma was fibromyxoid in 27% of cases, being moderate to severe (i.e. affecting ≥10% of the total tumor stroma per tissue section) in two thirds of the cases. The fibromyxoid stroma was characterized typically by a dense fibrous stroma with variable multifocal to coalescing accumulations of intercellular, myxomatous substance (Figures 4.1 and 4.2). The presence of fibromyxoid stroma was strongly associated with tumor muscle invasive growth ($p < 0.0001$). Tumors with evident (5–100% of the tumor tissue section) squamous or glandular differentiation were associated with the presence of moderate to predominant fibromyxoid stroma. This association was stronger in tumors with glandular ($p < 0.0001$) compared with squamous differentiation ($p = 0.005$). Inflammation, peritumoral (including tumor front) as well as intratumoral, was common and seen in 89% and 75% of cases, respectively. The inflammation was predominantly lymphoplasmacytic, multifocal to coalescing, and typically mild. Almost one third of all cases (115 of 381; 30%) showed a variable, ranging from mild to severe, peri- and/or intratumoral infiltration with eosinophils (Fig. 4.3). Fewer cases (58 of 381;

15%) presented with formations of one or several lymphoid follicles, typically located in peritumoral tissue (Fig. 4.4). Moderate to severe intratumoral and peritumoral inflammation was associated with squamous ($p < 0.04$) and glandular ($p = 0.001$) differentiation, respectively. Moderate to severe peritumoral inflammation was associated with moderate to severe intratumoral inflammation ($p < 0.0001$). Twenty-four percent of all cases had variable tumor necrosis, which was typically mild and multifocal to coalescing (Table 4.3). In the majority (91%) of cases, the necrosis was comedo-like (Fig. 4.5). Moderate to severe tumor necrosis was associated with the presence of moderate to predominant fibromyxoid tumor stroma ($p < 0.02$). No other significant associations were observed between the different studied parameters.

4.5 Discussion

UC is known to have a variably dense fibrous tumor stroma (Amin, 2009; Humphrey et al., 2016). UC with myxoid stroma is rare in people (Tavora and Epstein, 2009) and has not been described in dogs or other animals. In people, myxoid stroma is reported in both invasive and non-invasive UC (Amin, 2009; Humphrey et al., 2016). The proposed terminology for UC with prominent myxoid stroma includes 'myxoid UC with abundant myxoid stroma' (Behzatoglu et al., 2012). In cases with chordoid morphology, characterized by prominent cellular cording and associated myxoid stromal matrix, the UCs are proposed to be referred to as 'UC with abundant myxoid stroma showing chordoid-like features' (Cox et al., 2009). In man, the myxoid stroma is typically loose with no significant collagenous stromal component. This contrasts with the canine cases reported here, which were characterized by a dense, mixed collagenous and myxoid (hence the term 'fibromyxoid') tumor stroma. The primarily dense fibromyxoid stroma in the canine cases studied here appears to closely resemble the fibromyxoid stroma described in human vulvar squamous cell carcinoma (Jeffus et al., 2015). In accordance with previous studies (Ambros et al., 1996; Pinto et al., 1999), Jeffus et al. (Jeffus et al., 2015) defined a fibromyxoid stromal response as extracellular matrix composed of immature

collagen and fibroblasts with a myxoid component, which had a blue hue on HE-stained tissue sections compared with the fibrous stroma. This histomorphological description defines well the appearance of the fibromyxoid stroma observed in the canine cases in the present study. The blue hue of the myxoid stromal component was observed in HE-stained tissue sections and was even more evident when the tissue was stained with Alcian blue. In people, UC may be associated with an exuberant stroma with variable myxoid matrix and extensive mesenchymal changes, which may stimulate a sarcoma or sarcomatoid differentiation, referred to as 'pseudosarcomatous stromal reaction' (Ambrosini-Spaltro and Melissari, 2011; Ro et al., 1993). In the present canine cases, such a highly proliferative stromal spindle cell population, characterized by a high cellularity of plump fibroblasts, was absent. Canine cases in the present study lacked any chordoid-like features (i.e. cellular cording in a loose myxoid stroma).

The fact that the presence of fibromyxoid stroma was strongly associated with muscle invasive tumor growth in these dogs with UC is significant. Muscle invasion per se is an indicator for higher tumor stage and poor prognosis in patients with UC (Humphrey et al., 2016). In a study of human UC, all cases with abundant myxoid stroma were invasive, with 69% and 31% of cases invading the lamina propria and tunica muscularis, respectively (Tavora and Epstein, 2009). The presence of fibromyxoid stroma is also known to be a poor prognostic factor in vulvar squamous cell carcinoma (Ambros et al., 1996; Jeffus et al., 2015) and uterine endometrioid endometrial carcinoma (Murray et al., 2003). In vulvar squamous cell carcinoma, the presence of a fibromyxoid stroma was associated with older age group, poorer survival rate and more extensive lymph node metastases (Ambros et al., 1996) as well as infiltrative tumor morphology, perineural invasion and lymph node metastasis (Jeffus et al., 2015). In endometrial carcinoma, a fibromyxoid stromal reaction is known to be associated with a higher frequency of death or recurrence and is frequently accompanied by lymphatic or blood vessel invasion (Murray et al., 2003). The role of fibromyxoid tumor stroma in the pathomechanism of

aggressive tumor growth remains unknown. Infiltrative tumors with a fibromyxoid stromal response have been proposed to behave more aggressively through epithelial-to-mesenchymal transition (Holthoff et al., 2017).

Tumor necrosis was a common finding in the present study, and was observed in ~25% of cases. This is in agreement with human upper and lower urinary tract UC where tumor necrosis is a frequent and a well-described feature (Hodgson et al., 2018; Lee et al., 2007; Soave et al., 2015; Zigeuner et al., 2010). Tumor necrosis is a poor prognostic factor in human UC, and is associated with increased tumor size, decreased recurrence-free survival and decreased disease-specific survival, older age, advanced tumor stage, higher tumor grade, lymph node metastasis, positive surgical margin status and lymphovascular invasion (Hodgson et al., 2018; Lee et al., 2007; Soave et al., 2015; Zigeuner et al., 2010). In these canine cases, no association of tumor necrosis with older age or tumor muscle invasion was observed. It was not possible to determine additional clinicopathological associations, as information with respect to tumor size, survival time, lymph node metastasis and surgical margins was not available, which is a limitation of this study. Interestingly however, moderate (affecting 5–20% of the tissue section) to severe (affecting >50% of the tissue section) tumor necrosis was significantly associated ($p < 0.02$) with the presence of moderate (10–50% of the total tumor stroma) to predominant (>50% of the total tumor stroma) fibromyxoid tumor stroma, which in turn is strongly associated with muscle invasion. Nevertheless, no direct association was observed between tumor necrosis and muscle invasion.

In the canine UCs reported here, tumor necrosis presented primarily as comedo-type necrosis, closely resembling comedonecrosis in human and canine breast and prostate cancer (Akter et al., 2015; Al-Mansour et al., 2018; Epstein et al., 2017; Fine et al., 2018; Palmieri and Grieco, 2015; Yagata et al., 2003). The histomorphological description of comedonecrosis (i.e. intraluminal necrotic cells and/or karyorrhexis displaying cribriform or solid

architecture)(Fine et al., 2018), describes well the comedo-type necrosis in the examined canine UCs. However, the term comedonecrosis is not commonly used when referring to tumor necrosis in human or canine UCs, except in cases with prostatic UC (Humphrey et al., 2016). Reasons for this may be: (1) necrosis in human (non-prostatic) UC is not of comedo-type, and/or (2) necrosis in canine UC has not previously been further characterized. Given that comedonecrosis in human UC appears to be rare, in contrast to canine UC, its presence may indicate a different pathogenesis of tumor necrosis in people and dogs. Given the frequent presence of comedonecrosis in canine UC in the present study, which includes over 380 dogs of different breeds, ages and gender, with origin in two different countries, it seems reasonable to assume that comedonecrosis is a common feature of canine UC.

Regarding the prognostic significance of comedonecrosis in the present study, only an indirect association between the presence of moderate to severe tumor necrosis and tumor muscle invasion was found. No significant association between the presence of comedonecrosis and age, sex, neutering status or dog breed was identified. In human breast carcinoma, disease-free survival was significantly shorter in patients with the comedo-type compared with the non-comedo-type tumor (Yagata et al., 2003). Due to the lack of information about survival times of the dogs studied here, no conclusions could be drawn for canine UC. In PC, a finding of comedonecrosis has been near universally associated with high-grade disease, and comedonecrosis is a defined feature of Gleason grade 5 tumors (Epstein et al., 2017). Considering that canine UC is typically a high-grade disease per se, the frequently occurring comedonecrosis may potentially reflect, and be associated with, high tumor grades.

Tumor inflammation, both peritumoural and intratumoral, was common in the studied canine UCs. Lymphocytes and plasma cells were the predominate inflammatory cell type and most cases had only a mild inflammatory response. This is in agreement with previous studies of human and canine UC (Inoue et al., 2017; Mihatsch et al., 1979; Offersen et al., 2002; Samaratunga et al., 2005). The prognostic significance of peri- and intratumoral inflammation in UC is

controversial in the human literature (Samaratunga et al., 2005). Inflammation has been reported to be associated with longer survival times, particularly in cases with an intense, tumor-front inflammatory response (Hodgson et al., 2018; Offersen et al., 2002). This association could unfortunately not be tested in the present canine cohort due to a lack of information about survival times. Apart from mononuclear inflammatory cells, polymorphonuclear cells, in particular neutrophils and eosinophils, are also described in human UC (Offersen et al., 2002; Samaratunga et al., 2005). Almost one third of all cases in the present series showed a variable, peri- and/or intratumoral infiltration with eosinophils. The occurrence of eosinophils within neoplastic tissue is referred to as tumor-associated tissue eosinophilia (TATE) (Popov et al., 2018). Similar to TATE in human UC, the extent of the eosinophilic inflammatory response in canine cases varied greatly, ranging from absent to a high-density inflammation. The prognostic significance of TATE in UC remains controversial (Hodgson et al., 2018; Lowe et al., 1984; Mihatsch et al., 1979; Popov et al., 2018). In addition to lymphoplasmacytic and eosinophilic inflammation, about 15% of all canine UCs presented with formations of one or several lymphoid follicles, typically located in peritumoral tissue. The presence of tertiary lymphoid structures (TLSs) has been reported to occur in bladder and other types of cancer (Koti et al., 2017). Studies of the prognostic significance of TLSs in BC are rare. Koti et al. (Koti et al., 2017) reported a poor prognostic significance of TLSs, which was seen more commonly in high-grade muscle invasive, compared with non-muscle invasive, BC. In the current series, no association between the presence and extent of TATE or TLS, and muscle invasive growth, age, sex, neutering status or dog breed was identified. In conclusion, TATE and TLS are regularly occurring features in canine UC, but are of unknown prognostic significance.

Divergent, including squamous and glandular, differentiation is frequent in human UC and has diagnostic, prognostic and therapeutic implications (Amin, 2009; Minato et al., 2017; Shanks and Iczkowski, 2009). In the present study, squamous differentiation (8%) was found more commonly than glandular

differentiation (3%). This has already been reported and discussed in a previous study, which included histological assessment of a subset of 260 out of the currently reported 383 cases (de Brot et al., 2018). As an additional finding, the present study shows an association between divergent (i.e. glandular, and to a lesser extent, squamous differentiation) and the presence of fibromyxoid tumor stroma. Partly based on evidence from the literature, and partly speculative, it could be proposed that this association may be explained as follows: (1) tumor cells with squamous or glandular differentiation promote the development of a tumor stroma with a myxoid component, (2) tumor stroma with a myxoid component promotes the divergent differentiation of neoplastic urothelial cells, or (3) divergent differentiation (Amin, 2009; Minato et al., 2017; Shanks and Iczkowski, 2009) and myxoid stroma (Tavora and Epstein, 2009) both represent poor prognostic features and are therefore likely to be seen together in highly malignant subtypes of UC. These explanations are, however, speculative and require further studies for clarification. Another feature which was associated with divergent (i.e. glandular, and to a lesser extent, squamous differentiation) was the presence of moderate to severe inflammation. As for the association with myxoid stroma, it remains unknown whether in these cases inflammation promoted divergent differentiation of neoplastic urothelial cells or vice versa.

In conclusion, the presence of fibromyxoid tumor stroma is common in canine UC and is strongly associated with muscle-invasive growth, which is an indicator of poor prognosis. Tumor inflammation and necrosis are common in UC, but their prognostic significance remains unknown. Based on histomorphology, tumor necrosis in canine UC is predominantly comedo-like and therefore best referred to as comedonecrosis.

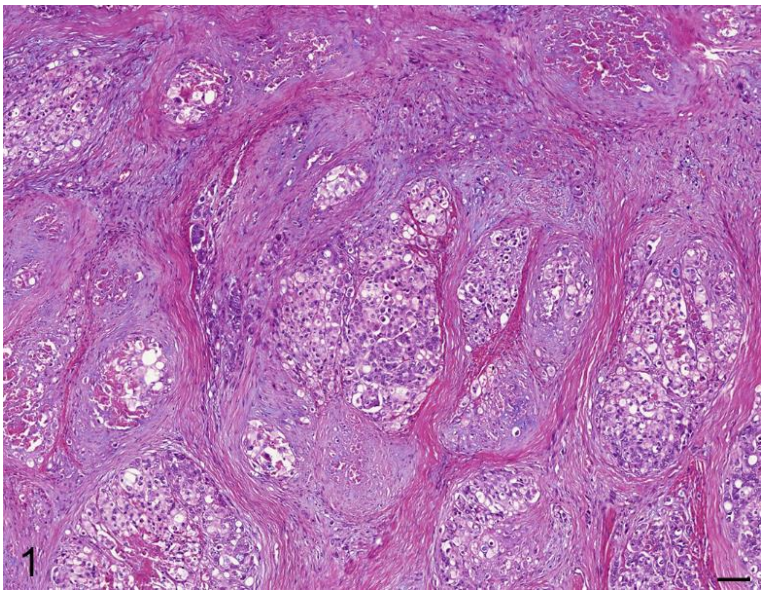


Figure 4.1. Muscle-invasive UC in the urinary bladder of a 7-year-old neutered male crossbreed dog. Note the mixed collagenous and myxoid (fibromyxoid) tumor stroma. HE. Bar, 100 µm.

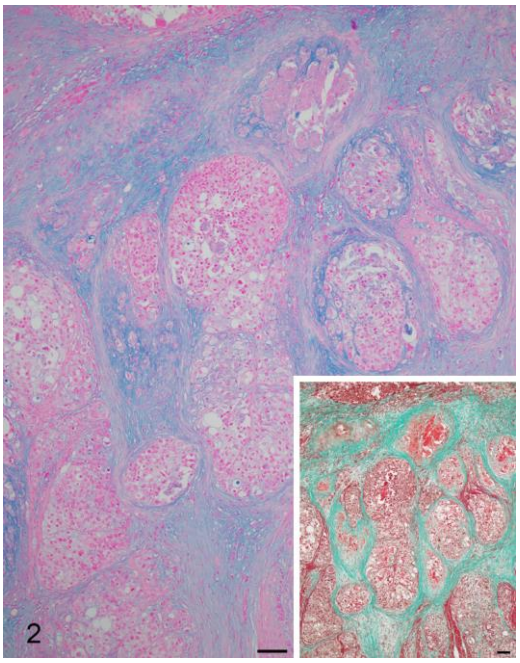


Figure 4.2. Muscle-invasive UC in the urinary bladder of a 7-year-old neutered male crossbreed dog (same case and approximately same location within the tumor as shown in Figure 4.1). Note the mixed collagenous and myxoid (fibromyxoid) tumor stroma with positive Alcian blue and green Masson's trichrome (inset) staining. Alcian blue stain with nuclear fast red counterstain. Bar, 100 µm. Inset: Masson's trichrome stain. Bar, 100 µm.

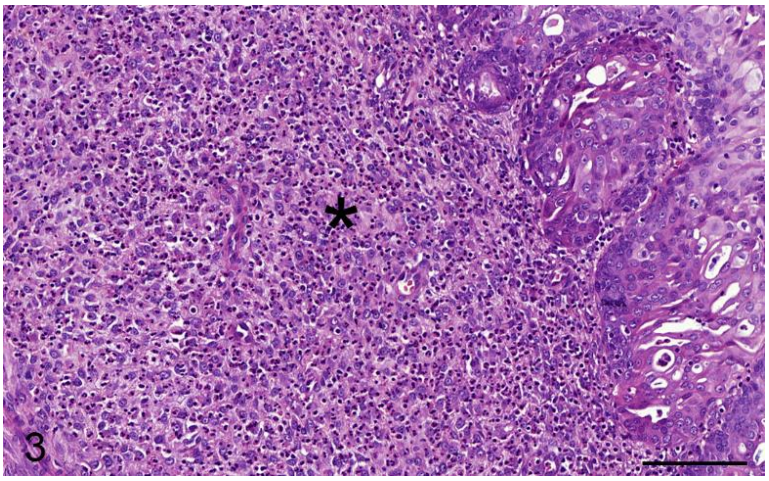


Figure 4.3. UC in the urethra of a 12-year-old male curly-coated retriever. Note the marked infiltration of the lamina propria with eosinophils (*). HE. Bar, 100 µm.

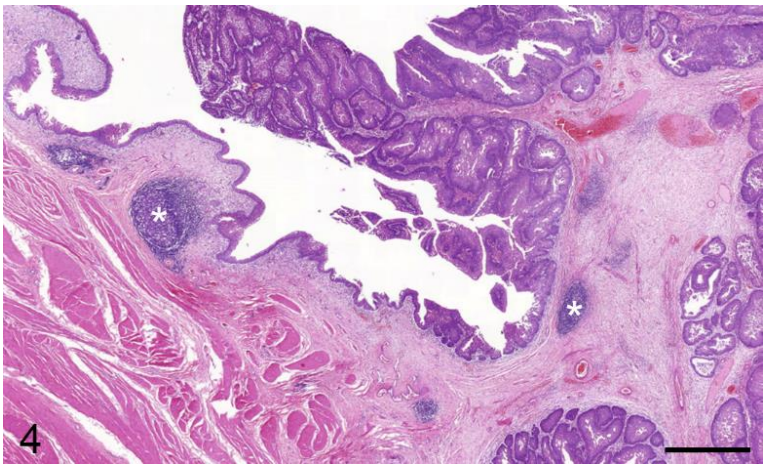


Figure 4.4. Non-muscle invasive UC in the urinary bladder of a 6-year-old giant schnauzer. Note the formations of lymphoid follicles (*) in the peritumoral lamina propria. HE. Bar, 1000 µm.

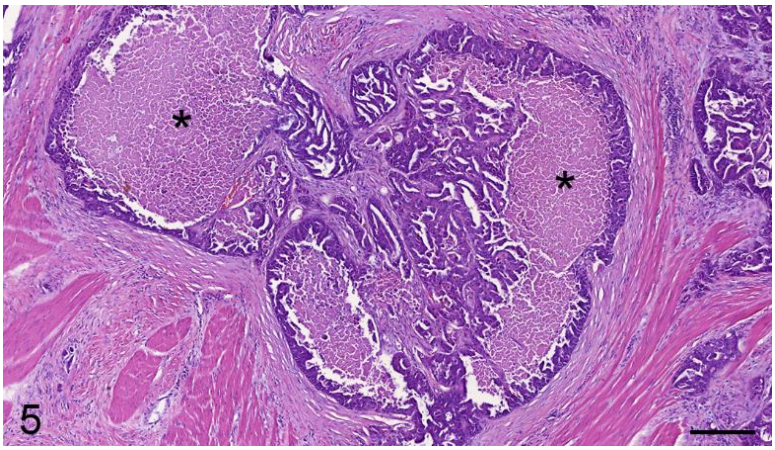


Figure 4.5. Muscle-invasive UC in the urinary bladder of a 5-year-old female Labrador retriever. Note the severe comedonecrosis, characterized by well-demarcated, large central areas of necrotic material (*) surrounded by neoplastic epithelial cells. The tumor stroma is fibromyxoid. HE. Bar, 200 µm

5. STUDY 3. Transcriptome profile analysis of canine urothelial carcinoma by RNA-sequencing

Authors' contributions

List of authors (in alphabetical order):
Simone de Brot (SdB), Tim Scase (TS), Nigel P. Mongan (NPM)

Contributions:
- SdB selected the cases and tissue areas for RNA-sequencing based on clinical data and histomorphology, with support of NPM.
- NPM further processed the selected tissue (tissue deparaffinization, RNA extraction and quantification) and sent the samples to the Barts and London Genomics Centre for library preparation and RNA-sequencing
- SdB and NPM performed the RNA-sequencing data analysis
- SdB interpreted the data, in comparison with data available from scientific human literature, with support of NPM.
- SdB wrote the manuscript, with support of NPM.

5.1 Abstract

Background: Canine bladder UC is a cancer, which is strongly linked to few specific dog breeds, proposing a strong genetic contribution. To date, very little is known about relevant genetic factors of UC in dogs, and the transcriptome of this disease has poorly been described. Differential gene expression, including genes of the p53 pathway, and certain chromosomal abnormalities have been reported to occur in dogs with UC. In contrast, differential splicing, a feature of UC in people, has not previously been reported for canine UC.

Aims: To i) characterize and assess differential gene expression and AS of canine UC by RNAseq, and to ii) compare the genetic alterations in canine UC with the transcriptional features of human BC.

Material and methods: Canine FFPE bladder UC tissue of 9 different dogs (n=3 paired non-tumor and tumor specimen, and n=6 non-paired tumor samples) with high grade UC were analyzed for the presence of different gene expression and AS by RNAseq. Assessed types of AS included skipped exons (SE), retained introns (RI), mutually exclusive exons (MXE), alternative 3' (A3SS) and 5' (A5SS)

start sites. Identified differentially expressed genes and significant altered AS were examined for any associated KEGG pathways and for any relevance in human BC.

Results: No significant differently expressed genes were found when canine UC and histopathologically non-malignant bladder mucosa were compared. In contrast, AS was common, with presence of numerous significant differently spliced genes in all five assessed types of AS. Many of the identified altered genes (*SVIL, PXN, KAT7, ACIN1, TPCN2, SLIT2, MTNR1A, DDR1, APAF1, PKN1, F11R, TCF7L2, ALKBH, COL6A3*) and KEGG pathways (focal adhesion, pathways in cancer, PI3K-Akt signalling among others) have been found to be relevant in human BC. Finally, human BC, as well as acute myeloid leukemia and thyroid cancer pathways were shown to be enriched pathways in the assessed canine UC with differential AS.

Conclusions: Canine UC is characterized by frequent differential splicing of cancer-relevant genes. Many of the identified altered cancer-relevant genes and pathways are known to be associated with human BC, confirming the resemblance of canine and human BC on a molecular level. This study is the first to describe AS in canine UC.

5.2 Introduction

Canine UC is a cancer with one of the strongest breed predisposition in dogs, proposing a strong genetic background (de Brot et al., 2018; Fulkerson and Knapp, 2015; Mutsaers et al., 2003). Scottish and the closely related West Highland White terriers are at highest risk, up to 20-fold, to develop the disease, presumably due to certain genetic factors in this breed. Despite awareness of this strong breed association (Norris et al., 1992), studies which address the genetic variations in these high-risk breeds are rare. So far, chromosomal number abnormalities as well as aberrant expression of genes involved in p53 pathways (*APC, BAX, CTNNB1, HDAC1, MDM2, NOXA1, PTEN*) and epithelial mesenchymal transition (*CDH1, CLDN3, VIM, ZEB1, ZEB2*) have been reported in canine UC (Dhawan et al., 2015; Shapiro et al., 2015). Gene expression analysis based on RNAseq has rarely been performed on canine UC tissue or

cells. Recently, RNAseq revealed a 7-fold upregulation of immune checkpoint B7x when comparing 29 cystoscopic UC biopsy samples with 4 normal canine bladder tissue samples (Chand et al., 2019). The B7x expression however did not correlate with clinical features. Previously, the results of a gene expression analysis of the same canine RNA have already been published, based on a microarray expression profile analysis (Dhawan et al., 2015) and RNAseq, respectively (Dhawan et al., 2018). In the earlier study, 18 canine UC were compared with 4 normal dog bladder tissues, using the GeneChip™ Canine Genome Array 2.0 (Affymetrix canine 2.0), which contains over 20,000 predicted genes. The gene expression profile indicated two different molecular subtypes of UC, consisting of a basal and luminal types. Furthermore, p53 pathway genes were upregulated in tumor compared to normal bladder tissue samples. In the more recent study, RNAseq of 29 UC and 4 normal bladder samples confirmed the presence of two different, i.e. a basal and luminal, subtypes of UC. Basal tumors were characterized by upregulation of *MMP9, SERPINE2, CAV1, KRT14*, and *RASA3*, whereas luminal tumors showed increased expressions of *PPARG, LY6E, CTSE, CDK3,* and *TBX2,* among other genes. A major limitation to these studies was that the breeds of dogs, from which the tissue samples were collected, were not reported. AS is an important post-transcriptional modification, which allows the generation of different mRNA species from a single gene. From the different mRNA isoforms, a variety of proteins can be translated, some of which may differ in their function or location within the cell or tissue. Given its important role in the generation of different proteins, it is not surprising that altered AS has been shown to be associated with disease, including cancer (Scotti 2015, Singh 2012). In human bladder UC, AS has been demonstrated to have an important role in cancer progression as well as prognosis (Duenas 2019, He 2018, Gosalbez 2014, Malentacchi 2012, Atlasi 2009). More specifically, UC development has been considered to depend on AS, which has an effect on certain key oncogenic pathways (Duenas 2019). The same group of researchers have proposed that AS of *MDM2* is responsible for UC recurrence. Furthermore, a prognostic role has been suggested for AS via the construction of splicing event signatures (He

2018). One specific gene, *SDF-1*, has been reported to be present as different isoforms in human UC, with a poor prognostic role for the isoform β. SDF-1 β has also been demonstrated to have a diagnostic implication due to its high sensitivity in the detection of UC (Gosalbez 2014). Another gene, which has been proposed to be valuable for UC detection is carbonic anhydrase 9 (*CAIX*). For that purpose, it has been recommended to only measure the full-length isoform, rather than the concentration of all the splice variants of this gene (Malentacchi 2012). Finally, when assessing the expression of surviving (a protein with anti-apoptotic properties) for diagnostic or therapeutic purposes, it has been proposed to differentiate between different splice variants due to their variable expression in UC (Atlasi 2009).

In dogs, the role of AS in cancer has poorly been investigated up to present. Only few studies are available, which report the occurrence of AS in a small number of cancer types. In canine mast cell tumors, AS has been demonstrated to result in a truncated GNAI2 protein even though it has not been determined what role this altered protein plays in this type of canine cancer (Arendt 2015). When investigating canine breast cancer, AS has been shown to be responsible for a reduced expression of a functional tumor suppressor gene *p16/INK4A* (Kabir 2013) and kallikrein-related peptidases 8 and 14 (Angelopoulou 2010, Angelopoulou 2009). In canine BC, AS has however not been reported up to present. In the present study, AS in canine UC is described for the first time.

The aim of the present study is to i) analyze the global transcriptional profile, i.e. differential gene expression and AS, of canine UC from Scottish terriers and the closely related West Highland White terriers by RNAseq and to ii) compare the results with the transcriptional features of human BC.

5.3 Material and methods

Ethics and study design

The study was approved by the University of Nottingham AWERB and the School of Veterinary Medicine and Sciences ethics committees. Informed

consent of all cases was obtained upon submission of the tumor samples. Prior to the use of patient data, all canine cases was anonymized. The study is retrospective and includes archived FFPE tissue, which was provided by Bridge Pathology Ltd. Bristol UK, in a collaborative agreement.

Cases

Based on dog breed, tumor origin, tissue quality and tumor histomorphology, 9 different dogs with UC were selected. Only Scottish (n=1) and West Highland White terriers (n=2), primary urinary bladder UC, high grade tumors and samples with neglectable tissue artefacts were included. More detailed case information is provided in Table 5.1. Information about the presence of tumor metastasis and follow-up data were not available.

Sample ID	Paired TN	Breed	Gender	Age (years)	Clinical information	Tumor growth	Muscle invasion	Location of non-neoplastic (normal) tissue in relation to tumor
15 (normal) 14 (tumor)	Yes	WHWT	FN	12	Hematuria; bladder tumor detected on US; tumor removal via laparotomy	Papillary	No	Adjacent, on the same tissue block and tissue fragment like tumor.
47	No	WHWT	MN	9	Hematuria; bladder tumor detected on US	NA	No	NA
17	No	WHWT	MN	9	Tumor removal via laparotomy	Flat	Yes	NA
18 (normal) 19 (tumor)	Yes	WHWT	MN	12	Hematuria; bladder tumor detected on US	Papillary	No	Adjacent, on the same tissue block and tissue fragment like tumor.
21	No	WHWT	NR	12	Dysuria; bladder tumor detected on US	Flat	No	NA
24	No	ST	FN	9	Hematuria	Papillary	NA	NA
26	No	ST	FN	10	NR	Papillary	No	NA
25	No	ST	MN	9	NR	NA	Yes	NA
33 (normal) 34 (tumor)	Yes	ST	MN	9	Tumor removal via partial cystectomy	Papillary	No	On a different tissue block and fragment.

Table 5.1. Case information of the 9 dogs which were selected for RNAseq.

Abbreviations: FM: Female neutered; MN: Male neutered; N: Normal; NA: Not applicable/assessable; NR: Not reported; ST: Scottish terrier; T: Tumor; TN: Tumor/normal; WHWT: West Highland White terrier

RNA sequencing: Sample preparation and sequencing

From each case/FFPE tissue block, four 10 µm thick tissue sections were trimmed and transferred to sterile Eppendorf tubes for further processing for RNA extraction. Where necessary, tumor and benign tissue were separated and removed from non-neoplastic, inflamed, necrotic, or calcified tissue by manual microdissection of the 10 µm sections by using sterile microtome and scalpel blades. For that purpose, the corresponding digital histology slide was previously marked up as guidance, as illustrated (Figures 5.1 and 5.2). Samples were first treated with deparaffinization solution (Qiagen, Manchester, UK) as directed by the manufacturer. Total RNA was then isolated to the retrieved tissue isolated using an RNeasy FFPE kit (Qiagen, Manchester, UK), with on-column DNase (Sigma-Aldrich, Gillingham, UK) digestion. Samples were quantified using a Nanodrop spectrophotometer and Abs260/280 determined and values ~2.0 selected for further analysis. RNA quality [RNA integrity number (RIN) >7] was confirmed using an Agilent bioanalyser. Samples were submitted to the Barts and London Genomics Centre for library preparation and analyzed using an Illumina NextSeq500 platform using standard protocols.

i) Differential gene expression analysis

Paired end raw reads (fastq format) were quality- and adapter-trimmed using the Trimgalore wrapper for FastQC and Cutadapt. The resultant fastq files were then aligned to the canine reference genome (CanFam3.1) using the STAR aligner and gene expression quantified using HTSeq. The RobiNA (version 1.2.4_build656) implementation of EdgeR (Robinson et al., 2010) was used to calculate differential gene expression between non-malignant and UC specimens, which was determined based on a $q<0.05$ and fold changes >1.5 and using the Benjamini-Hochberg (Benjamini and Hochberg, 1995) method for multiple testing correction. Unsupervised hierarchical clustering analysis of either paired non-tumor and tumor samples, or non-tumor compared to all tumor samples, was created using Cluster3.0. Count data was filtered to remove genes which were not expressed in any samples, log transformed,

mean centred and average linkage determined. The resulting outputs were displayed using Java Treeview.

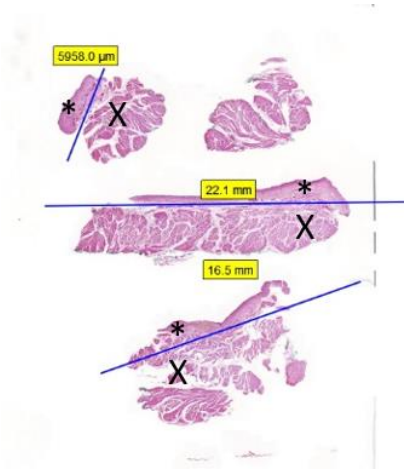


Figure 5.1. Case 33. Screenshot of a digital histology slide containing fragments of non-neoplastic canine urinary bladder tissue. Prior to manual microdissection, the areas of tissue to be sampled have been marked up by drawing blue lines (indicated lengths of lines are irrelevant). In this case, mucosa (here on the side marked with *) was selected and tunica muscularis (on the side marked with X) was excluded.

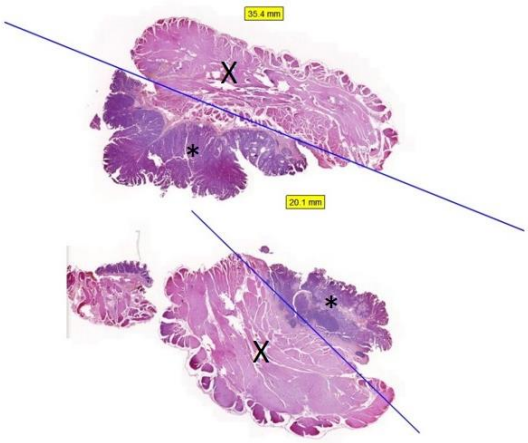
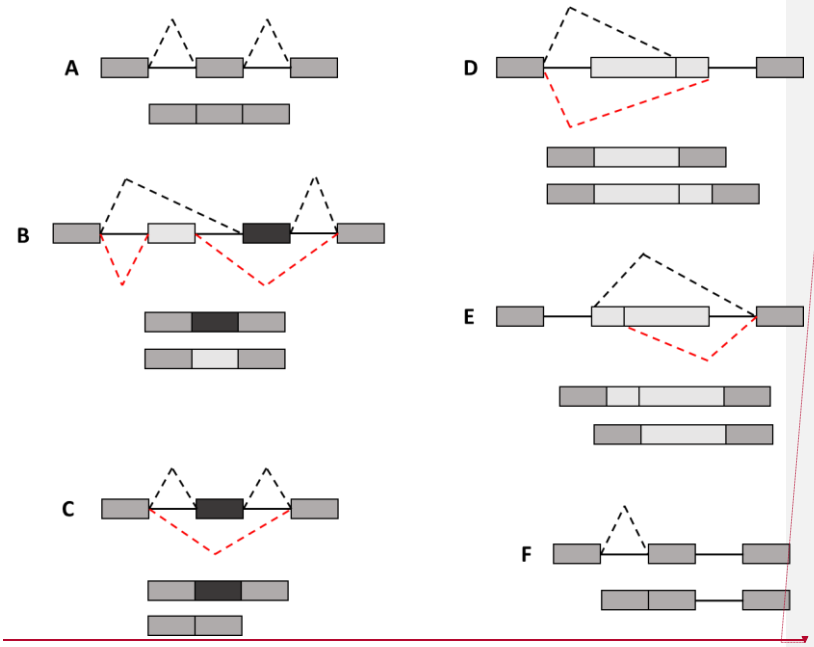


Figure 5.2. Case 26. Screenshot of a digital histology slide containing fragments of a urinary bladder UC. Prior to manual microdissection, the areas of tumor tissue to be sampled have been marked up by drawing a blue line, which separates tumor growth (*) from adjacent non-neoplastic tunica muscularis (X) (indicated length of line is irrelevant).

ii) Alternative splicing analysis

Reads were first trimmed to a uniform length (74 bp) using the rMATS trimming tool. AS events were detected and quantified with the rMATs (version 3.2.5) using the STAR aligner and the CanFam3.1 Ensembl annotated gene transfer format (GTF) file. Assessed events included the following: SE, MXE, A5SS, A3SS and RI (Figure 5.3). For this purpose, RNAseq data (as described above) from normal bladder tissue (n=3 cases; sample ID 15, 18 and 33) was compared to RNAseq data from BC tissue (n=3 cases; sample ID 14, 17 and 34). Splicing events with false discovery rate (FDR) <0.05 were considered significant. For each event, and separately for normal and cancer samples, the exon inclusion level (defined as exon-inclusion ratio, also known as PSI) as well as the difference of PSI (dPSI) between normal and cancer samples were calculated. A threshold of dPSI >20% was arbitrarily defined as a biologically relevant difference. The KEGG database (https://www.genome.jp/kegg/, accessed 13 November 2019) and WEB-based Gene SeT AnaLysis Toolkit (WebGestalt; http://www.webgestalt.org/, accessed 13 November 2019) was searched to identify relevant pathways and genes affected by the AS. Literature research on Pubmed (https://www.ncbi.nlm.nih.gov/pubmed, last access on 13 November 2019) was performed in order to identify any bladder or other cancer-specific relevance of genes with significant AS events.



Deleted:

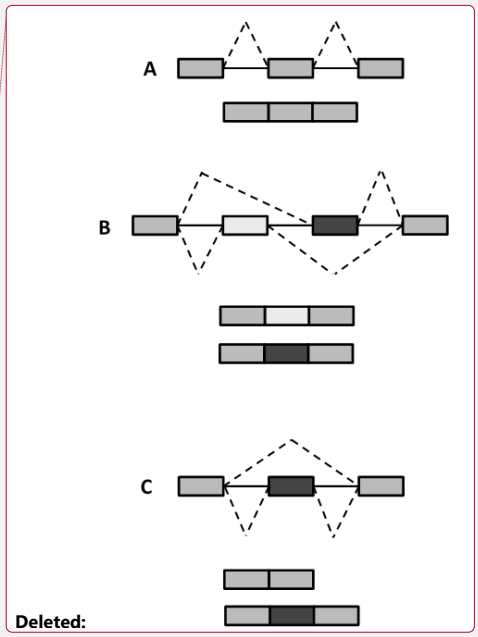


Figure 5.3. Illustration of the different types of AS events, which were assessed in the present study. Grey boxes indicate exonic regions. Pale and dark grey boxes indicate intronic sequences that are included in mature mRNA by alternative splicing. The black dashed lines indicate constitutive splicing, whereas the red dashed lines indicate alternative splicing. Five main types of AS events are shown. (A) Constitutive splicing; (B) mutually exclusive exons; (C) cassette alternative exon; (D) alternative 3' splice site; (E) alternative 5' splice site; and (F) intron retention.

Deleted:

5.4 Results

5.4.1 Differential gene expression

No significant differentially expressed genes were identified when setting the expression fold change to >1.5. Interestingly, when performing a hierarchical cluster analysis, paired samples failed to cluster together (Figures 5.4 and 5.5).

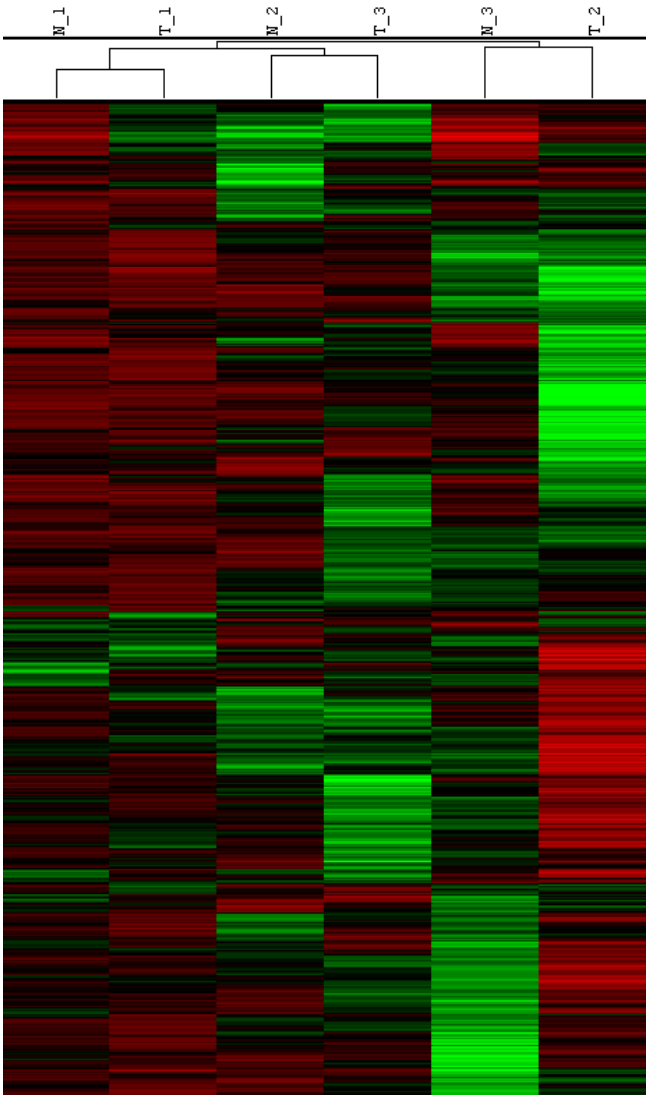


Figure 5.4. Heat map constructed by hierarchical clustering analysis of paired (N: normal; T: tumor) samples of n=3 dogs with canine urothelial carcinoma. Green and red indicate up- and downregulation of individual genes in the event of cancer, respectively. The numbers 1 to 3 correspond to the following cases (as indicated in Table 5.1): 1: 15(N) and 14(T); 2: 18(N) and 19(T); 3: 33(N) and 34(T).

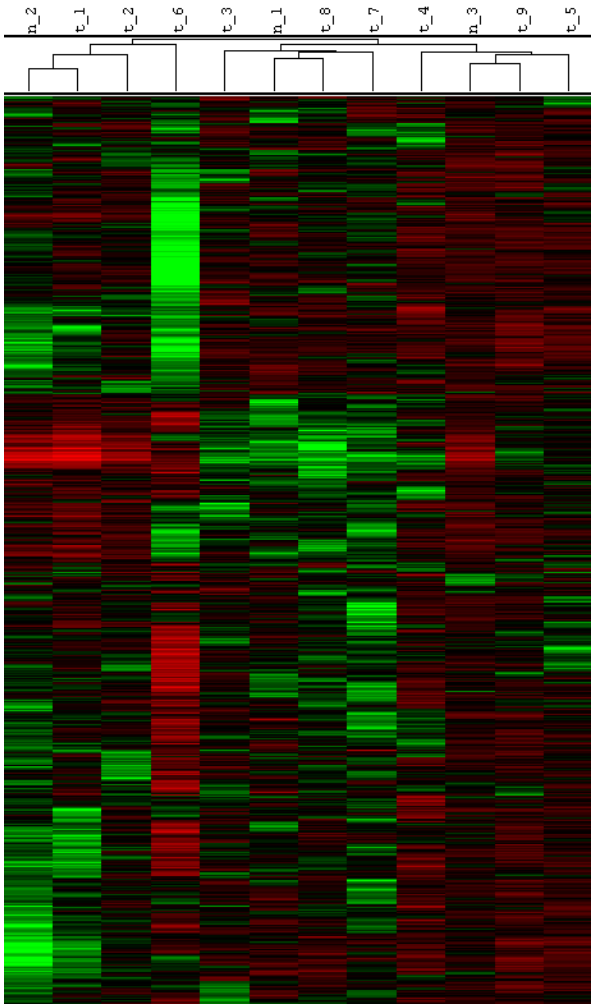


Figure 5.5. Heat map constructed by unsupervised hierarchical clustering analysis of paired (n=3) (N: normal; T: tumor) and non-paired (n=6) tumor samples of n=9 dogs with canine UC. Green and red indicate up- and downregulation of individual genes in the event of cancer, respectively. The numbers 1 to 9 correspond to the following cases (as indicated in Table 5.1): N_1: 18; N_2: 33; N_3: 15; T_1: 19; T_2: 21; T_3: 24; T_4: 25; T_5: 26; T_6: 17; T_7: 34; T_8: 47; T_9: 14.

5.4.2 Alternative splicing analysis

In addition to the differential gene expression analysis, the RNAseq data of the three paired canine UC cases (sample IDs 14, 15, 17, 18, 33, 34) was assessed for the presence and frequency of AS. The following five different types of AS were analyzed: SE, MXE, RI, A5SS, and A3SS. The results of the AS analysis are indicated individually for each subtype of AS, and have been summarized in the Table 5.2.

Skipped exon

A total of 12,286 events were detected using junction counts and reads on target, with 496 (4%) significant (FDR <0.05) events between normal and neoplastic samples. Of those, higher exon inclusion levels were slightly more common in normal (n=255) (51%) compared to cancer samples (n=241) (9%), and 78 (16%) events were considered significant based on dPSI (≥ 20%). These 78 events occurred in 71 different genes, which are associated with the following top 10 different KEGG pathways (all of them human-specific, unless indicated otherwise): Mitophagy (p<0.015), Th17 cell differentiation (p<0.038), autophagy – animal (p<0.052), spliceosome (p<0.056), apoptosis (p<0.058), Hepatitis B (p<0.064), Cushing syndrome (p<0.072), protein processing in endoplasmic reticulum (p<0.082), RNA transport (p<0.082), autophagy – other (p<0.089). The events were located on 29 (out of 39) different canine chromosomes, with a range of 2 (3%) to 8 (10%) events per chromosome.

Mutually exclusive exon

A total of 948 events were detected using junction counts and reads on target, with 90 (9%) significant (FDR<0.05) events. Of those, higher inclusion levels were slightly more common in cancer (n=47) (52%) compared to normal (n=43) (48%) cases, with 44 (49%) events with a significant dPSI (≥ 20%). These 44 events occurred in 41 different genes, which are associated with the following top 10 different KEGG pathways (all of them human-specific, unless indicated otherwise): Protein digestion and absorption (p<0.017), melanogenesis (p<0.021), ubiquitin mediated proteolysis (p<0.036), Wnt signalling pathway

(p<0.040), oxytocin signaling pathway (p<0.044), Hippo signalling pathway (p<0.045), Cushing syndrome (p<0.045), glycosylphosphatidylinositol (GPI)-anchor biosynthesis (p<0.054), axon guidance (p<0.056), Hippo signalling pathway – multiple species (p<0.063). The events were located on 24 (out of 39) different canine chromosomes, with a range of 1 (2%) to 4 (9%) events per chromosome.

Retained intron

A total of 334 events were detected using junction counts and reads on target, with 23 (7%) significant (FDR<0.05) events. Of those, higher exon inclusion levels were seen more frequently in normal (n=14) (61%) compared to cancer (n=9) (39%) cases, with 6 (26%) events with a significant dPSI (≥ 20%). These 6 events occurred in 6 different genes, which are associated with the following top 10 different KEGG pathways (all of them human-specific, unless indicated otherwise): Epithelial cell signaling in Helicobacter pylori infection (p<0.037), Salmonella infection (p<0.047), insulin resistance (p<0.058), leukocyte transendothelial migration (p<0.061), signaling pathways regulating pluripotency of stem cells (p<0.075), cell adhesion molecules (CAMs) (p<0.077), non-alcoholic fatty liver disease (NAFLD) (p<0.080), tight junction (p<0.091), PI3K-Akt signaling pathway (p<0.182). The events were located on 5 (out of 39) different canine chromosomes, with a range of 1 (17%) to 2 (33%) events per chromosome.

Alternative 5' splice site

A total of 3982 events were detected using junction counts and reads on target, with 157 (4%) significant (FDR<0.05) events. Of those, higher inclusion levels were more frequent in normal (n=98) (62%) compared to neoplastic (n=59) (38%) samples, with n=31 (20%) events with a significant dPSI (≥ 20%). These 31 events occurred in 30 different genes, which are associated with the following top 10 different KEGG pathways (all of them human-specific, unless indicated otherwise): Endocrine resistance (p<0.010), thyroid hormone signalling pathway (p<0.013), neurotrophin signaling pathway (p<0.014),

transcriptional misregulation in cancer (p<0.031), nicotinate and nicotinamide metabolism (p<0.045), thyroid cancer (p<0.055), ferroptosis (p<0.059), homologous recombination (p<0.061), BC (p<0.061), amyotrophic lateral sclerosis (ALS) (p<0.075). The events were located on 16 (out of 39) different canine chromosomes, with a range of 1 (3%) to 4 (13%) events per chromosome.

Alternative 3' splice site

A total of 7597 events were detected using junction counts and reads on target, with n=255 (3%) significant (FDR<0.05) events. Of those, higher inclusion levels were more common in normal (n=153) (60%) compared to cancer (n=102) (40%) cases, with n=72 (28%) events with significant dPSI (≥ 20%). These 72 events occurred in 69 different genes, which are associated with the following top 10 different KEGG pathways (all of them human-specific, unless indicated otherwise): Shigellosis (p<0.003), adipocytokine signalling pathway (p<0.004), microRNAs in cancer (p<0.004), antifolate resistance (p<0.008), Th17 cell differentiation (p<0.011), neurotrophin signalling pathway (p<0.014), Ras signalling pathway (p<0.017), ubiquitin mediated proteolysis (p<0.020), cytosolic DNA-sensing pathway (p<0.030), acute myeloid leukemia (p<0.032). The events were located on 23 (out of 39) different canine chromosomes, with a range of 1 (1%) to 7 (10%) events per chromosome.

Assessed parameter	SE	MXE	RI	A5SS	A3SS
Number of significant events[1)] (normal:tumor)	496 (255:241)	90 (43:47)	23 (14:9)	157 (98:59)	255 (153:102)
Number of events with dPSI ≥20% (range)	78 (20.1-81.6)	44 (20.0-52.7)	6 (20.5-48.6)	31 (20.4-57.7)	72 (20.2-63.7)
Associated top ten KEGG pathways* (in decreasing order of p-values; cancer-specific pathways in bold)	Mitophagy Th17 cell differentiation Autophagy - Animal Spliceosome Apoptosis Hepatitis B Cushing syndrome Protein processing in endoplasmic reticulum RNA transport Autophagy - other	Protein digestion and absorption Melanogenesis Ubiquitin mediated proteolysis Wnt signaling pathway Oxytocin signaling pathway Hippo signaling pathway Cushing syndrome Glycosylphosphatidylinositol (GPI)-anchor biosynthesis Axon guidance Hippo signaling pathway – multiple species	Epithelial cell signaling in Helicobacter pylori infection Salmonella infection Insulin resistance Leukocyte transendothelial migration Signaling pathways regulating pluripotency of stem cells Cell adhesion molecules (CAMs) Non-alcoholic fatty liver disease (NAFLD) Tight junction PI3K-Akt signaling pathway	Endocrine resistance Thyroid hormone signaling pathway Neurotrophin signaling pathway Transcriptional misregulation in cancer Nicotinate and nicotinamide metabolism **Thyroid cancer** Ferroptosis Homologous recombination **Bladder cancer** Amyotrophic lateral sclerosis (ALS)	Shigellosis Adipocytokine signaling pathway MicroRNAs in cancer Antifolate resistance Th17 cell differentiation Neurotrophin signaling pathway Ras signaling pathway Ubiquitin mediated proteolysis Cytosolic DNA-sensing pathway **Acute myeloid leukemia**

Number of affected known genes	71	41	6	30	69
Number of different chromosomes with AS	29/39	24/39	5/39	16/39	23/39
Frequency of AS event per chromosome	8/78(10%) Chr 6,9 6/78(8%) Chr 2 4/78(5%) Chr 3,7,24,27,30 3/78(4%) Chr 8,14,25 2/78(3%) Chr 4,5,10,11,12,18,26,31	4/44(9%) Chr 20 3/44(7%) Chr 1,13,25,26 2/44(5%) Chr 2,6,9,11,16,18,28,32 1/44(2%) Chr X,3,4,7,8,10,17,19,23,30,31, 33	2/6(33%) Chr 38 1/6(17%) Chr 10,17,20,26	4/31(13%) Chr 5,20 3/31(10%) Chr 9,17 2/31(7%) Chr 1,2,10,16,30 1/31(3%) Chr 7,8,14,26,33,36,38	7/72(10%) Chr 1,20 6/72(8%) Chr 6,28 5/72(7%) Chr 9,18 4/72(6%) Chr 8,13, 3/72(4%) Chr 10,22 2/72(3%) Chr 3,5,16,19,25,26,29,30,34 1/72(1%) Chr 12,23,24,27
Frequency of AS event per mRNA strand	36/78(46%) neg 42/78(54%) pos	24/44(55%) neg 20/44(46%) pos	3/6(50%) neg 3/6(50%) pos	16/31(52%) neg 15/31(48%) pos	40/72(56%) neg 32/72(44%) pos

Table 5.2. Summary of the AS analysis of 3 paired cases of canine UC, indicating the results for each subtype of AS in a separate column.

Abbreviations: AS: Alternative splicing; A3SS: Alternative 3' site splicing; A5SS: Alternative 5' splicing; Chr: Chromosome; dPSI: difference of percent spliced in; KEGG: Kyoto Encyclopedia of Genes and Genomes; MXE: Mutually exclusive exon; neg: negative (mRNA strand); pos: positive (mRNA strand); RI: Retained intron; SE: Skipped exon

[1)]based on junction counts and target reads; *all human-specific unless indicated otherwise

All genes affected by AS events with expected altered amino acid sequence (i.e. SE, MXE or RI) and with dPSI of ≥20% were assessed for any reported association with human or animal BC by performing a literature research on PubMed (https://www.ncbi.nlm.nih.gov/pubmed, last access on 13 November 2019). The results are shown in Table 5.3, and are summarized in Table 5.4. A total of 14 different genes were identified, all of which were found to also be relevant for different types of non-BC. These genes have been reported to either have an altered gene and/or protein expression in cancer, with prognostic significance for some of the genes. Corresponding references are indicated in Table 5.3. More specifically, 9 (64%) and 5 (36%) out of 14 genes were up- and downregulated in BC, respectively. In different non-BC, 5 (36%) and 4 (29%) out of the 14 genes were up- and downregulated, respectively. The remaining 5 (36%) genes were either up- or downregulated within different or the same type of cancer. When comparing the individual gene expression between BC and non-BC, 3 (21%) and another 3 (21%) of 14 genes were up- or downregulated in both cancer groups. The remaining 8 (57%) genes were expressed in different directions in BC compared to other cancer types, in at least some of the reported studies. When comparing the dPSI (i.e. the ratio between reads including or excluding exons) for each of the 14 genes, *SVIL* had the highest (81.6%) and *APAF-1* the lowest (24.1%) value. The type of AS of both genes was SE. When dPSI was compared between the different splicing events, mean dPSI values were highest in genes with SE (41.7%), followed by RI (40.6) and MXE (37.4%). All but one gene (*KAT7*) had only undergone one subtype of AS event. SE was most common (8/14; 57%), followed by MXE (4/14; 29%) and RI (14%). Eight out of 14 (57%) genes were associated with between one and 13 different cancer-relevant KEGG pathways. Three of the total 29 pathways, i.e. focal adhesion, pathways in cancer, and PI3K-Akt signaling, were observed to be relevant for two different genes each. The remaining 26 pathways were associated with only one of the genes.

Gene	Altered expression in BC	Altered expression in non-BC	Combined change of expression in BC and other cancer	dPSI present study	AS event	KEGG pathways with relevance in cancer*
SVIL	Altered (suspected decreased) gene expression (Lamy et al., 2016)	- Increased protein expression (different human carcinoma cell lines) (Chen et al., 2017)	Up & down	81.6	SE	NA
PXN	Decreased protein expression, prognostic (Athanasopoulou et al., 2013)	- Increased protein expression, prognostic (colorectal) (Du et al., 2016; Mantonakis et al., 2017); (larynx) (Li et al., 2015b) - Decreased protein expression (liver metastasis compared to primary tumor) (Mantonakis et al., 2017)	Up & down	58.1	SE	N=4 Focal adhesion Proteoglycans in cancer Regulation of actin cytoskeleton VEGF signaling
KAT7	Increased protein expression, prognostic (Chen et al., 2018; Iizuka et al., 2009)	- Increased protein expression (breast) (Hu et al., 2009; Iizuka et al., 2013)	Up	48.5 (SE) 20.4 (MXE)	SE, MXE	NA
ACIN1	Decreased gene expression (inactivating genetic mutation)(Majewski et al., 2019)	- Hypermethylation of the gene (lung) (Shu et al., 2006)	Down	42.9	SE	N=3 mRNA surveillance pathway RNA transport Spliceosome
TPCN2	Increased gene expression (Shivakumar et al., 2017)	- Increased gene expression (6-gene signature), prognostic (prostate) (Li et al., 2019a)	Up	34.7	SE	N=1 Calcium signaling

SLIT2	Increased gene expression, prognostic (Krafft et al., 2018); decreased gene expression (hypermethylation of the gene)(Roperch et al., 2016)	-	Decreased protein expression, prognostic (brain) (Liu et al., 2016) (breast) (Bhattacharya et al., 2016; Qin et al., 2015); (leukemia) (Golos et al., 2019); (lymphoma) (Mohamed et al., 2019); (stomach) (Kim et al., 2016); (thyroid) (Jeon et al., 2019; Shi et al., 2016)	Up & down	31.9	SE	NA
		-	Decreased gene expression (hypermethylation of the gene) (colorectal) (Patai et al., 2015); (nasopharynx) (Li et al., 2018)				
MTNR1A	Decreased gene expression (genetic mutation) (Lin et al., 2017)	-	Decreased protein expression (oral (Nakamura et al., 2008))	Down	28	SE	NA
		-	Genetic mutation (breast) (Pham et al., 2019); (liver) (Su et al., 2017); (oral) (Lin et al., 2015a)				
DDR1	Increased protein expression, prognostic (Xie et al., 2017)	-	Decreased protein expression, prognostic (kidney) (Krazinski et al., 2019)	Up & down	25.7	SE	NA
		-	Increased protein expression, prognostic (stomach) (Hur et al., 2017)				
		-	Variable protein expression (breast) (Jing et al., 2018)				

APAF1	Decreased gene expression (hypermethylation of the gene) (Christoph et al., 2007a; Christoph et al., 2006)	- Decreased protein expression (breast) (Loginov et al., 2017); (ovary) (Abdelrahman et al., 2018) - Decreased gene expression (genetic mutation) (colorectal) (Sho et al., 2017); (hypermethylation of the gene) (rectal) (Benard et al., 2014)	Down	24.1	SE	N=4 Apoptosis P53 signaling Pathways in cancer Small cell lung cancer
PKN1	Increased protein expression (Lachmann et al., 2011)	- Increased protein expression (prostate) (Venkadakrishnan et al., 2019); (breast) (Turner et al., 2010) - Variable protein expression (breast) (Awadelkarim et al., 2012)	Up and down	47.8	RI	N=2 NOD-like receptor signaling PI3K-Akt signaling
F11R (JAM-A)	Increased gene expression, prognostic (Riester et al., 2014)	- Decreased protein expression (breast) (Naik et al., 2008); (kidney) (Gutwein et al., 2009) - Increased protein expression (breast) (McSherry et al., 2009) (brain) (Pong et al., 2013) - Decreased gene expression (adrenal) (Alshabi et al., 2019); (breast) (Yen et al., 2017)	Up & down	33.4	RI	N=2 Cell adhesion molecules (CAMs) Tight junction

TCF7L2	Increased protein expression (Wang et al., 2017b)	- Increased protein expression, prognostic (pancreas) (Xiang et al., 2018) - Increased gene expression (breast) (Zheng et al., 2017) - Genetic mutations, prognostic (colorectal) (De Nicola et al., 2018; Song et al., 2018); (oral) (Damani Shah et al., 2019)	Up	52.7	MXE	N=13 Acute myeloid leukemia; Adherens junction; Basal cell carcinoma; Breast cancer; Colorectal cancer; Endometrial cancer; Gastric cancer; Hepatocellular carcinoma; Hippo signaling; Pathways in cancer; Prostate cancer; Thyroid cancer; Wnt signaling
ALKBH3	Increased protein expression (Shimada et al., 2009)	- Increased protein expression, prognostic (kidney) (Hotta et al., 2015); (lung) (Tasaki et al., 2011) - Decreased gene expression, prognostic (various cancers) (Knijnenburg et al., 2018); (hypermethylation of the gene) (breast) (Stefansson et al., 2017)	Up & down	51.1	MXE	NA
COL6A3	Increased protein expression (Huang et al., 2018; Thorsen et al., 2008); increased gene expression, prognostic (Di et al., 2019; Zhu et al., 2019)	- Increased protein expression, prognostic (colorectal) (Qiao et al., 2015) (pancreas) (Arafat et al., 2011) - Increased gene expression (colorectal) (Liu et al., 2018b) (Snezhkina et al., 2016) - Genetic mutation (esophageal) (Li et al., 2019b); (lung) (Duan et al., 2019)	Up & down	25.4	MXE	N=3 ECM-receptor interaction Focal adhesion PI3K-Akt signaling

Table 5.3. Fourteen different genes with significant AS events (SE, MXE or RI) with reported relevance in human bladder and non-BC are listed. The genes are sorted in decreasing order of their calculated dPSI values from the present AS analysis, and are grouped for the different type of AS events.

Abbreviations: AS: Alternative splicing; BC: Bladder cancer; down: downregulated (expression); dPSI: Difference of percent spliced in; KEGG: Kyoto Encyclopedia of Genes and Genomes; MXE: Mutually exclusive exon; RI: retained intron; SE: skipped exon; up: upregulated (expression)

*All referring to human pathways unless indicated otherwise

Total number of genes	Altered expression in BC	Altered expression in other cancer	Combined altered expression	dPSI (mean)	Subtype of AS event	KEGG pathways with relevance in cancer
N=14	Increased expression (potential oncogenes) N=9 Decreased expression (potential tumor suppressor genes) N= 4 (plus n=1 suspected)	Increased expression (potential oncogenes) N=5 Decreased expression (potential tumor suppressor genes) N=3 (plus 1 suspected) Genes with variable expression N=5	Up only N=3 Down only N=3 Up & down N=8	SE 41.7 RI 40.6 MXE 37.4	N=13 genes with 1 AS event subtype each; n=1 gene with 2 different AS event subtypes SE N=8 RI N=2 MXE N=4	Total n=29 different pathways with relevance in n=8 different genes N=3 pathways with relevance in 2 different genes each: Focal adhesion, Pathways in cancer, PI3K-Akt signaling N=26 pathways with relevance in 1 gene each: Acute myeloid leukemia, Adherens junction, Apoptosis, Basal cell carcinoma, Breast cancer, Calcium signaling, Cell adhesion molecules (CAMs), Colorectal cancer, ECM-receptor interaction, Endometrial cancer, Gastric cancer, Hepatocellular carcinoma, Hippo signaling, mRNA surveillance pathway, NOD-like receptor signaling, P53 signaling, Prostate cancer, Proteoglycans in cancer, Regulation of actin cytoskeleton, RNA transport, Small cell lung cancer, Spliceosome, Thyroid cancer, Tight junction, VEGF signaling, Wnt signaling

Table 5.4. Relevance in BC and other cancer, and associated KEGG pathways are summarized for n=14 different genes with significant AS events in the present study (Summary of Table 5.3).

Abbreviations: BC: Bladder cancer; dPSI: Difference of percent spliced in; KEGG: Kyoto Encyclopedia of Genes and Genomes; MXE: Mutually exclusive exon; RI: retained intron; SE: skipped exon; up: upregulated (expression)

From the identified top ten KEGG pathways, which were found to be associated with the different types of AS events, three cancer-specific pathways were detected (Table 5.5), including acute myeloid leukemia ($p<0.032$), thyroid cancer ($p<0.055$) and BC ($p<0.061$). The thyroid and bladder cancer pathways were identified in the group of genes with differential A5SS, whereas the acute myeloid leukemia pathway was found to be relevant within the group of genes with altered A3SS. Three different relevant genes with significant AS were associated with these cancer-specific pathways. TP53 was associated with thyroid as well as bladder cancer, whereas IKBKB and TCF7L2 was linked to the acute myeloid leukemia pathway.

KEGG pathway*	**P value**	**AS event**	**Number of different genes**	**Relevant genes within the pathway**
Acute myeloid leukemia	0.032	A3SS	2	*IKBKB*, *TCF7L2*
Thyroid cancer	0.055	A5SS	1	*TP53*
Bladder cancer	0.060	A5SS	1	*TP53*

Table 5.5. Identified cancer-specific KEGG pathways and relevant genes in the AS analysis of 3 paired canine UC cases.

*Cancer-specific pathways identified within the top 10 KEGG pathways of each type of AS

5.5 Discussion

Canine UC is expected to have a strong genetic background, primarily based on the well-known high predisposition for certain dog breeds to develop the disease (Norris et al., 1992). Studies, which investigate the genetic contribution of UC in dogs are however rare, and very little is known about potential cancer-relevant genes. The assessment of differential gene expression and chromosomal number abnormalities of a relatively small number of UC-affected dogs revealed aberrant expression of genes involved in p53 pathways and epithelial mesenchymal transition (Sommer et al., 2018). Next-generation-sequencing has been performed only on a limited number of samples and studies about AS in canine UC are lacking. In the present RNAseq study, bladder UC tissue of nine different dogs was assessed for the level of differential gene expression and AS. Cancer samples were collected from either Scottish terriers (i.e. the breed with highest predisposition to develop UC) or their close relatives, the West Highland White terriers. Close to 900 significant events of five different types of AS were detected, in absence of any significant differentially expressed genes (DEG). The lack of DEG prompts the question if this observation corresponds to inappropriate sampling or if it represents a true finding. There is no doubt that the small number of normal tissue specimens included in the study represents a limitation, which could potentially explain the failure to find altered gene expression. Furthermore, normal and adjacent cancer tissue from the same patient may be similar on a molecular basis, due to a field effect, which alters the entire urothelium in cases of UC (Jones et al., 2005). Moreover, a caveat includes the used canine reference database (CanFam3.1), which represents the genome of a female boxer (Lindbad-Toh et al. 2005). Even though the level of annotation of the dog genome has improved recently, it is still far from perfect (Jagannathan et al. 2019). A more detailed characterization of the canine transcriptome has recently been performed by Hoeppner et al. (2014) who assessed the following ten types of tissues: blood, brain, heart, kidney, liver, lung, ovary, skeletal muscle, skin, and testis. Urinary bladder tissue was however not included. In addition, the canine transcriptome has been described to differ between a variety of different dog breeds

(Megquier 2019). In the present study, the dog breed differed between the reference genome and the assessed urinary bladder tissue, possibly interfering with the interpretation of the generated RNAseq data. Finally, the assessed transcriptome of benign and malignant bladder tissues in the present study included two different dog breeds. Even though the two types of terriers are considered being relatively closely related, they may still be too genetically heterogenous to be compared directly. Therefore, the observed lack of DEG may be explained by a high genetic heterogeneity of the assessed tissue samples. Despite all these limitations and the lack of DEG, AS was found to be frequent, possibly providing evidence that AS is more relevant than alternative expression levels in the carcinogenesis of canine UC in these high-risk breeds. This phenomenon has been reported before in human diseases, including cancer. In invasive ductal carcinomas of the breast, AS was primarily seen in genes with low or no differential expression (Bjorklund et al., 2017). In idiopathic pulmonary fibrosis, significant AS occurred in approximately equal numbers of genes with and without significant altered expression levels (Deng et al., 2013).

Deleted:

Deleted: potential

Deleted: ,

Deleted: in the presence of

Deleted: AS could

Deleted: e

For the first time, AS splicing has been described to occur in canine UC. Interestingly, numerous relevant genes and disease pathways are altered in both human and canine UC. More specifically, 14 different genes with significant AS with relevance in human BC have been identified in the assessed canine cancer tissue. The gene with the highest dPSI value was *SVIL*, which has been demonstrated to have an altered expression level in human BC (Lamy et al., 2016). In addition, this gene has been shown to have a prognostic value in human UC (Ponten et al., 2008; Uhlen et al., 2015) (https://www.proteinatlas.org/, accessed 13 November 2019), and increased expression has been observed in different human carcinoma cell lines (Chen et al., 2017). *SVIL* is an actin and myosin-binding protein, with an important role in cell contraction and migration, including tissue invasion (Crowley et al., 2009). Considering the highly invasive nature of canine UC, it seems reasonable to propose that *SVIL* could potentially, contribute to the tissue invasion of cancer cells, at least to a certain extent. It could be speculated that the

observed significant increase in skipped exons may lead to the generation different isoforms of the *SVIL* gene, which may be translated into proteins with a higher functional activity. In order to correlate changes in AS with the level of protein expression and function, for SVIL or any other genes, further protein expression studies are required. The gene with the second highest dPSI value in the present study was *PXN*, which is known to have prognostic significance in human bladder and other cancer. Primary BC as well as colorectal cancer metastases in the liver were shown to have reduced *PXN* expression (Athanasopoulou et al., 2013; Mantonakis et al., 2017). This is in contrast to an increased expression of the same gene in laryngeal and primary colorectal cancer when compared to benign tissue (Du et al., 2016; Li et al., 2015b; Mantonakis et al., 2017). Similar to *SVIL*, *PXN* is a cytoskeletal, actin-binding protein, which is located at sites of cell adhesion to the extracellular matrix (Deakin and Turner, 2008). The reported reduced *PXN* expression in BC could potentially explain the increased motility of cancer cells. Indeed, *PXN* has been shown to have a promoting effect on cell motility (West et al., 2001). Depending on the type of tissue and environmental factors, the same protein has been demonstrated to have an inhibitory effect on cell motility (Yano et al., 2004). This dual effect may possibly explain the presumably contradictory level of *PXN* expression in different types of cancer. The observed significant increased level of exon skipping in neoplastic compared to benign canine urothelium could result in the generation of a less or even non-functional *PXN* protein. Decreased levels of *PXN*, associated with increased cell motility, may further contribute to the invasive nature and frequent metastatic spread of UC in dogs. For canine *PXN*, the functional implication of the altered AS remains however speculation so far.

Three genes with significant AS in the present canine study, which are known to have increased expression in human bladder and other cancers include *COL6A3, KAT7, TPCN2* and *TCF7L2*.

COL6A3 has been demonstrated to be overexpressed in BC and a variety of other malignancies, with a prognostic value for bladder, pancreas and colorectal cancer (Arafat et al., 2011; Di et al., 2019; Duan et al., 2019; Huang

et al., 2018; Li et al., 2019b; Liu et al., 2018b; Qiao et al., 2015; Snezhkina et al., 2016; Thorsen et al., 2008; Zhu et al., 2019). *COL6A3* is a component of collagen type VI, which is present in most types of connective tissue (Nissen et al., 2019). In addition to its physiological role in tissue structure, collagen VI has also been shown to have a tumor-promoting effect by increasing cell proliferation and decreasing apoptosis (Cheng et al., 2011a; Park and Scherer, 2012). The observed significant differential MXE in the studied canine UC tissue may lead to the generation of more functional *COL6A3* proteins, thereby contributing to BC development in dogs. *KAT7* (also known as HBO1) has been reported to have a prognostic role in human BC (Chen et al., 2018; Iizuka et al., 2009) and is overexpressed in breast cancer (Hu et al., 2009; Iizuka et al., 2013). Interestingly, *KAT7* presented with significant AS events in two different types of AS (i.e. SE and MXE) in the present study, potentially emphasizing an important role of differential splicing for regulating the expression of this gene. The function of *KAT7* is to acetylate H4 histones, thereby unfolding the chromatin in order DNA transcription can take place (Miotto and Struhl, 2010). Despite a well-recognized oncogenic effect of *KAT7*, it remains poorly understood how exactly overexpression of this gene causes malignant disease. It may be speculated that increased AS generates *KAT7* isoforms, which are translated into functionally active proteins, eventually leading to an overall increase of unfolded chromatin. Consequently, potential oncogenes may be expressed to a higher extent, finally contributing to the development of cancer. *TPCN2* is a highly selective Ca2+ channel, which is located in the lysosomal membrane (Pitt et al., 2010). Increased expression of this gene has been observed in bladder (Shivakumar et al., 2017) and prostate cancer (Li et al., 2019a) even though little is known about the mechanisms by which this gene causes malignant disease. In a recent study, which investigates mouse breast and human cervical cancer cell lines, *TPCN2* has been demonstrated to inhibit the fusion between autophagosome and lysosome, resulting in the accumulation of autophagosomes (Sun and Yue, 2018; Wang et al., 2017b). In the context of cancer, *TPCN2* has been poorly investigated. In a more recent study, this gene has been shown to be relevant for cancer cell migration, and

has therefore been proposed to be important for metastasis (Nguyen et al., 2017). Accordingly, the observed significant differential splicing in the present canine UC tissues, which presumably alters the level of functional *TPCN2* protein, could play an important role in the metastatic behavior of UC in dogs. Up to present, the expression and function of *TPCN2* has not been investigated in any canine benign or neoplastic condition in dogs. The present study is the first to report the level of expression and AS of this gene in canines. Transcription factor 7 like 2 (*TCF7L2*) has been shown to be overexpressed in BC (Wang et al., 2017b), as well as other cancer, including breast and pancreas malignancies, with a prognostic significance in the latter (Xiang et al., 2018; Zheng et al., 2017). *TCF7L2* is a transcription factor with relevance for a variety of different genes, with a key role in the Wnt signaling pathway (Graham et al., 2000). More specifically, the effector of this cancer-relevant pathway, β-catenin, accumulates in malignant cells and forms a complex with *TCF7L2*, leading to the transcription of several genes with a role in cell proliferation. In the currently studied canine UC, *TCF7L2* presented with significant differential MXE splicing. Even though MXE is not expected to change protein size or structure, this type of AS is able to produce proteins with altered functions (Mathur et al., 2019). Significant differences in the level of MXE may therefore generate *TCF7L2* proteins with increased functional activity, potentially promoting cell proliferation, which may lead to the development of canine UC.

Three genes with significant AS in the present canine study, which are either suspected or confirmed to have decreased expression levels in human bladder and other cancers include *ACIN1*, *APAF1* and *MTNR1A*. *ACIN1* has been reported to be mutated or hypermethylated in human bladder (Majewski et al., 2019) and lung cancer (Shu et al., 2006). These genetic and epigenetic changes are expected to lead to decreased expression of this gene. *ACIN1* is relevant for apoptosis, specifically for the condensation of chromatin, which is known to play a key role in the inhibition of cancer development (Brown and Attardi, 2005). It is therefore unsurprising that decreased *ACIN1* expression has been linked to cancer. Likewise, the observed significant AS of this gene in the

studied canine UC tissue is expected to be associated with an altered, most likely reduced, level of functional *ACIN1* protein. Furthermore, in addition to its role in apoptosis, *ACIN1* has also been demonstrated to be important for the regulation of splicing (Rodor et al., 2016). It has been suggested that it has a direct role in the definition of exon and intron. AS of this gene may consequently also have an effect on the splicing of a range of different genes, with or without cancer relevance. The gene *APAF1* has been demonstrated to be hypermethylated in human BC, presumably corresponding to a reduced gene expression (Christoph et al., 2007b; Christoph et al., 2006). Decreased expression has also been observed in non-bladder malignancies, including breast, ovary, and colorectal cancer (Abdelrahman et al., 2018; Loginov et al., 2017; Sho et al., 2017). *APAF1* is a key protein for apoptosis, with the capacity to initiate this pathway. Similar to *ACIN1*, reduced expression of *APAF1* is an expected finding in cancer. The observed significant differential SE of this gene in the studied canine UC tissue is therefore likely to be relevant for BC carcinogenesis in dogs. As for any of the genes with AS, the level of functional protein expression would needed to be known in order to better understand better relevance of differential splicing for UC in dogs. *MTNR1A* has been reported to be mutated in BC (Lin et al., 2017) and other malignancies, including breast, liver, and oral cancer, with either confirmed or at least suspected decreased expression (Lin et al., 2015a; Nakamura et al., 2008; Pham et al., 2019; Su et al., 2017). In the healthy organism, this receptor is responsible for melatonin effects on sleep and circadian rhythm regulation (Jockers et al., 2016). In the context of cancer, melatonin has also been demonstrated to have an oncostatic role, with inhibitory effects on tumor proliferation, invasion, and metastasis among other mechanisms (Reiter, 2004). Decreased expression of *MTNR1A*, potentially caused by AS, is expected to lead to decreased action of melatonin and therefore to increased risk of cancer. The same can be proposed to be true for canine UC, which has been shown to be characterized by significant AS of *MTNR1A* in the present study.

Four genes (*DDR1, F11R, PKN1* and *SLIT2*) with significant differential splicing in the studied canine tissues have been reported to be overexpressed in human BC, with either down or upregulation in other types of cancer. Discoidin domain receptor tyrosine kinase 1 (DDR1) protein has been demonstrated to be overexpressed in bladder and gastric cancer, with prognostic value for both types of malignancies (Hur et al., 2017; Xie et al., 2017). In contrast, kidney cancer has been shown to have decreased levels of DDR1 protein, with prognostic significance (Krazinski et al., 2019), whereas DDR1 expression levels varied in breast cancer (Jing et al., 2018). DDR1 is a receptor tyrosine kinase, which is activated by collagen, with various effects, including cellular proliferation and adhesion, among others (Henriet et al., 2018). It could be speculated that the wide range of functions may explain the variable levels of expression in the different cancers. Similarly, the observed significant AS in the studied canine UC may either correspond to an increased or decreased DDR1 functional protein expression. *F11R* (also known as *JAM-A*) has been described to be upregulated in human BC, with a prognostic role (Riester et al., 2014). In other cancer, *F11R* has been shown to be either increased (breast and brain) or decreased (adrenal, breast and kidney) (Gutwein et al., 2009; McSherry et al., 2009; Naik et al., 2008; Pong et al., 2013; Yen et al., 2017). F11R is a component of the epithelial and endothelial tight junctions, and therefore relevant for the regulation of transmigration and cell-to-cell contact (Martin-Padura et al., 1998). As expected, reduced expression of this protein has been confirmed to promote invasive growth and metastasis in certain cancers. (Fong et al., 2012; Gotte et al., 2010; Gutwein et al., 2009; McSherry et al., 2009). The association of cancer development and promotion with increased levels of *F11R* are less well understood. It has been proposed that increased expression of *F11R* may facilitate cancer cell migration through downstream effects on β1-integrin (McSherry et al., 2009). Regarding the observed significant differential splicing of *F11R* in the studied canine population, it remains unknown if AS results in either increased or decreased levels of functional protein. As required for other genes with significant AS in the present study, the level of F11R protein expression needs to be measured in order to better estimate the potential

relevance of differential splicing of selected genes. *PKN1* has been demonstrated to be upregulated in BC (Lachmann et al., 2011) and other malignancies, including cancer of the prostate and breast (Turner et al., 2010; Venkadakrishnan et al., 2019). In contrast, *PKN1* expression remained either unaltered or was both down- and upregulated in breast cancer (Awadelkarim et al., 2012). PKN1 belongs to the protein kinase C superfamily, which may be activated by Rho-proteins and apoptosis-relevant proteases (Mukai, 2003). The relevance of PKN1 in Rho, apoptosis and other cancer-relevant pathways explain its importance in cancer development and progression. The variable level of *PKN1* expression in some cancers suggest to evaluate the expression of *PKN1* together with other protein kinases C, rather than measuring *PKN1* individually (Awadelkarim et al., 2012). The detected significant AS of *PKN1* in the studied canine UC tissues is expected to be associated with altered levels of functional protein. Considering the observed increased PKN1 protein expression in human BC, it is tempting to speculate that the same protein may also be upregulated in canine UC. This needs confirmation by further investigating the level of functional PKN1 protein in BC of dogs.

SLIT2 has been detected to be differentially expressed in human BC, with either increased or decreased levels of the gene (Krafft et al., 2018; Roperch et al., 2016). Other malignancies, including brain, breast, colorectal, leukemia, lymphoma, nasopharyngeal, stomach and thyroid cancer, have been reported to consistently show a decreased level of expression, on a gene as well as protein level (Bhattacharya et al., 2016; Golos et al., 2019; Jeon et al., 2019; Kim et al., 2016; Li et al., 2018; Liu et al., 2016; Mohamed et al., 2019; Patai et al., 2015; Qin et al., 2015; Shi et al., 2016). One of the key roles of SLIT2 includes the regulation of cellular migration, primarily of nervous cells and leukocytes (Chaturvedi and Robinson, 2015; Yuan et al., 1999). It is therefore little surprising that the reduced level of *SLIT2* in numerous different cancers have been shown to be associated with increased cancer cell migration and invasion. The association of human BC with increased *SLIT2* levels in one of two studies may however seem contradictory. This conflicting result may be explained by the fact that increased levels of *SLIT2* could only be demonstrated on a genetic,

but not protein, level (Krafft et al., 2018). Based on the known downregulation of *SLIT2* in most studied cancers, the observed AS of *SLIT* in the currently studied canine UC is more likely to result in decreased rather than increased protein expression. Protein expression analysis (e.g. IHC or Western blot) would be required to confirm this speculation.

In addition to the observed significant differential splicing of individual cancer-relevant genes, AS analysis of canine UC tissue also revealed an association with certain human cancer-specific pathways. More specifically, differential A3SS was associated with acute myeloid leukemia pathway, whereas differential A5SS was linked to the pathways of thyroid and bladder cancer. Moreover, the identified genes with significant differential AS in the studied canine UC and with known relevance in human BC could be linked to up to two different cancer-relevant pathways per gene. Pathways, which were associated with two genes each included focal adhesion, pathways in cancer, and PI3K-Akt signaling, all of which are known to have a key role in cancer. Interestingly, in human BC, the top five enriched pathways obtained in the KEGG pathway analysis were demonstrated to include focal adhesion and PI3K-Akt signaling pathway (Gao et al., 2018). BC cell invasion and migration has been reported to be regulated by focal adhesion kinases (Kong et al., 2017a). Furthermore, differential gene expression analysis of BC revealed decreased expression of genes, which have been associated to the focal adhesion pathway (Zhang et al., 2018b). One gene, which has been shown to be overrepresented in the focal adhesion pathway, includes *COL3A1*, which is associated with BC progression (Yuan et al., 2017). Similar observations were made based on differential protein expression analysis of BC, which confirmed a key role of the focal adhesion pathway in tumor development and progression (Wu et al., 2017). In addition to altered expression of genes and proteins with relevance in focal adhesion, PI3K-Akt signaling pathway alterations are common in human BC (Korkolopoulou et al., 2012; Platt et al., 2009). This pathway has been found to be altered in many cancer types, and is a well-known target for cancer therapeutics due to its role in cell growth, survival and metastasis (Fresno Vara et al., 2004; Hou et al.,

2017). For BC initiation, as well as progression, PI3K-Akt pathway activation is known to be highly relevant, and occurs through different mechanisms (Kachrilas et al., 2019; Platt et al., 2009). Independent of tumor stage and certain molecular alterations, PI3K-Akt pathway is activated in any type of bladder UC (Calderaro et al., 2014). As for any of the cancer-relevant pathways, the role of focal adhesion and PI3K-Akt pathways has poorly been investigated in canine BC (Maeda et al., 2018; Ramsey et al., 2017). The few available reports describe altered ERBB2 and TP53 pathways in canine BC and confirm that molecular alterations are comparable between human and canine BC (Maeda et al., 2018). In the currently studied canine UC tissues, one of the three altered cancer-specific pathways was specific for human BC. This pathway was associated with altered A5SS, and TP53 was the relevant gene with significant differential splicing in the studied BC of dogs. In agreement with previous studies, this observation confirms the resemblance of canine and human BC on a molecular level.

In conclusion, differential gene expression analysis failed to identify any significantly altered genes in the currently assessed canine UC when compared to histomorphologically non-malignant bladder tissue. In contrast, AS was common in the same examined bladder UC tissue samples, with presence of numerous significant differently spliced genes in all assessed types of AS (SE, RI, MXE, A3SS, A5SS). Many of the identified altered genes (*SVIL, PXN, KAT7, ACIN1, TPCN2, SLIT2, MTNR1A, DDR1, APAF1, PKN1, F11R, TCF7L2, ALKBH, COL6A3*) and KEGG pathways (focal adhesion, pathways in cancer, PI3K-Akt signaling among others) are known to be relevant in human BC. Finally, human BC pathway was one of the top ten enriched pathways in the assessed canine UC with differential A5SS. This study is the first to describe AS in canine UC. Results provide evidence that AS is common in UC of dogs, and confirm that canine and human BC share significantly altered cancer-relevant genes and pathways.

6. STUDY 4. Histopathological and immunohistochemical (p63 and Uroplakin III) study of canine benign and malignant prostate tissue

The following study was presented as a short oral communication and poster at the Joint European Congress of Clinical and Anatomical Veterinary Pathology (ECVP-ESVP-ECVCP-ESVCP) in September 2019 in Arnhem, The Netherlands.

Authors' contributions

List of authors (in order as in the oral and poster presentation):

Simone de Brot (SdB), Llorenç Grau-Roma (LGR), Emily White (EW), Tim Scase (TS), Brian Robinson (BDR), Franco Guscetti (FC), Nigel Mongan (NPM)

Contributions:

- SdB contributed to the acquisition of canine tissue and analysis of the epidemiological data (age at the time of tumor diagnosis, neutering status, and dog breed), with support of EW, FC and TS.
- SdB performed the histomorphological and immunohistochemical examinations (including tumor and benign tissue diagnosis and classification), with support of LGR, EW, FC, BDR and TS.
- SdB performed the statistical analysis (using the software SPSS v.24.0), with support of LGR.
- SdB interpreted the data, with support of LGR, BDR and NPM.
- SdB wrote the manuscript, with support of NPM.

6.1 Abstract

Canine PCa (CaPCa) is a highly aggressive type of cancer, arising from glandular, ductal or urethral cells. The histomorphological distinction between PGlC and UC can be challenging. IHC may be useful, however routinely available and established canine markers are limited. The aim of this study was to assess the expression of p63 and UPIII in canine PCa (n=41), in comparison with non-

neoplastic prostate tissue (n=17 normal adult, n=15 hyperplasia, n=16 atrophy, n=14 normal premature).

Based on histomorphology, 18/41 (44%), 16/41 (39%) and 7/41 (17%) were classified as poorly differentiated carcinoma, UC and PGlC, respectively. With the aid of UPIII IHC, 9/18 (50%) of the poorly differentiated carcinomas were further classified as UC, resulting in a total of 25/41 (61%) UC and 7/41 (17%) PGlC. The remaining 9/41 (22%) carcinomas were not further classifiable, compatible with anaplastic carcinoma.

Most PCa contained only scattered p63 positive cells (21/39, 54%) or were p63 negative (14/39, 36%). The remaining 4 cases (10%), characterized by squamous (n=2) or low-grade, urothelial differentiation (n=2), were strongly and almost diffusely p63 positive. In non-neoplastic prostate tissue, nuclear staining for p63 was detected in basal and urothelial cells. The expression of UPIII was absent, weak, moderate or strong in 20/39 (51%), 13/39 (33%), 4/39 (10%) and 2/39 (5%) PCa, respectively and present in <10% of neoplastic cells in most (74%) cases. In non-neoplastic tissue, UPIII expression was limited to prostatic urethra and ducts.

In conclusion, canine PCa is typically characterized by a poor differentiation, which makes the histomorphological distinction between urothelial and glandular carcinomas difficult. P63 expression in canine PCa is typically absent or limited to scattered neoplastic cells. The expression of UPIII in PCa of dogs varies, but tends to be weak if present, most likely corresponding to poorly differentiated UC. For the differentiation of canine UC and PGlC, IHC for UPIII can be helpful for the differentiation of UC and anaplastic, not further classifiable, carcinomas. P63 is of limited value in poorly differentiated canine PCa, but may potentially be a valuable marker for detecting squamous or urothelial differentiation.

6.2 Introduction

In men, PC is the most common type of urological tumor, accounting for 1-2% of all cancers (Humphrey et al., 2016). This is in contrast to animals, which rarely develop this malignancy spontaneously. In fact, only one animal species, the

dog, is known to develop PC on a regular basis (Cornell et al., 2000; Leroy and Northrup, 2009; Obradovich et al., 1987; Teske et al., 2002). The dog has therefore been proposed as an animal model for human prostatic disease (Ittmann et al., 2013; Leroy and Northrup, 2009; Sun et al., 2017; Waters et al., 1998). PC in species other than men and canines is extremely rare or has not been described at all (Caney et al., 1998; LeRoy and Lech, 2004; Leroy and Northrup, 2009). Canine PC is characterized by high tumor grade and aggressive biological behavior with presence of metastasis in up to 40% of dogs at the time of diagnosis (Cornell et al., 2000; Ravicini et al., 2018). PCa is the most common type of prostatic tumor (Meuten and Meuten, 2016), arising from glandular, ductal or urethral epithelial cells. Unfortunately, most cases are diagnosed at late stage of the disease, and the cell of origin often remains unknown (Cornell et al., 2000; Lai et al., 2008a; Leroy and Northrup, 2009; Sorenmo et al., 2004). The histopathological tumor classification tends to be challenging due to poor and heterogeneous differentiation of PCa in dogs (Bryan et al., 2007; Lai et al., 2008a; Leroy and Northrup, 2009; Palmieri and Grieco, 2015; Sorenmo et al., 2004). IHC may be useful for a better tumor characterization, but only few markers are routinely available and have been established in dogs (Gallardo et al., 2007; Lai et al., 2008a; Rivera-Calderon et al., 2016; Romanucci et al., 2016; Wagner et al., 2015).

Prostate-specific antigen (PSA), which is a routinely used, well-established diagnostic as well as prognostic marker for prostatic disease in men (Altwein and Luboldt, 1999; Stamey et al., 1987; Wang et al., 1979), remains controversial in dogs. In contrast to the situation in men, serum PSA fails to significantly increase in dogs with prostate pathologies (Bell et al., 1995). More specifically, this marker could not be detected in the serum or seminal plasma of dogs with or without prostatic disease. In the same study, canine tissue of PCa was however reported to show a slight to moderate PSA expression by IHC. Tissue expression of PSA was also reported to occur in normal canine prostates (Lai et al., 2008b). More specifically, benign acinar, urethral as well as ductal cells showed immunohistochemical staining for this marker. A further prostate-specific marker with relevance in PC of men, the prostate-specific membrane

antigen (PSMA), also failed to directly be applied to dogs so far. In normal prostate tissue of dogs, PSMA could not be identified using different protein detecting methods (Aggarwal et al., 2006). In some cases, PSMA could however be detected in benign prostatic urethral cells (Lai 2008). Since the failure of PSA as a serum marker for canine prostate disorder, the search for alternative potentially high-impact markers has started and is ongoing. To date, a canine marker with comparable sensitivity and specificity as PSA in men has not been identified. So far, the markers with reported highest relevance in the canine genital tract include alkaline phosphatase (AP), carnitine, and CPSE (Alonge et al., 2018a; Chapdelaine et al., 1984b; Gobello et al., 2002; Wolf et al., 2012). Of those, CPSE seems to perform best in detecting prostate disease in dogs. This enzyme was reported to be increased in dogs with benign prostatic hyperplasia (BPH) compared to normal dogs. The level of this marker in the serum did however not significantly differ between BPH, prostatitis and PC (Bell et al., 1995). Furthermore, CPSE expression in PC tissue could not be demonstrated by IHC.

P63, a marker for prostate basal cells, is routinely used for the diagnosis of human PCa (Brimo and Epstein, 2012; Dabir et al., 2012; Epstein et al., 2014; Signoretti et al., 2000). In the normal human gland, acini are lined by a continuous basal cell layer. This layer is however lost during carcinogenesis, and human PCa typically lacks p63 expression. In contrast to the human prostate, the normal canine gland is characterized by a discontinuous basal cell layer, with fewer basal cells than in men (Leav et al., 2001; Romanucci et al., 2016). Therefore, the discontinuity of the basal cell layer is not a diagnostic criteria for canine PC, and basal cell markers are not routinely used for PCa diagnosis in dogs. In the canine and human normal prostate, luminal glandular cells lack p63 expression. In most PCa of men and dogs, the expression of p63 is either absent or restricted to a low number of neoplastic cells (Della Salda et al., 2019; Fonseca-Alves et al., 2018b; Romanucci et al., 2016). One rare subtype of PCa with p63 expression of luminal cells has however been described in both men and dogs (Fonseca-Alves et al., 2018b; Romanucci et al., 2016). P63 is also used

as urothelial marker, and has been proposed to be valuable for differentiating poorly differentiated human glandular prostatic from urothelial carcinoma (Alshenawy and Saied, 2015; Chuang et al., 2007; Kunju et al., 2006; Oh et al., 2016). As far as the authors are aware, comparative studies of p63 in canine urologic malignancies have not been reported.

UPIII, a highly specific but less sensitive marker for urothelial differentiation, may be used in cases of human or canine PCa where UC is a differential diagnosis (Hameed and Humphrey, 2005; Kaufmann et al., 2000; Mhawech et al., 2002; Ramos-Vara et al., 2003). In human PCa, urothelial and prostatic glandular markers are often used in combination and are needed if UC and PC cannot be reliably differentiated based on histomorphology alone. In dogs, prostate markers, either urothelial or glandular, are less well established and usually not used in the routine diagnostic work. UPIII expression was demonstrated in canine PCa, leading to a suggested conclusion that canine PC may have its origin in prostatic ducts (Lai et al., 2008a). Studies reporting the expression of UPIII in canine prostate tissue are however extremely rare. Furthermore, to the authors' best knowledge, studies which describe the combination of p63 and UPIII expression in the canine prostate are currently not available.

The aim of the present study was to assess the expression of p63 and UPIII in canine PCa, in comparison with non-neoplastic prostate tissue.

6.3 Material and methods

Samples

The study was reviewed and approved by the University of Nottingham AWERB and School of Veterinary Medicine and Sciences ethics committees. Informed written consent was obtained from the dog owners upon sample submission. All patient data has been anonymized. Formalin-fixed and paraffin wax-embedded prostate tissue (between one to three complete cross sections of the gland) from 104 male dogs (n=41 carcinoma, n=17 normal gland, n=15 BPH, n=16 glandular atrophy, n=14 neonatal or premature gland) was included. The

41 cases with neoplasia were submitted to Bridge Pathology Ltd. Bristol UK or the Veterinary Pathology Service, University of Nottingham UK, as either biopsies or necropsies. Non-neoplastic prostate tissue was collected from 63 necropsy cases, which were submitted to the University of Nottingham UK. The following case information was available: age at the time of prostate tissue sampling/disease diagnosis, neutering status and dog breed. No follow-up data was available. Within the PC cases, the following breeds were represented: n=12 Labrador retriever, n=5 cross breeds, n=2 Border collies, n=2 Jack Russell terriers, n=2 Rottweiler, n=2 Yorkshire terriers, one of each: Belgian shepherd, boxer, cairn terrier, cocker spaniel, Welsh corgi, field spaniel, flat coated retriever, fox terrier, giant schnauzer, miniature schnauzer, Samoyed, Spanish water spaniel, springer spaniel, Staffordshire bullterrier, viszla, weimaraner. All dogs with normal gland, BPH and neonatal/premature gland were entire. Dogs with diffuse glandular atrophy were either neutered (n=14, surgical castration) or entire (n=2, starvation due to neglect). Cases with cancer were either neutered (n=24), entire (n=7) or of unknown neutering status (n=10). The age of dogs belonging to the different groups were as follows: Neoplasia: Mean 9.63 years (standard deviation (SD) 1.63, standard error of the mean (SEM) 0.27, range 5-13); normal: Mean 3.41 years (SD 2.82, SEM 0.68, range 0.5-11); hyperplasia: Mean 8.07 years (SD 2.56, SEM 0.68, range 3-11); atrophy: Mean 8.53 years (SD 4.17, SEM 1.01, range 2-15); neonatal/premature: 71 days (SD 67.13, SEM 17.94, range 1-212).

Histology

HE-stained tissue sections from all 104 cases were available. The samples were assessed histologically by a board-certified veterinary pathologist (SdB), with support of three certified veterinary pathologists (LGR, FG and TS), and a certified human uropathologist (BDR). IHC with p63 (Agilent Technologies, mouse, 1:100) (n=39 PCa, n=60 non-neoplastic prostates) and UPIII (CellMarque, mouse, 1:100) (n=39 PCa, n=2 normal urinary bladder, n=4 non-neoplastic prostate tissue adjacent to carcinoma) was performed. The following semi quantitative scoring system was used for p63: 0=negative; 1=rare (<5%)

stained cells; 2=moderate number (5-70%) of stained cells; 3=strong staining (>70% of stained cells); for UPIII, staining intensity and distribution were semi-quantified separately, as follows. Positive UPIII staining was defined as a focal, multifocal or diffuse membranous neoplastic cellular staining, of weak to strong intensity. UPIII staining intensity: 0=negative; 1=weak; 2=moderate; 3=strong. UPIII staining distribution (including percentage of stained neoplastic cells): 1=multifocal, <10%; 2=multifocal, 10-80%; 3=multifocal to diffuse, >80%. In a first step, all tumors were classified based on the histomorphology (Humphrey et al., 2016) as i) adenocarcinoma (PGlC), ii) UC or iii) poorly differentiated carcinoma. In a second step, the poorly differentiated carcinomas were re-classified as UC in case they showed positive immunohistochemical UPIII staining. The presence of inflammation was assessed in all cancer cases and semi quantified as follows (including percentage of affected tissue): 0=absent; 1=mild (<5%), 2=moderate (5-50%), 3=severe (>50%).

Statistical analysis

Statistics were performed using SPSS v.24.0 (IBM Corp., Armonk, New York, USA). The Chi-square test was used to test for associations between the dogs' age and any of the assessed histological parameters; between the presence and extent of tumor inflammation and neutering as well as tumor type (urothelial versus non-urothelial), and between neutering and type of tumor. $p < 0.05$ was accepted as significant.

6.4 Results

The examined cancerous prostate tissue was collected from dogs which were surgically neutered [24/41 (59%)] or entire [7/41 (17%)], respectively. The neutering status remained unknown in 10/41 (24%) cases. The mean age of dogs with PCa was 9.63 years (SEM 0.265, SD 1.634, range 5-13). Twenty-two different breeds were affected (see material and methods), with most cases seen in Labradors (12/41, 29%) and cross breeds (5/41, 12%), presumably

representing two of the most common breeds in the UK (https://www.thekennelclub.org.uk/, accessed 13 November 2019). Based on histomorphology, 18/41 (44%), 16/41 (39%) and 7/41 (17%) were classified as poorly differentiated carcinoma, UC and PGlC, respectively. Two cases of UC consisted of a rather well-differentiated neoplastic epithelial growth, with morphology suggestive of urothelium. One case of UC and one case of poorly differentiated carcinoma presented with a diffuse, and multifocal squamous differentiation. With the aid of UPIII IHC (see material and methods), 9/18 (50%) of the poorly differentiated carcinomas were classified as UC, resulting in a total of 25/41 (61%) UC, 7/41 (17%) PGlC, and 9/41 (22%) poorly differentiated carcinomas (Figures 6.1 to 6.7). All but two (39/41, 95%) of PCa were accompanied by a certain degree of inflammatory reaction, which was severe in 20/39 (51%), moderate in 8/39 (21%), and mild in 11/39 (28%) of cases. The inflammation consisted typically of a multifocal to coalescing, lymphoplasmacytic infiltrate. The presence of moderate to severe inflammation (28/41, 68%) was more common in neutered compared to entire dogs ($p<0.02$). The same was true for dogs with UC compared to non-UC ($p<0.05$). When comparing the dogs with urothelial versus non-UC, neutering was significantly ($p<0.001$) more common in the UC group. No significant age differences were observed between UC and PGlC or between entire and neutered dogs, respectively. Immunohistochemical staining for p63 was performed in 39/41 PCa cases and was present in 25/39 (61%). It was characterized by a consistently strong, nuclear signal in a varying number of neoplastic cells. Twenty-one out of 39 (54%) PCa had rare (<5%), individual positive cells (Figure 6.8), 14/39 (36%) lacked p63 expression, and 4/39 (10%) showed p63 staining in a large percent (>70%) of neoplastic cells. None of the cases had only moderate p63 staining, with 5-70% of positive cells. The four cases with strong p63 expression consisted of two well-differentiated, histomorphologically interpreted as urothelial, carcinomas and two carcinomas with squamous differentiation. In the two cases with urothelial morphology, p63 staining was restricted to basal and intermediate epithelial cells. In cases with rare stained neoplastic cells, most cases (16/21, 76%) presented with

Deleted: 1

neoplastic lobules which were multifocally lined by a single layer of strongly stained cells (Figure 6.9). The p63 staining in non-neoplastic glands is summarized in Table 6.1. In benign prostate glandular tissue, p63 staining was limited to basal cells. In normal and hyperplastic glands, the basal cell layer was discontinuous (Figure 6.10), whereas neonatal/premature glands presented with a continuous layer of basal cells (Figure 6.11). In atrophic glands, a mixture of continuous, and to a lesser extent, discontinuous basal cell layers was observed. The urothelium lining prostate duct and urethra showed consistent p63 staining of basal and intermediate cells. Distal, non-urothelial, portions of the duct, however, presented with a multifocally discontinuous layer of stained basal cells. Ejaculatory ducts, which were seen in some tissue sections of normal, hyperplastic and atrophic glands were characterized by a discontinuous basal cell staining. In neonatal/premature dogs, p63 expression was not only seen in basal but also intermediate, and to a lesser extent apical ejaculatory duct cells.

In 39/41 PCa, IHC for UPIII was performed, which was characterized by a variably intense membranous staining, which was most pronounced along luminal surfaces. UPIII expression was negative in 20/39 (51%) of cases or consisted of a weak 13/39 (33%), moderate 4/39 (10%), or strong staining intensity in 2/41 (5%) cases, respectively (Figure 6.12). The distribution and percentage of stained cells was multifocal, <10% in 14/19 (74%), multifocal to diffuse, >80% in 3/19 (16%) or multifocal, 10-80% in 2/19 (11%) of cases. In non-neoplastic prostate tissue, duct as well as urethra presented with apical membranous staining. The co-expression of p63 and UPIII could be assessed in 38/41 cases. Results are provided in Table 6.2. Double negative PCa were most common (11/38, 29%), closely followed by PCa with weak UPIII and rare p63 staining (10/38, 26%). The four PCa cases with strong p63 expression did not express UPIII.

Deleted: 2

Deleted: 3

Deleted: 4

Deleted: 5

6.5 Discussion

The prostate gland of dogs has a comparable morphology and function as in men (Ittmann et al., 2013; Leroy and Northrup, 2009; Sun et al., 2017). Even though less common than in men, PC in dogs occurs spontaneously and on a regular basis (Cornell et al., 2000; Leroy and Northrup, 2009; Obradovich et al., 1987; Teske et al., 2002). This is in contrast to other animals with a prostate, which develop PC extremely rarely or not at all (Caney et al., 1998; LeRoy and Lech, 2004; Leroy and Northrup, 2009). Curative therapeutics, including androgen deprivation therapy, are currently not successful in affected dogs, and mean survival times may be less than three months (Ravicini et al., 2018). Interestingly, neutered, i.e. surgically castrated, dogs are at higher risk to develop PC compared to entire animals, proposing that canines may suffer from a hormone-resistant form of cancer (Bryan et al., 2007; Cornell et al., 2000; Sorenmo et al., 2004; Teske et al., 2002). The present study confirms this observation and shows a trend for neutered dogs to be at higher risk to be diagnosed with PCa. Unfortunately, the cell of origin remains unknown in many cases of canine PCa, primarily due to the similar histomorphology of already advanced disease at the time of diagnosis. Potentially, these neoplasms could originate from prostatic acinar epithelium (containing basal, luminal/secretory and few neuroendocrine cells), urethral urothelium or ductal epithelium. The distinction between acinar, urothelial and ductal carcinoma is important as the different subtypes may differ in their prognosis as well as therapeutic approach. The prognostic significance of the different histologic canine tumor subtypes remains controversial, there is however a tendency for a higher metastatic rate in cancers with a mixed morphology (Cornell et al., 2000).

In addition, knowing the histogenesis of canine PC is crucial when considering using the dog as animal model for PC in men. When comparing UC versus PGlC, the present study shows a higher ratio of neutered dogs in UC compared to PGlC. Similar findings have been described in a study with 76 dogs, which reports a higher risk for entire dogs to suffer from prostate adenocarcinoma

compared to carcinomas with a mixed (including urothelial) morphology (Cornell et al., 2000).

Canine PCa, which develops from either ductal or acinar epithelial cells, is currently further classified as adenocarcinoma or poorly differentiated carcinoma, based on the histomorphological appearance (Owen 1980). In contrast to the human WHO tumor classification system (Humphrey et al., 2016), the WHO classification for tumors in domestic animals (Kennedy 1998) does not include carcinoma of the prostatic urethra in the section of prostatic epithelial tumors. Instead, urethral tumors are included in the WHO classification of Tumors of the Urinary System (Meuten 2004). The histomorphological classification of (prostatic or non-prostatic) urethral tumors are reported to be similar to those in the urinary bladder (Meuten and Meuten, 2016). UC are most common, followed by SSC. Other types of primary urethral carcinomas (e.g. adenocarcinoma or undifferentiated carcinoma) are less common and poorly described in dogs (Norris et al., 1992). Unfortunately, poorly differentiated PCa are not uncommon in dogs, making the histomorphological distinction between PGlC and UC difficult. In the present study, 18 out of 41 (44%) PCa were classified as poorly differentiated carcinomas based on histomorphology alone. IHC can be useful for a better characterization of canine PCa, PC specific markers are however rarely used in the routine veterinary diagnostic work, often due to limited availability, but also due to difficulty in their interpretation (Bassily et al., 2000; LeRoy and Lech, 2004). It has been demonstrated that some canine PCa may express both urothelial and glandular prostate markers, making it even more difficult to distinguish between PGlC and UC in dogs (Cornell et al., 2000; LeRoy and Lech, 2004; Leroy and Northrup, 2009).

Uroplakin, a transmembrane protein expressed by apical urothelial (umbrella) cells, is known to be a specific marker for terminal urothelial differentiation in both men and dogs (Kaufmann et al., 2000; Ramos-Vara et al., 2003), its sensitivity is however often only in the range of 40-60% (Amin et al., 2014;

Chang et al., 2012; Hoang et al., 2015; Kaufmann et al., 2000; Parker et al., 2003) In men, most studies have been performed using UPIII. More recently, UPII has however been shown to be slightly more sensitive (Hoang et al., 2015; Tian et al., 2015). Canine studies which examine the expression of UP in urothelial tumors are limited to UPIII and only rarely include prostate tissue (Fonseca-Alves et al., 2018b; Lai et al., 2008a; Ramos-Vara et al., 2003; Sledge et al., 2015). To the authors' best knowledge, there are currently only two studies which describe the expression of UPIII in canine PCa (Fonseca-Alves et al., 2018b; Lai et al., 2008a). In the more recent work, 47 of 90 PCa expressed UPIII, whereas in non-neoplastic prostate glands, UPIII expression was only observed in urothelial cells of the urethra. Non-neoplastic acini and ducts (not further specified) were reported to lack UPIII expression (Fonseca-Alves et al., 2018b). In the study of Lai et al. (Lai et al., 2008a), a similar percentage (60%) of PCa expressed UPIII, including carcinomas with a micropapillary, cribriform and solid growth pattern. Tumors or tumor areas with a sarcomatoid, acinar/ductal or tubular papillary growth remained UPIII negative (Lai et al., 2008a). Based on the staining with UPIII and other markers, including different cytokeratins, PSA and PSMA, Lai et al. (Lai et al., 2008a) proposed that canine PCa may derive from prostate ducts rather than from acini. Similar to the findings of Fonseca-Alves et al. (Fonseca-Alves et al., 2018b), almost half of all PCa expressed UPIII in the present study. The half of these cases were poorly differentiated carcinomas based on HE staining. Considering that UPIII is known to be highly specific for urothelial differentiation and due to the fact that in the present examined benign canine prostates, convincing membranous UPIII staining was restricted to urethra and proximal ducts, we concluded that UPIII positive cases most likely correspond to prostatic UC. When referring to prostate UC in men (Humphrey et al., 2016), this tumor is presumed to have its origin in the urothelium of the urethra and the proximal ducts. If the same definition is applied to canine UC, UPIII positive canine PCa may either have a ductal, as suggested by Lai et al. (Lai et al., 2008a), or a urethral origin.

P63, which belongs to the p53 family (Arrowsmith, 1999), is one of the more commonly used basal cell as well as urothelial cell marker when diagnosing PCa in men. In this setting, its two main purposes are i) as a basal cell marker, to help distinguishing neoplastic from non-neoplastic prostate tissue by assessing the continuity of the glands' basal cell layer (Dabir et al., 2012; Epstein et al., 2014; Signoretti et al., 2000) and ii) as a marker for urothelial differentiation, to aid in the differentiation between poorly differentiated adenocarcinoma (PGlC) and high-grade UC (Alshenawy and Saied, 2015; Hodges et al., 2010; Kunju et al., 2006; Oh et al., 2016; Srinivasan and Parwani, 2011). In dogs, the first aim of p63 is not directly applicable since the basal cell layer in the healthy canine prostate gland is discontinuous (Leav et al., 2001; Romanucci et al., 2016), which has been confirmed in the present study. Furthermore, the diagnosis of canine PCa is usually straightforward due to advanced disease once the dog is presented with suspicion of PC. IHC is rarely needed in order to distinguish neoplastic from non-neoplastic prostate tissue. In contrast, the differentiation between glandular and urothelial PCa is frequently challenging in cases of canine PC, primarily due to their resembling clinical presentation and poor as well as heterogeneous differentiation at the time of diagnosis (Cornell et al., 2000; Lai et al., 2008a; Palmieri and Grieco, 2015). This has been confirmed in the present study, where 18 out of 41 PCa were poorly differentiated based on histomorphology. In men, p63 is known to be highly specific and moderately sensitive for UC, when compared to PGlC (Alshenawy and Saied, 2015; Kunju et al., 2006). To date, the specificity and sensitivity of p63 for urothelial differentiation remains unknown in dogs with PC, due to a lack of canine studies, which evaluate and compare the expression of p63 between urothelial and glandular prostatic tumors. When referring to the few available canine studies which evaluate p63 in PCa, the tumors are characterized by rare or absent expression of p63 (Della Salda et al., 2019; Fonseca-Alves et al., 2018b; Romanucci et al., 2016), with the exception of a very rare subtype of PGlC, which aberrantly expresses p63 (Fonseca-Alves et al., 2018b). In the present canine cases, p63 expression was either limited to rare (<5%) cells or observed in at least 70% of tumor cells. In agreement with previous studies (Della Salda

et al., 2019), p63 positive neoplastic cells were rare or not detected in most (90%) PCa in the present studied canine tumors. In the cases with only rare, multifocal p63 positive cells, it remains however uncertain if they truly represent individual neoplastic cells or if they correspond to remaining non-neoplastic basal cells, intermingled with the neoplastic growth. Interestingly, more than three quarters of PCa with rare p63 staining showed a discontinuous layer of stained cells, multifocally lining the periphery of the tumors. Most likely, these peripheral rim of stained cells correspond to suspected non-neoplastic basal cells of pre-existing acini or ducts. This finding may be interpreted as follows: i) PCa originates from these acini or ducts and extends into the surrounding parenchyma or ii) PCa spreads within acini or ducts. Both possibilities have been proposed in previous studies (Bostwick et al., 2004; Leav et al., 2001).

The remaining four cases, consisting of two carcinomas with squamous differentiation and two well-differentiated, suspected UC, were characterized by a strong expression of p63. The two cases with squamous morphology most likely represent UC with squamous differentiation, which is common in canine and human UC (Arva and Das, 2011; de Brot et al., 2018; Humphrey et al., 2016). The differential diagnosis, primary prostate squamous cell carcinoma, cannot be ruled out, but was considered less likely due its rare occurrence (Arva and Das, 2011). While squamous cell carcinomas are well known to express p63 in both men and dogs (Mestrinho et al., 2015; Thaiwong et al., 2018), little is known about the level of p63 expression in canine urothelial tumors. In a study including 25 dogs with bladder UC, p63 has been shown to be rarely detected in neoplastic cells, in contrast to a strong expression in urothelial cells of normal and inflamed bladder tissue (Hanazono et al., 2016). As far as the authors are aware, canine studies comparing the p63 expression between urothelial and glandular PCa are lacking.

When combining the two markers, p63 and UPIII, most PCa were either double negative or had a low expression of both UPIII and p63 in the present study. Even if PCa fail to stain with p63 and UPIII, UC cannot be excluded since both

markers have limited sensitivities and because poorly differentiated human and canine, urothelial or non-urothelial, PCa are known to have only rare or absent expression of one or both of these markers (Della Salda et al., 2019; Koga et al., 2003; Romanucci et al., 2016). Considering the high specificity of UPIII, it can however be assumed that a UPIII positive PCa, with or without p63 expression, has a urothelial origin, even if the UPIII staining is only weak and focal. In half of the poorly differentiated PCa, UPIII therefore aided in establishing a final diagnosis of UC in the present canine cases. Interestingly, the two cases consisting of rather well differentiated neoplastic epithelium with strong p63 expression were UPIII negative. Based on histomorphology, these two cases were suggestive of UC even though a ductal, or less likely, glandular origin could not be ruled out with certainty. Further IHC with different urothelial markers would be needed in order to establish a definite diagnosis of UC in these cases. If the suspicion of UC can be confirmed in these cases, p63 would consequently be more sensitive than UPIII for canine prostate UC, which would be comparable to the situation in men (Oh et al., 2016). Alternatively, if these two p63 positive cases were non-urothelial, they may represent rare cases of a prostate basal cell carcinoma or an aberrant p63-expressing PGlC. The five UPIII negative cases with rare p63 expression are difficult to interpret and do not allow to be further classified as either UC or PGlC. Even though the rare p63 positive cells could potentially correspond to neoplastic urothelial cells, it cannot be excluded that these cells represent individual, remaining non-neoplastic prostate basal cells, which would render the tumor p63 negative. Finally, all cases with moderate or strong UPIII expression, which convincingly represent UC, were also p63 positive even though p63 was only detected in a low number of cells. In the examined canine prostate UC, higher expression of UPIII therefore does not appear to correspond to higher p63 expression. In fact, previous studies report that only p63 negative tumor cells expressed UPIII (Koga et al., 2003). It was proposed that loss of p63 is required for terminal urothelial differentiation, in both normal as well as neoplastic urothelium. To the authors' best knowledge, studies evaluating the combination of UPIII and p63 in canine PCa are lacking.

In conclusion, canine PCa is typically characterized by a poor differentiation, which makes the histomorphological distinction between urothelial and glandular carcinomas difficult. P63 expression in canine PCa is typically absent or limited to scattered neoplastic cells. In contrast, in PCa with either squamous differentiation or in few cases of well-differentiated UC, p63 staining tends to be strong. The expression of UPIII in PCa varies, but tends to be weak if present, most likely corresponding to poorly differentiated UC. For the differentiation of canine UC and PGlC, IHC for UPIII can be helpful. In the present study, 50% of anaplastic carcinomas were reclassified as UC with the aid of UPIII. P63 is of limited value in poorly differentiated canine PCa, but may potentially be a valuable diagnostic marker for lower grade carcinomas with squamous or urothelial differentiation.

Deleted: ¶
¶

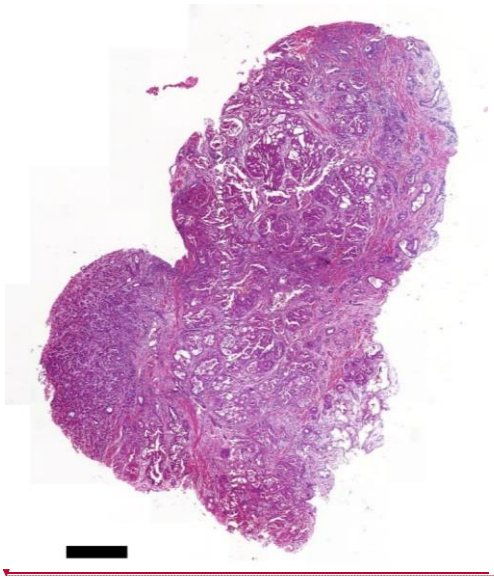


Figure 6.1. Poorly differentiated, UPIII negative prostate carcinoma of a 9-year-old male surgically neutered Labrador retriever. HE. Bar indicates 500 µm.

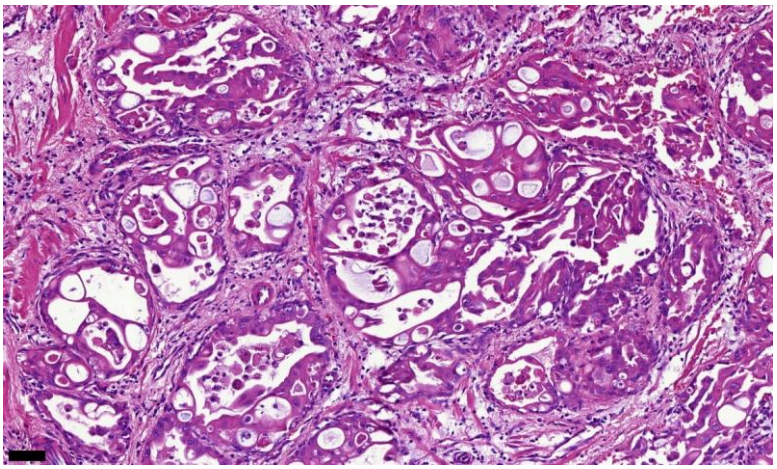


Figure 6.2. Higher magnification of Figure 6.1. Bar indicates 50 µm.

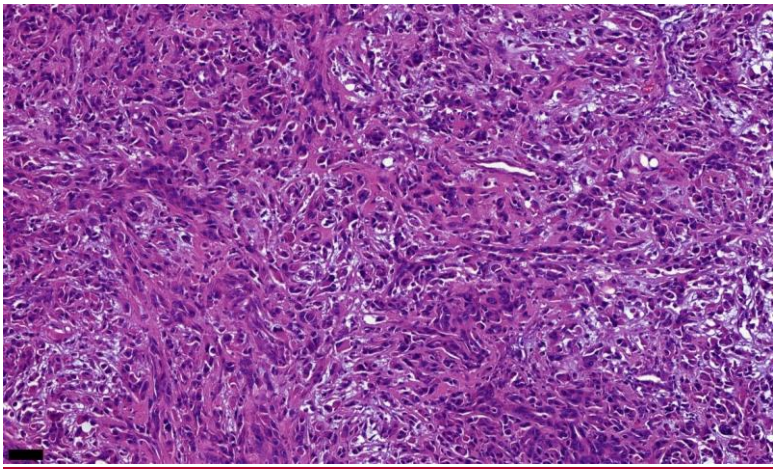


Figure 6.3. Same case as shown in Figure 6.1 and 6.2, depicting an area with a different, predominantly sarcomatous growth pattern. HE. Bar indicates 50 µm.

Formatted: Font: Bold

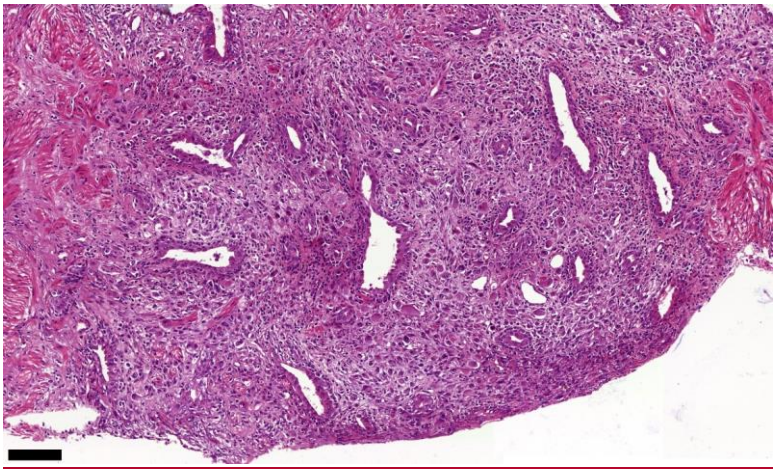


Figure 6.4. Poorly differentiated (suspected glandular), UPIII negative prostate carcinoma of an adult giant schnauzer. Neoplastic cells appear anaplastic and a highly infiltrative growth is evident. HE. Bar indicates 100 µm.

Formatted: Font: Bold

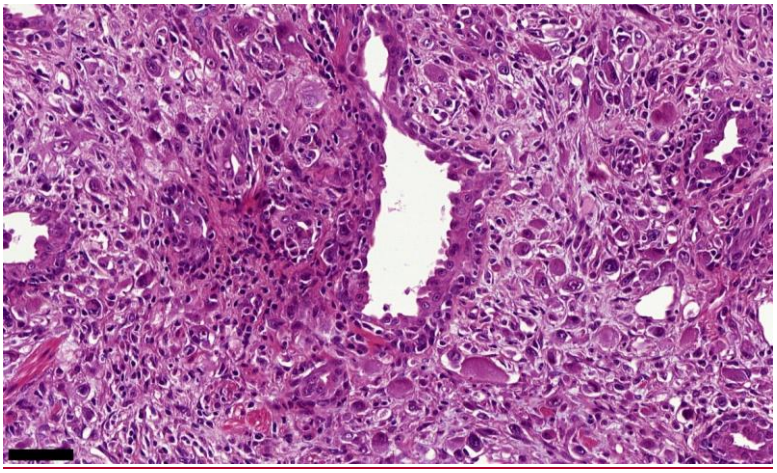


Figure 6.5. Higher magnification of Figure 6.4. Bar indicates 50 µm.

Formatted: Font: Bold

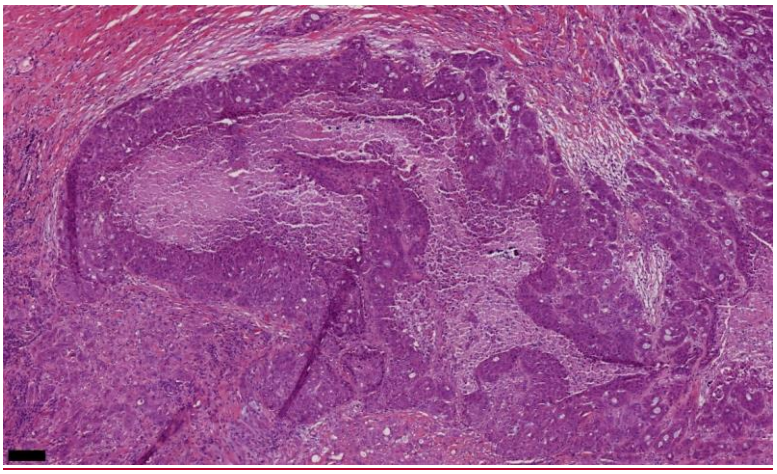


Figure 6.6. Poorly differentiated (suspected urothelial) carcinoma of a 10-year-old male surgically neutered Labrador retriever. Extensive tumor necrosis is present. HE. Bar indicates 100 µm.

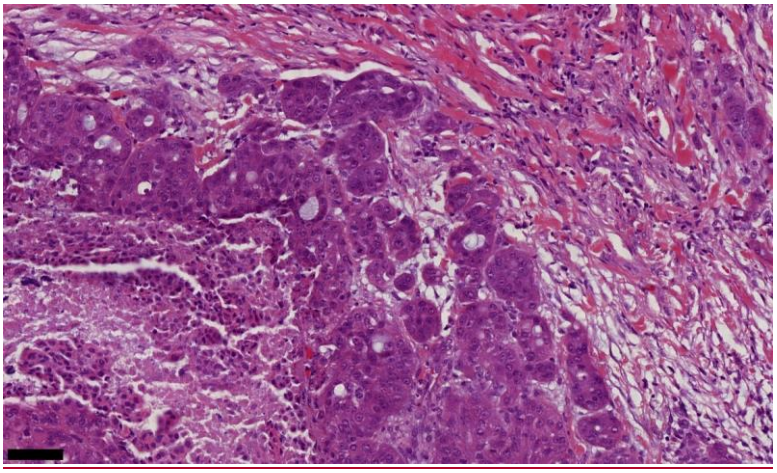


Figure 6.7. Higher magnification of figure 6.6, indicating the highly invasive tumor growth. HE. Bar indicates 50 µm.

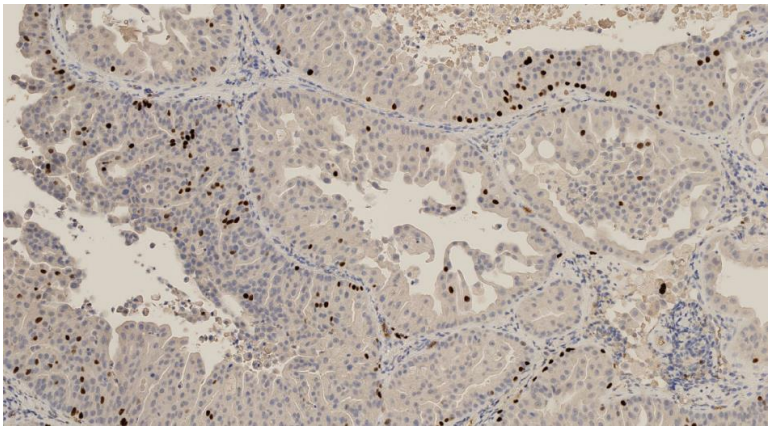


Figure 6.8, P63 IHC of a UC in the prostate of a 9-year-old male neutered Labrador retriever. A low number of neoplastic cells show strong nuclear staining.

Deleted: 1

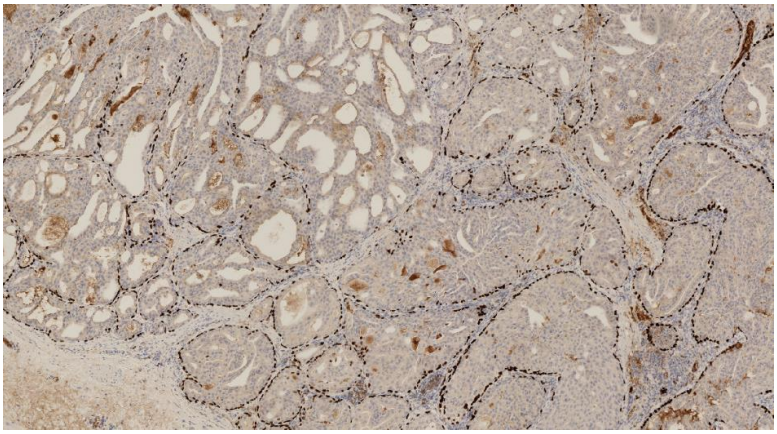


Figure 6.9. P63 IHC of a UC in the prostate of a 11-year-old male neutered Welsh corgi. Multifocally, neoplastic lobules are lined by a single layer of strongly stained cells.

Deleted: 2

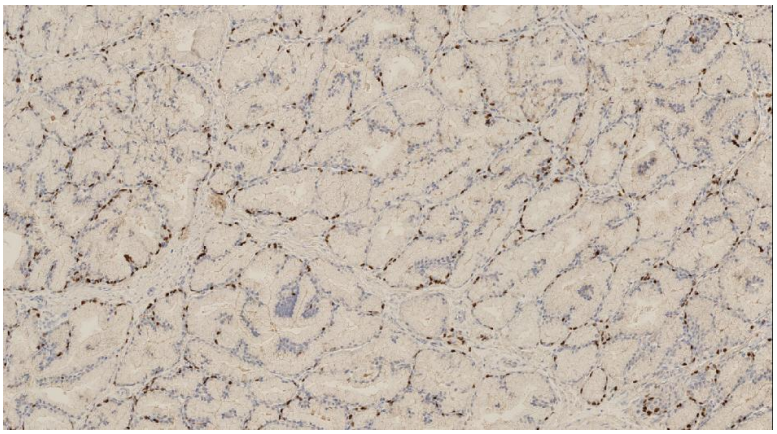


Figure 6.10. P63 IHC of a normal prostate gland from a 9-year-old intact German shepherd x Rottweiler crossbreed dog. Acini are lined by a discontinuous layer of stained basal cells.

Deleted: 3

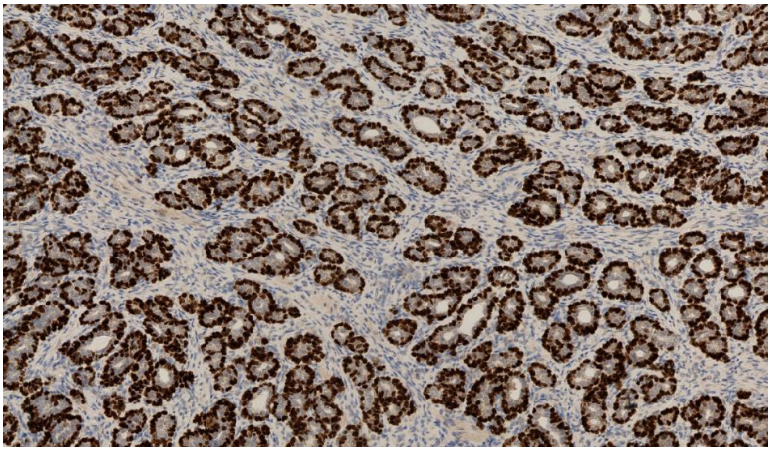


Figure 6.11. P63 IHC of a premature prostate gland from a 8-week-old intact Cavalier King Charles spaniel. Acini are lined by a continuous layer of stained basal cells.

Deleted: 4

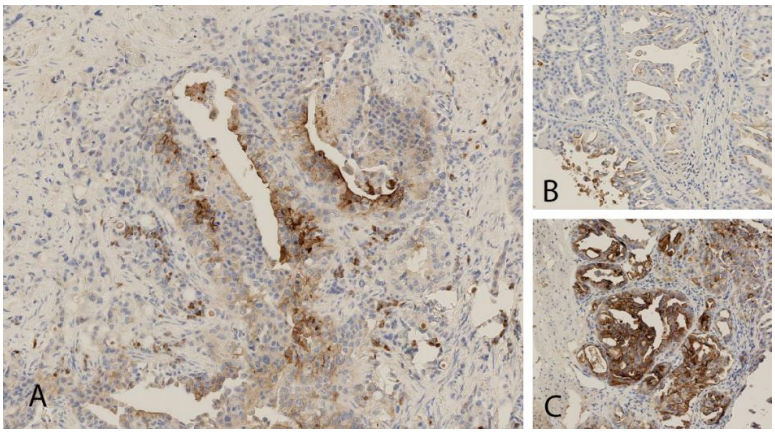


Figure 6.12. UPIII IHC of three different prostate UC with variably intense, multifocal, apical membranous staining of neoplastic cells. A) Moderate, staining in a 10-year-old male neutered Cairn terrier. B) Weak staining in a 11-year-old male neutered Welsh corgi (same case as shown in Figure 6.2). C) Strong staining in a 7-year-old male neutered Yorkshire terrier.

Deleted: 5

Type of cell or anatomic structure	Normal N=17	Hyperplasia N=15	Atrophy N= 16	Neonatal/premature N=14
Acinar basal cells	Discontinuous layer of stained cells	Discontinuous layer of stained cells	Mixed continuous > discontinuous layer of stained cells	Continuous layer of stained cells*
Acinar secretory cells	Negative	Negative	Negative	Negative
Duct	Continuous (distal: discontinuous) layer of stained basal cells	Continuous (distal: discontinuous) layer of stained basal cells	Continuous (distal: discontinuous) layer of stained basal cells	Continuous layer of stained basal cells
Urethra and proximal duct (urothelium)	Basal and intermediate cells are positive	Basal and intermediate cells are positive	Basal and intermediate cells are positive	Basal and intermediate cells are positive
Ejaculatory duct	Discontinuous layer of stained basal cells	Discontinuous layer of stained basal cells	Discontinuous layer of stained basal cells	Discontinuous layer of stained basal, intermediate, and fewer apical cells

Table 6.1. P63 IHC staining of non-neoplastic canine prostate tissue.

*Multifocal discontinuous in areas where glands presented with well-differentiated acinar secretory cells (minimum 3 months of age)

P63 \ UroplakinIII	Negative	Weak	Moderate	Strong	Total
Negative	11	2	0	0	13
Rare (<5%) positive cells	5	10	4	2	21
Strong (>70%) staining	4	0	0	0	4
Total	20	12	4	2	38

Table 6.2. Combined p63 and UroplakinIII immunohistochemical staining of 38 canine prostate carcinomas.

7 STUDY 5. Expression of KDM7A and KDM5B in human prostate carcinoma

Authors' contributions

List of authors (in alphabetical order):

Simone de Brot (SdB), Llorenç Grau-Roma (LGR), Nigel Mongan (NPM), Jenny Persson (JP)

Contributions:

- JP provided the stained tissue microarrays and corresponding clinical diagnoses
- SdB performed the histomorphological and immunohistochemical examinations (including tumor and benign tissue diagnosis and classification), with support of LGR and JP.
- SdB performed the statistical analysis (using the software SPSS v.24.0), with support of LGR.
- SdB interpreted the data, with support of LGR and NPM.
- SdB wrote the manuscript, with support of NPM.

The following study investigates the expression of two potential PCa markers, KDM7A and KDM5B, in human benign and malignant prostate tissue. These two markers were selected since they were considered relevant for PCa based on their recently discovered role as AR co-regulators (personal communication Prof N. Mongan). In addition, these two proteins are known to have a high degree of conservation across species, which renders them valuable to study in animal models. The predicted protein sequences of human and canine KDM5B and KDM7A are 89.88% and 95.79% conserved respectively. Nevertheless, canine tissue has not been included in the present study due to the observed limited specific expression profile in human tissue.

Deleted: So far

Deleted: no

Deleted:

Deleted: ,

Deleted: but the same markers may be evaluated on PCa samples of dogs in the near future

7.1 Abstract

Background: Lysine (K)-specific demethylases (KDMs) are highly conserved chromatin-modifying enzymes, which may be altered in cancer. KDM7A (JHDM1D) and KDM5B (JARID1B, PLU-1) are two types of putative epigenetic regulator, which influence gene transcription. Their role in cancer development, progression and therapy is of interest, but has poorly been investigated until present.

Aims: To assess the level of KDM7A and KDM5B expression in benign and patient-matched malignant human prostate tissue by IHC.

Material and methods: Three TMAs containing a total of n=312 cores collected from n=62 benign and n=62 patient-matched malignant [n=15 metastatic PCa; n=47 organ-confined PCa] human prostatic tissues were assessed and compared for KDM7A and KDM5B expression by IHC.

Results:

KDM7A: Protein expression, either in the cytoplasm or nucleus, was present in the majority of benign (60-89%) and malignant (70-100%) prostate tissues. Within the same TMA, KDM7A expression was higher in organ-confined PCa compared to benign prostate tissue ($p<0.05$). PCa metastases had a highly variable level of expression depending on the site of tumor spread, ranging from 0% (kidney) to 100% (adrenal, liver, testis) of cases, with intermediate values of 67-88% in bone, lymph node and lung. Cytoplasmic expression was reduced in renal ($p<0.05$) and bone ($p<0.001$) metastases compared to the primary tumor. Staining intensity was weak in the majority of benign (50-100%) and malignant (61-100%) samples. Nuclear expression was higher than cytoplasmic staining in organ-confined PCa ($p<0.001$) and benign ($p<0.05$) prostate tissue, which was vice versa in metastatic PCa. Distinct and strong cytoplasmic staining of prostate basal cells was observed in 28-88% (benign) and 0-58% (malignant) of cases.

KDM5B: Protein expression was observed in all assessed benign and malignant tissue cores. Cytoplasmic staining was strong in 82-91% (benign), 78-91% (organ-confined PCa), and 100% (metastatic PCa), with the exception of bone metastases, which had strong staining in 61% of cases. Nuclear staining

intensity was strong in most benign (62-89%) as well as malignant (77-80%) tissues, with significantly decreased nuclear expression in bone metastases compared to benign prostate tissue ($p<0.001$).

Conclusions: KDM7A is weakly expressed in benign and malignant prostate tissue. Cytoplasmic KDM7A expression is higher in benign prostate compared to organ-confined PCa. Nuclear expression is higher in metastatic PCa in comparison to benign prostate tissue. Prostate basal cells frequently present with a distinct and strong cytoplasmic KDM7A expression, suggesting that KDM7A may have potential as basal cell marker. KDM5B is strongly expressed in benign and malignant prostate tissue. In comparison with benign prostate and primary tumors, bone PCa metastases show decreased nuclear KDM5B expression. The high KDM5B expression in the cytoplasm may provide evidence for a non-chromatin linked role for KDM5B.

7.2 Introduction

In cancer epigenetics, histone lysine demethylases (KDMs) play a crucial role (Janardhan et al., 2018). The lysine or arginine residues of histones can be methylated by distinct enzymes, with distinct functional consequences. Lysine side chains may be mono, di, or tri-methylated. The functional consequences of histone H3 lysine methylation at positions 4 (H3K4), 9 (H3K9) and 27 (H3K27) are best understood, with methylation of H3K9 and H3K27 associated with transcriptional repression and H3K4 methylation associated with transcriptional activation. The level of histone methylation does not change the structure of chromatin, but is believed to indirectly influence the level of gene transcription by rendering the DNA more accessible to the transcriptional machinery. Histone lysine methylation can be reverse by KDMs, the expression of which is believed to be regulated in temporal and tissue specific contexts. Different KDMs have different substrate specificities. Consequently, the level of gene activation varies with changing expression of KDMs. The best understood KDM is LSD1/KDM1A (Nilsson 2015, Willmann 2012, Kashyap 2013, Metzger 2005). More recently, the focus of research has turned to understanding the roles of other KDMs, most notably in the context of the

Deleted:

current project, KDM5B and KDM7A. Furthermore, KDMs are characterized by a high level of cross species conservation, which renders them suitable to study in animal models (Fellous 2019).

KDM7A, also known as JHDM1D, specifically demethylates lysine 9 (H3K9) and 27 (H3K27) of histone 3, thereby contributing to increased gene expression (Yang et al., 2010). KDM7A is known to have an important role in the development and differentiation of the nervous system (Tsukada et al., 2010). Its role in cancer development and progression has however only been studied to a limited extent. In 2011, KDM7A has been demonstrated to have a tumor-suppressive effect by downregulating angiogenesis (Osawa et al., 2011). In various cancer cell lines, this enzyme was shown to be highly expressed under nutrient-deprivation conditions. In the context of PC, KDM7A modulates AR expression and AR-positive tumor growth (Lee et al., 2018). Furthermore, it is overexpressed in a castration-resistant PC cell line, and upregulated in PC tissue, in correlation with the Gleason score. Based on this observation, KDM7A could be relevant as therapeutic target. Similar to the situation in PC, KDM7A overexpression and nuclear location has been observed in breast cancer (Meng et al., 2019). This effect was more pronounced in triple negative breast cancer compared to the luminal subtype. Suggested cancer-promoting mechanisms include increased levels of stem cell factors, such as KLF4 and c-MYC, as well as inhibition of apoptosis via upregulation of B-cell lymphoma-2 (Bcl-2).

KDM5B, also known under the names JARID1B or PLU-1, demethylates lysine 4 of histone H3 (H3K4), with a strong repressive effect on gene transcription. The main target genes are important for development, in particular of the nervous system. In normal adult tissue, the expression of KDM5B is mainly restricted to testis (Lu et al., 1999). Benign prostate tissue expresses very low levels of this enzyme (Xiang et al., 2007). Contrary to this, the level of KDM5B is increased in different types of cancer with a promoting effect on tumor initiation, invasion and metastasis (Han et al., 2017). For this reason, this enzyme may be important for therapeutic approaches. In PC, KDM5B is overexpressed, and has

an oncogenic effect through activation of AR target genes (Crea et al., 2012; Ke et al., 2009; Xiang et al., 2007). Tumor metastases had even higher levels of KDM5B compared to primary prostate tumors (Xiang et al., 2007). Its specific role in tumor development and progression remains however uncertain.

Recently, the tumor suppressor microRNA, hsa-miR-137 (miR137) was found to repress expression of an extended network of AR coregulators (Nilsson 2015), including KDM1A, and two additional KDMs (KDM5B and KDM7A) which at the time were not known to be involved in androgen signaling or PC. This led to the hypothesis that KDM5B and KDM7A were involved in androgen signaling in PCa. To test this hypothesis IHC was used to assess the level of expression of KDM7A and KDM5B in benign and malignant human prostate tissue.

7.3 Material and methods

Ethics, study design and patient information

The present case control study was approved by the University of Lund and Umea (Sweden) and the University of Nottingham AWERB and School of Veterinary Medicine and Sciences ethics committees, and the Helsinki Declaration of Human Rights was strictly observed. All patient data was anonymized prior to any performed analysis.

Histology/TMA

TMAs were kindly provided by Prof Jenny Persson (Lund and Umea Universities, Sweden). Before TMAs were created, all cases were examined and a diagnosis was established by a certified human pathologist (Dr. Thanasis Simoulis) by histological analysis of biopsies and staged pre-clinically with organ confined PC. All tissue processing was performed at Lund University using identical procedures. The TMAs were stained with HE stain and were digitally reviewed by a veterinary pathologist (SdB), using the software Aperio ImageScope v12.3.2.5030 (Leica Biosystems Inc., Buffalo Grove, Illinois, USA). TMAs included 1.0 mm in diameter cores from benign and malignant prostate tissue

(PCa), including tumor metastases in distant organs. Three different TMAs were available, with the following tissue characteristics:

Lubb43-10-1B ('block 1'):

N=14 cases with n=2 to 18 tissue cores per case, with a total of n=120 cores. The tissue cores consist of n=14 benign prostate, n=20 primary PCa, n=64 PCa metastases (n=24 bone, n=18 lymph node, n=8 lung, n=6 liver, n=2 adrenal gland, n=2 kidney, n=2 spleen, n=2 testis), and n=22 normal non-prostatic tissues (n=10 bone, n=6 spleen, n=4 liver, n=2 lymph node). All cases had metastatic events.

Lubb43-10:2 ('block 2'):

N=24 cases with n=4 cores per case (n=2 PCa and n=2 benign), with a total of n=96 cores. N=1 case (ID 335) had a metastatic event.

Lubb43-10:3 ('block 3'):

N=24 cases, with n=4 punches per case (n=2 PCa and n=2 benign), with a total of n=96 cores. None of the cases had any metastatic event.

Immunohistochemistry

The IHC staining of the TMAs was kindly performed by Prof Jenny Persson (Lund and Umea Universitites, Sweden). The following antibodies were used: KDM7A (Sigma-Aldrich USA, SAB2101190-5OUG, rabbit polyclonal, 1:100) and KDM5B (Novus Biologicals USA, NB100-97821, rabbit polyclonal, 1:200). All three TMAs were stained at the same time, under identical conditions, using an autostainer. Immunohistochemical scoring and analysis was performed digitally with the software Aperio ImageScope v12.3.2.5030. Staining intensity was scored as 0 (negative), 1 (weak), 2 (moderate), and 3 (strong). The following semi-quantification scheme was applied:

0 < 1% of stained cells

1 1-5% of stained cells

2 6-25% of stained cells

3 26-75% of stained cells

4 76-100% of stained cells

All tissue cores were examined for any IHC staining. The semi-quantification was however restricted to benign or malignant prostate epithelial cells. Control tissue consisted of normal myocardium in all three TMAs.

All IHC tissue cores were reviewed, and excluded if necessary due to poor tissue quality (e.g. lack or minimal amount of tissue, lack of prostate epithelial cells, large tissue folds etc.). In the case of missing evidence for malignancy in HE-stained tissue cores indicated as cancer or vice versa in benign tissues, the cores were re-labelled accordingly.

Statistics

Statistical analysis was performed using SPSS v.26.0 (IBM Corp., Armonk, New York, USA). The Mann-Whitney-U test has been used for the comparison of semi-quantitative values of staining intensity and percentage of stained cells within and between the different disease and tissue groups.

7.4 Results

7.4.1 KDM7A

Block 1

The nuclear and cytoplasmic KDM7A staining of normal prostate and PCa (primary tumor and metastases) was assessed and semi-quantified, with the following results. The staining of normal non-prostatic tissue was assessed, but not further quantified.

Primary and metastatic PCa and normal prostate

The results of the semi-quantitative assessment of KDM7A staining of normal prostate and PCa (primary tumor and metastases) are provided in Table 7.1 and are summarized in Table 7.2. Mean staining values per tissue and tissue group are indicated in Table 7.3 and 7.4, respectively. Cytoplasmic staining of primary PCa was weak in 11/18(61%), moderate in 5/18(28%), and strong in 2/18(11%) of assessable cases. Cytoplasmic staining intensity was weak in all metastatic tumor samples (Figure 7.1) with the exception of one out of 11 assessable lymph node samples (one punch of case 115-5) which showed moderate

staining intensity. Normal prostate tissue presented with equal numbers (4/8; 50%) of samples with weak and moderate cytoplasmic staining intensity (SI) (Figure 7.2). The percentage of stained cells varied between primary and metastatic PCa, between the different tissues with tumor metastases, as well as between individual samples of the same sample group. Both malignant as well as normal prostate tissue samples showed a marked variation in the number of cells with cytoplasmic staining, with less than 1% (semi-quantitative value of 0) until up to 76-100% (semi-quantitative value of 4) of stained cells. On average, both benign as well as malignant prostate tissue had roughly the same percentage of cytoplasmic stained cells, corresponding to the staining category 2, i.e. 6-25% of stained cells. Most cytoplasmic positive cells were seen in metastatic cancer samples of adrenal glands and testis, consisting of up to 100% of stained tumor cells (Figure 7.3). Kidney and bone metastases presented with the lowest percentage of cells with cytoplasmic staining, with significant differences ($p<0.005$) compared to the primary tumor. A complete lack of cytoplasmic positive tumor cells was observed in both tissue cores of the one available case with renal metastases and 12/15(80%) of bone metastases punches. The three remaining punches containing bone metastases had rare to a moderate percentage (26-75%) of cytoplasmic stained cells. Other organs with tumor metastases were characterized by a highly variable range of <1 to 100% (lymph node, lung) and 6-75% (liver) of cytoplasmic stained cells, respectively. Nuclear staining intensity was weak in all primary and metastatic tumor samples (Figure 7.4) as well as in the single positive case of benign prostate tissue. Similar to the situation in cytoplasmic staining, the percentage of nuclear stained cells varied between primary and metastatic PCa, between the different tissues with tumor metastases, as well as between individual samples of the same tissue group. In addition, and in contrast to cytoplasmic staining, benign and malignant prostate tissue differed significantly in the mean percentage of nuclear stained cells, with higher expression in malignant samples ($p<0.05$). PCa samples were characterized by a wide range (between <1 and 100%) of cells with nuclear staining, whereas benign prostate tissue lacked a nuclear signal in all but one case (181-1) which contained 6-25% of

positive nuclei. The mean percentage of cells with nuclear staining was significantly increased compared to the number of cells with cytoplasmic staining in bone metastases ($p<0.05$). Tissues with a comparable mean percentage of cells with cytoplasmic and nuclear staining included primary PCa, as well as tumor metastases in adrenal, liver, lymph node, lung, kidney, and testis. Finally, normal prostate tissue was characterized by a lower mean percentage of cells with nuclear compared to cytoplasmic staining ($p<0.05$). Overall, when comparing primary PCa with tumor metastases (with a separate group for bone metastases) and benign prostate tissue, the mean percentage of cells with cytoplasmic staining was significantly ($p<0.05$) lower in bone metastases. When comparing the mean percentage of cells with nuclear staining, benign prostate tissue had significantly ($p<0.05$) lower values than primary tumor tissue samples. Finally, the mean percentage of cells with nuclear versus cytoplasmic staining differed significantly in bone metastases and normal prostate ($p<0.05$). In benign tissue, cytoplasmic KDM7A expression was more frequent than nuclear positivity ($p<0.05$), whereas the opposite was true for bone metastases.

Prostate basal cells

In benign as well as malignant prostate tissue samples, a variable number of basal cells frequently showed a strong and distinct, cytoplasmic staining for KDM7A (Figure 7.5). The results of the basal cell staining assessment are provided in Table 7.1 and summarized in Table 7.4. When present, basal cell staining was most commonly multifocal, affecting a variable number of glands and typically consisted of a predominantly discontinuous layer of stained cells. Of all n=14 (benign or malignant) cases with basal cell staining, there was only one PCa tissue core (case 147-1), which presented with a predominantly continuous stained basal cell layer. In neoplastic prostate tissue, basal cell staining was observed in 8/21(38%) of cases, with a focal (2/8; 25%) to multifocal (6/8; 75%) distribution, affecting more than 50% of glands in 3/8(38%) of cases (Figure 7.6). In benign prostates, basal cell staining tended to be more frequent compared to neoplastic prostate tissue. Two thirds (6/9;

67%) of all benign prostate tissues presented with a discontinuous layer of stained basal cells, which was seen in one (1/6; 17%), or multiple (5/6; 83%) glands.

Prostate stroma

Only cellular KDM7A staining was assessed, and positive IHC signals in extracellular spaces were excluded from the analysis. The results of the stromal cellular staining are indicated in Table 7.1 and summarized in Table 7.4. Even though a relatively rare finding, few cases of PCa (2/21; 10%) and benign prostate tissue (1/9; 11%) showed individual, strongly (cytoplasmic) stained cells, which were embedded in the prostate stroma. It remains uncertain if these cells correspond to one or several types of stromal, i.e. fibroblastic, vascular, smooth muscular, nervous, or inflammatory cells.

Normal non-prostate tissue

Normal myocardium (Figure 7.7) and liver (Figure 7.8) showed a weak and moderate cytoplasmic KDM7A staining, respectively. Erythrocytes within normal tissue, most evident in bone (Figure 7.9) and spleen (Figure 7.10), were characterized by a consistently, moderate to strong cytoplasmic staining. Intracellular pigments (hemosiderin and lipofuscin) in myocardium and liver stained positive.

Case ID	Tissue	Group	C(%)	C(SI)	N(%)	N(SI)	Basal cell staining	Basal cell continuity	individual cells in stroma
125-11	Adrenal T	M	4	1	4	1	NA	NA	NA
125-11	Adrenal T	M	4	1	4	1	NA	NA	NA
147-3	Bone T	B	0	NA	0	NA	NA	NA	NA
147-3	Bone T	B	0	NA	0	NA	NA	NA	NA
98-3	Bone T	B	0	NA	4	1	NA	NA	NA
98-3	Bone T	B	0	NA	4	1	NA	NA	NA
105-4	Bone T	B	0	NA	1	1	NA	NA	NA
105-4	Bone T	B	0	NA	1	1	NA	NA	NA
115-4	Bone T	B	0	NA	0	NA	NA	NA	NA
115-4	Bone T	B	1	1	1	1	NA	NA	NA
125-4	Bone T	B	0	NA	1	1	NA	NA	NA
165-4	Bone T	B	0	NA	0	NA	NA	NA	NA
165-4	Bone T	B	0	NA	0	NA	NA	NA	NA
193-4	Bone T	B	3	1	3	1	NA	NA	NA
193-4	Bone T	B	3	1	3	1	NA	NA	NA
98-4	Bone T	B	0	NA	3	1	NA	NA	NA
98-4	Bone T	B	0	NA	3	1	NA	NA	NA
98-9	Kidney T	M	0	NA	0	NA	NA	NA	NA
98-9	Kidney T	M	0	NA	0	NA	NA	NA	NA
107-8	Liver T	M	3	1	2	1	NA	NA	NA
107-8	Liver T	M	2	1	1	1	NA	NA	NA
251-8	Liver T	M	2	1	1	1	NA	NA	NA
115-5	LN T	M	2	1	1	1	NA	NA	NA
115-5	LN T	M	1	2	1	1	NA	NA	NA
105-6	LN T	M	0	NA	0	NA	NA	NA	NA
105-6	LN T	M	0	NA	0	NA	NA	NA	NA
107-6	LN T	M	2	1	4	1	NA	NA	NA
107-6	LN T	M	0	NA	3	1	NA	NA	NA
115-6	LN T	M	3	1	2	1	NA	NA	NA
115-6	LN T	M	4	1	4	1	NA	NA	NA
119-6	LN T	M	0	NA	1	1	NA	NA	NA
119-6	LN T	M	0	NA	2	1	NA	NA	NA
251-6	LN T	M	2	1	2	1	NA	NA	NA
98-6	LN T	M	0	NA	2	1	NA	NA	NA
98-6	LN T	M	1	1	2	1	NA	NA	NA
98-6	LN T	M	2	1	3	1	NA	NA	NA
98-6	LN T	M	2	1	3	1	NA	NA	NA
98-6	LN T	M	1	1	3	1	NA	NA	NA
98-6	LN T	M	2	1	3	1	NA	NA	NA
105-7	Lung T	M	0	NA	2	1	NA	NA	NA
105-7	Lung T	M	0	NA	0	NA	NA	NA	NA
125-7	Lung T	M	4	1	4	1	NA	NA	NA
125-7	Lung T	M	4	1	4	1	NA	NA	NA
98-7	Lung T	M	2	1	3	1	NA	NA	NA
98-7	Lung T	M	2	1	3	1	NA	NA	NA
105-1	Prostate	P	0	NA	0	NA	0	NA	0
105-1	Prostate	P	1	2	0	NA	1	D	0
165-1	Prostate	P	4	2	0	NA	3	D	0
165-1	Prostate	P	3	2	0	NA	3	D	0
181-1	Prostate	P	3	1	2	1	3	D	1
193-1	Prostate	X	3	2	0	NA	2	D	0

193-1	Prostate	X	2	1	0	NA	2	D	0
105-2	Prostate	P	1	1	0	NA	0	NA	0
105-2	Prostate	P	1	1	0	NA	0	NA	0
167-2	Prostate T	T	4	2	0	NA	3	D	0
167-2	Prostate T	T	4	2	0	NA	3	D	0
193-2	Prostate T	X	2	2	0	NA	1	D	0
193-2	Prostate T	X	1	3	1	1	1	D	0
147-1	Prostate T	T	0	NA	2	1	2	D	1
147-1	Prostate T	T	2	3	1	1	3	Con	1
147-1	Prostate T	T	0	NA	1	1	0	NA	0
147-1	Prostate T	T	0	NA	1	1	0	NA	0
167-1	Prostate T	T	3	2	0	NA	2	D	0
107-2	Prostate T	T	2	1	3	1	0	NA	0
107-2	Prostate T	T	2	1	3	1	0	NA	0
115-2	Prostate T	T	1	1	1	1	0	NA	0
115-2	Prostate T	T	1	2	2	1	0	NA	0
125-2	Prostate T	T	4	1	4	1	2	D	0
125-2	Prostate T	T	4	1	4	1	0	NA	0
165-2	Prostate T	T	2	1	1	1	0	NA	0
165-2	Prostate T	T	2	1	2	1	0	NA	0
181-2	Prostate T	T	3	1	3	1	0	NA	0
181-2	Prostate T	T	3	1	2	1	0	NA	0
98-2	Prostate T	T	3	1	3	1	0	NA	0
98-2	Prostate T	T	2	1	4	1	0	NA	0
125-10	Testis T	M	4	1	4	1	NA	NA	NA

Table 7.1. Block 1. Semi-quantitative assessment of cytoplasmic and nuclear KDM7A staining of PCa (T) (primary tumor and metastases) and benign prostate tissue (Prostate), as indicated per individual tissue core (with up to 4 cores per case). Also indicated is the staining of prostate basal cells and individual, not further characterized prostate stromal cells. Semi-quantification of C(%) and N(%) was performed as follows: 0: <1%; 1: 1-5%; 2: 6-25%; 3: 26-75%; 4: 76-100% stained cells. Staining intensity was graded as: 1: weak; 2: moderate; 3: strong. The presence of prostate basal cell staining was indicated as follows: 0: Absent; 1: Focal; 2: Multifocal, <50% of glands; 3: Multifocal to diffuse, >50% of glands.

Abbreviations: B: Bone; C: Cytoplasmic staining; Con: Continuous (stained basal cell layer); D: Discontinuous (stained basal cell layer); LN: Lymph node; M: Metastasis; N: Nuclear staining; NA: Not applicable; P: Prostate (benign); SI: Staining intensity; T: Tumor (PCa).

Tissue	C(%)	C(SI)	N(%)	N(SI)
Prostate T	3/21(14 %) 0 3/21(14%) 1 7/21(33%) 2 4/21(19%) 3 4/21(19%) 4	11/18(61%) 1 5/18(28%) 2 2/18(11%) 3	4/21(19%) 0 6/21(29%) 1 4/21(19%) 2 4/21(19%) 3 3/21(14%) 4	17/17(100%) 1
Prostate (benign)	1/9(11%) 0 3/9(33%) 1 1/9(11%) 2 3/9(33%) 3 1/9(11%) 4	4/8(50%) 1 4/8(50%) 2	8/9(89%) 0 1/9(11%) 2	1/1(100%) 1
Adrenal Met	2/2(100%) 4	2/2(100%) 1	2/2(100%) 4	2/2(100%) 1
Bone Met	12/15(80%) 0 1/15(7%) 1 2/15(13%) 3	3/3(100%) 1	5/15(33%) 0 4/15(27%) 1 4/15(27%) 3 2/15(13%) 4	10/10(100%) 1
Kidney Met	2/2(100%) 0	NA	2/2(100%) 0	NA
Liver Met	2/3(67%) 2 1/3(33%) 3	3/3(100%) 1	2/3(67%) 1 1/3(33%) 2	3/3(100%) 1
LN Met	6/17(35%) 0 3/17(18%) 1 6/17(35%) 2 1/17(6%) 3 1/17(6%) 4	10/11(91%) 1 1/11(9%) 2	2/17(12%) 0 3/17(18%) 1 5/17(29%) 2 5/17(29%) 3 2/17(12%) 4	15/15(100%) 1
Lung Met	2/6(33%) 0 2/6(33%) 2 2/6(33%) 4	4/4(100%) 1	1/6(17%) 0 1/6(17%) 2 2/6(33%) 3 2/6(33%) 4	5/5(100%) 1
Testis Met	1/1(100%) 4	1/1(100%) 1	1/1(100%) 4	1/1(100%) 1

Table 7.2. TMA block 1. Overview of the semi-quantitative assessment of cytoplasmic and nuclear KDM7A staining of benign prostate and malignant primary and metastatic PCa (excluding basal cell staining), as indicated per tissue. C(%) and N(%) indicate the percentage of cells with cytoplasmic and nuclear staining, respectively. Semi-quantification of C(%) and N(%) was performed as follows: 0: <1%; 1: 1-5%; 2: 6-25%; 3: 26-75%; 4: 76-100% stained cells. Staining intensity was graded as: 1: weak; 2: moderate; 3: strong.
Abbreviations: C: Cytoplasm; LN: Lymph node; Met: Metastasis; N: Nuclear; NA: Not applicable; SI: Staining intensity; T: Tumor (PCa).

Tissue	Number of cores	C(%)	C(SI)	N(%)	N(SI)	N(%) vs C(%)
Prostate tumor	21	2(±1.31)	1.5(±0.71)	2.18(±1.36) *	1(±0)	↑
Adrenal met	2	4(±0)	1(±0)	4(±0)*	1(±0)	≙
Kidney met	2	0(±0)*	NA	0(±0)	NA	≙
Liver met	3	2.33(±0.58)	1(±0)	1.33(±0.58)	1(±0)	↓
LN met	17	1.29(±1.21)	1.2(±0.3)	2.12(±1.22)	1(±0)	↑
Lung met	6	2(±1.79)	1(±0)	2.67(±1.51)	1(±0)	↑
Testis met	1	4(±0)	1(±0)	4(±0)	1(±0)	≙
Bone met	15	0.47(±1.06)**	1(±0)	1.6(±1.55)	1(±0)	↑*
Prostate (benign)	9	2(±1.32)	1.5(±0.53)	0.22(±0.67)	1(±0)	↓*

Table 7.3. Block 1. Mean values (standard deviations in brackets) of the semi-quantitative assessment of KDM7A staining of PCa (primary tumor and metastases) and normal prostate, as indicated per tissue. Semi-quantification of C(%) and N(%) was performed as follows: 0: <1%; 1: 1-5%; 2: 6-25%; 3: 26-75%; 4: 76-100% stained cells. Staining intensity was graded as: 1: weak; 2: moderate; 3: strong.

Abbreviations: C: Cytoplasm; LN: Lymph node; met: Metastasis; N: Nuclear; SI: Staining intensity.

*significantly different ($p<0.05$); **highly significant different ($p<0.001$). For the parameters C(%) and N(%), the significant differences refer to the variations between the values of malignant compared to benign prostate tissue. For the column 'N(%) vs C(%)', significant differences refer to variations between N(%) and C(%) values.

↑: N(%) is higher than C(%); ↓: N(%) is lower than C(%); ≙: N(%) and C(%) are comparable.

Group	Number of cores	C(%)	C(SI)	N(%)	N(SI)	N(%) vs. C(%)	Prostate basal cell staining	Stained basal cell layer continuity	Presence of stained prostate stromal cells
T	21	2 (±1.31)	1.5 (±0.71)	2.18 (±1.36)	1 (±0)	↑	Absent 13/21(62%) Focal 2/21(10%) Multifocal moderate[a)] 3/21(14%) Multifocal to diffuse[b)] 3/21(14%)	Discontinuous 7/8(87.5%) Continuous 1/8(12.5%)	2/21(10%)
Met (M)	31	1.71 (±1.49)	1.05 (±0.71)	2.19 (±1.36)	1 (±0)	↑	NA	NA	NA
Bone met (B)	15	0.47* (±1.06)	1 (±0)	1.6 (±1.55)	1 (±0)	↑*	NA	NA	NA
Benign prostate (P)	9	2 (±1.32)	1.5 (±0.53)	0.22* (±0.67)	1 (±0)	↓*	Absent 3/9 (33%) Focal 1/9(11%) Multifocal, moderate[a)] 2/9(22%) Multifocal to diffuse[b)] 3/9(33%)	Discontinuous 6/6(100%)	1/9(11%)

Table 7.4. Block 1. Mean values (standard deviations in brackets) of the semi-quantitative assessment of cytoplasmic and nuclear KDM7A staining of PCa (primary tumor and metastases) and normal prostate, as indicated per tissue group. Also indicated is the staining of prostate basal cells and individual, not further characterized prostate stromal cells. Semi-quantification of C(%) and N(%) was performed as follows: 0: <1%; 1: 1-5%; 2: 6-25%; 3: 26-75%; 4: 76-100% stained cells. Staining intensity was graded as: 1: weak; 2: moderate; 3: strong

Abbreviations: C: Cytoplasmic staining; Met: Metastasis (any organ except bone); N: Nuclear staining; NA: Not applicable; P: Prostate (benign); SI: Staining intensity; T: Primary tumor (PCa);

[a)]<50% of glands with basal cell staining; [b)]≥50% of glands with basal cell staining

*significantly different ($p<0.05$). For the parameters C(%) and N(%), the significant differences refer to the variations between the values of malignant compared to benign prostate tissue. For the column 'N(%) vs C(%)', significant differences refer to variations between N(%) and C(%) values.

↑: N(%) is higher than C(%); ↓: N(%) is lower than C(%).

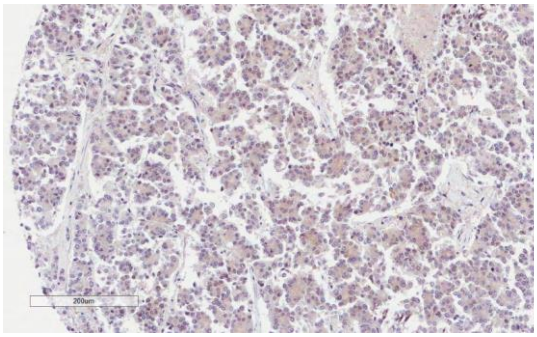


Figure 7.1. Case 107-8. PCa metastasis in the liver with weak, diffuse cytoplasmic and multifocal weak nuclear staining. KDM7A IHC.

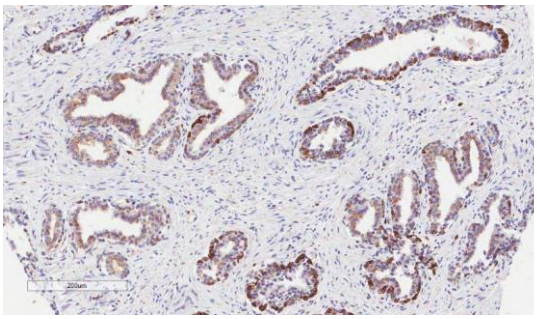


Figure 7.2. Case 165-1. Benign prostate tissue with weak to moderate cytoplasmic staining. Note the multifocally strongly cytoplasmic stained basal cells. KDM7A IHC.

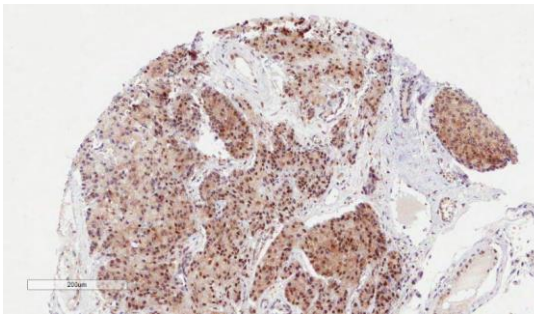


Figure 7.3. Case 125-10. PCa metastasis in the testis. Diffuse weak to moderate, cytoplasmic and multifocal nuclear staining of neoplastic cells. KDM7A IHC.

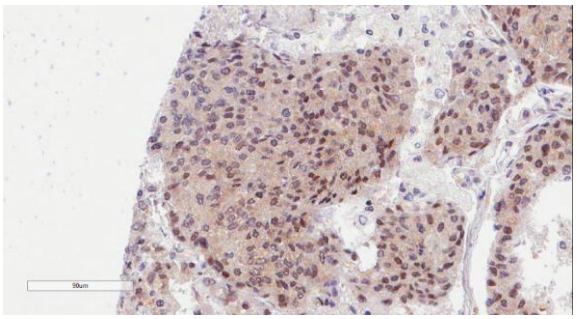


Figure 7.4. Case 125-7. PCa metastasis in the lung with diffuse weak cytoplasmic and multifocal nuclear staining. KDM7A IHC.

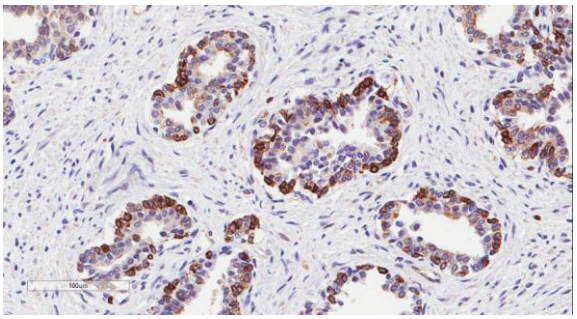


Figure 7.5. Case 165-1. Benign prostate tissue with strong and distinct cytoplasmic staining of basal cells and weak cytoplasmic staining of acinar cells. KDM7A IHC.

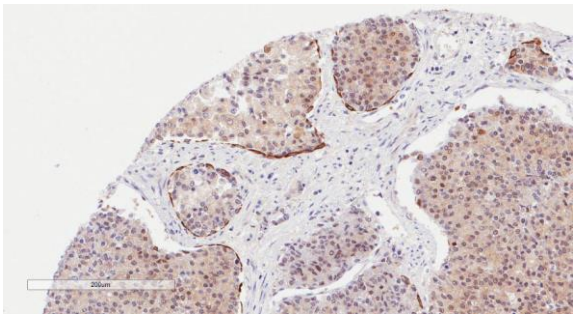


Figure 7.6. Case 125-2. PCa with diffuse weak cytoplasmic and multifocal nuclear staining of tumor cells and multifocal strong cytoplasmic staining of basal cells. KDM7A IHC.

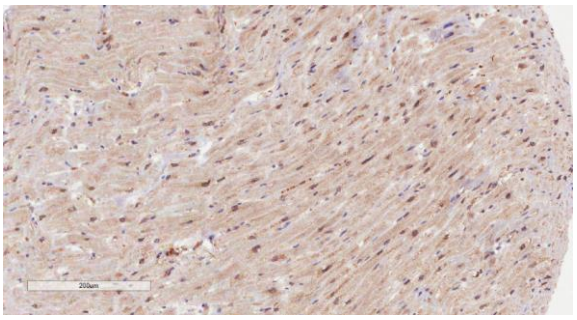


Figure 7.7. Normal myocardium (control) with weak diffuse cytoplasmic and multifocal nuclear staining. KDM7A IHC.

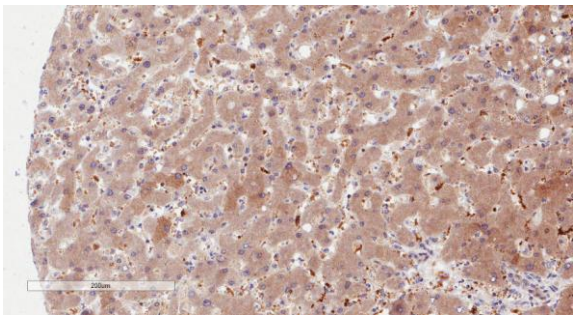


Figure 7.8. Case 125-15. Normal liver with moderate, diffuse cytoplasmic staining of hepatocytes. KDM7A IHC.

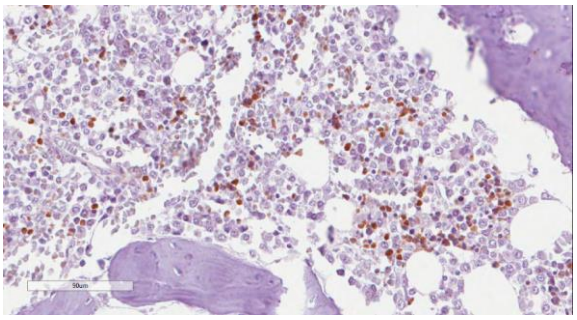


Figure 7.9. Case 224-4. Normal bone marrow with multifocal moderate to strong cytoplasmic staining of hematopoietic cells and erythrocytes. KDM7A IHC.

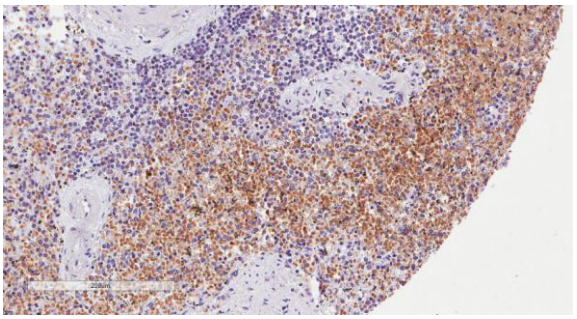


Figure 7.10. Case 251-12. Normal spleen with strong cytoplasmic staining of erythrocytes within the red pulp. KDM7A IHC.

Block 2

The nuclear and cytoplasmic KDM7A staining of benign and malignant (PCa) prostate tissue was assessed and semi-quantified, with the following results. Tissue cores, which were histologically not clearly identifiable as either benign or neoplastic were classified as 'X' (uncertain malignancy). These samples were assessed for KDM7A staining, but not further used for statistical analysis and interpretation.

Malignant and benign prostate

The results of the semi-quantitative assessment of KDM7A staining of benign and malignant prostate tissue are provided in Table 7.5 and are summarized in Table 7.6. Mean staining values per tissue group are indicated in Table 7.7. Cytoplasmic staining was weak in the majority of malignant (27/36; 75%) and benign (14/25; 56%) tissue samples (Figure 7.11). A substantial number of malignant (7/36; 19%) and benign (10/25; 40%) samples presented with moderately intense cytoplasmic staining (Figure 7.12), whereas strong staining was relatively rare and limited to one and two cases of benign tissue and PCa, respectively. All tumor cases had a positive KDM7A cytoplasmic staining, the percentage of stained cells varied however significantly between the different samples. The majority of malignant tissues (21/36; 58%) had 26-100% of positive cells, whereas KDM7A staining was seen in 25% or less of tumor cells in 15/36(42%) of cases. Benign tissue samples presented with cytoplasmic KDM7A staining in 25/34(74%) of cases, which was slightly less common compared to 88% of cases with cytoplasmic staining in malignant tissue samples. Accordingly, the mean values of the semi-quantitative assessment of cytoplasmic staining was significantly ($p<0.05$) higher in malignant (2.67) compared to benign (1.91) prostate tissue. Comparable to malignant prostate tissue, the percentage of stained benign cells varied significantly. In approximately equal numbers of cases, the percentage of stained cells was either less (13/34; 38%) or more (12/34; 35%) than 26%. Nuclear staining intensity was weak in all assessable benign and malignant prostate tissue samples (Figure 7.13). In contrast to the cytoplasmic staining, the relative

number of cases with nuclear staining was comparable between benign (15/34; 44%) and malignant (16/36; 44%) tissues. When present, the percentage of nuclear stained cells was less than 26% in the majority of both benign (12/16; 75%) and PCa (13/15; 87%) samples. The mean values of the semi-quantitative assessment of the nuclear staining was not significantly different between malignant and benign tissue. In PCa ($p<0.001$) and benign tissue ($p<0.05$), the mean percentage of cells with nuclear staining was significantly decreased compared to cells with cytoplasmic staining.

Prostate basal cells

In benign as well as malignant prostate tissue samples, a variable number of basal cells frequently showed a strong and distinct, cytoplasmic staining for KDM7A. The results of the basal cell staining assessment are provided in Table 7.5 and summarized in Table 7.7. When present, basal cell staining was most commonly multifocal, affecting a variable number of glands and typically consisted of a predominantly discontinuous layer of stained cells. Of all n=51 cases with basal cell staining, only a minority of tumor (1/21; 5%) and benign (4/30;13%) cases presented with a predominantly continuous layer of stained basal cells (Figure 7.14). Basal cell staining was significantly ($p<0.01$) more common in benign (30/34; 88%) compared to malignant (21/36; 58%) tissue. Similarly, the number of cases with widespread, multifocal basal cell staining, affecting >50% of glands, tended to be higher in benign (17/30; 57%) compared to malignant (7/21; 33%) prostate samples.

Prostate stroma

Only cellular KDM7A staining was assessed, and positive IHC signals in extracellular spaces were excluded from the analysis. Even though not a consistent finding, a substantial number of prostate tumors (8/36; 22%) and benign tissue (5/34; 15%) showed individual, strongly (cytoplasmic) stained cells, which were embedded in the prostate stroma (Figure 7.15). It remains uncertain if these cells correspond to one or several types of stromal, i.e. fibroblastic, vascular, smooth muscular, nervous, or inflammatory cells.

Case ID	Group	C(%)	C(SI)	N(%)	N(SI)	Basal cell staining	Basal cell continuity	individual cells in stroma
278	P	2	2	0	NA	2	D	0
291	P	4	2	1	1	3	Con	1
291	P	4	2	2	1	3	D	0
313	P	4	2	2	1	(2)	D	0
335	P	3	1	1	1	3	D	0
336	P	0	NA	0	NA	0	NA	0
386	P	0	NA	0	NA	(2)	D	0
431	P	0	NA	0	NA	0	NA	0
441	P	0	NA	0	NA	3	D	0
441	P	0	NA	0	NA	3	D	0
527	P	1	2	0	NA	(2)	D	0
527	P	1	1	0	NA	2	D	0
555	P	4	3	0	NA	0	NA	0
623	P	0	NA	0	NA	3	Con	0
623	P	1	1	0	NA	3	D	0
644	P	2	1	2	1	(2)	D	1
744	P	0	NA	0	NA	3	D	0
744	P	0	NA	0	NA	3	D	0
850	P	2	1	1	1	3	D	1
985	P	1	1	0	NA	1	D	1
986	P	4	1	1	1	(2)	D	0
986	P	3	2	0	NA	3	D	0
988	P	2	1	1	1	3	D	0
988	P	1	1	1	1	(1)	D	0
991	P	2	1	2	1	1	D	0
991	P	3	2	0	NA	3	D	0
994	P	4	2	0	NA	3	Con	0
994	P	4	2	0	NA	3	Con	1
996	P	1	1	1	1	(2)	D	0
996	P	0	NA	0	NA	3	D	0
1000	P	2	2	2	1	3	D	0
1000	P	2	1	2	1	0	NA	0
1013	P	4	1	4	1	(2)	D	0
1013	P	4	1	4	1	(2)	D	0
278	T	2	1	0	NA	0	NA	0
278	T	3	1	0	NA	0	NA	0
291	T	4	1	0	NA	0	NA	0
291	T	2	1	0	NA	2	D	1
313	T	3	1	2	1	0	NA	0
313	T	4	1	2	1	2	D	0
386	T	3	1	0	NA	(2)	D	1
386	T	3	1	0	NA	2	D	0
390	T	1	1	0	NA	2	D	0
390	T	1	1	0	NA	2	D	0
431	T	1	1	0	NA	1	D	0
441	T	2	3	0	NA	3	D	1
527	T	2	3	0	NA	3	D	1
527	T	1	1	0	NA	0	NA	0
555	T	2	1	1	1	0	NA	0

623	T	1	2	1	1	0	NA	1
623	T	2	1	0	NA	2	D	0
644	T	2	1	2	1	0	NA	0
644	T	3	1	2	1	0	NA	0
744	T	3	2	0	NA	3	D	0
850	T	4	1	4	1	2	D	1
981	T	4	1	4	1	0	NA	0
981	T	4	1	4	1	0	NA	0
985	T	4	1	0	NA	3	D	1
986	T	4	1	0	NA	3	D	0
988	T	1	2	0	NA	(2)	D	0
991	T	3	2	0	NA	3	D	0
991	T	1	1	0	NA	0	NA	0
994	T	3	2	1	1	0	NA	1
994	T	3	1	1	1	(2)	D	0
996	T	4	1	1	1	2	D	0
996	T	3	1	1	1	(2)	D	0
1000	T	4	2	3	1	2	D	0
1000	T	3	1	2	1	0	NA	0
1013	T	2	1	2	1	0	NA	0
335*	T	4	2	0	NA	0	Con	0
313	X	4	1	3	1	0	NA	0
390	X	3	2	0	NA	3	D	1
390	X	2	1	1	1	2	D	1
431	X	1	1	0	NA	2	D	0
431	X	1	2	0	NA	2	D	0
441	X	2	3	0	NA	3	D	0
555	X	4	2	0	NA	2	D	0
644	X	0	NA	2	1	2	D	0
850	X	3	2	1	1	3	D	1
850	X	4	2	0	NA	3	D	0
985	X	4	1	1	1	0	NA	0
986	X	4	1	3	1	(2)	D	0
988	X	1	1	0	NA	1	D	0

Table 7.5. Block 2. Semi-quantitative assessment of cytoplasmic and nuclear KDM7A staining of PCa (T) and benign prostate tissue (P), as indicated per individual tissue core (with up to 4 cores per case). Also indicated is the staining of prostate basal cells and individual, not further characterized prostate stromal cells. Semi-quantification of C(%) and N(%) was performed as follows: 0: <1%; 1: 1-5%; 2: 6-25%; 3: 26-75%; 4: 76-100% stained cells. Staining intensity was graded as: 1: weak; 2: moderate; 3: strong. The presence of prostate basal cell staining was indicated as follows: 0: Absent; 1: Focal; 2: Multifocal, <50% of glands; 3: Multifocal to diffuse, >50% of glands. Values in brackets indicate the presence of only rare stained basal cells.

Abbreviations: C: Cytoplasmic staining; Con: Continuous (stained basal cell layer); D: Discontinuous (stained basal cell layer); N: Nuclear staining; NA: Not applicable; P: Prostate (benign); SI: Staining intensity; T: Primary tumor (PCa); X: Prostate tissue of uncertain malignancy.

*only case with known metastatic event

Group	C(%)	C(SI)	N(%)	N(SI)
T	7/36(19%) 1 8/36(22%) 2 11/36(31%) 3 10/36(28%) 4	27/36(75%) 1 7/36(19%) 2 2/36(6%) 3	20/36(56%) 0 6/36(17%) 1 6/36(17%) 2 1/36(3%) 3 3/36(8%) 4	16/16(100%) 1
P	9/34 (26%) 0 6/34(18%) 1 7/34(21%) 2 3/34(9%) 3 9/34(26%) 4	14/25(56%) 1 10/25(40%) 2 1/25(4%) 3	19/34(56%) 0 7/34(21%) 1 6/34(18%) 2 2/34(6%) 4	15/15(100%) 1
X	1/13(8%) 0 3/13(23%) 1 2/13(15%) 2 2/13(15%) 3 5/13(38%) 4	6/12(50%) 1 5/12(42%) 2 1/12(8%) 3	7/13(54%) 0 3/13(23%) 1 1/13(8%) 2 2/13(15%) 3	6/6(100%) 1

Table 7.6. Block 2. Overview of the semi-quantitative assessment of cytoplasmic and nuclear KDM7A staining of malignant (T) and benign (P) prostate tissue (excluding basal cell staining), as indicated per tissue group. The group 'X' includes prostate tissue of uncertain malignancy. C(%) and N(%) indicate the percentage of cells with cytoplasmic and nuclear staining, respectively. Semi-quantification of C(%) and N(%) was performed as follows: 0: <1%; 1: 1-5%; 2: 6-25%; 3: 26-75%; 4: 76-100% stained cells. Staining intensity was graded as: 1: weak; 2: moderate; 3: strong.

Abbreviations: C: Cytoplasm; N: Nuclear; P: Prostate (benign); SI: Staining intensity; T: Tumor (PCa).

Group	Number of cores	C(%)	C(SI)	N(%)	N(SI)	N(%) vs. C(%)	Basal cell staining	Basal cell continuity	Presence of stained prostate stromal cells
T	36	2.67* (±1.10)	1.31 (±0.58)	0.92 (±1.27)	1(±0)	↓**	Absent 15/36(42%)* Focal 1/36(3%) Multifocal moderate[a)] 13/36(36%) Multifocal to diffuse [b)] 7/36(19%)	Discontinuous 20/21(95%) Continuous 1/21(5%)	8/36(22%)
P	34	1.91 (±1.56)	1.48 (±0.59)	0.79 (±1.12)	1(±0)	↓*	Absent 4/34(12%) Focal 3/34(9%) Multifocal moderate 10/34(29%) Multifocal to diffuse 17/34(50%)	Discontinuous 26/30(87%) Continuous 4/30(13%)	5/34(15%)
X	13	2.54 (±1.45)	1.58 (±0.67)	0.85 (±1.14)	1(±0)	↓	Absent 2/13(15%) Focal 1/13(8%) Multifocal moderate 6/13(46%) Multifocal to diffuse 4/13(31%)	Discontinuous 11/11(100%)	3/13(23%)

Table 7.7. Block 2. Mean values (standard deviation in brackets) of the semi-quantitative assessment of cytoplasmic and nuclear KDM7A staining of PCa (T) and benign prostate tissue (P), as indicated per tissue group. Also indicated is the staining of prostate basal cells and individual, not further characterized prostate stromal cells. Semi-quantification of C(%) and N(%) was performed as follows: 0: <1%; 1: 1-5%; 2: 6-25%; 3: 26-75%; 4: 76-100% stained cells. Staining intensity was graded as: 1: weak; 2: moderate; 3: strong

Abbreviations: C: Cytoplasmic staining; N: Nuclear staining; NA: Not applicable; P: Prostate (benign); SI: Staining intensity; T: Primary tumor (PCa); X: Prostate tissue of uncertain malignancy.

[a)]<50% of glands; [b)]≥50% of glands

*significantly different ($p<0.05$); **highly significant different ($p<0.001$). For the parameters C(%) and 'basal cell staining', the significant differences refer to the variations between the values of malignant compared to benign prostate tissue. For the column 'N(%) vs C(%)', significant differences refer to variations between N(%) and C(%) values.

↓: N(%) is lower than C(%).

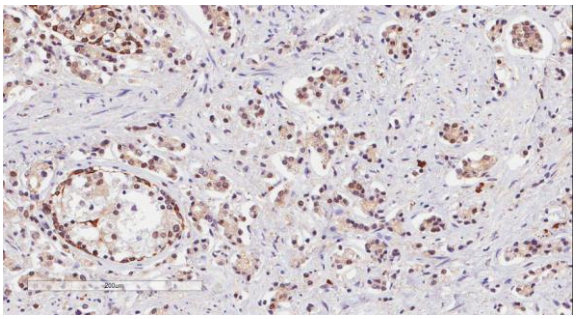


Figure 7.11. Case 850. PCa with diffuse weak cytoplasmic and multifocal weak to moderate nuclear staining. Note the strong cytoplasmic staining of remaining basal cells. KDM7A IHC.

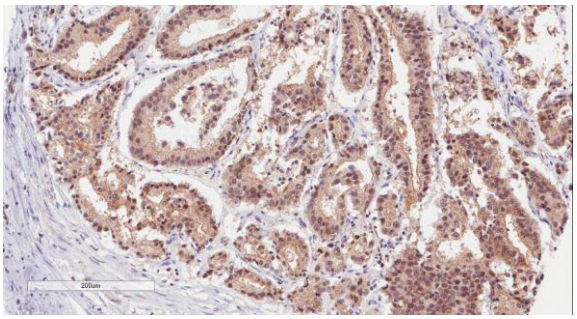


Figure 7.12. Case 335. PCa with diffuse, moderate cytoplasmic and multifocal weak to moderate nuclear staining. KDM7A IHC.

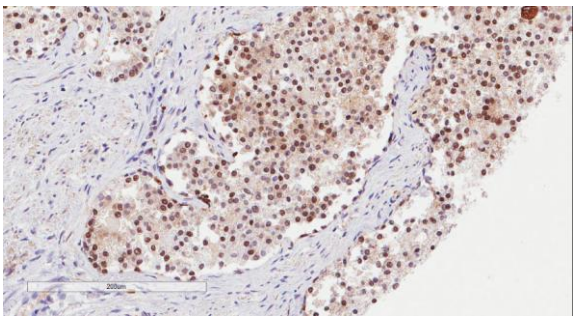


Figure 7.13. Case 1013. PCa with diffuse weak cytoplasmic and multifocal moderate to strong nuclear staining. KDM7A IHC.

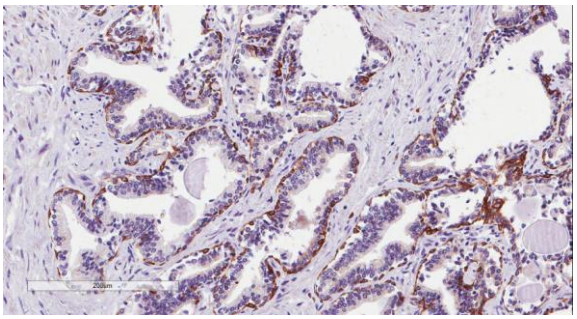


Figure 7.14. Case 623. Benign prostate tissue with a multifocally continuous layer of strongly (cytoplasmic) stained basal cells. KDM7A IHC.

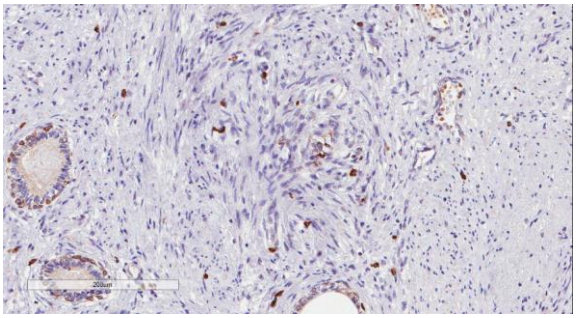


Figure 7.15. Case 850. Benign prostate with individual strongly (cytoplasmic) stained stromal cells. KDM7A IHC.

Block 3

The nuclear and cytoplasmic KDM7A staining of benign (P) and malignant (PCa) prostate tissue was assessed and semi-quantified, with the following results. Tissue cores, which were histologically not clearly identifiable as either benign or neoplastic were classified as 'X' (uncertain malignancy). These samples were assessed for KDM7A staining, but not further used for statistical analysis and interpretation.

Malignant and benign prostate

The results of the semi-quantitative assessment of KDM7A staining of benign and malignant prostate tissue are provided in Table 7.8 and are summarized in Table 7.9. Mean staining values per tissue group are indicated in Table 7.10. The presence of cytoplasmic staining tended to be more common in PCa (16/23; 70%) compared to benign tissue (12/25; 48%). Cytoplasmic staining was weak in the majority of malignant (14/16; 88%) and benign (8/12; 67%) tissue samples. The remaining cases showed moderately intense cytoplasmic staining. When present, half of the malignant and benign tissue samples had more than 75% (Figure 7.16) and less than 6% (Figure 7.17) of stained cells, respectively. Accordingly, the mean percentage of cytoplasmic stained cells were significantly ($p<0.05$) higher in PCa compared to benign tissue. Nuclear staining was weak in all assessable benign (15/15; 100%) and most (14/16; 88%) malignant tissues (Figure 7.18). The two remaining PCa samples had moderately intense staining of the nuclei. The percentage of cells with nuclear staining was comparable between PCa (16/23; 70%) and benign tissue (15/25; 60%). In benign tissue, nuclear staining was seen in a maximum of 25% of cells, whereas malignant tissue had a highly variable number of stained cells, ranging from 1 to 100%. The mean percentage of nuclear stained cells was comparable between PCa and benign tissue. In both malignant and benign tissues, the mean percentage of cells with nuclear staining was similar compared to the amount of cells with cytoplasmic expression.

Prostate basal cells

Limited to a few cases (7/25; 28%) of benign prostate tissue samples, a variable number of basal cells frequently showed a strong and distinct, cytoplasmic staining for KDM7A. The results of the basal cell staining assessment are provided in Table 7.8 and summarized in Table 7.10. Basal cell staining was significantly more common in benign compared to malignant prostate tissue ($p<0.01$), with complete absence of stained basal cells in any of the cancer tissue cores. When present, basal cell staining was multifocal, affecting a variable number of glands and consisted of a predominantly discontinuous layer of stained cells (Figure 7.19). In approximately equal number of benign cases, the basal cell staining was present in less (4/7; 57%) or more (3/7; 43%) than half of the glands.

Prostate stroma

Only cellular KDM7A staining was assessed, and positive IHC signals in extracellular spaces were excluded from the analysis. Even though not a consistent finding, a substantial number of prostate tumors (2/23; 9%) and benign tissues (5/25; 20%) showed individual, strongly stained cells, which were embedded in the prostate stroma (Figure 7.20). It remains uncertain if these cells correspond to one or several types of stromal, i.e. fibroblastic, vascular, smooth muscular, nervous, or inflammatory cells.

Case ID	Group	C(%)	C(SI)	N(%)	N(SI)	Basal cell staining	Basal cell continuity	individual cells in stroma
1015	T	3	1	0	NA	0	NA	0
1017	T	4	1	0	NA	0	NA	0
1017	T	4	1	0	NA	0	NA	0
1056	T	4	1	1	1	0	NA	0
1056	T	4	1	0	NA	0	NA	0
1069	T	0	NA	1	1	0	NA	1
1069	T	0	NA	1	1	0	NA	0
1070	T	3	1	2	1	0	NA	0
1070	T	3	1	2	1	0	NA	0
1140	T	2	1	2	2	0	NA	0
1140	T	3	1	3	2	0	NA	0
1104	T	2	1	1	1	0	NA	0
1104	T	3	1	1	1	0	NA	0
1105	T	0	NA	2	1	0	NA	0
1107	T	0	NA	0	NA	0	NA	1
1111	T	0	NA	1	1	0	NA	0
1111	T	0	NA	0	NA	0	NA	0
1024	T	4	1	3	1	0	NA	0
1024	T	4	2	3	1	0	NA	0
1032	T	4	1	3	1	0	NA	0
1032	T	4	2	4	1	0	NA	0
1140	T	1	1	1	1	0	NA	0
1140	T	0	NA	0	NA	0	NA	0
1021	P	0	NA	(1)	(1)	0	NA	0
1021	P	0	NA	(1)	(1)	0	NA	0
1045	P	1	1	1	1	0	NA	0
1051	P	0	NA	0	NA	0	NA	0
1051	P	0	NA	1	1	0	NA	0
1056	P	3	1	2	1	0	NA	0
1056	P	3	1	2	1	0	NA	0
1068	P	0	NA	1	1	0	NA	0
1068	P	0	NA	2	1	0	NA	0
1070	P	0	NA	2	1	0	NA	0
1070	P	0	NA	1	1	0	NA	0
1083	P	1	1	1	1	0	NA	0
1083	P	3	1	2	1	0	NA	0
1085	P	1	1	0	NA	2	D	0
1085	P	2	1	2	1	2	D	0
1086	P	2	2	0	NA	2	D	0
1086	P	1	2	0	NA	2	D	0
1093	P	2	2	0	NA	3	D	1
1093	P	1	2	0	NA	3	D	1
1107	P	0	NA	0	NA	0	NA	1
1107	P	0	NA	0	NA	0	NA	1
1111	P	0	NA	0	NA	3	D	0
1111	P	0	NA	0	NA	0	NA	0
1114	P	0	NA	1	1	0	NA	1
1114	P	1	1	1	1	0	NA	0
1014	X	1	1	0	NA	2	D	0
1014	X	3	1	1	1	0	NA	0

1014	X	0	NA	1	1	0	NA	0
1014	X	1	1	1	1	0	NA	0
1015	X	2	2	1	1	0	NA	0
1015	X	0	NA	1	1	0	NA	1
1021	X	0	NA	(1)	(1)	0	NA	0
1021	X	0	NA	(1)	(1)	0	NA	0
1032	X	4	1	3	1	0	NA	0
1032	X	4	2	3	2	0	NA	0
1051	X	0	NA	2	1	0	NA	0
1068	X	1	1	2	1	1	D	0
1068	X	1	1	2	1	0	NA	0
1069	X	1	1	1	1	0	NA	1
1069	X	1	1	1	1	0	NA	1
1083	X	3	1	2	1	0	NA	0
1083	X	2	1	2	1	0	NA	0
1086	X	1	1	0	NA	2	D	1
1086	X	0	NA	1	1	0	NA	1
1088	X	1	1	1	1	0	NA	0
1088	X	0	NA	1	1	0	NA	0
1093	X	0	NA	0	NA	0	NA	0
1093	X	1	1	0	NA	1	D	1
1105	X	0	NA	1	1	0	NA	0
1105	X	1	1	2	1	0	NA	0
1105	X	0	NA	0	NA	0	NA	0
1114	X	0	NA	1	1	0	NA	0
1114	X	2	1	1	1	0	NA	1

Table 7.8. Block 3. Semi-quantitative assessment of cytoplasmic and nuclear KDM7A staining of PCa (T) and benign prostate tissue (P), as indicated per individual tissue core (with up to 4 cores per case). Also indicated is the staining of prostate basal cells and individual, not further characterized prostate stromal cells. Semi-quantification of C(%) and N(%) was performed as follows: 0: <1%; 1: 1-5%; 2: 6-25%; 3: 26-75%; 4: 76-100% stained cells. Staining intensity was graded as: 1: weak; 2: moderate; 3: strong. The presence of prostate basal cell staining was indicated as follows: 0: Absent; 1: Focal; 2: Multifocal, <50% of glands; 3: Multifocal to diffuse, >50% of glands. Values in brackets indicate the presence of only rare stained nuclei with only very weak staining intensity.

Abbreviations: C: Cytoplasmic staining; D: Discontinuous (stained basal cell layer); N: Nuclear staining; NA: Not applicable; P: Prostate (benign); SI: Staining intensity; T: Primary tumor (PCa); X: Prostate tissue of uncertain malignancy.

Group	C(%)	C(SI)	N(%)	N(SI)
T	7/23(30%) 0 1/23(4%) 1 2/23(9%) 2 5/23(22%) 3 8/23(35%) 4	14/16(88%) 1 2/16(13%) 2	7/23(30%) 0 7/23(30%) 1 4/23(17%) 2 4/23(17%) 3 1/23(4%) 4	14/16(88%) 1 2/16(13%) 2
P	13/25(52%) 0 6/25(24%) 1 3/25(12%) 2 3/25(12%) 3	8/12(67%) 1 4/12(33%) 2	10/25(40%) 0 9/25(36%) 1 6/25(24%) 2	15/15(100%) 1
X	11/28(39%) 0 10/28(36%) 1 3/28(11%) 2 2/28(7%) 3 2/28(7%) 4	15/17(88%) 1 2/17(12%) 2	5/28(18%) 0 15/28(54%) 1 6/28(21%) 2 2/28(7%) 3	22/23(96%) 1 1/23(4%) 2

Table 7.9. Block 3. Overview of the semi-quantitative assessment of cytoplasmic and nuclear KDM7A staining of malignant (T) and benign (P) prostate tissue (excluding basal cell staining), as indicated per tissue group. The group 'X' includes prostate tissue of uncertain malignancy. C(%) and N(%) indicate the percentage of cells with cytoplasmic and nuclear staining, respectively. Semi-quantification of C(%) and N(%) was performed as follows: 0: <1%; 1: 1-5%; 2: 6-25%; 3: 26-75%; 4: 76-100% stained cells. Staining intensity was graded as: 1: weak; 2: moderate; 3: strong.

Abbreviations: C: Cytoplasm; N: Nuclear; P: Prostate (benign); SI: Staining intensity; T: Tumor (PCa).

Group	Number of cores	C(%)	C(SI)	N(%)	N(SI)	N(%) vs. C(%)	Basal cell staining	Basal cell continuity	Presence of stained cells in stroma
T	23	2.26* (±1.71)	1.13 (±0.34)	1.35 (±1.23)	1.13 (±0.34)	↓	Absent 23/23(100%)*	NA	2/23(9%)
P	25	0.67 (±1.07)	1 (±0.6)	1.06 (±0.8)	1 (±0.46)	↑	Absent 18/25(72%) Multifocal moderate[a)] 4/25(16%) Multifocal to diffuse[b)] 3/25(12%)	Discontinuous 7/7(100%)	5/25(20%)
X	28	1.08 (±1.21)	1.15 (±0.33)	1.29 (±0.82)	1.05 (±0.21)	↑	Absent 24/28(86%) Focal 2/28(7%) Multifocal moderate 2/28(7%)	Discontinuous 4/4(100%)	7/28(25%)

Table 7.10. Block 3. Mean values (standard deviation in brackets) of the semi-quantitative assessment of cytoplasmic and nuclear KDM7A staining of PCa (T) and benign prostate tissue (P), as indicated per tissue group. Also indicated is the staining of prostate basal cells and individual, not further characterized prostate stromal cells. Semi-quantification of C(%) and N(%) was performed as follows: 0: <1%; 1: 1-5%; 2: 6-25%; 3: 26-75%; 4: 76-100% stained cells. Staining intensity was graded as: 1: weak; 2: moderate; 3: strong

Abbreviations: C: Cytoplasmic staining; N: Nuclear staining; NA: Not applicable; P: Prostate (benign); SI: Staining intensity; T: Primary tumor (PCa); X: Prostate tissue of uncertain malignancy.

[a)]<50% of glands; [b)]≥50% of glands; *significantly different ($p<0.05$). For the parameters C(%) and 'basal cell staining', the significant differences refer to the variations between the values of malignant compared to benign prostate tissue.

↑: N(%) is higher than C(%); ↓: N(%) is lower than C(%).

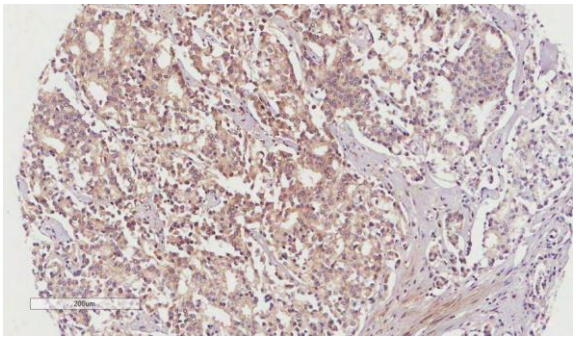


Figure 7.16. Case 1056. PCa with diffuse weak cytoplasmic staining of neoplastic cells. KDM7A IHC.

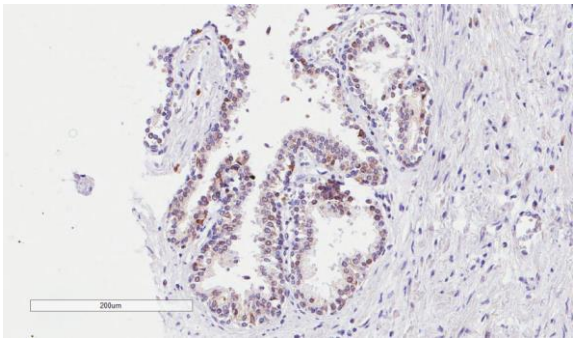


Figure 7.17. Case 1085. Benign prostate with less than 1-5% of cells with weak cytoplasmic and occasional weak nuclear staining. KDM7A IHC.

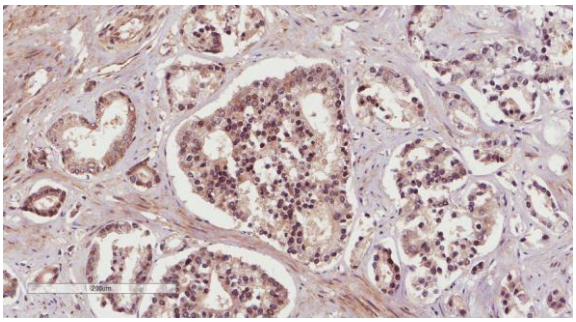


Figure 7.18. Case 1070. PCa with diffuse weak cytoplasmic and multifocal weak to moderate nuclear staining. KDM7A IHC.

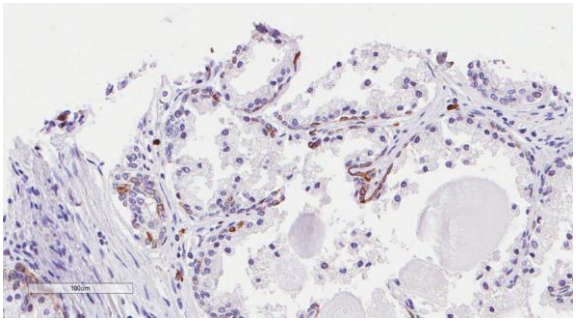


Figure 7.19. Case 1105. Benign prostate with a discontinuous layer of strongly (cytoplasmic) stained basal cells. KDM7A IHC.

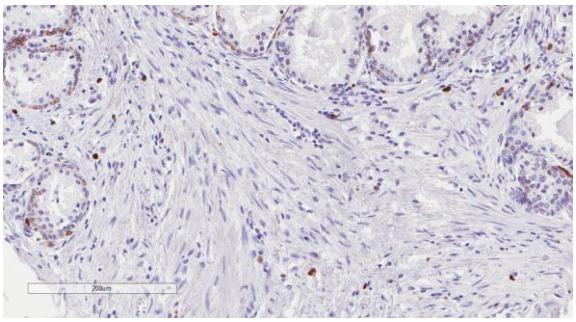


Figure 7.20. Case 1093. Benign prostate with individual strongly (cytoplasmic) stained stromal cells. KDM7A IHC.

Comparative KDM7A staining of all three blocks

The nuclear and cytoplasmic KDM7A staining of benign prostate (blocks 1, 2 and 3) and organ-confined (blocks 1 and 2) and metastatic (block 1) PCa tissue was compared, with the following results. Tissue cores, which were histologically not clearly identifiable as either benign or neoplastic (tissue group 'X') (see Tables 7.5-7.10) were excluded.

Primary and metastatic PCa and normal prostate

The results of the semi-quantitative assessment of KDM7A staining of benign and malignant prostate tissues are summarized in Table 7.11. Mean cytoplasmic and nuclear staining was weak, or between weak and moderate in all groups, with comparable semi-quantitative values, ranging from 1 to 1.5. In contrast, the mean percentage of cells with cytoplasmic or nuclear staining varied between the different disease groups as well as between the different tissue groups within the same group of disease. The mean percentage of cells with cytoplasmic staining was highest in organ-confined PCa, ranging between the semi-quantitative values of more than 2 (i.e. 6-25% of cells) and less than 3 (i.e. 26-75% of cells). Within the different tissue groups and blocks of metastatic PCa and benign prostate, the mean percentage of cytoplasmic stained cells was variable, but in general relatively low with maximal semi-quantitative values of 2, corresponding to 6-25% of stained cells. Bone metastases had the lowest semi-quantitative value (0.47, corresponding to less than 5% of stained cells) for the mean percentage of cells, which was significantly ($p<0.05$) decreased when compared to the primary tumor. The mean percentage of cells with nuclear staining was highest in metastatic PCa, with almost identical semi-quantitative values of 2.18 and 2.19 (corresponding to slightly more than 25% of cells) in primary and metastatic tumor, respectively. Bone metastases had lower mean percentages of nuclear stained cells, ranging between the semi-quantitative values of 1 (i.e. 1-5% of cells) and 2 (i.e. 6-25% of cells), which were significantly ($p<0.05$) lower compared to benign tissue on the same TMA. Benign prostate tissue had the lowest mean percentage of cells with nuclear

staining, with semi-quantitative values of 0.22 to 1.06 (corresponding to approximately 5% or less stained cells), with similar results for organ-confined PCa, which had mean semi-quantitative values of 0.92 to 1.35. Organ-confined PCa ($p<0.001$ in one of two TMAs) and benign prostate tissue ($p<0.05$ in two of three TMAs) had significantly lower mean percentages of nuclear compared to cytoplasmic stained cells. The opposite was true for metastatic PCa, with significant values for bone metastases ($p<0.05$). The ratio of the percentage of cells with nuclear versus cytoplasmic staining was contrary between the two blocks with BPH.

Prostate basal cells

Ranging from none (organ-confined PCa) to 88% (benign prostate) of cases, a variable number of basal cells frequently showed a strong and distinct, cytoplasmic staining for KDM7A (Table 7.11). When present, basal cell staining was most commonly multifocal, affecting a variable number of glands and consisted of a predominantly discontinuous, and rarely continuous, layer of stained cells. The number of cases with basal cell staining was variable between the different disease groups as well as tissue groups and blocks. In two of the three TMAs, basal cell staining was significantly ($p<0.01$) more common in benign compared to malignant prostate tissue.

Prostate stroma

Only cellular KDM7A staining was assessed, and positive IHC signals in extracellular spaces were excluded from the analysis. Even though with variable frequencies between the different disease and tissue groups and blocks, all benign and malignant tissue groups contained a significant number (9-22%) of cases, which showed low numbers of individual, strongly stained cells, which were embedded in the prostate stroma. It remains uncertain if these cells correspond to one or several types of stromal, i.e. fibroblastic, vascular, smooth muscular, nervous, or inflammatory cells.

Disease group	Tissue group	Block		C(%)	C(SI)	N(%)		N(SI)	N(%) vs. C(%)	Basal cell staining				Basal cell continuity	Presence of stained cells in stroma
										Absent	Focal	Multifocal moderate[a)]	Multifocal to diffuse[b)]		
Organ-confined PCa[1)]	T	2		2.67 (±1.10)	1.31 (±0.58)	0.92 (±1.27)		1 (±0)	↓**	15/36* (42%)	1/36 (3%)	13/36 (36%)	7/36 (19%)	1/21(5%)Con, 20/21(95%)D	8/36(22%)
	T	3		2.26 (±1.71)	1.13 (±0.34)	1.35 (±1.23)		1.13 (±0.34)	↓	23/23* (100%)	0	0	0	NA	2/23(9%)
Metastatic PCa	T	1	***	2 (±1.31)	1.5 (±0.71)	2.18 (±1.36)		1 (±0)	↑	13/21 (62%)	2/21 (10%)	3/21 (14%)	3/21 (14%)	1/8(12.5%)Con, 7/8(87.5%)	2/21(10%)
	Met	1		1.71 (±1.49)	1.05 (±0.71)	2.19 (±1.36)		1 (±0)	↑			NA		NA	NA
	Bone Met	1		0.47 (±1.06)	1 (±0)	1.6 (±1.55)	*	1 (±0)	↑*			NA		NA	NA
Benign	P	1		2 (±1.32)	1.5 (±0.53)	0.22 (±0.67)		1 (±0)	↓*	3/9 (33%)	1/9 (11%)	2/9(22%)	3/9(33%)	6/6(100%)D	1/9(11%)
	P	2		1.91 (±1.56)	1.48 (±0.59)	0.79 (±1.12)		1 (±0)	↓*	4/34 (12%)	3/34 (9%)	10/34(29%)	17/34(50%)	4/30(13%)Con, 26/30(87%)D	5/34(15%)
	P	3		0.67 (±1.07)	1 (±0.6)	1.06 (±0.8)		1 (±0.46)	↑	18/25(72%)	0	4/25(16%)	3/25(12%)	7/7(100%)D	5/25(20%)

Table 7.11. Summary of KDM7A staining of benign and malignant prostate tissue. Indicated are mean values (standard deviation in brackets) of the semi-quantitative assessment of cytoplasmic and nuclear staining as well as the staining of prostate basal cells and individual prostate stromal cells. Semi-quantification of C(%) and N(%) was performed as follows: 0: <1%; 1: 1-5%; 2: 6-25%; 3: 26-75%; 4: 76-100% stained cells. Staining intensity was graded as: 1: weak; 2: moderate; 3: strong

Abbreviations: C: Cytoplasmic staining; Con: Continuous; Met: Metastasis; N: Nuclear staining; NA: Not applicable; P: Prostate (benign); SI: Staining intensity; T: Primary tumor (PCa)

[1)]Organ-confined disease in all except one case (335), which had a metastatic event; [a)]<50% of glands; [b)]≥50% of glands.

*significantly different ($p<0.05$); **highly significant different ($p<0.001$). For the parameter 'Basal cell staining', the significant differences refer to variations between the values of malignant compared to benign prostate tissue. For the column 'N(%) vs C(%)', significant differences refer to variations between N(%) and C(%) values.[1)]Organ-confined disease in all except one case (335), which had a metastatic event.

7.4.2 KDM5B

Antibody optimization: comparison of antibody dilutions of 1:100 vs 1:200

At first attempt, an antibody dilution of 1:100 was used, which resulted in a diffusely strong nuclear and cytoplasmic KDM5B staining of benign and malignant prostate tissue (Figures 7.21 and 7.22).

More specifically, all tissue cores presented with a diffuse cytoplasmic and nuclear staining, with a strong cytoplasmic staining intensity in all except two cases of organ-confined PCa, which had moderate staining. Similarly, all tissue cores had strong nuclear staining, except n=7 (n=3 organ-confined PCa, n=2 lymph node and n=2 bone PCa metastases) tissue cores, which presented with moderate nuclear staining intensity. Due to a consistent strong staining, without recognizable differences between the different types of tissue, the staining was repeated, using an antibody dilution of 1:200, as described below.

KDM5B staining was assessed in benign and malignant prostate parenchyma. Results are described separately for each of the three blocks. The staining of the stroma of benign and malignant tissues was diffuse and moderate, without visible differences between the different tissues (Figure 7.23). Therefore, the stromal staining has not been assessed further.

Block 1

The nuclear and cytoplasmic KDM5B staining of benign prostate and PCa (primary tumor and metastases) was assessed and semi-quantified, with the following results. The staining of normal non-prostatic tissue was assessed, but not further quantified.

Primary and metastatic PCa and normal prostate

The results of the semi-quantitative assessment of KDM5B staining of benign prostate and PCa (primary tumor and metastases) are provided in Table 7.12 and are summarized in Table 7.13. Mean staining values per tissue and tissue group are indicated in Tables 7.14 and 7.15, respectively. Cytoplasmic staining of primary and non-osseous metastatic PCa was strong in all cases (Figures 7.24

and 7.25). In bone metastases, a significant number (9/23; 39%) had moderately intense cytoplasmic staining (Figure 7.26), which was strong in the remaining cases. Benign prostate gland had strong cytoplasmic staining (Figure 7.27) in all but one case, which had a moderate staining intensity. Accordingly, the mean values of cytoplasmic staining intensities were comparable between primary as well as metastatic PCa and benign prostate, with the exception of bone metastases, which had a significantly ($p<0.001$) less intense staining. The percentage of KDM5B cytoplasmic stained cells was high, i.e. 75-100% of cells were positive, in all benign and malignant tissue cores. The same was true for nuclear KDM5B staining. In contrast, the staining intensity of the nuclei varied between and within the different disease and tissue groups. The majority of normal (8/10; 80%) and primary PCa (17/22; 77%) had intense nuclear staining, with moderate staining intensity in the remaining cases. PCa metastases varied in their nuclear staining, depending on the tissue (Figure 7.28). PCa metastases in the lung and testis had strong nuclear staining in all cases, whereas the staining was moderate in the kidney. Other organs had variable nuclear staining intensity, ranging from weak to moderate. When comparing the mean values of the nuclear KDM5B staining intensity, PCa metastases in the bone had significantly ($p<0.001$) less intense nuclear staining compared to primary PCa (Tables 7.14 and 7.15) (Figure 7.29). Tumor metastases in other tissues as well as normal prostate tissue did not differ significantly in their nuclear staining intensity compared to primary PCa. With the exception of PCa metastases in the lung and testis, which had strong nuclear and cytoplasmic staining in all samples, the mean nuclear SI was reduced compared to cytoplasmic SI in all disease and tissue groups. This difference in SI was statistically significant in primary PCa ($p<0.05$) as well as metastatic PCa in the lymph node ($p<0.05$) and bone ($p<0.05$). In contrast to the KDM7A staining, the KDM5B staining of prostate basal and acinar cells was similar in staining intensity and distribution. There was only one case of PCa, which had more intense staining of basal compared to acinar cells.

Normal non-prostate tissue

Normal myocardium (control tissue) (Figure 7.30), bone (Figure 7.31), liver (Figure 7.32) and spleen (Figure 7.33) were characterized by a strong and diffuse KDM5B staining of parenchyma and stroma, including hematopoietic cells and leukocytes. In contrast to KDM7A, erythrocytes remained unstained (Figure 7.34).

Case ID	Tissue	Group	C(%)	C(SI)	N(%)	N(SI)
125-11	Adrenal T	M	4	3	4	2
125-11	Adrenal T	M	4	3	4	3
105-4	Bone T	B	4	3	4	2
105-4	Bone T	B	4	3	4	2
107-4	Bone T	B	4	3	4	2
115-4	Bone T	B	4	3	4	2
115-4	Bone T	B	4	3	4	2
125-4	Bone T	B	4	2	4	1
125-4	Bone T	B	4	3	4	3
147-3	Bone T	B	4	3	4	1
147-3	Bone T	B	4	3	4	1
147-4	Bone T	B	4	2	4	1
147-4	Bone T	B	4	2	4	2
165-4	Bone T	B	4	2	4	1
165-4	Bone T	B	4	2	4	1
167-4	Bone T	B	4	2	4	1
167-4	Bone T	B	4	2	4	2
181-4	Bone T	B	4	2	4	1
193-4	Bone T	B	4	3	4	3
193-4	Bone T	B	4	3	4	3
203-4	Bone T	B	4	2	4	1
98-3	Bone T	B	4	3	4	3
98-3	Bone T	B	4	3	4	3
98-4	Bone T	B	4	3	4	2
98-4	Bone T	B	4	3	4	3
98-9	Kidney T	M	4	3	4	2
98-9	Kidney T	M	4	3	4	2
107-8	Liver T	M	4	3	4	1
107-8	Liver T	M	4	3	4	1
251-8	Liver T	M	4	3	4	3
251-8	Liver T	M	4	3	4	3
105-6	LN T	M	4	3	4	2
105-6	LN T	M	4	3	4	2
107-6	LN T	M	4	3	4	1
107-6	LN T	M	4	3	4	1
115-5	LN T	M	4	3	4	2
115-5	LN T	M	4	3	4	3
115-6	LN T	M	4	3	4	3
115-6	LN T	M	4	3	4	3
119-6	LN T	M	4	3	4	2
119-6	LN T	M	4	3	4	2
251-6	LN T	M	4	3	4	3
251-6	LN T	M	4	3	4	3
98-6	LN T	M	4	3	4	3
98-6	LN T	M	4	3	4	3
98-6	LN T	M	4	3	4	3
98-6	LN T	M	4	3	4	3
98-6	LN T	M	4	3	4	3
98-6	LN T	M	4	3	4	3
105-7	Lung T	M	4	3	4	3
105-7	Lung T	M	4	3	4	3
125-7	Lung T	M	4	3	4	3
125-7	Lung T	M	4	3	4	3
98-7	Lung T	M	4	3	4	3
98-7	Lung T	M	4	3	4	3

105-1	Prostate	P	4	3	4	3
105-1	Prostate	P	4	2	4	2
105-2	Prostate	P	4	3	4	3
105-2	Prostate	P	4	3	4	3
165-1	Prostate	P	4	3	4	2
165-1	Prostate	P	4	3	4	3
181-1	Prostate	P	4	3	4	3
181-1	Prostate	P	4	3	4	3
193-1	Prostate	P	4	3	4	3
193-1	Prostate	P	4	3	4	3
107-2	Prostate T	T	4	3	4	3
107-2	Prostate T	T	4	3	4	3
115-2	Prostate T	T	4	3	4	3
115-2	Prostate T	T	4	3	4	3
125-2	Prostate T	T	4	3	4	3
125-2	Prostate T	T	4	3	4	3
147-1	Prostate T	T	4	3	4	3
147-1	Prostate T	T	4	3	4	3
147-1	Prostate T	T	4	3	4	2
147-1	Prostate T	T	4	3	4	2
165-2	Prostate T	T	4	3	4	2
165-2	Prostate T	T	4	3	4	2
167-1	Prostate T	T	4	3	4	3
167-2	Prostate T	T	4	3	4	3
167-2	Prostate T	T	4	3	4	2
181-2	Prostate T	T	4	3	4	3
181-2	Prostate T	T	4	3	4	3
193-2	Prostate T	T	4	3	4	3
193-2	Prostate T	T	4	3	4	3
251-2	Prostate T	T	4	3	4	3
98-2	Prostate T	T	4	3	4	3
98-2	Prostate T	T	4	3	4	3
119-13	Spleen T	M	4	3	4	2
119-13	Spleen T	M	4	3	4	2
125-10	Testis T	M	4	3	4	3
125-10	Testis T	M	4	3	4	3

Table 7.12. Block 1. Semi-quantitative assessment of cytoplasmic and nuclear KDM5B staining of PCa (T) (primary tumor and metastases) and benign prostate tissue (Prostate), as indicated per individual tissue core (with up to 4 cores per case). Also indicated is the staining of prostate basal cells and individual, not further characterized prostate stromal cells. Semi-quantification of C(%) and N(%) was performed as follows: 0: <1%; 1: 1-5%; 2: 6-25%; 3: 26-75%; 4: 76-100% stained cells. Staining intensity was graded as: 1: weak; 2: moderate; 3: strong.

Abbreviations: B: Bone; C: Cytoplasmic staining; LN: Lymph node; M: Metastasis; N: Nuclear staining; NA: Not applicable; P: Prostate (benign); SI: Staining intensity; T: Tumor (PCa)

Tissue	C(%)	C(SI)	N(%)	N(SI)
Prostate T	22/22(100%) 4	22/22(100%) 3	22/22(100%) 4	5/22(23%) 2 17/22(77%) 3
Prostate	10/10(100%) 4	9/10(90%) 3 1/10(10%) 2	10/10(100%) 4	2/10(20%) 2 8/10(80%) 3
Adrenal Met	2/2(100%) 4	2/2(100%) 3	2/2(100%) 4	1/2(50%) 2 1/2(50%) 3
Bone Met	23/23(100%) 4	9/23(39%) 2 14/23(61%) 3	23/23(100%) 4	9/23(39%) 1 8/23(35%) 2 6/23(27%) 3
Kidney Met	2/2(100%) 4	2/2(100%) 3	2/2(100%) 4	2/2(100%) 2
Liver Met	4/4(100%) 4	4/4(100%) 3	4/4(100%) 4	2/4(50%) 1 2/4(50%) 3
LN Met	18/18(100%) 4	18/18(100%) 3	18/18(100%) 4	2/18(11%) 1 5/18(28%) 2 11/18(61%) 3
Lung Met	6/6(100%) 4	6/6(100%) 3	6/6(100%) 4	6/6(100%) 3
Testis Met	2/2(100%) 4	2/2(100%) 3	2/2(100%) 4	2/2(100%) 3

Table 7.13. Block 1. Overview of the semi-quantitative assessment of cytoplasmic and nuclear KDM5B staining of normal prostate and malignant primary and metastatic PCa, as indicated per tissue. C(%) and N(%) indicate the percentage of cells with cytoplasmic and nuclear staining, respectively. Semi-quantification of C(%) and N(%) was performed as follows: 0: <1%; 1: 1-5%; 2: 6-25%; 3: 26-75%; 4: 76-100% stained cells. Staining intensity was graded as: 1: weak; 2: moderate; 3: strong.

Abbreviations: B: Bone; C: Cytoplasm; LN: Lymph node; Met: Metastasis; N: Nuclear; NA: Not applicable; P: Prostate; Prostate N: Normal prostate; SI: Staining intensity; T: Tumor (PCa).

Tissue	Number of cores	C(%)	C(SI)	N(%)	N(SI)	N(SI) vs C(SI)
Prostate tumor	22	4(±0)	3(±0)	4(±0)	2.77(±0.43)	↓*
Adrenal met	2	4(±0)	3(±0)	4(±0)	2.5(±0.71)	↓
Kidney met	2	4(±0)	3(±0)	4(±0)	2(±0)	↓
Liver met	4	4(±0)	3(±0)	4(±0)	2(±1.15)	↓
LN met	18	4(±0)	3(±0)	4(±0)	2.5(±0.71)	↓*
Lung met	6	4(±0)	3(±0)	4(±0)	3(±0)	≙
Spleen met	2	4(±0)	3(±0)	4(±0)	2(±0)	↓
Testis met	2	4(±0)	3(±0)	4(±0)	3(±0)	≙
Bone met	23	4(±0)	2.61(±0.5)**	4(±0)	1.87(±0.81)**	↓*
Benign prostate	10	4(±0)	2.9(±0.32)	4(±0)	2.8(±0.42)	↓

Table 7.14. Block 1. Mean values (standard deviations in brackets) of the semi-quantitative assessment of KDM5B staining of PCa (primary tumor and metastases) and normal prostate, as indicated per tissue. Semi-quantification of C(%) and N(%) was performed as follows: 0: <1%; 1: 1-5%; 2: 6-25%; 3: 26-75%; 4: 76-100% stained cells. Staining intensity was graded as: 1: weak; 2: moderate; 3: strong.

Abbreviations: C: Cytoplasm; LN: Lymph node; met: Metastasis; N: Nuclear; SI: Staining intensity

*significantly different ($p<0.05$); **highly significant different ($p<0.001$). For the parameters C(SI) and N(SI), the significant differences refer to the variations between the values of malignant compared to benign prostate tissue. For the column 'N(%) vs C(%)', significant differences refer to variations between N(%) and C(%) values.

↓: N(%) is lower than C(%); ≙: N(%) and C(%) are comparable

Group	Number of cores	C(%)	C(SI)	N(%)	N(SI)	N(SI) vs. C(SI)
T	22	4(±0)	3(±0)	4(±0)	2.77(±0.43)	↓*
Met (M)	36	4(±0)	3(±0)	4(±0)	2.50(± 0.70)	↓**
Bone met (B)	23	4(±0)	2.61(±0.5)**	4(±0)	1.87(±0.81)**	↓*
Benign prostate (P)	10	4(±0)	2.9(±0.32)	4(±0)	2.8(±0.42)	↓

Table 7.15. Block 1. Mean values (standard deviations in brackets) of the semi-quantitative assessment of cytoplasmic and nuclear KDM7A staining of PCa (primary tumor and metastases) and normal prostate, as indicated per tissue group. Also indicated is the staining of prostate basal cells and individual, not further characterized prostate stromal cells. Semi-quantification of C(%) and N(%) was performed as follows: 0: <1%; 1: 1-5%; 2: 6-25%; 3: 26-75%; 4: 76-100% stained cells. Staining intensity was graded as: 1: weak; 2: moderate; 3: strong

Abbreviations: C: Cytoplasmic staining; Met: Metastasis (any organ except bone); N: Nuclear staining; NA: Not applicable; SI: Staining intensity; T: Primary tumor (PCa);

*significantly different ($p<0.05$); **highly significant different ($p<0.001$). For the parameters C(SI) and N(SI), the significant differences refer to the variations between the values of malignant compared to benign prostate tissue. For the column 'N(%) vs C(%)', significant differences refer to variations between N(%) and C(%) values.

↓: N(%) is lower than C(%)



Figure 7.21. Case 165-1. Benign prostate with diffuse strong cytoplasmic and nuclear glandular cell staining. KDM5B IHC (1:100).

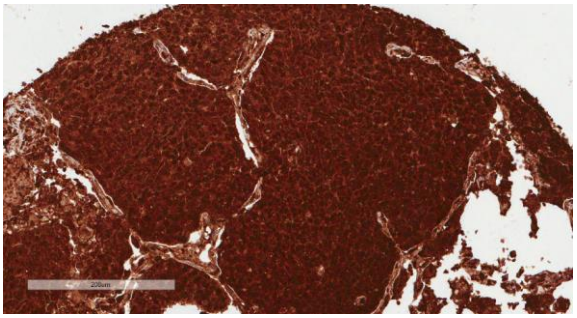


Figure 7.22. Case 125-7. PCa metastasis in the lung with diffuse strong cytoplasmic and nuclear staining of neoplastic cells. KDM5B IHC (1:100).

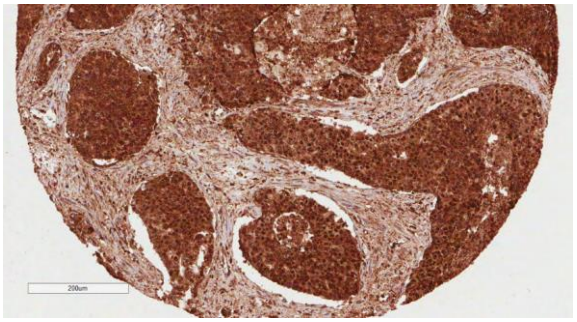


Figure 7.23. Case 125-2. PCa with diffuse strong cytoplasmic and moderate to strong nuclear staining of neoplastic cells. KDM5B IHC (1:200).

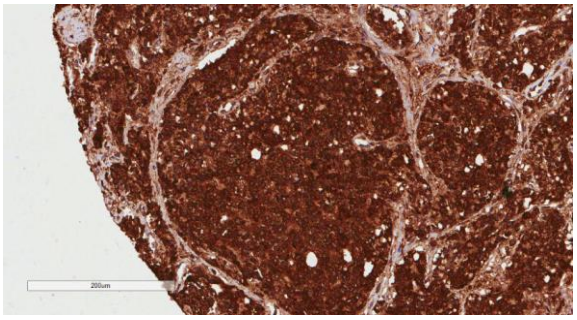


Figure 7.24. Case 115-6. PCa metastasis in the lymph node with diffuse strong cytoplasmic and moderate to strong nuclear staining of neoplastic cells. KDM5B IHC (1:200).

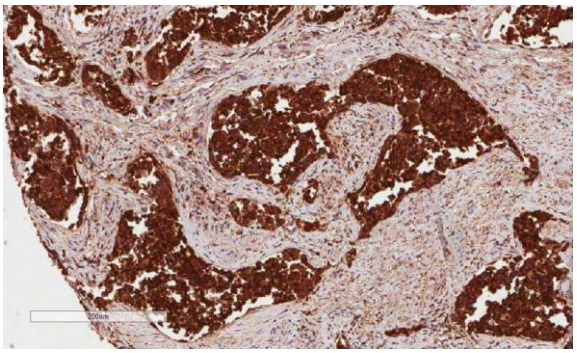


Figure 7.25. Case 107-2. PCa with diffuse strong cytoplasmic and nuclear staining of neoplastic cells. KDM5B IHC (1:200).

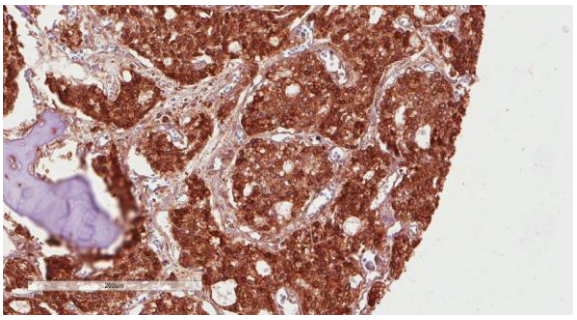


Figure 7.26. Case 105-4. PCa metastasis in the bone with diffuse moderate to strong cytoplasmic and nuclear staining of neoplastic cells. KDM5B IHC (1:200).

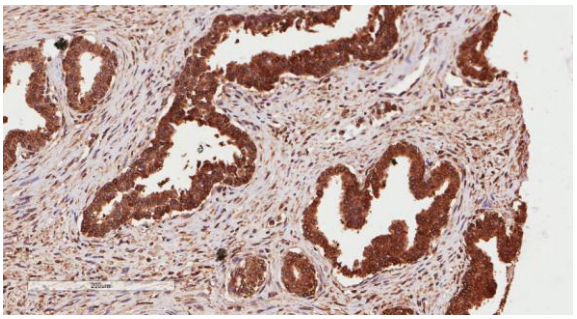


Figure 7.27. Case 165-1. Benign prostate with diffuse strong cytoplasmic and weak to moderate nuclear staining of glandular cells. KDM5B IHC (1:200).

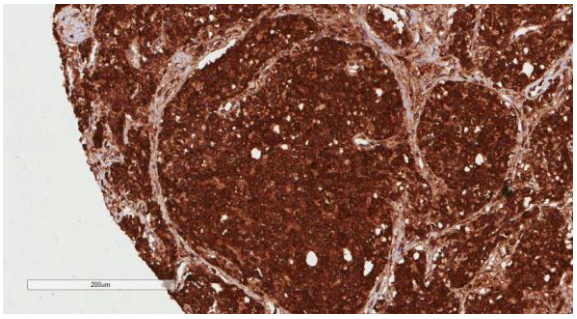


Figure 7.28. Case 115-6. PCa metastasis in the lymph node with diffuse strong cytoplasmic and nuclear staining of neoplastic cells. KDM5B IHC (1:200).

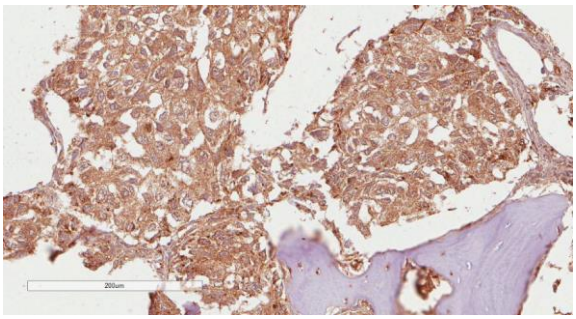


Figure 7.29. Case 165-4. PCa metastasis in the bone with diffuse weak to moderate cytoplasmic and weak nuclear staining. KDM5B IHC (1:200).

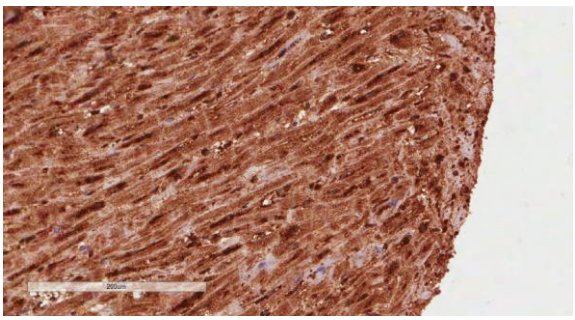


Figure 7.30. Normal myocardium (control case) with diffuse, strong cytoplasmic staining of myocardiocytes. KDM5B IHC (1:200).

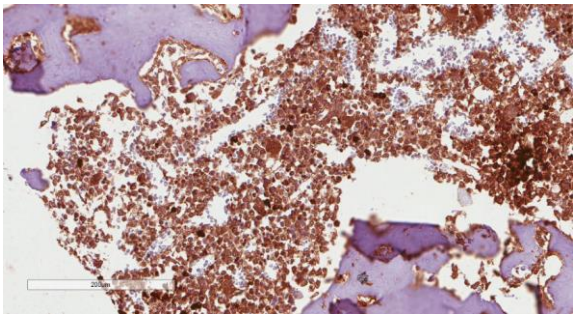


Figure 7.31. Case 224-4. Normal bone (marrow) with strong cytoplasmic staining of hematopoietic cells. KDM5B IHC (1:200).

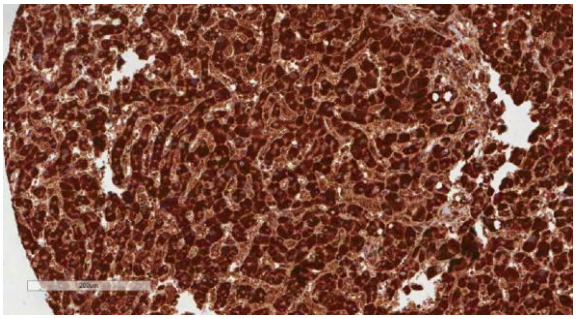


Figure 7.32. Case 125-11. Normal liver with strong diffuse cytoplasmic staining of hepatocytes. KDM5B IHC (1:200).

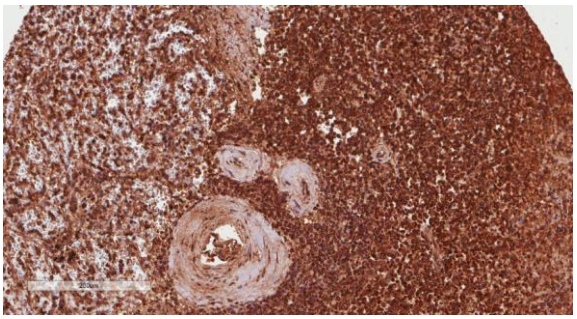


Figure 7.33. Case 251-12. Normal spleen with diffuse strong cytoplasmic staining of leukocytes. KDM5B IHC (1:200).

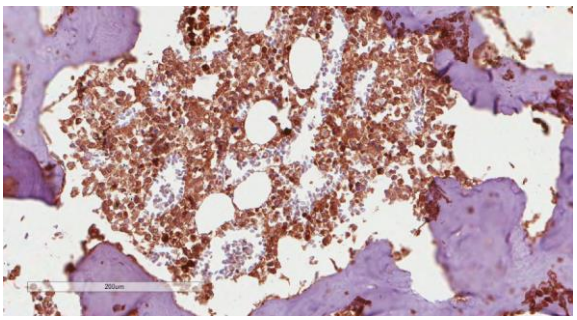


Figure 7.34. Case 224-4. Normal bone (marrow) with strong cytoplasmic staining of hematopoietic cells. Note the unstained erythrocytes. KDM5B IHC (1:200).

Block 2

The nuclear and cytoplasmic KDM5B staining of benign and malignant (PCa) prostate tissue was assessed and semi-quantified, with the following results.

Malignant and benign prostate

The results of the semi-quantitative assessment of KDM5B staining of benign and malignant prostate tissue are provided in Table 7.18 and are summarized in Table 7.19. Mean staining values per tissue group are indicated in Table 7.20. Cytoplasmic staining was strong in the majority of organ-confined PCa (41/45; 91%) (Figure 7.35) and benign (32/39; 82%) (Figure 7.36) samples, with moderate staining in the remaining cases. The mean cytoplasmic SI did not differ between malignant and benign prostates. The estimated percentage of cytoplasmic or nuclear stained cells was comparable in all cases of PCa and benign tissue, with 75-100% of positive cells in all assessed tissue cores. In contrast, nuclear staining intensity was variable within and between malignant and benign tissues. Even though most cases of PCa (36/45; 80%) and benign prostates (24/39; 62%) were characterized by strongly stained nuclei, the number of cores with weak nuclear staining was substantial (7/39; 18%) in benign tissues, but rare in PCa (1/45; 2%). Accordingly, mean nuclear SI was significantly ($p<0.05$) reduced in benign compared to organ-confined PCa. On average, SI in cytoplasm was higher than in nuclei in both malignant and benign prostate. This difference was however only statistically significant ($p<0.05$) in benign tissues.

In rare cases (n=2 PCa), KDM5B staining was stronger in areas with more disordered neoplastic epithelium.

In contrast to the KDM7A staining, the KDM5B staining of prostate basal and acinar cells was similar in staining intensity and distribution in most of the cases. There were however ten (n=4 benign; n=6 PCa) cases, which had more intense staining of basal compared to acinar cells (Figure 7.37).

Case ID	Group	C(%)	C(SI)	N(%)	N(SI)
278	P	4	3	4	2
278	P	4	3	4	2
278	P	4	3	4	3
278	P	4	3	4	2
291	P	4	3	4	3
291	P	4	3	4	3
291	P	4	3	4	3
291	P	4	3	4	2
335	P	4	3	4	3
336	P	4	3	4	2
386	P	4	3	4	2
431	P	4	3	4	2
431	P	4	3	4	3
441	P	4	2	4	1
441	P	4	2	4	1
527	P	4	2	4	1
527	P	4	2	4	1
555	P	4	2	4	1
555	P	4	2	4	1
623	P	4	3	4	3
623	P	4	3	4	3
623	P	4	3	4	3
623	P	4	3	4	3
644	P	4	3	4	3
644	P	4	3	4	3
644	P	4	3	4	3
644	P	4	3	4	3
981	P	4	3	4	3
981	P	4	3	4	3
985	P	4	3	4	3
985	P	4	2	4	1
985	P	4	3	4	2
991	P	4	3	4	3
991	P	4	3	4	3
991	P	4	3	4	3
991	P	4	3	4	3
994	P	4	3	4	3
994	P	4	3	4	3
994	P	4	3	4	3
278	T	4	3	4	3
291	T	4	3	4	2
291	T	4	2	4	1
313	T	4	3	4	3
313	T	4	3	4	3
313	T	4	3	4	3
313	T	4	3	4	3
386	T	4	3	4	2
386	T	4	3	4	3
390	T	4	3	4	3
390	T	4	3	4	3
431	T	4	3	4	2
431	T	4	3	4	3
441	T	4	2	4	2
441	T	4	2	4	2
527	T	4	2	4	2

555	T	4	3	4	3
555	T	4	3	4	3
744	T	4	3	4	2
744	T	4	3	4	3
744	T	4	3	4	2
850	T	4	3	4	3
850	T	4	3	4	3
850	T	4	3	4	3
850	T	4	3	4	3
986	T	4	3	4	3
986	T	4	3	4	3
986	T	4	3	4	3
986	T	4	3	4	3
988	T	4	3	4	3
988	T	4	3	4	3
988	T	4	3	4	3
988	T	4	3	4	3
996	T	4	3	4	3
996	T	4	3	4	3
996	T	4	3	4	3
996	T	4	3	4	3
1000	T	4	3	4	3
1000	T	4	3	4	3
1000	T	4	3	4	3
1000	T	4	3	4	3
1013	T	4	3	4	3
1013	T	4	3	4	3
1013	T	4	3	4	3
1013	T	4	3	4	3

Table 7.16. Block 2. Semi-quantitative assessment of cytoplasmic and nuclear KDM5B staining of organ-confined PCa (T) and benign prostate tissue (P), as indicated per individual tissue core (with up to 4 cores per case). Semi-quantification of C(%) and N(%) was performed as follows: 0: <1%; 1: 1-5%; 2: 6-25%; 3: 26-75%; 4: 76-100% stained cells. Staining intensity was graded as: 1: weak; 2: moderate; 3: strong.

Abbreviations: C: Cytoplasmic staining; N: Nuclear staining; P: Prostate (benign); SI: Staining intensity; T: Tumor (PCa)

Tissue	C(%)	C(SI)	N(%)	N(SI)
T	45/45(100%) 4	4/45(9%) 2 41/45(91%) 3	45/45(100%) 4	1/45(2%) 1 8/45(18%) 2 36/45(80%) 3
P	39/39(100%) 4	7/39(18%) 2 32/39(82%) 3	39/39(100%) 4	7/39(18%) 1 8/39(21%) 2 24/39(62%) 3

Table 7.17. Block 2. Overview of the semi-quantitative assessment of cytoplasmic and nuclear KDM5B staining of benign (P) prostate and organ-confined PCa, as indicated per tissue. C(%) and N(%) indicate the percentage of cells with cytoplasmic and nuclear staining, respectively. Semi-quantification of C(%) and N(%) was performed as follows: 0: <1%; 1: 1-5%; 2: 6-25%; 3: 26-75%; 4: 76-100% stained cells. Staining intensity was graded as: 1: weak; 2: moderate; 3: strong.

Abbreviations: C: Cytoplasm; N: Nuclear; P: Prostate (benign); SI: Staining intensity; T: Tumor (PCa)

Tissue	Number of cores	C(%)	C(SI)	N(%)	N(SI)	N(SI) vs C(SI)
T	45	4(±0)	2.91(±0.29)	4(±0)	2.78(±0.47)	↓
P	39	4(±0)	2.82(±0.39)	4(±0)	2.44(±0.79)*	↓*

Table 7.18. Block 2. Mean values (standard deviations in brackets) of the semi-quantitative assessment of KDM5B staining of PCa (primary tumor and metastases) and normal prostate, as indicated per tissue. Semi-quantification of C(%) and N(%) was performed as follows: 0: <1%; 1: 1-5%; 2: 6-25%; 3: 26-75%; 4: 76-100% stained cells. Staining intensity was graded as: 1: weak; 2: moderate; 3: strong.

Abbreviations: C: Cytoplasm; N: Nuclear; P: Prostate; SI: Staining intensity

*significantly different ($p<0.05$). For the parameter N(SI), the significant difference refers to the variations between the value of malignant compared to benign prostate tissue. For the column 'N(%) vs C(%)', significant differences refer to variations between N(%) and C(%) values.
↓: N(%) is lower than C(%).

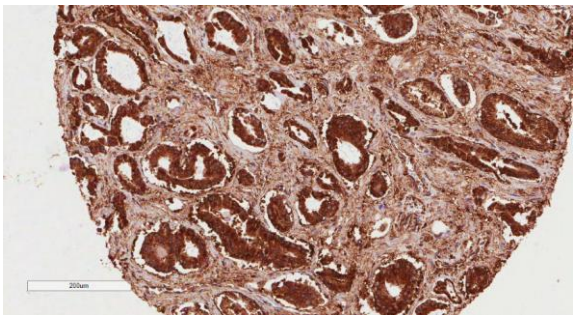


Figure 7.35. Case 335. PCa with diffuse strong cytoplasmic and weak to moderate nuclear staining of neoplastic cells. KDM5B IHC (1:200).

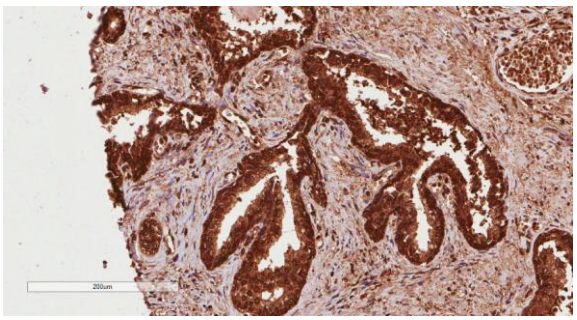


Figure 7.36. Case 291. Benign prostate with diffuse strong cytoplasmic and nuclear staining of acinar and basal cells. KDM5B IHC (1:200).

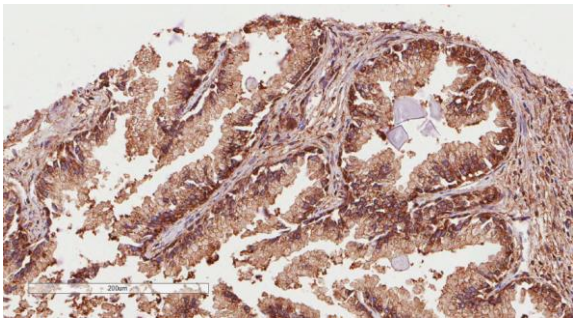


Figure 7.37. Case 441. Benign prostate with diffuse weak cytoplasmic staining of acinar cells. Note the multifocal strong staining of basal cells. KDM5B IHC (1:200).

Block 3

The nuclear and cytoplasmic KDM5B staining of benign (P) and malignant (PCa) prostate tissue was assessed and semi-quantified, with the following results.

Malignant and benign prostate

The results of the semi-quantitative assessment of KDM5B staining of benign and malignant prostate tissue are provided in Table 7.21 and are summarized in Table 7.22. Mean staining values per tissue group are indicated in Tables 7.23 and 7.24. Cytoplasmic staining was strong in the majority of malignant (36/46; 78%) (Figure 7.38) and benign (41/45; 91%) (Figure 7.39) tissues, with moderate cytoplasmic SI in the remaining cases. In all assessed PCa and benign tissue cores, the percentage of cells with nuclear or cytoplasmic staining was 75-100%. Similar to the cytoplasmic staining, the majority of benign (37/46; 80%) and malignant (40/45, 89%) (Figure 7.40) tissues had strong nuclear SI, without significant difference between PCa and benign prostates. Furthermore, mean staining intensities of nuclei and cytoplasm were comparable in both benign and malignant tissue cores. In summary, benign prostate tissue and PCa did not show any significant differences between the cytoplasmic or nuclear KDM5B staining intensity or percentage of stained cells.

In rare cases (n=3 PCa), KDM5B staining was stronger in areas with more disordered neoplastic epithelium.

In contrast to the KDM7A staining, the KDM5B staining of prostate basal and acinar cells was similar in staining intensity and distribution in most of the cases. There were however five (n=2 benign; n=3 PCa) cases, which had more intense staining of basal compared to acinar cells (Figure 7.41)

Case ID	group	C(%)	C(SI)	N(%)	N(SI)
1014	P	4	3	4	3
1014	P	4	3	4	3
1015	P	4	3	4	3
1017	P	4	3	4	3
1017	P	4	3	4	3
1021	P	4	3	4	3
1021	P	4	3	4	3
1024	P	4	3	4	3
1024	P	4	3	4	3
1032	P	4	3	4	3
1032	P	4	3	4	3
1045	P	4	3	4	3
1051	P	4	3	4	3
1051	P	4	3	4	3
1056	P	4	3	4	3
1056	P	4	3	4	3
1068	P	4	3	4	3
1068	P	4	3	4	3
1069	P	4	3	4	3
1069	P	4	3	4	3
1070	P	4	3	4	3
1070	P	4	3	4	3
1140	P	4	3	4	3
1140	P	4	3	4	3
1080	P	4	3	4	3
1080	P	4	3	4	3
1083	P	4	3	4	3
1083	P	4	3	4	3
1085	P	4	3	4	3
1085	P	4	3	4	3
1086	P	4	3	4	3
1086	P	4	3	4	3
1088	P	4	3	4	3
1088	P	4	3	4	3
1093	P	4	3	4	3
1093	P	4	3	4	3
1104	P	4	3	4	3
1105	P	4	3	4	3
1105	P	4	3	4	3
1107	P	4	3	4	3
1107	P	4	3	4	3
1111	P	4	3	4	3
1111	P	4	3	4	3
1114	P	4	3	4	3
1114	P	4	3	4	3
1014	T	4	3	4	3
1014	T	4	3	4	3
1015	T	4	3	4	3
1015	T	4	3	4	3
1017	T	4	3	4	3
1017	T	4	3	4	3
1021	T	4	3	4	3
1021	T	4	2	4	2
1024	T	4	3	4	3
1032	T	4	3	4	3

1032	T	4	3	4	3
1045	T	4	3	4	3
1045	T	4	3	4	3
1051	T	4	3	4	3
1056	T	4	3	4	3
1056	T	4	3	4	3
1068	T	4	3	4	3
1068	T	4	3	4	3
1069	T	4	3	4	3
1069	T	4	3	4	3
1070	T	4	3	4	3
1070	T	4	3	4	3
1140	T	4	3	4	3
1140	T	4	3	4	3
1080	T	4	3	4	3
1080	T	4	3	4	3
1083	T	4	3	4	3
1083	T	4	3	4	3
1085	T	4	3	4	3
1085	T	4	3	4	3
1086	T	4	3	4	3
1086	T	4	3	4	3
1088	T	4	3	4	3
1088	T	4	3	4	3
1093	T	4	3	4	3
1093	T	4	3	4	3
1104	T	4	3	4	3
1104	T	4	3	4	3
1105	T	4	3	4	3
1105	T	4	3	4	3
1107	T	4	3	4	3
1111	T	4	3	4	3
1111	T	4	2	4	2
1114	T	4	3	4	3
1114	T	4	3	4	3

Table 7.19. Block 3. Semi-quantitative assessment of cytoplasmic and nuclear KDM5B staining of organ-confined PCa (T) and benign prostate tissue (P), as indicated per individual tissue core (with up to 4 cores per case). Semi-quantification of C(%) and N(%) was performed as follows: 0: <1%; 1: 1-5%; 2: 6-25%; 3: 26-75%; 4: 76-100% stained cells. Staining intensity was graded as: 1: weak; 2: moderate; 3: strong.

Abbreviations: C: Cytoplasmic staining; N: Nuclear staining; P: Prostate (benign); SI: Staining intensity; T: Tumor (PCa)

Tissue	C(%)	C(SI)	N(%)	N(SI)
T	46/46(100%) 4	10/46(22%) 2 36/46(78%) 3	46/46(100%) 4	2/46(4%) 1 7/46(15%) 2 37/46(80%) 3
P	45/45(100%) 4	4/45(9%) 2 41/45(91%) 3	45/45(100%) 4	1/45(2%) 1 4/45(9%) 2 40/45(89%) 3

Table 7.20. Block 3. Overview of the semi-quantitative assessment of cytoplasmic and nuclear KDM5B staining of benign (P) prostate and organ-confined PCa, as indicated per tissue. C(%) and N(%) indicate the percentage of cells with cytoplasmic and nuclear staining, respectively. Semi-quantification of C(%) and N(%) was performed as follows: 0: <1%; 1: 1-5%; 2: 6-25%; 3: 26-75%; 4: 76-100% stained cells. Staining intensity was graded as: 1: weak; 2: moderate; 3: strong.

Abbreviations: C: Cytoplasm; N: Nuclear; P: Prostate (benign); SI: Staining intensity; T: Tumor (PCa)

Tissue	Number of cores	C(%)	C(SI)	N(%)	N(SI)	N(SI) vs C(SI)
T	46	4(±0)	2.78(±0.42)	4(±0)	2.76(±0.52)	≙
P	45	4(±0)	3(±0)	4(±0)	3(±0)	≙

Table 7.21. Block 3. Mean values (standard deviations in brackets) of the semi-quantitative assessment of KDM5B staining of PCa (primary tumor and metastases) and benign prostate, as indicated per tissue. Semi-quantification of C(%) and N(%) was performed as follows: 0: <1%; 1: 1-5%; 2: 6-25%; 3: 26-75%; 4: 76-100% stained cells. Staining intensity was graded as: 1: weak; 2: moderate; 3: strong.

Abbreviations: C: Cytoplasm; N: Nuclear; P: Prostate (benign); SI: Staining intensity

Disease group	Tissue group	Block	No. of cores	C(%)	C(SI)	N(%)	N(SI)	N(SI) vs. C(SI)
Organ-confined PCa[1)]	T	2	45	4(±0)	2.91(±0.29)	4(±0)	2.78(±0.47)	↓
	T	3	46	4(±0)	2.78(±0.42)	4(±0)	2.76(±0.52)	≙
Metastatic PCa	T	1	22	4(±0)	3(±0)	4(±0)	2.77(±0.43)	↓*
	Met	1	36	4(±0)	3(±0)	4(±0)	2.50(± 0.70)	↓**
	Bone Met	1	23	4(±0)	2.61(±0.5)**	4(±0)	1.87(±0.81)**	↓*
Benign	P	1	10	4(±0)	2.9(±0.32)	4(±0)	2.8(±0.42)	↓
	P	2	39	4(±0)	2.82(±0.39)	4(±0)	2.44(±0.79)*	↓*
	P	3	45	4(±0)	3(±0)	4(±0)	3(±0)	≙

Table 7.22. Summary of KDM5B staining of benign and malignant prostate tissue. Mean values (standard deviation in brackets) of the semi-quantitative assessment of cytoplasmic and nuclear KDM5B staining of PCa (T) and benign prostate tissue (P), as indicated per tissue and disease

group. Semi-quantification of C(%) and N(%) was performed as follows: 0: <1%; 1: 1-5%; 2: 6-25%; 3: 26-75%; 4: 76-100% stained cells. Staining intensity was graded as: 1: weak; 2: moderate; 3: strong.

[1)]All cases with organ-confined PCa, except for one case, which had a metastatic event.

Abbreviations: C: Cytoplasmic staining; N: Nuclear staining; P: Prostate (benign); SI: Staining intensity; T: Primary tumor (PCa).

*significantly different ($p<0.05$); **highly significant different ($p<0.001$). For the parameters C(SI) and N(SI), the significant differences refer to the variations between the values of malignant compared to benign prostate tissue within the same tissue block. For the column 'N(%) vs C(%)', significant differences refer to variations between N(%) and C(%) values.

↓: N(%) is lower than C(%); ≙: N(%) and C(%) are comparable.

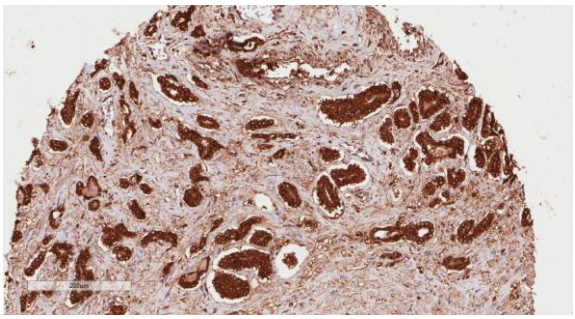


Figure 7.38. Case 1015. PCa with diffuse strong cytoplasmic and weak to moderate nuclear staining of neoplastic cells. KDM5B IHC (1:200).

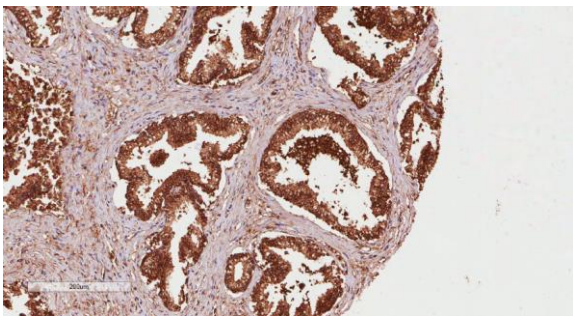


Figure 7.39. Case 1068. Benign prostate with diffuse moderate to strong cytoplasmic and weak to moderate nuclear staining of glands. KDM5B IHC (1:200).

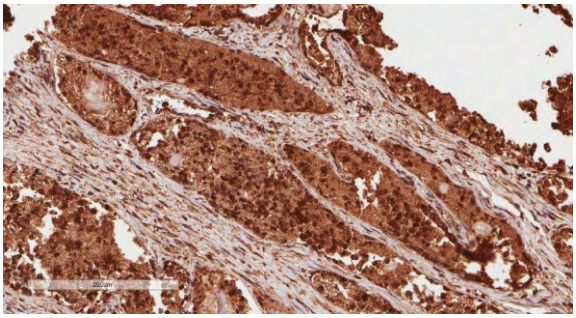


Figure 7.40. Case 1086. PCa with diffuse strong cytoplasmic and nuclear staining. KDM5B IHC (1:200).

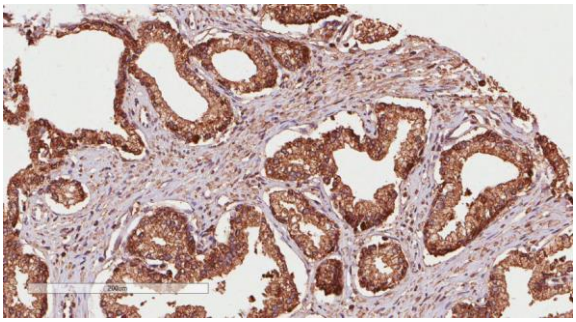


Figure 7.41. Case 1021. Benign prostate with diffuse moderate to strong cytoplasmic staining of glands with multifocal strong cytoplasmic staining of basal cells. KDM5B IHC (1:200).

7.5 Discussion

Both benign and malignant prostate tissue stained positive for KDM7A and KDM5B. IHC staining intensity (SI) as well as the percentage of stained cells varied however between the two markers and between the different types of tissues.

When present, cytoplasmic and nuclear IHC expression of KDM7A was weak to, less commonly, moderate in most benign and malignant tissues. Strong staining was rare. The majority of benign (50-67%), organ-confined PCa (75-88%), primary tumors of metastatic PCa (61%) and PCa metastases (91%) tissue samples had weak cytoplasmic staining. If present, nuclear staining was weak in all benign, all metastatic PCa and almost all (except of two tissue cores with moderate SI) organ-confined PCa tissue samples. In contrast to a common, predominantly weak SI in all different groups of disease and tissue, the presence of staining as well as the estimated percentage of stained cells varied between the the different groups and samples. Cytoplasmic or nuclear stained cells were present in 60-89% of benign tissue samples. Compared to benign prostate tissue, the presence of KDM7A staining tended to be more common in organ-confined PCa, which contained stained tumor cells in 70 to 100% of all tissue cores. This observation confirms the findings of a recent study published in 2018 (Lee et al., 2018), which describes increased KDM7A protein and mRNA expression in PC tissue, in correlation with Gleason score. The finding of cytoplasmic KDM7A expression in most normal prostate tissues of the present study, with similar or even sometimes stronger staining intensities than in malignant tissues, is however more difficult to interpret. Especially when taking into consideration that normal prostate tissue is known to express KDM7A (Ponten et al., 2008; Uhlen et al., 2015) (https://www.proteinatlas.org/, accessed 13 November 2019). The presence of (either cytoplasmic or nuclear) stained cells in metastatic PCa was seen in 86% of primary tumors, varied however significantly in the different tumor metastases. PCa metastases in adrenal, liver and testis were all positive for KDM7A, but remained negative in the kidney. Metastatic tissue in the bone, lymph node and lung contained KDM7A expressing cells in 67 to 88% of tissue samples. Given the relatively low

number of studied cases, it remains uncertain if the different expression levels observed in the different tissues with metastases are a consistent finding in metastatic PCa. The percentage of cytoplasmic stained cells varied strongly between and within the different disease and tissue groups. The percentage of positive cells in benign prostate tissue was highly variable, ranging from less than 1% to up to 100% of cells. The same was true for organ-confined and metastatic PCa. Nevertheless, when calculating mean values of the semi-quantitatively assessed percentages of stained cells, certain significant differences were observed between different tissue groups. More specifically, the mean semi-quantitative values of the percentage of cytoplasmic stained cells were significantly ($p<0.05$) higher in organ-confined PCa compared to benign prostate tissue. This finding is comparable to the overall increased presence of KDM7A positive cases in local PCa compared to benign prostate tissue, as described above. Interestingly, in cases of metastatic PCa, tumor metastases tend to have lower mean percentage values of cells with cytoplasmic staining compared to the primary tumor. This difference was significant ($p<0.05$) when bone metastases were assessed separately. When comparing semi-quantitative values of the amount of cells with cytoplasmic staining, benign prostate and metastatic PCa did not differ significantly. This is in contrast to a significant difference in the mean percentage of cells with nuclear staining in benign compared to metastatic PCa. Benign prostate tissue has significantly ($p<0.05$) lower mean percentages of nuclear stained cells than primary tumors of metastatic PCa. While metastatic PCa samples had a wide range (between <1 and 100%) of cells with nuclear staining, benign prostate tissue had nuclear KDM7A expression in 11-60% of cases. The mean percentage of cells with nuclear staining was much higher in metastatic PCa, with almost identical semi-quantitative values of 2.18 and 2.19 (corresponding to slightly more than 25% of cells) in primary and metastatic tumors, respectively. In conclusion, the nuclear KDM7A expression was increased in metastatic PCa compared to benign prostate tissue. The same phenomenon, i.e. increased KDM7A expression with nuclear location, has recently been described in breast cancer (Meng et al., 2019). Noteworthy, unlike primary tumor and non-osseous

metastases, bone metastases had relatively low numbers of nuclear stained cells, which were comparable to normal prostate tissue. The observed lower KDM7A expression in bone tissue however needs to be interpreted with caution as this finding may represent an artefact caused by decalcification of the tissue (which is required for routine tissue processing of bone), which is known to frequently reduce the sensitivity of IHC (Bussolati and Leonardo, 2008). When comparing benign prostate tissue and organ-confined PCa, the overall mean semi-quantitatively assessed percentage of cells with nuclear staining was comparable, but lower than in metastatic PCa. In benign prostate tissue, the majority (94-100%) of cases had less than 26% of nuclear stained cells whereas organ-confined PCa presented with highly variable numbers of stained cells, ranging from 1 to 100%.

The ratio of cytoplasmic versus nuclear KDM7A staining differed between and within different groups of benign and malignant prostate tissue. Organ-confined PCa and benign prostate tended to have higher mean percentages of nuclear compared to cytoplasmic stained cells. A predominant nuclear location is also reported for KDM7A in various types of normal tissue when referring to the Human protein atlas (Ponten et al., 2008; Uhlen et al., 2015) (https://www.proteinatlas.org/, accessed 13 November 2019). The opposite was true for metastatic PCa, which, on average, had higher numbers of cytoplasmic compared to nuclear stained cells per sample. This observation may be interpreted as increase in nuclear KDM7A expression in malignant prostate tissue. The reason for this phenomenon remains unknown..

In addition to KDM7A expression in benign and malignant prostate secretory cells, a highly variable number (0 – 88%) of benign and cancer cases showed a strong and distinct, cytoplasmic staining of prostate basal cells. In most cases, basal cell staining was multifocal, was present in a variable number of glands and consisted of a predominantly discontinuous layer of stained cells. In two of the three TMAs, basal cell staining was more common in benign (28-88%) compared to malignant (0-58%) tissue cores ($p<0.01$). This finding may simply reflect the loss of basal cells, which is a feature of PCa in men. Comparable

KDM7A IHC staining of benign prostate basal cells is reported in the Human Protein Atlas (Ponten et al., 2008; Uhlen et al., 2015) (https://www.proteinatlas.org/, accessed 13 November 2019). The observed distinct and strong staining of prostate basal cells provides evidence for substantial KDM7A expression in this type of cells. Therefore, KDM7A may have the potential to be used as a prostate basal cell marker.

Apart from prostate glandular cell staining, a significant number (9-22% of cases) of malignant and benign prostate tissue contained low numbers of individual, strongly KDM7A stained cells, which were embedded in the prostate stroma. The number of stromal cell positive cases did not differ significantly between benign and malignant glands. It remains uncertain what cell type they represent. One or several types of stromal, i.e. fibroblastic, vascular, smooth muscular, nervous, or inflammatory cells are possible. Based on their plump-spindle to polygonal cell shape, round cells (including leukocytes) seem less likely. They are unlikely to represent benign or malignant prostate glandular cells, based on their cell morphology and individual distribution without forming cellular aggregates. For a better characterization of these cells, further IHC would however be required to identify the type of cell.
Finally, few tissue cores of normal myocardium, bone, liver, and spleen were also stained, which showed diffuse, weak to moderate cytoplasmic KDM7A staining of myocardiocytes, hematopoietic cells, erythrocytes and hepatocytes. The type of stained cells and staining distribution was comparable to the reported KDM7A staining pattern for the same tissues in the Human Protein Atlas (Ponten et al., 2008; Uhlen et al., 2015) (https://www.proteinatlas.org/, accessed 13 November 2019).

In strong contrast to KDM7A, the KDM5B staining was characterized by a strong staining intensity in most benign and malignant tissues. This is in strong contrast to previous studies, which describe a weak to absent KDM5B expression in benign prostate (Lu et al., 1999; Xiang et al., 2007). Indeed, significant KDM5B gene expression was restricted to testis when benign tissues,

including prostate, were assessed (Lu et al., 1999). When consulting the Human Protein Atlas, the reported KDM5B protein expression in benign prostate tissue is controversial, ranging from complete lack of expression to a diffuse and marked nuclear positivity in prostate parenchyma and stroma (Ponten et al., 2008; Uhlen et al., 2015) (https://www.proteinatlas.org/, accessed 13 November 2019). In the present study, there was however a tendency for a mild reduction in nuclear compared to cytoplasmic KDM5B staining intensity in a certain number of benign and malignant tissue cores. Normal prostate had a strong cytoplasmic staining in all but one case, which had moderate SI. Similarly, metastatic PCa was characterized by an intense cytoplasmic KDM5B positivity in all primary tumors and non-osseous metastases. This observation confirms the previously reported high KDM5B expression in metastatic PC (Crea et al., 2012; Xiang et al., 2007). In a significant number (39%) of bone metastases in the present study, the staining in the cytoplasm was only moderate. This finding needs interpretation with caution because of potential reduction in staining due to the decalcification, which is required for processing bone tissue for histological examination. Cytoplasmic SI was comparable between BPH and organ-confined PCa, with strong staining in 82-91% and 78-91% of benign and malignant tissue, respectively. Remaining cases had moderate cytoplasmic staining. Contrary to KDM7A staining, the percentage of either nuclear or cytoplasmic KDM5B stained cells was comparable in benign and malignant tissues, with 75-100% of positive cells in all assessed tissue cores. Nuclear staining did however show some differences between malignant and benign tissues. Normal prostate as well as primary tumors of metastatic PCa had intense nuclear KDM5B staining in the majority of cases. Unlike primary tumors, PCa metastases varied in their nuclear staining, depending on the type of tissue. More specifically, metastatic PCa in the kidney, spleen and bone had less intense mean nuclear staining compared to primary PCa, which was significant ($p<0.05$) in the case of bone. As mentioned before, this finding needs interpretation with caution as the reduced staining may correspond to an artefact caused by the bone tissue processing. When comparing benign tissue with organ-confined PCa, differences in nuclear staining intensity were only

observed in one of the two examined TMAs. The mean nuclear SI was significantly ($p<0.05$) reduced in benign prostates compared to PCa in one TMA. However, this effect could not be demonstrated in the second TMA, which contained benign tissue and organ-confined PCa. The reason for this phenomenon remains unknown. It cannot be excluded that the two TMAs had different staining due to potential differences in the staining or tissue processing procedure.

When comparing the level of nuclear versus cytoplasmic expression, the mean nuclear SI was reduced in all disease and tissue groups, except in lung and testicular PCa metastases, which had strong staining in both cellular compartments. This difference in nuclear versus cytoplasmic location was significant ($p<0.05$) in benign tissue, as well as primary and metastatic tumor samples. The high KDM5B expression in the cytoplasm may provide evidence for a non-chromatin linked role for this type of KDM. Even though little is known about the function of KDMs outside the nucleus, cytoplasmic expression of KDM4A has been demonstrated, with a regulatory function in protein synthesis (Van Rechem et al., 2015). Similarly, KDM5B is expressed in the cytoplasm of BC cells during certain phases of the cell cycle (Hayami et al., 2010). Interestingly, KDM1A inhibitors have been demonstrated to cause cytoplasmic translocation of the enzyme (Yabuta and Shidoji, 2019). Therefore, the present study may potentially highlight an important cytoplasmic role for KDM5B in benign and malignant prostate tissue.

In contrast to KDM7A, intense staining was present in both basal and acinar glandular cells, with only few cases of more pronounced basal cell staining. Consequently, KDM5B is likely to have relevant functions in both types of prostate glandular cells. In addition, benign and malignant prostate stroma presented with diffuse, moderate KDM5B expression. Despite evident lack of differential expression between benign and malignant prostate tissue, this observation may provide evidence for a potential role of this enzyme in the non-glandular compartment.

In conclusion, KDM7A was weakly expressed in both benign and malignant prostate tissue. The level of expression, i.e. the number of positive cases and the percentage of stained cells, was increased in benign prostate compared to organ-confined PCa. In PCa metastases, the percentage of cells with cytoplasmic KDM7A expression was similar like in normal prostate tissue, but decreased when compared to the primary tumor. In contrast, nuclear expression was increased in metastatic PCa, in comparison with normal prostate tissue. Benign prostate tissue and organ-confined PCa had similar nuclear KDM7A expression, which was higher than in normal prostate, but lower than in metastatic PCa. Nuclear expression was higher than in the cytoplasm in organ-confined PCa and normal prostate tissue, which was vice versa in metastatic PCa. Prostate basal cells presented with a distinct and strong cytoplasmic KDM7A expression, forming a discontinuous layer of stained cells in most of the cases. Finally, benign as well as malignant prostate stroma contained a low number of individual, strongly KDM7A stained, not further characterized cells in the minority of cases.

KDM5B expression was strong in most benign and malignant prostate tissue. The percentage of stained cells was high, often reaching 100%, in all tissue samples, without significant differences between benign and malignant cases. In comparison with benign prostate and primary tumors, PCa metastases had decreased nuclear KDM5B expression. Nuclear compared to cytoplasmic expression was significantly reduced in bening tissue and metastatic PCa. The high KDM5B expression in the cytoplasm may provide evidence for a non-chromatin linked role for KDM5B.

8. STUDY 6. Histopathology and expression of RBP4 and MYC in TRACK (transgenic model of cancer of the kidney) mice

Formatted: Line spacing: 1.5 lines

The present study includes the histomorphological analysis of a subset of tissue samples collected from transgenic mice with kidney-specific HIF-1α overexpression, referred to as TRACK mice. This model was previously shown to develop neoplastic renal proximal tubular changes. In addition, the expression of RBP4 and MYC was assessed by IHC in a small number of animals.

8.1. Abstract

Background: In 2011, the TRACK mouse model for clear cell renal cell carcinoma (ccRCC) was established, to recapitulate the molecular and morphological features present in spontaneous human ccRCC. This model was shown to successfully produce renal histomorphological lesions, which resemble the phenotype of VHL disease. Other microscopic changes within the kidney, including features of inflammation and degeneration, as well as the histological appearance of other organs have not yet been described for the TRACK model. Furthermore, the expression of certain RCC-associated proteins, including MYC and RBP4 has not previously been investigated in the TRACK and other RCC animal models.

Aims: To characterize the histomorphology of the kidney and other organs of TRACK and control mice and to evaluate the tissues' protein expression of MYC and RBP4 by IHC.

Material and methods: Murine FFPE tissues were assessed, collected from n=66 mice. Tissue samples (heart, lung, spleen, liver, pancreas, kidney, small intestine, testis, skeletal muscle) of n=44 TRACK (HIF-1α overexpressing) and n=22 control (n=5 HIF-2α overexpressing and n=17 WT) mice were histomorphologically assessed. Three TRACK and two WT mice were further evaluated for the expression of RBP4 and MYC by IHC.

Results: All TRACK mice presented with moderate to severe vacuolar tubular changes in the kidney, with presence of tubular dysplasia in 5/44 (11%) cases.

Additional significant renal lesions included a mild, chronic interstitial inflammation, fibrosis, and tubular regeneration. Inflammation was seen in 41/44 (93%) of HIF-1α mice, in none of the HIF-2α mice and in a number (5 out of 17, 29%) of WT animals. Mild chronic tubular atrophy and interstitial fibrosis was seen in 6/44 (14%) HIF-1α mice, and in none of the control animals. These fibrotic areas were indicative of chronic infarcts based on their histological appearance. Features of tubular regeneration was limited to HIF-1α mice, and was seen in 31/44 (70%) of cases. The most relevant non-renal histopathology included a mild, chronic inflammatory response in the liver, which was seen in 7/24 (29%) of HIF-1α mice, none of the WT. RBP4 was expressed in the renal proximal tubular and parietal epithelial cells of 3/3 (100%) TRACK mice and remained undetectable in WT. Moderate to strong expression of MYC was seen in the renal tubules of TRACK and WT animals. Other organs showed variable MYC staining, without evident differences between TRACK and WT mice.

Conclusions: The TRACK model reliably develops pre-neoplastic and early neoplastic renal tubular changes with comparable histomorphology as seen in early stages of spontaneous ccRCC. In addition to the tubular lesions, other mild renal changes occur in TRACK mice, including tubular regeneration, chronic infarcts, and chronic interstitial inflammation. Chronic hepatic inflammatory infiltrates have been observed in a significant number of TRACK mice, which may possibly be related to increased renal HIF-1 α levels. MYC is strongly expressed in renal tubules, and to a variable extent in other tissues, with a similar IHC staining between TRACK and WT animals. RBP4 expression is present in the apical cytoplasm of proximal tubular and parietal epithelial cells of TRACK mice, which is absent in WT. Other organs, including the liver, fail to demonstrate convincing RBP4 expression by IHC. This observation prompts to further evaluate the potential use of RBP4 as biomarker for ccRCC.

This study confirms the previously reported premalignant and early neoplastic renal proximal tubular histopathological lesions in the TRACK model. In addition, degenerative and inflammatory changes within the kidney and the liver, as well as the immunohistochemical expression of MYC and RBP4 are reported in this model for the first time.

8.2 Introduction

Clear cell renal cell carcinoma (ccRCC), the most common subtype of RCC, has been given its name based on the histological appearance of the neoplastic cells. Even though primarily true for low-grade, well differentiated ccRCC, tumor cells are characterized by abundant, optically clear cytoplasm, and are arranged in a nested, trabecular and/or alveolar pattern (Moch et al., 2016; Udager and Mehra, 2016). When generating animal models for ccRCC or any other type of cancer, it is crucial that the model mirrors spontaneous human disease on a morphological as well as molecular level. Even though a range of animal models for ccRCC has been generated, few succeeded in establishing a tumor with 'clear' cell morphology. In 2011, Fu and colleagues (Fu et al., 2011) established a mouse model with the desired histological features, including 'clear' neoplastic cells, renal cysts, disorganized proximal tubules, and tumors with cyst formations. This model, referred to as TRACK, is based on a kidney-specific, constitutively expressed HIF-1α in proximal tubules. TRACK mice reliably produce dysplastic, pre-neoplastic and early neoplastic proximal tubular changes with convincing resemblance to human ccRCC.

On a molecular level, ccRCC is characterized by a variety of genetic abnormalities, most commonly including loss of *VHL* gene, which leads to accumulation of HIF-1α. In addition, overexpression of *MYC* is a frequent finding in ccRCC (Shroff et al., 2015; Tang et al., 2009). *MYC* is an important oncogene in different types of cancer, with a promoting effect on cell cycle progression, cellular proliferation and angiogenesis (Nesbit et al., 1999). For investigating the role of MYC in ccRCC, as well as testing potential therapeutic strategies, a robust animal model is highly valuable. Four years ago, a transgenic mouse model with conditional expression of *MYC* has been established (Shroff et al., 2015). These mice developed renal collecting duct carcinomas, and MYC was shown to have an important role in inducing and maintaining neoplastic growth. Furthermore, tumor regression was achieved upon inactivation of *MYC*. Two years later, the generation of two RCC mouse

models was reported, which were characterized by an activated *MYC*, either alone or in combination with other genes (Bailey et al., 2017). Upon sole activation of *MYC*, the mice developed papillary RCC, whereas *MYC* activation combined with inactivation of *Ink4a/Arf* (*Cdkn2a*) resulted in the formation ccRCC. The association of MYC and HIF-α in ccRCC tumorigenesis is well known, with opposing effects of HIF-1α and HIF-2α. HIF-2α promotes tumor growth through activation of MYC, while HIF-1α has a tumor inhibitory effect via suppression of MYC (Gordan et al., 2007; Zhang et al., 2007). The tumor-repressing effect of HIF-1α has however been questioned and requires further investigation (Gudas et al., 2014). The TRACK (transgenic cancer of the kidney) ccRCC mouse model expresses a mutated, constitutively active *HIF-1α* in renal proximal tubule epithelia, without evidence of *HIF-2α* activity (Fu et al., 2011). Mice of this model were reported to develop early neoplastic changes of ccRCC, histologically and genetically comparable to human disease (Fu et al., 2015; Minton et al., 2015). The expression level of *MYC* has not yet been evaluated in this animal model.

RCC is clearly associated with obesity, which is a strong risk factor for this disease (Chow et al., 2000; Nam et al., 2019). Adipokines are hormones, which are secreted by adipose tissue, and their serum and tissue levels vary depending on the amount of people's body fat (Schrover 2018). RBP4 is one type of adipokine, which has been shown to be associated with renal disease, including cancer (Choi 2016). The liver is the main site of RBP4 synthesis, the protein can however also be expressed by other tissues, including kidney. In renal dysfunction, as for example in diabetic patients, serum RBP4 protein levels are increased (Cabre et al., 2007; Domingos et al., 2017; Klisic et al., 2017). The same has been shown to be true for patients with RCC, thereby proposing to use RBP4 as biomarker for this disease (Choi et al., 2016). In contrast to increased protein levels in the serum, *RBP4* gene expression in kidney tissue of ccRCC patients has been suggested to be reduced in one study from 2017 (Kudryavtseva et al., 2017). The extent of RBP4 expression on a

protein level in kidneys of people, or alternatively lab mice, with RCC, remains however unknown.

The aim of this study is to characterize the histomorphology of the kidney and other organs of TRACK mice and to evaluate the tissues' protein expression of MYC and RBP4 by IHC.

8.3 Material and methods

Ethics and study design

This animal research study has been performed in collaboration with Prof Lorraine Gudas from Weill Cornell Medicine, New York USA. The care and use of animals in this study were approved by the Institutional Animal Care and Use Committee of Will Cornell Medical College (WCMC) of Cornell University, New York USA and the University of Nottingham AWERB and School of Veterinary Medicine and Sciences ethics committees.

Animals

Transgenic (TRACK) and control {wild type (WT) and HIF-2α-overexpressing} C57BL/6 mice were generated at WCMC as previously published (Fu et al., 2011). The animals were euthanized at the age of 6-28 weeks, and full necropsies were performed, including sampling of relevant tissues, which were routinely processed for histological examination.

Deleted: months

Histology

HE stained tissue samples of a total of n=66 TRACK and control mice were available (generously provided by Prof Gudas), which were histologically assessed by light microscopy (Leica DM 2500). The following tissues were available: Kidney (all cases) and, for some of the cases, other tissues (heart, lung, spleen, liver, pancreas, and testis) from n=44 transgenic (HIF-1α overexpressing) TRACK and 22 control (n=5 HIF-2α overexpressing and n=17 WT) mice.

Kidney sections were examined and evaluated by assessing certain parameters as indicated in Table 8.1.

8. STUDY 6. Histopathology and expression of RBP4 and MYC in TRACK mice

Evaluated parameter	Scoring value			
	0	1	2	3
Tubular damage (TD)[1] (degeneration, necrosis)	Absence	<25% of tubules affected	25-50% of tubules affected	>50% of tubules affected
Tubular regeneration (TR)[2]	Absence	Mild and focal	Mild to moderate, multifocal	Moderate to marked, multifocal
Tubulointerstitial inflammation (TI)	Absence	<25% of the interstitium occupied by inflammatory cells	25-50% of the interstitium occupied by inflammatory cells	>50% of the interstitium occupied by inflammatory cells
Tubular atrophy and interstitial fibrosis (TAF)	Absence	<25% of tubules and interstitium affected	25-50% of tubules and interstitium affected	>50% of tubules and interstitium affected
Proteinuria (PU)	Absence	Mild	Moderate	Marked
Tubular mineralization (TM) (intraluminal, medullary)	Absence	<25% of tubules affected	25-50% of tubules affected	>50% of tubules affected
Glomerular damage (GD)	Absence	Glomerulitis and/or glomerulosclerosis in <25% of glomeruli	Glomerulitis and/or glomerulosclerosis in 25-50% of glomeruli	Glomerulitis and/or glomerulosclerosis in >50% of glomeruli
Pyelonephritis (PN)	Absence	Mild	Moderate	Marked

Table 8.1. Histopathological scoring system kidney.

[1]Tubular epithelial cells show one or more of the following features: Vacuolar degeneration, hypereosinophilic cytoplasm, loss of cellular detail, karyorrhexis, karyolysis, pyknosis

[2]Tubular epithelial cells show one or more of the following features: Hyperplasia/hypertrophy, increased nuclear-cytoplasmic ratio, basophilic cytoplasm, mitotic figure(s)

Immunohistochemistry

Kidney (all cases) and, for some of the cases, other tissues (heart, lung, spleen, liver, pancreas, intestine, testis, tongue) from 6 transgenic TRACK mice and 4 WT mice have been stained by Prof Gudas and her team, using two different antibodies: RBP4 (Santa Cruz, rabbit polyclonal, SC-25850, 1:100) and MYC (Santa Cruz, mouse monoclonal, SC-40, 9E10, 1:100). The staining distribution within the cells and tissue (cytoplasmic versus nuclear; multifocal versus diffuse) was recorded and the staining intensity was semiquantitatively assessed as follow: 0: negative; 1: weak; 2: moderate; 3: severe.

8.4 Results

8.4.1 Histology

Kidney

The results of the evaluated histopathological features are indicated in Table 8.2. and summarized in Table 8.3. All TRACK (HIF-1α overexpressing) mice had evidence of moderate to severe vacuolar degeneration of proximal tubular epithelial cells, which was absent in all control (HIF-2α overexpressing and WT) animals (Figure 8.1). Changes indicative of mild proteinuria and intratubular (intraluminal, medullary) mineralization was observed in 42/44 (95%) and 43/44 (98%) of HIF-1α mice, respectively. Both lesions were absent in control mice. Evidence of renal tubular regeneration was seen in a 31/44 (70%) of HIF-1α mice and was absent in control animals (Figure 8.2). Few focal, small, radiating, sharply demarcated areas of tubular atrophy and interstitial fibrosis (interpreted as chronic infarcts) were seen in 6/44 (14%) of HIF-1α mice and in none of the control animals. Glomerular changes, characterized by a segmental to diffuse thickening of the basement membrane (membranous glomerular change) were restricted to HIF-1α mice, with mild lesions in 5/44 (11%) and severe changes in 5/44 (11%) animals. A mild multifocal chronic lymphoplasmacytic interstitial inflammatory reaction was seen in 41/44 (93%) HIF-1α mice, in none of the HIF-2α mice and in a minority (5 out of 17, 29%) of WT animals (Figure 8.3). A mild to moderate chronic lymphoplasmacytic pyelonephritis was observed in all TRACK and WT mice. Five out of 44 (11%)

HIF-1α mice had dysplastic tubular changes, located in the outer medulla and characterized by an irregular tubular shape and epithelial lining (Figures 8.4 and 8.5). One HIF-1α mouse had focal glomerular parietal epithelial hyperplasia, which was not seen in any of the control mice. One HIF-1α mouse presented with a focal area of vascular and perivascular mesenchymal hyperplasia on the corticomedullary junction (Figure 8.6). Finally, three out of 17 (18%) WT showed mild, focal glomerular mesangial thickening through deposition of homogenous, eosinophilic, extracellular material (Figure 8.7).

Other organs

Potentially relevant histological changes were limited to the liver and spleen, which are provided in Table 8.4. Examined heart, lung, pancreas and testis sections did not reveal any relevant microscopic lesions. Liver sections were available for HIF-1α and WT mice, but not for HIF-2α animals. A mild periportal and perivenular predominantly mononuclear inflammatory reaction was seen in 7/24 (29%) HIF-1α mice and was absent in all WT. The mice with hepatic inflammatory lesions correspond to the cases with most pronounced regenerative tubular changes in the kidney. Another rather uncommon liver lesion was a mild multifocal hepatocellular necrosis of rare individual hepatocytes (single cell necrosis), which was observed in 4/24 (17%) HIF-1α mice and in none of the WT. The mice with these necrotic changes correspond to the cases with evidence of tubular dysplasia in the kidney, which also had mild to moderate renal interstitial inflammation. Eventually, all examined splenic tissue sections of HIF-1α (24/24, 100%) and WT (12/12, 100%) mice showed moderate extramedullary hematopoiesis.

Case	Expressed protein	TD	TR	TI	TAF	PU	TM	GD	PN	Other lesions
1a43-334 15-261 P1	HIF-1α	3	1	1	0	1	1	0	1	
1a43-334 15-261 P2	HIF-1α	3	0	1	0	1	1	0	1	
1a43-334 15-261 P3	HIF-1α	3	0	1	0	1	1	0	1	
1a43-334 15-261 P4	HIF-1α	3	0	1	0	1	1	0	1	
1a43-334 15-261 P5	HIF-1α	3	(1)	1	0	1	1	0	1	
1a43-335 15-261 P1	HIF-1α	3	1	1[1)]	0	1	1	0	1	
1a43-335 15-261 P2	HIF-1α	3	1	1[1)]	0	1	1	0	1	
1a43-335 15-261 P3	HIF-1α	3	1	1[1)]	0	1	1	0	1	
1a43-335 15-261 P4	HIF-1α	3	1	1[1)]	0	1	1	0	1	
1a43-335 15-261 P5	HIF-1α	3	0	1[1)]	0	1	1	0	1	
1a43-341 15-317 P1	HIF-1α	3	1	(1[1)])	0	1	1	0	1	
1a43-341 15-317 P2	HIF-1α	3	0	0	0	1	1	0	1	
1a43-341 15-317 P3	HIF-1α	3	0	0	0	1	1	0	1	
1a43-341 15-317 P4	HIF-1α	3	0	0	0	1	1	0	1	
1a43-342 15-317 P1	HIF-1α	3	2	1	0	1	1	0	1	Focal corticomedullary vascular/perivascular mesenchymal hyperplasia
1a43-342 15-317 P2	HIF-1α	3	2	1	0	0	1	0	1	
1a43-342 15-317 P3	HIF-1α	3	2	1	0	1	1	0	1	
1a43-342 15-317 P4	HIF-1α	3	2	1	0	0	1	0	1	
1a43-343 15-317 P1	HIF-1α	3	1	1[1)]	0	1	1	0	2	Focal tubular dysplasia (outer medulla)
1a43-343 15-317 P2	HIF-1α	3	0	1[1)]	0	1	1	0	2	Focal tubular dysplasia (outer medulla)
1a43-343 15-317 P3	HIF-1α	3	0	1	0	1	1	0	2	Focal tubular dysplasia (outer medulla)
1a43-343 15-317 P4	HIF-1α	3	1	1	0	1	1	0	2	
1a43-344 15-317 P1	HIF-1α	3	2	1	0	1	1	0	1	
1a43-344 15-317 P2	HIF-1α	3	1	1	0	1	1	0	1	
1a43-344 15-317 P3	HIF-1α	3	1	1	0	1	1	0	1	

1a43-344 15-317 P4	HIF-1α	3	1	1	0	1	1	0	1	
1a43-345 15-317 P1	HIF-1α	3	0	1	0	1	1	0	1	
1a43-345 15-317 P2	HIF-1α	3	0	1	0	1	1	0	1	
1a43-345 15-317 P3	HIF-1α	3	0	1	0	1	1	0	1	
1a43-345 15-317 P4	HIF-1α	3	0	1	0	1	1	0	1	
1a43-346 15-317 P1	HIF-1α	3	1	1	0	1	1	0	1	
1a43-346 15-317 P2	HIF-1α	3	1	1	0	1	1	0	1	
1a43-346 15-317 P3	HIF-1α	3	1	1	0	1	1	0	1	
1a43-346 15-317 P4	HIF-1α	3	1	1	0	1	1	0	1	
2a1-160 15-261 P1	HIF-2α	0	0	0	0	0	0	0	1	
2a1-160 15-261 P2	HIF-2α	0	0	0	0	0	0	0	1	
2a1-160 15-261 P3	HIF-2α	0	0	0	0	0	0	0	1	
2a1-160 15-261 P4	HIF-2α	0	0	0	0	0	0	0	1	
2a1-160 15-261 P5	HIF-2α	0	0	0	0	0	0	0	1	
43x1-23 15-261 P1	HIF-1α	2	2	1	1[2)]	1	1	3	1	
43x1-23 15-261 P2	HIF-1α	2	2	1	1[2]	1	1	3	1	
43x1-23 15-261 P3	HIF-1α	2	2	1	1[2]	1	1	3	1	
43x1-23 15-261 P4	HIF-1α	2	2	1	1[2]	1	1	3	1	
43x1-23 15-261 P5	HIF-1α	2	1	1	1[2]	1	0	3	1	
43x1-24 15-261 P1	HIF-1α	3	1	1	0	1	1	1	1	
43x1-24 15-261 P2	HIF-1α	3	1	1	0	1	1	1	1	
43x1-24 15-261 P3	HIF-1α	3	1	1	0	1	1	1	1	
43x1-24 15-261 P4	HIF-1α	3	1	1	0	1	1	1	1	Focal tubular dysplasia (outer medulla)
43x1-24 15-261 P5	HIF-1α	3	2	1	1[2)]	1	1	1	1	Focal tubular dysplasia (outer medulla); focal glomerular parietal epithelial hyperplasia
WT♂7m1 15-317 P1	WT	0	0	0	0	0	0	0	1	
WT♂7m1 15-317 P2	WT	0	0	0	0	0	0	0	1	
WT♂7m1 15-317 P3	WT	0	0	0	0	0	0	0	1	

WT♂7m1 15-317 P4	WT	0	0	0	0	0	0	0	1	
WT♂7m2 15-317 P1	WT	0	0	0	0	0	0	0	(1)	
WT♂7m2 15-317 P2	WT	0	0	0	0	0	0	0	(1)	
WT♂7m2 15-317 P3	WT	0	0	0	0	0	0	0	(1)	
WT♂7m2 15-317 P4	WT	0	0	0	0	0	0	0	(1)	
WT♂7m3 15-317 P1	WT	0	0	0	0	0	0	0	1	
WT♂7m3 15-317 P2	WT	0	0	0	0	0	0	0	1	
WT♂7m3 15-317 P3	WT	0	0	0	0	0	0	0	1	
WT♂7m3 15-317 P4	WT	0	0	0	0	0	0	0	1	
WT♂10m 15-261 P1	WT	0	0	(1)	0	0	0	0	1	Focal glomerular mesangial hyaline deposits
WT♂10m 15-261 P2	WT	0	0	(1)	0	0	0	0	1	Focal glomerular mesangial hyaline deposits
WT♂10m 15-261 P3	WT	0	0	(1)	0	0	0	0	1	Focal glomerular mesangial hyaline deposits
WT♂10m 15-261 P4	WT	0	0	(1)	0	0	0	0	1	
WT♂10m 15-261 P5	WT	0	0	(1)	0	0	0	0	1	

Table 8.2. Histopathological evaluation of the kidney.

() Lesion is minimal if indicated in brackets

[1)] The interstitial inflammation is perivascular around the interlobar blood vessels

[2)] One well-demarcated radiating area of TAF (chronic infarct), often with intralesional tubular cystic dilation

Abbreviations: GD: Glomerular damage; HIF: Hypoxia-inducible factor; PN: Pyelonephritis; PU: Proteinuria; TAF: Tubular atrophy and interstitial fibrosis; TD: Tubular damage; TI: Tubulointerstitial inflammation; TM: Tubular mineralization; TR: Tubular regeneration; WT: wild type

Expressed protein	TD	TR	TI	TAF	PU	TM	GD	PN
HIF-1α (n=44)	39/44 (89%) severe 5/44 (11%) moderate	21/44 (48%) mild 10/44 (23%) moderate	41/44 (93%) mild	6/44 (14%) mild (chronic infarcts)	42/44 (95%) mild	42/44 (95%) mild	5/44 (11%) mild 5/44 (11%) severe	40/44 (91%) mild 4/44 (9%) moderate
HIF-2α (n=5)	0/5	0/5	0/5	0/5	0/5	0/5	0/5	5/5 (100%) mild
WT (n=17)	0/17	0/217	5/17 (29%) mild	0/17	0/17	0/17	0/17	17/17 (100%) mild

Table 8.3. Summary of the renal histopathological findings per animal group.

Abbreviations: GD: Glomerular damage; HIF: Hypoxia-inducible factor; PN: Pyelonephritis; PU: Proteinuria; TAF: Tubular atrophy and interstitial fibrosis; TD: Tubular damage; TI: Tubulointerstitial inflammation; TM: Tubular mineralization; TR: Tubular regeneration; WT: wild type

Case	Expressed protein	Liver		Spleen
		Inflammation[1)]	Necrosis[2)]	Hematopoiesis
1a43-334 15-261 P1	HIF-1α	NP	NP	NP
1a43-334 15-261 P2	HIF-1α	NP	NP	NP
1a43-334 15-261 P3	HIF-1α	NP	NP	NP
1a43-334 15-261 P4	HIF-1α	NP	NP	NP
1a43-334 15-261 P5	HIF-1α	NP	NP	NP
1a43-335 15-261 P1	HIF-1α	NP	NP	NP
1a43-335 15-261 P2	HIF-1α	NP	NP	NP
1a43-335 15-261 P3	HIF-1α	NP	NP	NP
1a43-335 15-261 P4	HIF-1α	NP	NP	NP
1a43-335 15-261 P5	HIF-1α	NP	NP	NP
1a43-341 15-317 P1	HIF-1α	-	-	Moderate
1a43-341 15-317 P2	HIF-1α	-	-	Moderate
1a43-341 15-317 P3	HIF-1α	-	-	Moderate
1a43-341 15-317 P4	HIF-1α	-	-	Moderate
1a43-342 15-317 P1	HIF-1α	Mild	-	Moderate
1a43-342 15-317 P2	HIF-1α	Mild	-	Moderate
1a43-342 15-317 P3	HIF-1α	Mild	-	Moderate
1a43-342 15-317 P4	HIF-1α	Mild	-	Moderate
1a43-343 15-317 P1	HIF-1α	Mild*	Mild	Moderate
1a43-343 15-317 P2	HIF-1α	Mild	Mild	Moderate
1a43-343 15-317 P3	HIF-1α	Mild*	Mild	Moderate
1a43-343 15-317 P4	HIF-1α	-	Mild	Moderate
1a43-344 15-317 P1	HIF-1α	-	-	Moderate
1a43-344 15-317 P2	HIF-1α	-	-	Moderate
1a43-344 15-317 P3	HIF-1α	-	-	Moderate
1a43-344 15-317 P4	HIF-1α	-	-	Moderate
1a43-345 15-317 P1	HIF-1α	-	-	Moderate
1a43-345 15-317 P2	HIF-1α	-	-	Moderate
1a43-345 15-317 P3	HIF-1α	-	-	Moderate
1a43-345 15-317 P4	HIF-1α	-	-	Moderate
1a43-346 15-317 P1	HIF-1α	-	-	Moderate
1a43-346 15-317 P2	HIF-1α	-	-	Moderate
1a43-346 15-317 P3	HIF-1α	-	-	Moderate
1a43-346 15-317 P4	HIF-1α	-	-	Moderate
2a1-160 15-261 P1	HIF-2α	NP	NP	NP
2a1-160 15-261 P2	HIF-2α	NP	NP	NP
2a1-160 15-261 P3	HIF-2α	NP	NP	NP
2a1-160 15-261 P4	HIF-2α	NP	NP	NP
2a1-160 15-261 P5	HIF-2α	NP	NP	NP
43x1-23 15-261 P1	HIF-1α	NP	NP	NP
43x1-23 15-261 P2	HIF-1α	NP	NP	NP
43x1-23 15-261 P3	HIF-1α	NP	NP	NP
43x1-23 15-261 P4	HIF-1α	NP	NP	NP
43x1-23 15-261 P5	HIF-1α	NP	NP	NP
43x1-24 15-261 P1	HIF-1α	NP	NP	NP
43x1-24 15-261 P2	HIF-1α	NP	NP	NP
43x1-24 15-261 P3	HIF-1α	NP	NP	NP
43x1-24 15-261 P4	HIF-1α	NP	NP	NP
43x1-24 15-261 P5	HIF-1α	NP	NP	NP
WT♂7m1 15-317 P1	WT	-	-	Moderate

WT♂7m1 15-317 P2	WT	-	-	Moderate
WT♂7m1 15-317 P3	WT	-	-	Moderate
WT♂7m1 15-317 P4	WT	-	-	Moderate
WT♂7m2 15-317 P1	WT	-	-	Moderate
WT♂7m2 15-317 P2	WT	-	-	Moderate
WT♂7m2 15-317 P3	WT	-	-	Moderate
WT♂7m2 15-317 P4	WT	-	-	Moderate
WT♂7m3 15-317 P1	WT	-	-	Moderate
WT♂7m3 15-317 P2	WT	-	-	Moderate
WT♂7m3 15-317 P3	WT	-	-	Moderate
WT♂7m3 15-317 P4	WT	-	-	Moderate
WT♂10m 15-261 P1	WT	NP	NP	NP
WT♂10m 15-261 P2	WT	NP	NP	NP
WT♂10m 15-261 P3	WT	NP	NP	NP
WT♂10m 15-261 P4	WT	NP	NP	NP
WT♂10m 15-261 P5	WT	NP	NP	NP
Total	HIF-1α	7/24 (29%)	4/24 (17%)	24/24 (100%)
	HIF-2α	NP	NP	NP
	WT	0/12	0/12	12/12 (100%)

Table 8.4. Histopathological evaluation of the liver.

Abbreviations: HIF: Hypoxia-inducible factor; NP: Not provided; WT: wild type

[1)]Mild periportal and perivenular mainly mononuclear cellular infiltrates

[2)]Multifocal single cell hepatocellular necrosis

*Changes were only minimal

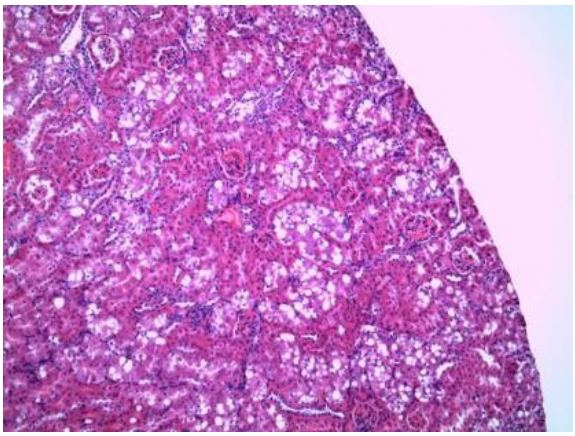


Figure 8.1A. Case 1α43-344 15-317 P2. Microphotograph of the kidney. Severe tubular vacuolar degeneration. HE stain, 10x objective.

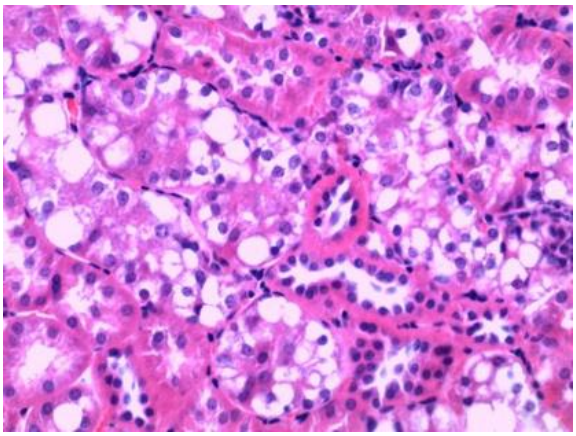


Figure 8.1B. Closer view of Figure 8.1A. Severely vacuolated cytoplasm of tubular epithelial cells. HE stain, 40x objective.

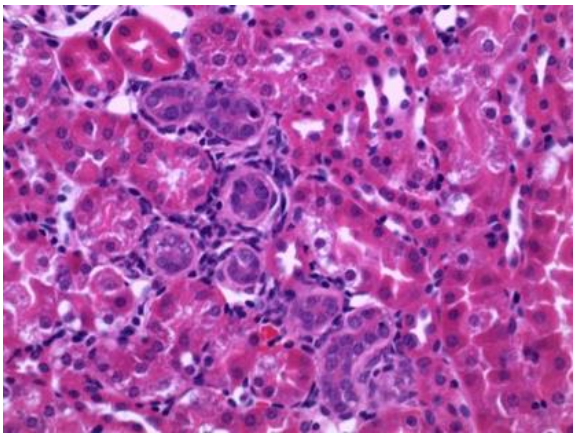


Figure 8.2. Case 1α43-342 15-317 P3. Basophilic tubular epithelial cells, with an increased nuclear:cytoplasmic ration, indicative of regeneration. HE stain, 40x objective.

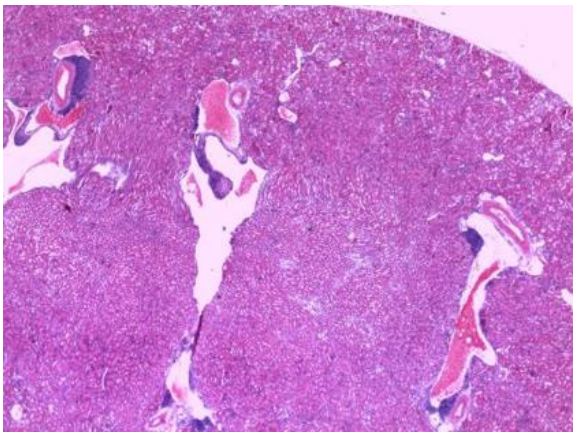


Figure 8.3A. Case 1α43 335 15-261 P3. Microphotograph of the kidney. Perivascular inflammation in the area of interlobar blood vessels. HE stain, 2.5x objective.

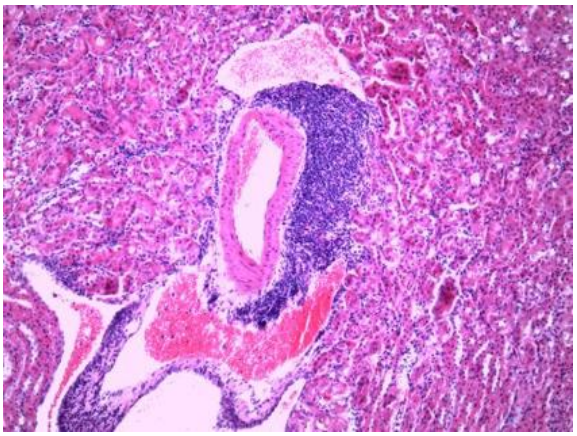


Figure 8.3B. Closer view of Figure 8.6A. Densely cellular mononuclear inflammation surrounding the interlobar artery and vein. HE stain, 10x objective.

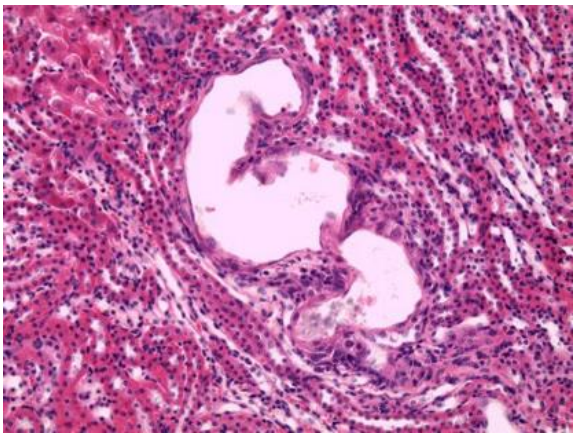


Figure 8.4. Case 1α43-343 15-317 P2. Microphotograph of the kidney. Irregular and distended (interpreted as dysplastic) tubule. HE stain, 20x objective.

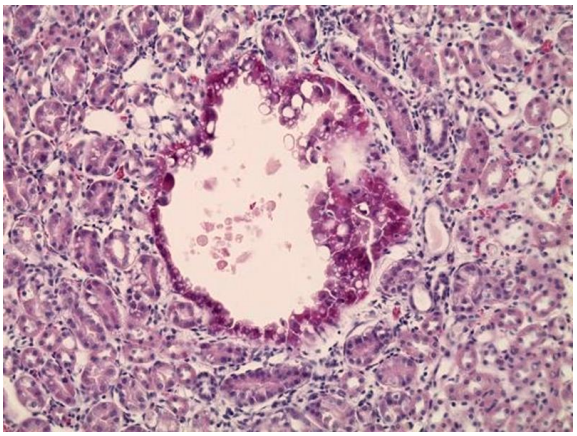


Figure 8.5. Case 43x-1-24 15-261 P5. Microphotograph of the kidney. Irregular and distended (interpreted as dysplastic) tubule, lined by several disorganized layers of cells with marked cytoplasmic vacuolation. HE stain, 20x objective.

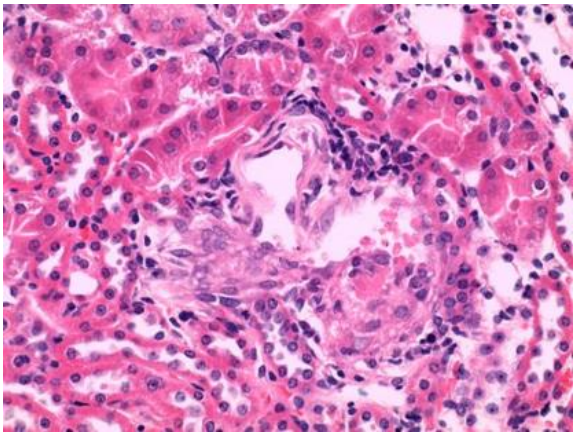


Figure 8.6. Case 1α43-342 15-317 P1. Microphotograph of the kidney. Irregular (suspected vascular) spindle cell proliferation. HE stain, 40x objective.

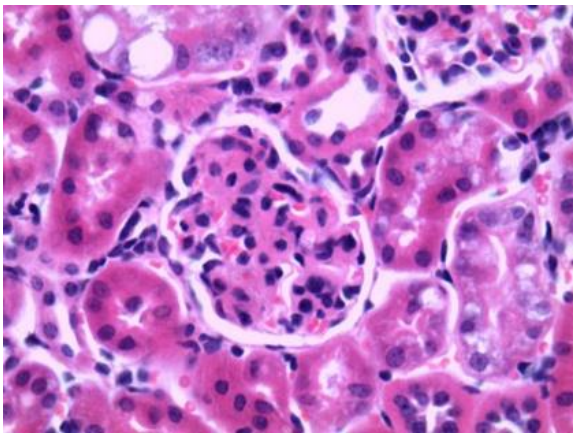


Figure 8.7. Case 43x-1-23 15-261 P1. Microphotograph of the kidney. Note the glomerular membranous thickening, indicative of glomerular damage. HE stain, 63x objective.

8.4.2 Immunohistochemistry

8.4.2.1 RBP4

Immunohistochemical staining was limited to kidney tissue of HIF-1α overexpressing TRACK mice (3/3, 100%) and was absent in WT animals (0/2) (Table 8.5). More specifically, TRACK mice had 20-40% of cortical nephrons with multifocal moderate granular apical cytoplasmic staining of predominantly proximal tubular cells and glomerular parietal epithelial cells (Figure 8.8). The entire kidney sections of all animals presented with a weak, diffuse staining, which was interpreted as background staining. Other organs, including heart, lung, liver, pancreas, spleen, intestine, testis, and tongue lacked any convincing positive staining.

Case	Subgroup	Kidney
WT♂ 8m-1 RBP4 15-331 P4	WT	Negative
WT♂ 8m-2 RBP4 15-331 P4	WT	Negative
43-348 RBP4 15-331 P4	TRACK	Moderately intense staining of 20-30% of cortical nephrons (proximal tubules, glomerular parietal cells)
43-349 RBP4 15-331 P4	TRACK	Moderately intense staining of 30-40% of cortical nephrons (proximal tubules, glomerular parietal cells)
43-358 RBP4 15-331 P4	TRACK	Moderately intense staining of 20-30% of cortical nephrons (proximal tubules, glomerular parietal cells)

Table 8.5. The results of the RBP4 immunohistochemical staining of the kidney. Abbreviations: RBP4: Retinol-binding protein 4; TRACK: Transgenic model of cancer of the kidney; WT: Wild type.

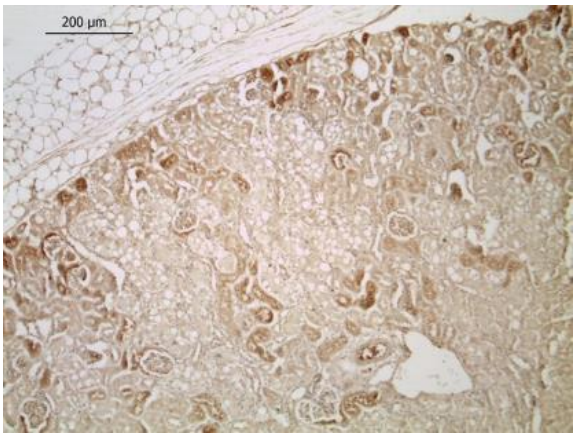


Figure 8.8A. Case 43-348 RBP4 15-331 P4. Kidney. Multifocal moderate RBP4 staining of proximal tubules and glomerular parietal layers, with diffuse weak staining of the entire kidney section. RBP4 IHC, 10x objective.

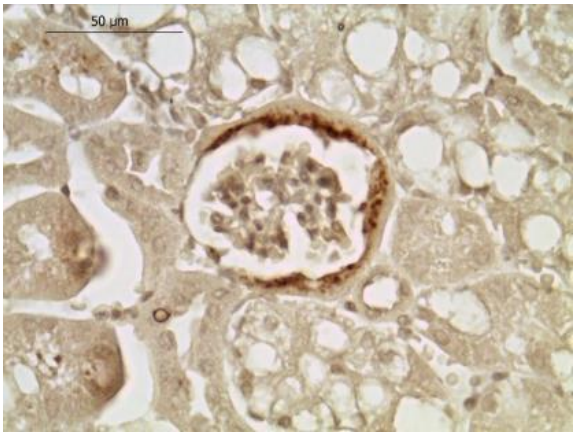


Figure 8.8B. Closer view of Figure 8.8A. Granular apical cytoplasmic RBP4 staining of glomerular parietal epithelial cells. The diffuse weak tubular staining is interpreted as background staining. RBP4 IHC, 63x objective.

8.4.2.2 MYC

Immunohistochemical staining was observed in all TRACK (3 out of 3) and WT (2 out of 2) animals in all examined tissues to a certain extent, including kidney, heart, liver, lung, pancreas, spleen, testis and tongue (Table 8.6). In the intestine (excluded from the table), the staining was restricted to leukocytes within the lamina propria. Staining intensity and distribution did not appear to significantly differ between TRACK and WT animals. In all animals, the staining was diffuse and cytoplasmic with weak to strong intensity depending on the type of stained tissue and cells. The staining in the kidney was characterized by a moderate to strong, diffuse, cytoplasmic staining of renal tubules (Figures 8.9 and 8.10). Additional structures or cells with the most distinct staining included: mononuclear leukocytes (spleen and intestine) (Figures 8.11 and 8.12), ductus epididymis epithelial cells, and testicular Leydig cells.

Organ	Group	Kidney	Heart	Lung	Liver	Spleen	Pancreas	Testis	Tongue
Staining distribution		diffuse, cytoplasmic	diffuse, cytoplasmic	diffuse, cytoplasmic	diffuse, cytoplasmic	diffuse, cytoplasmic	diffuse, cytoplasmic	diffuse, cytoplasmic	diffuse, cytoplasmic
Stained cell or structure		Tubules	Myocytes	Alveolar septae, bronchiolar epithelial cells	Hepatocytes	Leukocytes (macrophages)	exocrine cells	Leydig cells, seminiferous tubules (and ductus epididymis)	Myocytes, glossal epithelium
WT♂ 8m-1 MYC 15-331 P3	WT	+++	-	+	+	+++	+	++	+
WT♂ 8m-2 MYC 15-331 P3	WT	++	+	-	NP	+++	(+)	+++	+
43-350 MYC 15-331 P3	TRACK	++	++	-	+	+++	++	++	++
43-349 MYC 15-331 P3	TRACK	++	+	+	(+)	+++	-	+++	+
43-348 MYC 15-331 P3	TRACK	+++	+	+	+	+++	(+)	+++	(+)
Total	TRACK	2/3 mod 1/3 strong	2/3 weak 1/3 mod	1/3 neg 2/3 weak	3/3 weak	3/3 strong	1/3 neg 1/3 weak 1/3 mod	1/3 mod 2/3 strong	2/3 weak 1/3 mod
	WT	1/2 mod 1/2 strong	1/2 neg 1/2 weak	1/2 neg 1/2 weak	1/1 weak	2/2 strong	2/2 weak	1/2 mod 1/2 strong	2/2 weak

Table 8.6. The results of the MYC immunohistochemical staining of all examined tissues.

Abbreviations: Mod: Moderate; Neg: Negative; TRACK: Transgenic model of cancer of the kidney; WT: Wild type; -: negative; +: weak; ++: moderate; +++: strong; () lesion is minimal if indicated in brackets.

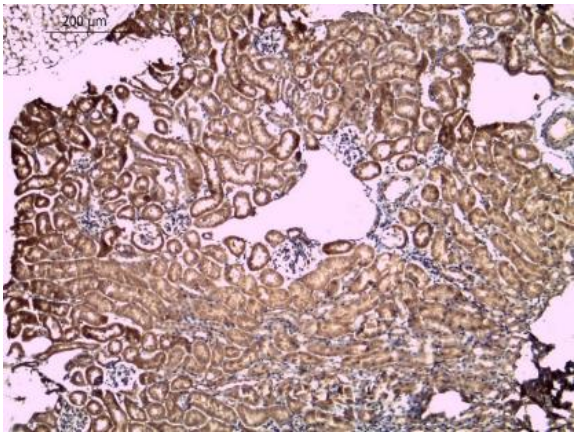


Figure 8.9A. Case WT♂ 8m-2 MYC 15-331 P3. MYC staining, kidney. Diffuse moderate staining of tubules. MYC IHC, 10x objective

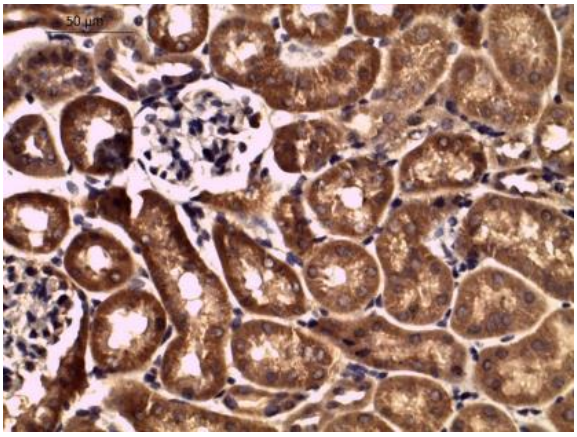


Figure 8.9B. Closer view of Figure 8.9A. Note the moderate cytoplasmic staining of tubular epithelial cells. MYC IHC, 40x objective.

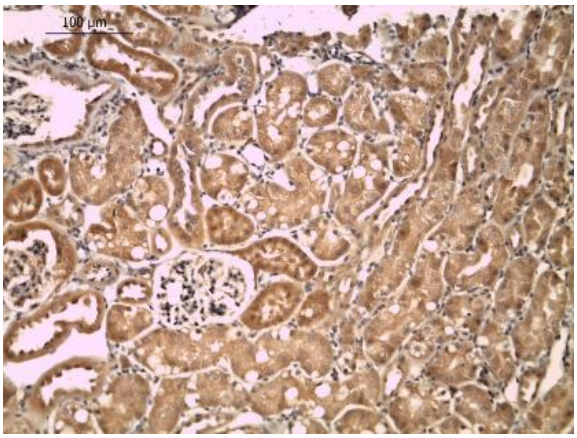


Figure 8.10. Case 43-350 MYC 15-331 P3. MYC staining, kidney. Note the diffuse moderate staining of tubules. MYC IHC, 20x objective.

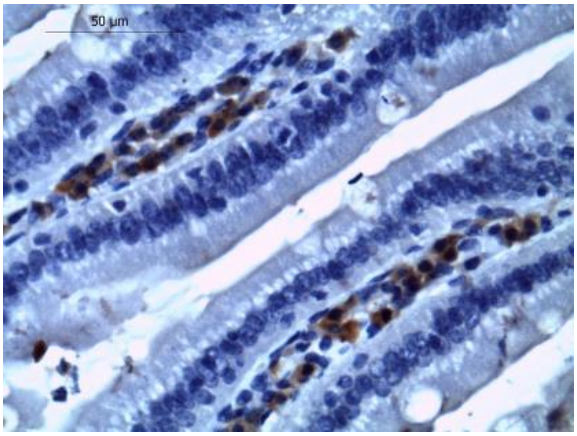


Figure 8.11. Case 43-350 MYC 15-331 P3. Small intestine. Strong cytoplasmic MYC staining of leukocytes within the lamina propria of the villi. MYC IHC, 63x objective.

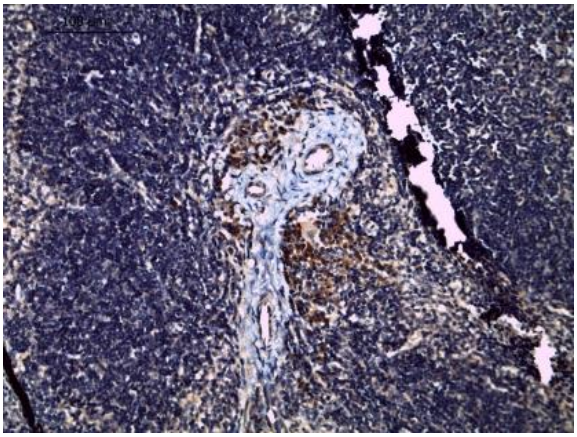


Figure 8.12A. Case 43-349 MYC 15-331 P3. Spleen. MYC staining of leukocytes within the red pulp (mainly periarteriolar). MYC IHC, 20x objective.

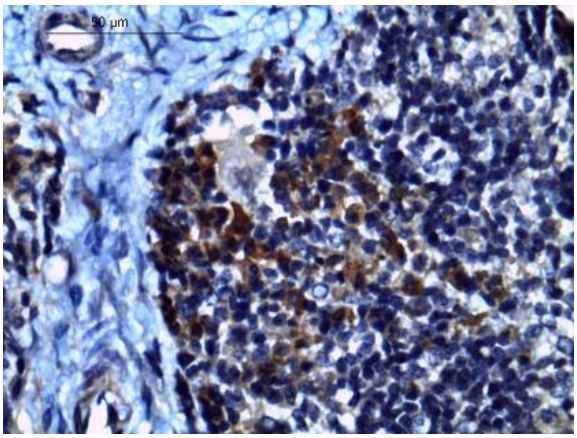


Figure 8.12B. Closer view of Figure 8.12A. Marked cytoplasmic MYC staining of leukocytes. MYC IHC, 63x objective.

8.5 Discussion

In 2011, the TRACK mouse model was generated, characterized by a constitutively active HIF-1α, leading to histological kidney lesions, which resemble the changes observed in human VHL (Fu et al., 2011). In this model, the HIF-1α expression is restricted to the kidney by using a renal proximal tubule specific promoter (type 1 γ-glutamyl transpeptidase). In the present study, a collection of different tissues from 66 TRACK mice have been examined histologically. In addition to the previously reported potentially premalignant lesions in the kidney, the renal tissue was also assessed for any other histopathological changes, including features of inflammation and degeneration. Moreover, other, non-renal tissues were also examined for any histopathological abnormalities.

The histological examination of the kidneys revealed comparable renal tubular histopathological changes as previously reported by Fu et al. (Fu 2011). The main lesion in the kidney consisted of a severe vacuolar swelling of proximal tubular epithelial cells, resembling 'clear' cells. These changes were absent in control (WT) or HIF-2α expressing mice. Occasionally, distorted tubules have been observed in a few TRACK mice, indicative of tubular dysplasia, which may be interpreted as a preneoplastic change. Alternatively, these lesions could already represent a neoplastic transformation, more specifically, a carcinoma in situ. True formations of, either microscopic or macroscopic, carcinomas have however not been identified in the mice examined here. Other frequent findings included intraluminal tubular accumulations of protein-rich substance (referred to as proteinuria), and fewer intraluminal calcifications. These changes were only present in TRACK mice and were considered secondary to the proximal tubular changes. Rarely, individual or small groups of proximal tubular cross sections presented with features suggestive of regeneration, such as cellular hypertrophy and hyperplasia, cytoplasmic basophilia, increased nuclear:cytoplasmic ratio, and presence of mitotic figures. Considering the association of HIF-1α expression and renal tubular regeneration and proliferation (Conde et al., 2012; Shu et al., 2019; Zepeda-Orozco et al., 2017), and given the absence of these lesions in WT and HIF-2α expressing mice, these

regenerative changes are most likely to be, at least partially, attributable to the overexpression of HIF-1α. Some TRACK mice showed one or several features of microvascular-related pathology, including multiple chronic renal infarcts and glomerular membranous changes. These changes were not observed in any of the control mice. The role of HIF-1α and HIF-2α in renal disease is controversial (Kong et al., 2017b; Li et al., 2017). Even though HIF-1α is known to have a protective role in renal disease (Fang et al., 2013; Nordquist et al., 2015), overexpression of the same protein has also been shown to be harmful (Baumann et al., 2016; Higgins et al., 2007). Increased levels of HIF-1α have been demonstrated to be associated with glomerular injury, through the activation of vasoactive substances leading to vasoconstriction (Luo et al., 2015). The observed glomerular lesions in the HIF-1α overexpressing mice of the present study may support this association. Furthermore, HIF-1α has been reported to promote renal fibrosis via the expression of lysyl oxidase genes and other profibrogenic factors (Higgins et al., 2007). This observation may potentially explain the chronic fibrotic changes, including the chronic infarcts, which occurred in a significant number (14%) of HIF-1α expressing mice. Another very common, even though little specific, histopathological lesion observed in the present study was a mild, chronic interstitial inflammation of the kidney, which was seen in more than 93% of HIF-1α mice, none of the HIF-2α animals and in 29% of WT. Considering that this change was absent in HIF-2α mice and much more common in HIF-1α compared to WT animals, this lesion is likely associated with increased expression of HIF-1α, either directly, or through the HIF-induced histopathological changes. Indeed, hypoxia and inflammation are known to coexist and regulate each other. HIF-1α has been demonstrated to have a direct regulatory effect on inflammation (Corcoran and O'Neill, 2016; Cramer et al., 2003; Liu et al., 2017). Alternatively, the severe renal tubular changes may have caused the interstitial inflammatory reaction, possibly by tubular cellular leakage. The association of tubular injury and inflammation is well-known to occur in the kidney, and interstitial inflammation is observed in the early phases of a variety of renal diseases (Cantaluppi et al., 2014; Liu et al., 2018a). Another option could be that the frequently observed

inflammation could correspond to a cancer (or at least precancerous condition)-associated process, which is known to occur in RCC (Geissler et al., 2015; Joung et al., 2018; Zhao et al., 2019). Furthermore, given the presence of the mild chronic renal inflammation in a significant number (29%) of WT mice, this histological change may correspond to a common background lesion in these mice. Therefore, the speculated association between the renal inflammatory changes and the overexpression of HIF-1α remains uncertain in the studied TRACK model. Finally, all HIF-overexpressing as well as WT mice showed a mild to occasionally moderate chronic pyelonephritis. Because of the omnipresent nature of this lesion, this change was considered incidental and unrelated to HIF expression. In agreement, inflammatory infiltrates in the submucosa of the renal pelvis have been demonstrated to be a frequent, spontaneous background finding in mice, without any biologic significance (Frazier et al., 2012).

Other organs than the kidney showed little (liver, pancreas, spleen) or no (heart, lung, small intestine, testis, skeletal muscle) potentially relevant histopathological changes. This finding was expected due to the fact that TRACK mice have been generated using a kidney-specific promoter (Fu et al., 2011). Nevertheless, a mild perivascular inflammatory reaction was observed in the liver of a significant number (29%) of HIF-1α expressing mice. None of the WT had evidence of hepatic inflammation, proposing that this lesion is likely associated with HIF-1α expression in the kidney, either directly or indirectly via its induced renal changes. Considering the link between liver and kidney (Cantaluppi et al., 2014), even a kidney-specific lesion may produce morphological changes in the liver. In addition to the inflammatory changes, four out of 24 (17%) HIF-1α expressing mice presented with minimal, single cell hepatocellular necrosis, which was absent in WT animals. It remains uncertain if and to what extent this change is associated with renal HIF-1α expression and associated lesions. Considering that, in this mouse model, HIF-1α is not overexpressed in the liver, the observed hepatocellular damage may be the result of an indirect effect of the HIF-1α induced renal changes. Finally, the

presence of mild extramedullary hematopoiesis in the spleen of all examined HIF-1α and WT mice was interpreted as incidental finding, likely unassociated with HIF-1α overexpression. Even though hematopoiesis in the spleen is not supposed to occur in adult mice, it may do so in older animals as it may be the case in the here examined mouse population (Loukov et al., 2016).

MYC was expressed in all examined tissues in at least certain types of cells, with a diffuse, cytoplasmic distribution in all cases. Assessed by IHC, the intensity of MYC protein expression varied markedly between the different sorts of tissue and cells and between some of the individual animals. When comparing TRACK and control mice, a convincingly different expression profile was not evident. This finding, however, needs to be interpreted with caution due to the limited number of animals examined. A predominantly absent to weak, and rarely moderate, expression of MYC was seen in the heart, lung, liver, pancreas, tongue of TRACK and WT mice. The IHC staining pattern and intensity in these tissues are comparable to the immunohistochemical protein expression profile reported in the Human Protein Atlas (HPA) (Ponten et al., 2008; Uhlen et al., 2015) (http://www.proteinatlas.org, accessed 13 November 2019), with the exception of the tongue, which currently lacks a MYC expression profile in the HPA. A moderate to strong expression of MYC was seen in the kidney, spleen, and testis. More specifically, IHC staining was present in renal tubules, splenic leukocytes (macrophages), testicular seminiferous tubules, Leydig cells and ductus epididymis. Available expression profiles on HPA are similar even though MYC has also been reported to be expressed in nuclei of testicular and splenic tissue, which is in contrast to the restricted cytoplasmic expression in the mouse tissue of the present study. In the small intestine, MYC expression was restricted to leukocytes within the lamina propria mucosae. From previous studies, it is known that MYC is overexpressed in ccRCC (Shroff et al., 2015; Tang et al., 2009). Considering the strong renal tubular staining in the kidney of TRACK mice in the present study, this ccRCC animal model may be able to reproduce MYC overexpression. A similar expression profile was however observed in WT animals, which hampers the interpretation of MYC expression

in TRACK mice. Thus, additional, ideally more specific, techniques (e.g. proteomics, transcriptomics) for assessing the expression of MYC should be performed. The effect of HIF-1α on tumorigenesis, as well as its association with MYC is controversial. For HIF-1α, a tumor inhibitory (Gordan et al., 2007; Zhang et al., 2007) as well as promoting (Fu et al., 2011; Gudas et al., 2014) effect has been demonstrated. The tumor suppressive effect of HIF-1α has been shown to be associated with reduced expression of MYC (Gordan et al., 2007; Zhang et al., 2007). Overexpression of HIF-1α in the kidney, as reproduced in TRACK mice, should therefore parallel decreased renal MYC expression. Alternatively, it could be hypothesized that the HIF-1α-induced metabolic changes could contribute to kidney damage, which may result in increased expression of MYC as a mechanism to accelerate kidney regeneration. Upregulation of MYC may then further promote cancer development. In the present study, none of these hypotheses could be proven neither to be true nor false, because of the comparable MYC expression profile of TRACK and WT mice. In order to detect a potential differential expression between TRACK and WT animals, larger sample sizes would be required or alternative methods of protein or RNA detection should be applied.

In the examined TRACK mice, RBP4 showed a kidney-specific protein expression, which was absent in WT animals. This cancer-related RBP4 expression provides further evidence that RBP4 may be valuable as biomarker for ccRCC, as suggested by Choi and his team who reported increased RBP4 serum levels in RCC patients (Choi et al., 2016). Other studies, which investigate the level of RBP4 protein expression in the kidney of ccRCC patients or animal models are lacking in the current literature. So far, the evaluation of renal RBP4 expression has been limited to a genetic level. In contrast to the observed increased protein levels, Kudryavtseva and her team demonstrated a reduced renal RBP4 gene expression in ccRCC patients (Kudryavtseva et al., 2017). In normal kidney, RBP4 is strongly expressed in the cytoplasm of renal tubular cells, without the limitation to a certain cellular location (Ponten et al., 2008; Uhlen et al., 2015) (https://www.proteinatlas.org/, accessed 13 November

2019). With the exception of a weak (interpreted as background), diffuse, cytoplasmic tubular IHC staining in TRACK and WT mice, RBP4 expression was restricted to the apical cytoplasm of proximal tubular and parietal epithelial cells of TRACK mice examined in the present study. This specific cellular distribution of RBP4 has not been reported and its significance remains uncertain. Non-specific staining cannot be ruled out with certainty. Furthermore, non-renal, including liver, tissue sections lacked RBP staining in TRACK as well as WT animals. The failure to detect RBP4 expression in the liver was unexpected, given that murine and human liver tissue is known to express this protein under normal and neoplastic conditions (Noy et al., 2015; Quadro et al., 1999; Thompson et al., 2017; Wang et al., 2011). The lack of detectable liver RBP4 expression in the present study raises concerns and requires further investigation.

In summary, in the present study, which was based on the histological examination of only a subset of tissue samples, the most relevant renal changes were restricted to microscopic, dysplastic to non-invasive, i.e. in-situ, neoplastic tubular lesions. Invasive cancerous growth could not be demonstrated on the examined kidney samples. Therefore, these observations indicate that the TRACK model reliably develops pre-neoplastic and early neoplastic renal tubular changes with comparable histomorphology as seen in spontaneous human disease. Certain adaptations of the experiments may be required in order to confirm the suitability of the TRACK model to induce invasive renal cancer. A longer duration of the experiment may be considered in order to achieve more advanced histological neoplastic changes. Alternatively, in order to improve the model, the concentration of HIF-1α could be increased by experimentally inducing i) direct HIF-1α overexpression, ii) inactivation of VHL, or iii) creating a hypoxic environment. In addition to the tubular lesions, other mild renal changes were frequently observed in TRACK mice, including tubular regeneration, chronic infarcts, glomerular changes and chronic interstitial inflammation. These changes are suspected to be associated with HIF-1α expression, and deserve further investigation. Histological lesions

Deleted: conclusion

Deleted: the TRACK model is a robust model for ccRCC, which reliably develops pre-neoplastic and early neoplastic renal tubular changes with comparable histomorphology as seen in spontaneous human disease.

in other organs than the kidney, primarily chronic inflammatory infiltrates in the liver, have been observed in a significant number of TRACK mice, and may possibly be related to increased renal HIF-1α levels. Mild, chronic pyelonephritis is a common background lesion, which was present in all examined TRACK and WT mice. MYC is strongly expressed in renal tubules, and to a variable extent in other tissues, with similar immunohistochemical expression profiles between TRACK and WT animals. Consequently, neither a decrease nor increase of MYC protein levels could be demonstrated in this animal model. Further investigation, with larger sample sizes or alternative protein expression detection methods, is recommended. RBP4 expression was present in the apical cytoplasm of proximal tubular and parietal epithelial cells of TRACK mice, which was absent in WT. This observation prompts to further evaluate the potential use of RBP4 as biomarker for ccRCC. Other organs, including the liver, failed to demonstrate convincing RBP4 expression by IHC.

This study confirms the previously reported premalignant renal proximal tubular histopathological lesions in the TRACK model. In addition, degenerative and inflammatory changes within the kidney and the liver, as well as the immunohistochemical expression of MYC and RBP4 are reported in this model for the first time.

9. Conclusions

The present study is a comparative, morphological and molecular pathological study of urological cancers. More specifically, dogs with spontaneous urological cancers were assessed as a non-rodent animal model for UC and PCa in men. In addition, two novel potential therapeutic targets have been evaluated in human PCa specimens. Furthermore, the TRACK mouse model was evaluated histopathologically. The main conclusions are summarized below, with reference to the aims of this dissertation. In addition, observations, which, to the author's best knowledge, are reported for the first time, are summarized under 'new insights'.

i) Aim: Pathological and molecular characterization of the canine UC model

Main conclusions

- Canine and human UC are epidemiologically and pathologically directly comparable, supporting the dog as a valuable animal model. The two most striking common features of canine and human UC include high sex predilection and histological tumor appearance.
- Canine UC has an extraordinarily high predisposition for certain genetically closely related dog breeds (top leader: Scottish terriers), which suggests a strong genetic component.
- Female surgically neutered (ovariohysterectomized) dogs are at highest risk to develop UC which leads to the speculation that the level of sex hormones and their receptors are relevant for UC carcinogenesis in dogs.
- Most canine UC are of high tumor grade and stage, with frequent muscle-invasive growth. Therefore, UC in dogs appears to mimic the malignant muscle-invasive form of UC in people.
- Tumor-associated inflammation is very common (>75%) in canine UC, consisting of a mild lymphoplasmacytic reaction in most cases. This is in agreement with the situation in human UC, where tumor inflammation is known to be frequent.

New insights

- To date, the present study is the largest reported comparative histological canine UC study, which includes a total of 381 dogs.
- The three dog breeds with highest risk to develop UC are significantly younger at the time of tumor diagnosis, compared to other dog breeds.
- In dogs, papillary UC is equally as common as UC with a non-papillary (flat) growth.
- In canine UC, non-papillary tumor growth is strongly associated with muscle invasion. This observation is in agreement with non-papillary UC in people, which are known to be associated with higher tumor grade, muscle invasion and poor prognosis.
- Fibromyxoid tumor stroma is common (27%) in canine UC and represents a strong indicator for muscle invasive tumor growth, presumably indicative of poor prognosis. This observation is in agreement with reported prognostic significance of a myxoid stroma in human urothelial and non-urothelial cancers.
- Uncommon variants of divergent histological differentiation are occasionally present in canine UC, including micropapillary and microcystic growth, as well as rhabdoid, signet-ring cell, lipid-rich and glycogen-rich appearance of neoplastic cells. Comparable histological tumor features are well known in human UC.
- Rare urinary tract tumors, including plasmacytoid UC and neuroendocrine tumor, occur spontaneously in dogs.
- Tumor necrosis in canine UC is relatively common (24%), and is mild and comedo-like in most (>90%) of the cases. This is in agreement with human UC, where necrosis is also a frequent tumor feature.
- In canine UC, the presence of tumor necrosis is associated with the presence of fibromyxoid tumor stroma. Considering the demonstrated association of fibromyxoid stroma and muscle-invasive tumor growth, tumor necrosis may have potential prognostic significance in canine UC. In human UC, tumor necrosis is a well-known feature for poor prognosis.

- In addition to the most commonly lympoplasmacytic tumor-associated inflammatory reaction, there is a variable (mild to marked) eosinophilic inflammatory component in almost one third of canine UC. In human oncology, the occurrence of eosinophils within neoplastic tissue is referred to as TATE. TATE is known to occur in human UC, with a controversial prognostic significance.
- This study is the first to describe AS in canine UC, revealing frequent differential splicing of cancer-relevant genes. Many of the identified altered cancer-relevant genes and pathways are known to be associated with human BC, confirming the resemblance of canine and human BC on a molecular level.
- Certain identified altered genes (*SVIL, PXN, KAT7, ACIN1, TPCN2, SLIT2, MTNR1A, DDR1, APAF1, PKN1, F11R, TCF7L2, ALKBH, COL6A3*) and KEGG pathways (focal adhesion, pathways in cancer, PI3K-Akt signalling among others) in canine UC are known to be relevant in human BC. Furthermore, human BC, as well as acute myeloid leukemia and thyroid cancer pathways are enriched pathways in the assessed canine UC with differential AS.
- Based on a low number (n=3 paired normal and tumor) of cases, significant differential gene expression was not observed in canine UC. In contrast to AS, the analysis of differentially expressed genes is less likely to provide new insights into UC oncogenesis in dogs.

ii) Aim: Pathological and molecular characterization of the canine PCa model

Main conclusions

- Entire as well as surgically castrated (orchiectomized) dogs develop spontaneous PCa. There is a trend for castrated dogs to be at higher risk for developing this cancer, proposing that canines may suffer from a hormone-resistant form of cancer.
- In dogs, PCa is a high-grade tumor, which is often diagnosed late at high cancer stage.

- Canine PCa is characterized by a poor histological differentiation, which makes a further histomorphological tumor classification difficult. The cell of PCa origin remains uncertain in the majority of affected dogs.
- The majority (84%) of canine PCa either lack (51%) UPIII expression or express it at very low levels (33%). In benign canine prostate tissue, UPIII expression is present in urothelial cells of the urethra and ducts.
- IHC for UPIII can be helpful for the differentiation of UC and anaplastic, not further classifiable, canine PCa.
- For canine PCa, IHC for p63 is of limited value. Most (90%) canine PCa contain only scattered p63 positive cells (54%) or are p63 negative (36%). In benign canine prostate tissue, strong nuclear p63 expression is present in basal and urothelial cells.

New insights

- The origin of canine PCa remains uncertain. Acinar (including neuroendocrine), urethral as well as ductal cells need to be considered as potential cell of tumor origin.

iii) Pathological and immunohistochemical evaluation of novel potential therapeutic targets in human PCa specimens

New insights

- Two potential PCa-relevant markers, KDM7A and KDM5B, have been identified. Both markers are expressed in benign and malignant human prostate tissue.
- KDM7A is consistently, even though weakly, expressed in the majority of benign (60-89%) and malignant (70-100%) prostate tissues. PCa metastases vary in their KDM7A expression, ranging from 0% (kidney) to 100% (adrenal, liver, testis) of cases, with intermediate values of 67-88% in bone, lymph node and lung.

- In men, cytoplasmic KDM7A expression is higher in benign prostate compared to organ-confined PCa. Nuclear expression is higher in metastatic PCa in comparison to benign prostate tissue
- In human prostates, distinct and strong cytoplasmic KDM7A staining of prostate basal cells is seen, suggesting that this KDM may have potential as basal cell marker.
- KDM5B is consistently and strongly expressed in the cytoplasm and nuclei of benign (100%) and malignant (100%) human prostate tissue. The cytoplasmic expression may represent a previously undiscovered non-chromatin linked role.
- Nuclear KDM5B expression is reduced in bone PCa metastases compared to benign prostate tissue of men.

iv) Aim: Pathological and molecular investigation of mechanistic contributors to kidney clear cell cancer

Main conclusions

- The TRACK mouse model reliably develops pre-neoplastic and early neoplastic renal tubular changes with comparable histomorphology as seen in early stages of spontaneous ccRCC. This confirms its suitability as animal model for early stages of kidney cancer.
- TRACK mice present with moderate to severe vacuolar renal tubular changes, with presence of tubular dysplasia in some (11%) cases.

New insights

- In addition to the pre-malignant renal changes, significant lesions in the kidney of TRACK mice include a mild, chronic interstitial inflammation, fibrosis, and tubular regeneration. These changes are suspected to be associated with an increased HIF-1α expression, which defines this mouse model.

- A mild, chronic interstitial renal inflammation is present in the majority (93%) of TRACK mice. A substantial number (29%) of wild type (WT) animals present with similar changes.
- Mild chronic tubular atrophy and interstitial fibrosis in the kidney, indicative of chronic infarctions, occurs in a moderate number (14%) of TRACK mice. These lesions are not seen in the control animals.
- Features of renal tubular regeneration is seen in a large number (70%) of TRACK mice. This feature is not observed in control animals.
- In the TRACK model, the most relevant non-renal histopathology includes a mild, chronic inflammatory response in the liver, which is seen in a moderate number (29%) of TRACK mice. This feature is not seen in WT mice.
- RBP4 is expressed in the renal proximal tubular and glomerular parietal epithelial cells of TRACK mice. Other assessed organs, including the liver, lack RBP4 expression. WT mice lack RBP4 expression in the kidney. Therefore, RBP4 has the potential to be used as biomarker for renal cancer.
- Moderate to strong expression of MYC is seen in the renal tubules of TRACK and WT animals. Other organs from the same animals show variable MYC staining, without evident differences between TRACK and WT mice.

As a final concluding remark, these studies support the use of comparative models to advance understanding of oncogenic mechanisms.

Potential future work

Considering the results of all the performed individual studies, the canine bladder cancer as well as prostate cancer model appear to be most promising for the following main reasons:

- The extraordinarily high breed predisposition of canine BC strongly suggests a genetic cause, which has not been identified to date
- The histomorphology of canine UC is directly comparable to human disease
- Canine BC is fairly common, which will enable disease investigation and potential future therapeutic trials

- The dog is the only animal species which does develop spontaneous PC on a regular basis
- In contrast to most PC lab animal models, canine PC is characterized by frequent metastatic spread, with comparable sites of metastases as in men

The main challenges of the spontaneous canine model are the late onset (between 5 to 15 years) of the disease, and difficulties to plan experiments including tissue sampling. However, these can be overcome by using already archived FFPE and biobanked fresh tissues. Future planned next steps in this field of research are:

- Identification of the canine BC causing gene(s) by genetic analysis (ideally whole genome sequencing) of dog tissue, followed by in vitro experiments for the study of the affected gene(s) in animal and human cells and tissue
- Establishment of a canine BC and PC cell culture for testing potential anti-cancer drugs before they are applied to pet dogs with cancer
- Screen canine PC for known human-relevant driver mutations by targeted RNA and DNA in order to further evaluate the dog as animal model for human PC
- Reduce the number of lab animals by testing therapeutic drugs *in vitro* on canine cancer cell culture or organoids

The first series of follow-up studies in our group are planned to start in spring 2020, in collaboration with Prof Mark Rubin from the University of Bern.

10. Publications and presentations

During the time period, when the present study was performed, the following 9 studies and three book chapters were published in scientific, peer-reviewed journals. Two of these studies directly derive from this dissertation and are included in this thesis. In addition, some parts of the performed investigations were presented at 7 different national and international scientific meetings, as indicated below.

Studies included in this thesis

- **de Brot S**, Grau-Roma L, Stirling-Stainsby C, Dettwiler M, Guscetti F, Meier D, Scase T, Robinson BD, Gardner D, Mongan NP. A fibromyxoid stromal response is associated with muscle invasion in canine urothelial carcinoma. Journal of Comparative Pathology. 2019, 169:35-46.
- **de Brot S**, Robinson BD, Scase, T, Grau-Roma L, Wilkinson E, Boorjian SA, Gardner D, Mongan NP. The dog as an animal model for bladder and urethral urothelial carcinoma: Comparative epidemiology and histology. Oncology Letters. 2018, 16(2):1641-1649.

Other cancer studies

- Corbetta D, Edery E, Polledo L, Grau-Roma L, **de Brot S**. Concurrent ectopic ureter and primary ureteral carcinoma in a cat. Journal of the American Veterinary Medical Association. IN PRESS
- Morey-Matamalas A, de Stefani A, Corbetta D, Grau-Roma L, **de Brot S**. Pulmonary basaloid squamous cell carcinoma in a dog. Journal of Comparative Pathology. 2018, 159:11-15.
- REVIEW. Simpson S, Dunning MD, **de Brot S**, Grau-Roma L, Mongan NP, Rutland CS. Comparative review of human and canine Osteosarcoma: morphology, epidemiology, prognosis, treatment and genetics. Acta Veterinaria Scandinavica. 2017, 59(1):71.
- REVIEW. Metzler VM, **de Brot S**, Robinson RS, Jeyapalan JN, Rakha E, Walton T3, Gardner DS, Lund EF, Whitchurch J, Haigh D, Lochray JM, Robinson BD,

Allegrucci C, Fray RG, Persson JL, Ødum N, Miftakhova RR, Rizvanov AA, Hughes IA, Tadokoro-Cuccaro R, Heery DM, Rutland CS, Mongan NP. Androgen dependent mechanisms of pro-angiogenic networks in placental and tumor development. Placenta. 2017, 56:79-85.

- **de Brot S**, Mongan NP. Key molecular pathways in prostate cancer development and progression: The cell cycle and androgen signaling interactions in prostate cancer. In: Robinson B, Mosquera JM, editors. Precision Molecular Pathology of Prostate Cancer. New York, NY, USA: Springer. 2017
- Rutland CS, **de Brot S**, James V, Mongan NP. Book Cancer and Noncoding RNAs, chapter 19: Heterochromatin modulation and PcG control of gene expression mediated by noncoding RNA in cancer. In Cancer and Noncoding RNAs. Editors: Jayprokas Chakrabarti, Sanga Mitra, Peter Linsley, Series Editor: Trygve Tollefsbol, Genetics & Genomics: Elsevier. 2017
- **de Brot S**, Rutland CS, Mongan NP, James V. Book Cancer and Noncoding RNAs, chapter 20: Epigenetic Control of microRNA Expression and Cancer. 2017 In Cancer and Noncoding RNAs. Editors: Jayprokas Chakrabarti, Sanga Mitra, Peter Linsley, Series Editor: Trygve Tollefsbol, Genetics & Genomics: Elsevier. 2017
- **de Brot S**, Schade B, Croci M, Dettwiler M, Guscetti F. Sequence and partial functional analysis of canine Bcl-2 family proteins. Research in Veterinary Science. 2016, 104:126-35.
- REVIEW. **de Brot S**, Ntekim A, Cardenas R, James V, Allegrucci C, Heery DM, Bates DO, Ødum N, Persson JL, Mongan NP. Regulation of vascular endothelial growth factor in prostate cancer. Endocrine Related Cancer. 2015, 22(3):R107-23.
- **de Brot S**, Sydler T, Nufer L, Ruetten M. Histological, immunohistochemical and electron microscopic characterization of a malignant iridophoroma in a dwarf bearded dragon (pogona henrylawsoni). Journal of Zoo and Wildlife Medicine. 2015, 46(3):583-7.

Presentations

- **Joint meeting of the European Society of Veterinary Pathology (ESVP), the European College of Veterinary Pathologists (ECVP), the European Society of Veterinary Clinical Pathology (ESVCP) and the European College of Veterinary Clinical Pathology (ECVCP).** Arnhem, The Netherlands. **de Brot S**, Grau-Roma L, White E, Scase T, Robinson BD, Guscetti F, Mongan NP. Immunohistochemical expression of p63 and Uroplakin III in non-neoplastic and neoplastic canine prostate tissue. Short oral and poster presentation. September 2019
- **Faculty Research Forum, University of Nottingham, UK. de Brot S**, Robinson BD, Scase T, Grau Roma L, Gardner D, Mongan MP. Can old dogs teach us new tricks in bladder cancer? Poster and oral presentation. June 2017
- **Postgraduate Research Symposium, University of Nottingham, UK. de Brot S**, Robinson BD, Grau Roma L, Scase T, Wilkinson E, Boorjian S, Dunning M, Gardner D, Mongan NP. Bladder cancer in people and dogs. A comparative epidemiological and histological study. Poster presentation (second prize). May 2017
- **Prostate Cancer UK Event, Nottingham, UK. de Brot S**, Robinson BD, Grau-Roma L, Scase T, Mongan NP. Animal model for prostatic disease and Animal model for prostate cancer. Poster presentations. March 2017
- **Joint meeting of the European Society of Veterinary Pathology (ESVP) and the European College of Veterinary Pathologists (ECVP)** Bologna, Italy. **de Brot S**, Grau-Roma L, Wilkinson E, Dunning M, Gardner D, Scase T, Mongan NP. Histologic characterization of 100 urinary bladder and urethral transitional cell urothelial carcinomas in dogs from the United Kingdom. Oral presentation. September 2016
- **Thermo Fisher Workshop for Animal Health Customers Schlieren, Switzerland. de Brot S**, Rutland C, Dunning M, Cobb M, Simpson S, Mongan NP. University of Nottingham. Canine Genomic Health Group. Oral presentation. April 2016

- **Cancer Genomics, EMBL** Heidelberg, Germany. **de Brot S**, Fu L, Devonald MA, Fuentes-Utrillia P, Johannson M, Nanus DM, Gudas LJ, Gardner DS, Mongan NP. An acute kidney injury model shares molecular characteristics of renal clear cell carcinoma. Poster presentation. November 2015

11. References

Abbo, A.H., Jones, D.R., Masters, A.R., Stewart, J.C., Fourez, L., Knapp, D.W., 2010. Phase I clinical trial and pharmacokinetics of intravesical mitomycin C in dogs with localized transitional cell carcinoma of the urinary bladder. J Vet Intern Med 24, 1124-1130.

Abdel-Rahman, O., 2019. Prostate Cancer Incidence and Mortality in Relationship to Family History of Prostate Cancer; Findings From The PLCO Trial. Clin Genitourin Cancer 17, e837-e844.

Abdelrahman, A.E., Fathy, A., Elsebai, E.A., Nawar, N., Etman, W.M., 2018. Prognostic impact of Apaf-1, Cyclin D1, and AQP-5 in serous ovarian carcinoma treated with the first-line chemotherapy. Ann Diagn Pathol 35, 27-37.

Aggarwal, S., Ricklis, R.M., Williams, S.A., Denmeade, S.R., 2006. Comparative study of PSMA expression in the prostate of mouse, dog, monkey, and human. Prostate 66, 903-910.

Akter, S.H., Lean, F.Z., Lu, J., Grieco, V., Palmieri, C., 2015. Different Growth Patterns of Canine Prostatic Carcinoma Suggests Different Models of Tumor-Initiating Cells. Vet Pathol 52, 1027-1033.

Al-Bayati, O., Hasan, A., Pruthi, D., Kaushik, D., Liss, M.A., 2019. Systematic review of modifiable risk factors for kidney cancer. Urol Oncol 37, 359-371.

Al-Mansour, M.A., Kubba, M.A.G., Al-Azreg, S.A., Dribika, S.A., 2018. Comparative histopathology and immunohistochemistry of human and canine mammary tumors. Open Vet J 8, 243-249.

Alford, A.V., Brito, J.M., Yadav, K.K., Yadav, S.S., Tewari, A.K., Renzulli, J., 2017. The Use of Biomarkers in Prostate Cancer Screening and Treatment. Rev Urol 19, 221-234.

Alfred Witjes, J., Lebret, T., Comperat, E.M., Cowan, N.C., De Santis, M., Bruins, H.M., Hernandez, V., Espinos, E.L., Dunn, J., Rouanne, M., Neuzillet, Y., Veskimae, E., van der Heijden, A.G., Gakis, G., Ribal, M.J., 2017. Updated 2016 EAU Guidelines on Muscle-invasive and Metastatic Bladder Cancer. Eur Urol 71, 462-475.

Allard, P., Bernard, P., Fradet, Y., Tetu, B., 1998. The early clinical course of primary Ta and T1 bladder cancer: a proposed prognostic index. Br J Urol 81, 692-698.

Allstadt, S.D., Rodriguez, C.O., Jr., Boostrom, B., Rebhun, R.B., Skorupski, K.A., 2015. Randomized phase III trial of piroxicam in combination with mitoxantrone or carboplatin for first-line treatment of urogenital tract transitional cell carcinoma in dogs. J Vet Intern Med 29, 261-267.

Alonge, S., Melandri, M., Aiudi, G., Lacalandra, G.M., 2018a. Advances in Prostatic Diagnostics in Dogs: The Role of Canine Prostatic Specific Esterase in the Early Diagnosis of Prostatic Disorders. Top Companion Anim Med 33, 105-108.

Alonge, S., Melandri, M., Leoci, R., Lacalandra, G.M., Aiudi, G., 2018b. Canine prostate specific esterase (CPSE) as an useful biomarker in preventive

screening programme of canine prostate: CPSE threshold value assessment and its correlation with ultrasonographic prostatic abnormalities in asymptomatic dogs. Reprod Domest Anim 53, 359-364.

Alshabi, A.M., Vastrad, B., Shaikh, I.A., Vastrad, C., 2019. Identification of important invasion and proliferation related genes in adrenocortical carcinoma. Med Oncol 36, 73.

Alshenawy, H.A., Saied, E., 2015. Do HOXB13 and P63 have a role in differentiating poorly differentiated prostatic carcinoma from urothelial high-grade carcinoma? APMIS 123, 772-778.

Altwein, J.E., Luboldt, H.J., 1999. Prognostic factors for carcinoma of the prostate. Urol Int 63, 62-71.

Ambros, R.A., Malfetano, J.H., Mihm, M.C., 1996. Clinicopathologic features of vulvar squamous cell carcinomas exhibiting prominent fibromyxoid stromal response. Int J Gynecol Pathol 15, 137-145.

Ambrosini-Spaltro, A., Melissari, M., 2011. Papillary urothelial carcinoma of the bladder with exuberant pseudosarcomatous stromal reaction following radiation therapy. Int J Surg Pathol 19, 263-267.

Amin, M.B., 2009. Histological variants of urothelial carcinoma: diagnostic, therapeutic and prognostic implications. Mod Pathol 22 Suppl 2, S96-S118.

Amin, M.B., Epstein, J.I., Ulbright, T.M., Humphrey, P.A., Egevad, L., Montironi, R., Grignon, D., Trpkov, K., Lopez-Beltran, A., Zhou, M., Argani, P., Delahunt, B., Berney, D.M., Srigley, J.R., Tickoo, S.K., Reuter, V.E., Members of the ISUP Immunohistochemistry in Diagnostic Urologic Pathology Group, 2014. Best practices recommendations in the application of immunohistochemistry in urologic pathology: report from the International Society of Urological Pathology consensus conference. Am J Surg Pathol 38, 1017-1022.

Amin, M.B. and Tickoo, S.K.: Genitourinary Diagnostic Pathology. Second ed: Elsevier; 2016.

Amini, A., Jones, B., Jackson, M.W., Yeh, N., Waxweiler, T.V., Maroni, P., Kavanagh, B.D., Raben, D., 2016. Survival Outcomes of Dose-Escalated External Beam Radiotherapy versus Combined Brachytherapy for Intermediate and High Risk Prostate Cancer Using the National Cancer Data Base. J Urol 195, 1453-1458.

Andreassen, B.K., Aagnes, B., Gislefoss, R., Andreassen, M., Wahlqvist, R., 2016. Incidence and Survival of urothelial carcinoma of the urinary bladder in Norway 1981-2014. BMC Cancer 16, 799.

Angulo, J.C., Shapiro, O., 2019. The Changing Therapeutic Landscape of Metastatic Renal Cancer. Cancers (Basel) 11.

Anidjar, M., Scarlata, E., Cury, F.L., Rocha, J., Hamel, L., Luz, M., Chevalier, S., 2012. Refining the orthotopic dog prostate cancer (DPC)-1 model to better bridge the gap between rodents and men. Prostate 72, 752-761.

Anidjar, M., Villette, J.M., Devauchelle, P., Delisle, F., Cotard, J.P., Billotey, C., Cochand-Priollet, B., Copin, H., Barnoux, M., Triballeau, S., Rain, J.D., Fiet, J., Teillac, P., Berthon, P., Cussenot, O., 2001. In vivo model

mimicking natural history of dog prostate cancer using DPC-1, a new canine prostate carcinoma cell line. Prostate 46, 2-10.

Annan, A.C., Stevens, K.A., Osunkoya, A.O., 2017. Urothelial carcinoma involving the ureteral orifice: a clinicopathologic analysis of 93 cases. Human Pathology 65, 101-106.

Antoni, S., Ferlay, J., Soerjomataram, I., Znaor, A., Jemal, A., Bray, F., 2017. Bladder Cancer Incidence and Mortality: A Global Overview and Recent Trends. Eur Urol 71, 96-108.

Apolo, A.B., Milowsky, M., Bajorin, D.F., 2009. Clinical states model for biomarkers in bladder cancer. Future Oncol 5, 977-992.

Arafat, H., Lazar, M., Salem, K., Chipitsyna, G., Gong, Q., Pan, T.C., Zhang, R.Z., Yeo, C.J., Chu, M.L., 2011. Tumor-specific expression and alternative splicing of the COL6A3 gene in pancreatic cancer. Surgery 150, 306-315.

Arcangeli, G., Strigari, L., Arcangeli, S., 2015. Radical cystectomy versus organ-sparing trimodality treatment in muscle-invasive bladder cancer: A systematic review of clinical trials. Crit Rev Oncol Hematol 95, 387-396.

Arnold, E.J., Childress, M.O., Fourez, L.M., Tan, K.M., Stewart, J.C., Bonney, P.L., Knapp, D.W., 2011. Clinical trial of vinblastine in dogs with transitional cell carcinoma of the urinary bladder. J Vet Intern Med 25, 1385-1390.

Arrowsmith, C.H., 1999. Structure and function in the p53 family. Cell Death Differ 6, 1169-1173.

Arva, N.C., Das, K., 2011. Diagnostic dilemmas of squamous differentiation in prostate carcinoma case report and review of the literature. Diagn Pathol 6, 46.

Athanasopoulou, A., Aroukatos, P., Nakas, D., Repanti, M., Papadaki, H., Bravou, V., 2013. Decreased ezrin and paxillin expression in human urothelial bladder tumors correlate with tumor progression. Urol Oncol 31, 836-842.

Awadelkarim, K.D., Callens, C., Rosse, C., Susini, A., Vacher, S., Rouleau, E., Lidereau, R., Bieche, I., 2012. Quantification of PKC family genes in sporadic breast cancer by qRT-PCR: evidence that PKCiota/lambda overexpression is an independent prognostic factor. Int J Cancer 131, 2852-2862.

Babjuk, M., Bohle, A., Burger, M., Capoun, O., Cohen, D., Comperat, E.M., Hernandez, V., Kaasinen, E., Palou, J., Roupret, M., van Rhijn, B.W.G., Shariat, S.F., Soukup, V., Sylvester, R.J., Zigeuner, R., 2017. EAU Guidelines on Non-Muscle-invasive Urothelial Carcinoma of the Bladder: Update 2016. Eur Urol 71, 447-461.

Babjuk, M., Burger, M., Zigeuner, R., Shariat, S.F., van Rhijn, B.W., Comperat, E., Sylvester, R.J., Kaasinen, E., Bohle, A., Palou Redorta, J., Roupret, M., European Association of, U., 2013. EAU guidelines on non-muscle-invasive urothelial carcinoma of the bladder: update 2013. Eur Urol 64, 639-653.

Bailey, S.T., Smith, A.M., Kardos, J., Wobker, S.E., Wilson, H.L., Krishnan, B., Saito, R., Lee, H.J., Zhang, J., Eaton, S.C., Williams, L.A., Manocha, U., Peters, D.J., Pan, X., Carroll, T.J., Felsher, D.W., Walter, V., Zhang, Q., Parker, J.S., Yeh, J.J., Moffitt, R.A., Leung, J.Y., Kim, W.Y., 2017. MYC

activation cooperates with Vhl and Ink4a/Arf loss to induce clear cell renal cell carcinoma. Nat Commun 8, 15770.

Barbieri, C.E., Tomlins, S.A., 2014. The prostate cancer genome: perspectives and potential. Urol Oncol 32, 53.

Bassily, N.H., Vallorosi, C.J., Akdas, G., Montie, J.E., Rubin, M.A., 2000. Coordinate expression of cytokeratins 7 and 20 in prostate adenocarcinoma and bladder urothelial carcinoma. Am J Clin Pathol 113, 383-388.

Baumann, B., Hayashida, T., Liang, X., Schnaper, H.W., 2016. Hypoxia-inducible factor-1alpha promotes glomerulosclerosis and regulates COL1A2 expression through interactions with Smad3. Kidney Int 90, 797-808.

Behzatoglu, K., Yildiz, P., Oznur, M., Bozkurt, E.R., 2012. A synchronous occurrence of urothelial carcinoma with abundant myxoid stroma and inverted papilloma of the urinary bladder. Rare Tumors 4, e45.

Bell, F.W., Klausner, J.S., Hayden, D.W., Feeney, D.A., Johnston, S.D., 1991. Clinical and pathologic features of prostatic adenocarcinoma in sexually intact and castrated dogs: 31 cases (1970-1987). J Am Vet Med Assoc 199, 1623-1630.

Bell, F.W., Klausner, J.S., Hayden, D.W., Lund, E.M., Liebenstein, B.B., Feeney, D.A., Johnston, S.D., Shivers, J.L., Ewing, C.M., Isaacs, W.B., 1995. Evaluation of Serum and Seminal Plasma Markers in the Diagnosis of Canine Prostatic Disorders. J Vet Intern Med 9, 149-153.

Benard, A., Zeestraten, E.C.M., Goossens-Beumer, I.J., Putter, H., van de Velde, C.J.H., Hoon, D.S.B., Kuppen, P.J.K., 2014. DNA methylation of apoptosis genes in rectal cancer predicts patient survival and tumor recurrence. Apoptosis 19, 1581-1593.

Benjamini, Y., Hochberg, Y., 1995. Controlling the False Discovery Rate - a Practical and Powerful Approach to Multiple Testing. J R Stat Soc B 57, 289-300.

Beukers, W., van der Keur, K.A., Kandimalla, R., Vergouwe, Y., Steyerberg, E.W., Boormans, J.L., Jensen, J.B., Lorente, J.A., Real, F.X., Segersten, U., Orntoft, T.F., Malats, N., Malmstrom, P.U., Dyrskjot, L., Zwarthoff, E.C., 2017. FGFR3, TERT and OTX1 as a Urinary Biomarker Combination for Surveillance of Patients with Bladder Cancer in a Large Prospective Multicenter Study. J Urol 197, 1410-1418.

Bhattacharya, R., Mukherjee, N., Dasgupta, H., Islam, M.S., Alam, N., Roy, A., Das, P., Roychoudhury, S., Panda, C.K., 2016. Frequent alterations of SLIT2-ROBO1-CDC42 signalling pathway in breast cancer: clinicopathological correlation. J Genet 95, 551-563.

Bill-Axelson, A., Holmberg, L., Garmo, H., Taari, K., Busch, C., Nordling, S., Haggman, M., Andersson, S.O., Andren, O., Steineck, G., Adami, H.O., Johansson, J.E., 2018. Radical Prostatectomy or Watchful Waiting in Prostate Cancer - 29-Year Follow-up. N Engl J Med 379, 2319-2329.

Biller, B., Berg, J., Garrett, L., Ruslander, D., Wearing, R., Abbott, B., Patel, M., Smith, D., Bryan, C., 2016. 2016 AAHA Oncology Guidelines for Dogs and Cats. J Am Anim Hosp Assoc 52, 181-204.

Birkhahn, M., Mitra, A.P., Williams, A.J., Lam, G., Ye, W., Datar, R.H., Balic, M., Groshen, S., Steven, K.E., Cote, R.J., 2010. Predicting recurrence and progression of noninvasive papillary bladder cancer at initial presentation based on quantitative gene expression profiles. Eur Urol 57, 12-20.

Bismar, T.A., Hegazy, S., Feng, Z., Yu, D., Donnelly, B., Palanisamy, N., Trock, B.J., 2018. Clinical utility of assessing PTEN and ERG protein expression in prostate cancer patients: a proposed method for risk stratification. J Cancer Res Clin Oncol 144, 2117-2125.

Bjorklund, S.S., Panda, A., Kumar, S., Seiler, M., Robinson, D., Gheeya, J., Yao, M., Alnaes, G.I.G., Toppmeyer, D., Riis, M., Naume, B., Borresen-Dale, A.L., Kristensen, V.N., Ganesan, S., Bhanot, G., 2017. Widespread alternative exon usage in clinically distinct subtypes of Invasive Ductal Carcinoma. Sci Rep 7, 5568.

Black, P.C., Brown, G.A., Dinney, C.P., 2009. The impact of variant histology on the outcome of bladder cancer treated with curative intent. Urol Oncol 27, 3-7.

Bohle, A., Jocham, D., Bock, P.R., 2003. Intravesical bacillus Calmette-Guerin versus mitomycin C for superficial bladder cancer: a formal meta-analysis of comparative studies on recurrence and toxicity. J Urol 169, 90-95.

Boorjian, S., Ugras, S., Mongan, N.P., Gudas, L.J., You, X., Tickoo, S.K., Scherr, D.S., 2004. Androgen receptor expression is inversely correlated with pathologic tumor stage in bladder cancer. Urology 64, 383-388.

Boria, P.A., Glickman, N.W., Schmidt, B.R., Widmer, W.R., Mutsaers, A.J., Adams, L.G., Snyder, P.W., DiBernardi, L., de Gortari, A.E., Bonney, P.L., Knapp, D.W., 2005. Carboplatin and piroxicam therapy in 31 dogs with transitional cell carcinoma of the urinary bladder. Vet Comp Oncol 3, 73-80.

Borjesson, D.L., Christopher, M.M., Ling, G.V., 1999. Detection of canine transitional cell carcinoma using a bladder tumor antigen urine dipstick test. Vet Clin Pathol 28, 33-38.

Bostrom, P.J., van Rhijn, B.W.G., Fleshner, N., Finelli, A., Jewett, M., Thoms, J., Hanna, S., Kuk, C., Zlotta, A.R., 2010. Staging and Staging Errors in Bladder Cancer. Eur Urol Suppl 9, 2-9.

Bostwick, D.G., Liu, L., Brawer, M.K., Qian, J., 2004. High-grade prostatic intraepithelial neoplasia. Rev Urol 6, 171-179.

Bray, F., Ferlay, J., Soerjomataram, I., Siegel, R.L., Torre, L.A., Jemal, A., 2018. Global cancer statistics 2018: GLOBOCAN estimates of incidence and mortality worldwide for 36 cancers in 185 countries. CA Cancer J Clin 68, 394-424.

Breau, R.H., Karnes, R.J., Farmer, S.A., Thapa, P., Cagiannos, I., Morash, C., Frank, I., 2014. Progression to detrusor muscle invasion during urothelial carcinoma surveillance is associated with poor prognosis. BJU Int 113, 900-906.

Brimo, F., Epstein, J.I., 2012. Immunohistochemical pitfalls in prostate pathology. Hum Pathol 43, 313-324.

Brockman, J.A., Alanee, S., Vickers, A.J., Scardino, P.T., Wood, D.P., Kibel, A.S., Lin, D.W., Bianco, F.J., Jr., Rabah, D.M., Klein, E.A., Ciezki, J.P., Gao, T., Kattan, M.W., Stephenson, A.J., 2015. Nomogram Predicting Prostate Cancer-specific Mortality for Men with Biochemical Recurrence After Radical Prostatectomy. Eur Urol 67, 1160-1167.

Brown, J.M., Attardi, L.D., 2005. The role of apoptosis in cancer development and treatment response. Nat Rev Cancer 5, 231-237.

Bryan, J.N., Keeler, M.R., Henry, C.J., Bryan, M.E., Hahn, A.W., Caldwell, C.W., 2007. A population study of neutering status as a risk factor for canine prostate cancer. Prostate 67, 1174-1181.

Buhagen, M., Gronskag, A., Ragde, S.F., Hilt, B., 2016. Association Between Kidney Cancer and Occupational Exposure to Trichloroethylene. J Occup Environ Med 58, 957-959.

Burger, M., Catto, J.W., Dalbagni, G., Grossman, H.B., Herr, H., Karakiewicz, P., Kassouf, W., Kiemeney, L.A., La Vecchia, C., Shariat, S., Lotan, Y., 2013. Epidemiology and risk factors of urothelial bladder cancer. Eur Urol 63, 234-241.

Bussolati, G., Leonardo, E., 2008. Technical pitfalls potentially affecting diagnoses in immunohistochemistry. J Clin Pathol 61, 1184-1192.

Cabre, A., Lazaro, I., Girona, J., Manzanares, J., Marimon, F., Plana, N., Heras, M., Masana, L., 2007. Retinol-binding protein 4 as a plasma biomarker of renal dysfunction and cardiovascular disease in type 2 diabetes. J Intern Med 262, 496-503.

Cai, M., Wei, J., Zhang, Z., Zhao, H., Qiu, Y., Fang, Y., Gao, Z., Cao, J., Chen, W., Zhou, F., Xie, D., Luo, J., 2012. Impact of age on the cancer-specific survival of patients with localized renal cell carcinoma: martingale residual and competing risks analysis. PLoS One 7, e48489.

Calderaro, J., Rebouissou, S., de Koning, L., Masmoudi, A., Herault, A., Dubois, T., Maille, P., Soyeux, P., Sibony, M., de la Taille, A., Vordos, D., Lebret, T., Radvanyi, F., Allory, Y., 2014. PI3K/AKT pathway activation in bladder carcinogenesis. Int J Cancer 134, 1776-1784.

Cancer Genome Atlas Research, N., 2014. Comprehensive molecular characterization of urothelial bladder carcinoma. Nature 507, 315-322.

Caney, S.M., Holt, P.E., Day, M.J., Rudorf, H., Gruffydd-Jones, T.J., 1998. Prostatic carcinoma in two cats. J Small Anim Pract 39, 140-143.

Cannon, C.M., Allstadt, S.D., 2015. Lower urinary tract cancer. Vet Clin North Am Small Anim Pract 45, 807-824.

Cantaluppi, V., Quercia, A.D., Dellepiane, S., Ferrario, S., Camussi, G., Biancone, L., 2014. Interaction between systemic inflammation and renal tubular epithelial cells. Nephrol Dial Transplant 29, 2004-2011.

Caraway, N.P., Katz, R.L., 2010. A review on the current state of urine cytology emphasizing the role of fluorescence in situ hybridization as an adjunct to diagnosis. Cancer Cytopathol 118, 175-183.

Carlo, M.I., Hakimi, A.A., Stewart, G.D., Bratslavsky, G., Brugarolas, J., Chen, Y.B., Linehan, W.M., Maher, E.R., Merino, M.J., Offit, K., Reuter, V.E., Shuch, B., Coleman, J.A., 2019. Familial Kidney Cancer: Implications of New Syndromes and Molecular Insights. Eur Urol.

Carlsson, S., Maschino, A., Schroder, F., Bangma, C., Steyerberg, E.W., van der Kwast, T., van Leenders, G., Vickers, A., Lilja, H., Roobol, M.J., 2013. Predictive value of four kallikrein markers for pathologically insignificant compared with aggressive prostate cancer in radical prostatectomy specimens: results from the European Randomized Study of Screening for Prostate Cancer section Rotterdam. Eur Urol 64, 693-699.

Carneiro, A., Barbosa, A.R.G., Takemura, L.S., Kayano, P.P., Moran, N.K.S., Chen, C.K., Wroclawski, M.L., Lemos, G.C., da Cunha, I.W., Obara, M.T., Tobias-Machado, M., Sowalsky, A.G., Bianco, B., 2018. The Role of Immunohistochemical Analysis as a Tool for the Diagnosis, Prognostic Evaluation and Treatment of Prostate Cancer: A Systematic Review of the Literature. Front Oncol 8, 377.

Caruso, R., Parisi, A., Bonanno, A., Paparo, D., Quattrocchi, E., Branca, G., Scardigno, M., Fedele, F., 2012. Histologic coagulative tumour necrosis as a prognostic indicator of aggressiveness in renal, lung, thyroid and colorectal carcinomas: A brief review. Oncol Lett 3, 16-18.

Caruso, R.A., Branca, G., Fedele, F., Irato, E., Finocchiaro, G., Parisi, A., Ieni, A., 2014. Mechanisms of coagulative necrosis in malignant epithelial tumors (Review). Oncol Lett 8, 1397-1402.

Carver, B.S., Bianco, F.J., Jr., Scardino, P.T., Eastham, J.A., 2006. Long-term outcome following radical prostatectomy in men with clinical stage T3 prostate cancer. J Urol 176, 564-568.

Chalasani, V., Chin, J.L., Izawa, J.I., 2009. Histologic variants of urothelial bladder cancer and nonurothelial histology in bladder cancer. Can Urol Assoc J 3, S193-198.

Chamie, K., Litwin, M.S., Bassett, J.C., Daskivich, T.J., Lai, J., Hanley, J.M., Konety, B.R., Saigal, C.S., Urologic Diseases in America, P., 2013. Recurrence of high-risk bladder cancer: a population-based analysis. Cancer 119, 3219-3227.

Chan, E., Patel, A., Heston, W., Larchian, W., 2009. Mouse orthotopic models for bladder cancer research. BJU Int 104, 1286-1291.

Chand, D., Dhawan, D., Sankin, A., Ren, X., Lin, J., Schoenberg, M., Knapp, D.W., Zang, X., 2019. Immune Checkpoint B7x (B7-H4/B7S1/VTCN1) is Over Expressed in Spontaneous Canine Bladder Cancer: The First Report and its Implications in a Preclinical Model. Bladder Cancer 5, 63-71.

Chang, A., Amin, A., Gabrielson, E., Illei, P., Roden, R.B., Sharma, R., Epstein, J.I., 2012. Utility of GATA3 immunohistochemistry in differentiating urothelial carcinoma from prostate adenocarcinoma and squamous cell carcinomas of the uterine cervix, anus, and lung. Am J Surg Pathol 36, 1472-1476.

Chapdelaine, P., Dube, J.Y., Frenette, G., Tremblay, R.R., 1984a. Identification of Arginine Esterase as the Major Androgen-Dependent Protein Secreted by Dog Prostate and Preliminary Molecular Characterization in Seminal Plasma. J Androl 5, 206-210.

Chapdelaine, P., Dube, J.Y., Frenette, G., Tremblay, R.R., 1984b. Identification of arginine esterase as the major androgen-dependent protein secreted

by dog prostate and preliminary molecular characterization in seminal plasma. J Androl 5, 206-210.
Chaturvedi, S., Robinson, L.A., 2015. Slit2-Robo signaling in inflammation and kidney injury. Pediatr Nephrol 30, 561-566.
Chen, R.C., 2019. Radiation therapy for prostate cancer: An evolving treatment modality. Urol Oncol 37, 579-581.
Chen, X., Yang, H., Zhang, S., Wang, Z., Ye, F., Liang, C., Wang, H., Fang, Z., 2017. A novel splice variant of supervillin, SV5, promotes carcinoma cell proliferation and cell migration. Biochem Biophys Res Commun 482, 43-49.
Chen, Z., Zhou, L., Wang, L., Kazobinka, G., Zhang, X., Han, X., Li, B., Hou, T., 2018. HBO1 promotes cell proliferation in bladder cancer via activation of Wnt/beta-catenin signaling. Mol Carcinog 57, 12-21.
Cheng, H.H., Sokolova, A.O., Schaeffer, E.M., Small, E.J., Higano, C.S., 2019. Germline and Somatic Mutations in Prostate Cancer for the Clinician. J Natl Compr Canc Netw 17, 515-521.
Cheng, I.H., Lin, Y.C., Hwang, E., Huang, H.T., Chang, W.H., Liu, Y.L., Chao, C.Y., 2011a. Collagen VI protects against neuronal apoptosis elicited by ultraviolet irradiation via an Akt/phosphatidylinositol 3-kinase signaling pathway. Neuroscience 183, 178-188.
Cheng, L., Montironi, R., Davidson, D.D., Lopez-Beltran, A., 2009. Staging and reporting of urothelial carcinoma of the urinary bladder. Mod Pathol 22 Suppl 2, S70-95.
Cheng, L., Zhang, S., MacLennan, G.T., Williamson, S.R., Lopez-Beltran, A., Montironi, R., 2011b. Bladder cancer: translating molecular genetic insights into clinical practice. Hum Pathol 42, 455-481.
Cheville, J.C., Lohse, C.M., Zincke, H., Weaver, A.L., Blute, M.L., 2003. Comparisons of outcome and prognostic features among histologic subtypes of renal cell carcinoma. Am J Surg Pathol 27, 612-624.
Childress, M.O., Adams, L.G., Ramos-Vara, J.A., Freeman, L.J., He, S., Constable, P.D., Knapp, D.W., 2011. Results of biopsy via transurethral cystoscopy and cystotomy for diagnosis of transitional cell carcinoma of the urinary bladder and urethra in dogs: 92 cases (2003-2008). J Am Vet Med Assoc 239, 350-356.
Choi, S.H., Chun, S.Y., Kim, T.H., Kwon, T.G., 2016. Identifying the emerging role of adipokine as a diagnostic and prognostic biomarker of renal cell carcinoma. Urol Oncol 34, 259.
Chow, W.H., Devesa, S.S., 2008. Contemporary epidemiology of renal cell cancer. Cancer J 14, 288-301.
Chow, W.H., Gridley, G., Fraumeni, J.F., Jr., Jarvholm, B., 2000. Obesity, hypertension, and the risk of kidney cancer in men. N Engl J Med 343, 1305-1311.
Chow, W.H., Shuch, B., Linehan, W.M., Devesa, S.S., 2013. Racial disparity in renal cell carcinoma patient survival according to demographic and clinical characteristics. Cancer 119, 388-394.
Choy, K., Fidel, J., 2016. Tolerability and Tumor Response of a Novel Low-Dose Palliative Radiation Therapy Protocol in Dogs with Transitional Cell

Carcinoma of the Bladder and Urethra. Vet Radiol Ultrasound 57, 341-351.

Christoph, F., Hinz, S., Kempkensteffen, C., Schostak, M., Schrader, M., Miller, K., 2007a. mRNA expression profiles of methylated APAF-1 and DAPK-1 tumor suppressor genes uncover clear cell renal cell carcinomas with aggressive phenotype. J Urol 178, 2655-2659.

Christoph, F., Hinz, S., Kempkensteffen, C., Weikert, S., Krause, H., Schostak, M., Schrader, M., Miller, K., 2007b. A gene expression profile of tumor suppressor genes commonly methylated in bladder cancer. J Cancer Res Clin Oncol 133, 343-349.

Christoph, F., Kempkensteffen, C., Weikert, S., Kollermann, J., Krause, H., Miller, K., Schostak, M., Schrader, M., 2006. Methylation of tumour suppressor genes APAF-1 and DAPK-1 and in vitro effects of demethylating agents in bladder and kidney cancer. Br J Cancer 95, 1701-1707.

Chuang, A.Y., DeMarzo, A.M., Veltri, R.W., Sharma, R.B., Bieberich, C.J., Epstein, J.I., 2007. Immunohistochemical differentiation of high-grade prostate carcinoma from urothelial carcinoma. Am J Surg Pathol 31, 1246-1255.

Conde, E., Alegre, L., Blanco-Sanchez, I., Saenz-Morales, D., Aguado-Fraile, E., Ponte, B., Ramos, E., Saiz, A., Jimenez, C., Ordonez, A., Lopez-Cabrera, M., del Peso, L., de Landazuri, M.O., Liano, F., Selgas, R., Sanchez-Tomero, J.A., Garcia-Bermejo, M.L., 2012. Hypoxia inducible factor 1-alpha (HIF-1 alpha) is induced during reperfusion after renal ischemia and is critical for proximal tubule cell survival. PLoS One 7, e33258.

Corcoran, S.E., O'Neill, L.A., 2016. HIF1alpha and metabolic reprogramming in inflammation. J Clin Invest 126, 3699-3707.

Cornell, K.K., Bostwick, D.G., Cooley, D.M., Hall, G., Harvey, H.J., Hendrick, M.J., Pauli, B.U., Render, J.A., Stoica, G., Sweet, D.C., Waters, D.J., 2000. Clinical and pathologic aspects of spontaneous canine prostate carcinoma: a retrospective analysis of 76 cases. Prostate 45, 173-183.

Cox, R.M., Schneider, A.G., Sangoi, A.R., Clingan, W.J., Gokden, N., McKenney, J.K., 2009. Invasive urothelial carcinoma with chordoid features: a report of 12 distinct cases characterized by prominent myxoid stroma and cordlike epithelial architecture. Am J Surg Pathol 33, 1213-1219.

Crallan, R.A., Georgopoulos, N.T., Southgate, J., 2006. Experimental models of human bladder carcinogenesis. Carcinogenesis 27, 374-381.

Cramer, T., Yamanishi, Y., Clausen, B.E., Forster, I., Pawlinski, R., Mackman, N., Haase, V.H., Jaenisch, R., Corr, M., Nizet, V., Firestein, G.S., Gerber, H.P., Ferrara, N., Johnson, R.S., 2003. HIF-1alpha is essential for myeloid cell-mediated inflammation. Cell 112, 645-657.

Crea, F., Sun, L., Mai, A., Chiang, Y.T., Farrar, W.L., Danesi, R., Helgason, C.D., 2012. The emerging role of histone lysine demethylases in prostate cancer. Mol Cancer 11, 52.

Crowley, J.L., Smith, T.C., Fang, Z., Takizawa, N., Luna, E.J., 2009. Supervillin reorganizes the actin cytoskeleton and increases invadopodial efficiency. Mol Biol Cell 20, 948-962.

Cui, Y., Cao, W., Li, Q., Shen, H., Liu, C., Deng, J., Xu, J., Shao, Q., 2016. Evaluation of prostate cancer antigen 3 for detecting prostate cancer: a systematic review and meta-analysis. Sci Rep 6, 25776.

Cunto, M., Mariani, E., Anicito Guido, E., Ballotta, G., Zambelli, D., 2019. Clinical approach to prostatic diseases in the dog. Reprod Domest Anim 54, 815-822.

Cuzick, J., Yang, Z.H., Fisher, G., Tikishvili, E., Stone, S., Lanchbury, J.S., Camacho, N., Merson, S., Brewer, D., Cooper, C.S., Clark, J., Berney, D.M., Moller, H., Scardino, P., Sangale, Z., Transatlantic Prostate, G., 2013. Prognostic value of PTEN loss in men with conservatively managed localised prostate cancer. Br J Cancer 108, 2582-2589.

D'Avella, C., Abbosh, P., Pal, S.K., Geynisman, D.M., 2018. Mutations in renal cell carcinoma. Urol Oncol.

Dabir, P.D., Ottosen, P., Hoyer, S., Hamilton-Dutoit, S., 2012. Comparative analysis of three- and two-antibody cocktails to AMACR and basal cell markers for the immunohistochemical diagnosis of prostate carcinoma. Diagn Pathol 7, 81.

Damani Shah, H., Saranath, D., Pradhan, S., 2019. Single nucleotide polymorphisms in transcription factor genes associated with susceptibility to oral cancer. J Cell Biochem.

Dayyani, F., Hoffman, K., Eifel, P., Guo, C., Vikram, R., Pagliaro, L.C., Pettaway, C., 2014. Management of advanced primary urethral carcinomas. Bju International 114, 25-31.

de Brot, S., Robinson, B.D., Scase, T., Grau-Roma, L., Wilkinson, E., Boorjian, S.A., Gardner, D., Mongan, N.P., 2018. The dog as an animal model for bladder and urethral urothelial carcinoma: Comparative epidemiology and histology. Oncol Lett 16, 1641-1649.

De Nicola, F., Goeman, F., Pallocca, M., Sperati, F., Pizzuti, L., Melucci, E., Casini, B., Amoreo, C.A., Gallo, E., Diodoro, M.G., Buglioni, S., Mazzotta, M., Vici, P., Sergi, D., Di Lauro, L., Barba, M., Pescarmona, E., Ciliberto, G., De Maria, R., Fanciulli, M., Maugeri-Sacca, M., 2018. Deep sequencing and pathway-focused analysis revealed multigene oncodriver signatures predicting survival outcomes in advanced colorectal cancer. Oncogenesis 7, 55.

Deakin, N.O., Turner, C.E., 2008. Paxillin comes of age. J Cell Sci 121, 2435-2444.

Dearnaley, D.P., Jovic, G., Syndikus, I., Khoo, V., Cowan, R.A., Graham, J.D., Aird, E.G., Bottomley, D., Huddart, R.A., Jose, C.C., Matthews, J.H.L., Millar, J.L., Murphy, C., Russell, J.M., Scrase, C.D., Parmar, M.K.B., Sydes, M.R., 2014. Escalated-dose versus control-dose conformal radiotherapy for prostate cancer: long-term results from the MRC RT01 randomised controlled trial. The Lancet Oncology 15, 464-473.

Decker, B., Parker, H.G., Dhawan, D., Kwon, E.M., Karlins, E., Davis, B.W., Ramos-Vara, J.A., Bonney, P.L., McNiel, E.A., Knapp, D.W., Ostrander, E.A., 2015. Homologous Mutation to Human BRAF V600E Is Common in Naturally Occurring Canine Bladder Cancer--Evidence for a Relevant Model System and Urine-Based Diagnostic Test. Mol Cancer Res 13, 993-1002.

Delahunt, B., Cheville, J.C., Martignoni, G., Humphrey, P.A., Magi-Galluzzi, C., McKenney, J., Egevad, L., Algaba, F., Moch, H., Grignon, D.J., Montironi, R., Srigley, J.R., Members of the, I.R.T.P., 2013a. The International Society of Urological Pathology (ISUP) grading system for renal cell carcinoma and other prognostic parameters. Am J Surg Pathol 37, 1490-1504.

Delahunt, B., Eble, J.N., Egevad, L., Samaratunga, H., 2019. Grading of renal cell carcinoma. Histopathology 74, 4-17.

Delahunt, B., Egevad, L., Montironi, R., Srigley, J.R., 2013b. International Society of Urological Pathology (ISUP) consensus conference on renal neoplasia: rationale and organization. Am J Surg Pathol 37, 1463-1468.

Delahunt, B., Kittelson, J.M., McCredie, M.R., Reeve, A.E., Stewart, J.H., Bilous, A.M., 2002. Prognostic importance of tumor size for localized conventional (clear cell) renal cell carcinoma: assessment of TNM T1 and T2 tumor categories and comparison with other prognostic parameters. Cancer 94, 658-664.

Delahunt, B., Sika-Paotonu, D., Bethwaite, P.B., William Jordan, T., Magi-Galluzzi, C., Zhou, M., Samaratunga, H., Srigley, J.R., 2011. Grading of clear cell renal cell carcinoma should be based on nucleolar prominence. Am J Surg Pathol 35, 1134-1139.

Della Salda, L., Massimini, M., Romanucci, M., Palmieri, C., Perillo, A., Grieco, V., Malatesta, D., Spinillo, M.A., Passantino, G., Dondi, F., Benazzi, C., 2019. Nectin-4 and p63 immunohistochemical expression in canine prostate tumourigenesis. Vet Comp Oncol 17, 298-307.

Deng, N., Sanchez, C.G., Lasky, J.A., Zhu, D., 2013. Detecting splicing variants in idiopathic pulmonary fibrosis from non-differentially expressed genes. PLoS One 8, e68352.

Devitt, M.E., Dreicer, R., 2019. Evolving Role of Genomics in Genitourinary Neoplasms. Acta Med Acad 48, 68-77.

Dhawan, D., Hahn, N.M., Ramos-Vara, J.A., Knapp, D.W., 2018. Naturally-occurring canine invasive urothelial carcinoma harbors luminal and basal transcriptional subtypes found in human muscle invasive bladder cancer. PLoS Genet 14, e1007571.

Dhawan, D., Paoloni, M., Shukradas, S., Choudhury, D.R., Craig, B.A., Ramos-Vara, J.A., Hahn, N., Bonney, P.L., Khanna, C., Knapp, D.W., 2015. Comparative Gene Expression Analyses Identify Luminal and Basal Subtypes of Canine Invasive Urothelial Carcinoma That Mimic Patterns in Human Invasive Bladder Cancer. PLoS One 10, e0136688.

Di, Y., Chen, D., Yu, W., Yan, L., 2019. Bladder cancer stage-associated hub genes revealed by WGCNA co-expression network analysis. Hereditas 156, 7.

Dietrich, K., Demidenko, E., Schned, A., Zens, M.S., Heaney, J., Karagas, M.R., 2011. Parity, early menopause and the incidence of bladder cancer in women: a case-control study and meta-analysis. Eur J Cancer 47, 592-599.

Ding, J., Xu, D., Pan, C., Ye, M., Kang, J., Bai, Q., Qi, J., 2014. Current animal models of bladder cancer: Awareness of translatability (Review). Exp Ther Med 8, 691-699.

Domingos, M.A.M., Queiroz, M., Lotufo, P.A., Bensenor, I.J., Titan, S.M.O., 2017. Serum RBP4 and CKD: Association with insulin resistance and lipids. J Diabetes Complications 31, 1132-1138.

Draulans, C., Everaerts, W., Isebaert, S., Gevaert, T., Oyen, R., Joniau, S., Lerut, E., De Wever, L., Weynand, B., Vanhoutte, E., De Meerleer, G., Haustermans, K., 2019. Impact of Magnetic Resonance Imaging on Prostate Cancer Staging and European Association of Urology Risk Classification. Urology 130, 113-119.

Du, C., Wang, X., Zhang, J., Liu, X., Zhu, J., Liu, Y., 2016. Paxillin is positively correlated with the clinicopathological factors of colorectal cancer, and knockdown of Paxillin improves sensitivity to cetuximab in colorectal cancer cells. Oncol Rep 35, 409-417.

Duan, Y., Liu, G., Sun, Y., Wu, J., Xiong, Z., Jin, T., Chen, M., 2019. COL6A3 polymorphisms were associated with lung cancer risk in a Chinese population. Respir Res 20, 143.

Dy, G.W., Gore, J.L., Forouzanfar, M.H., Naghavi, M., Fitzmaurice, C., 2017. Global Burden of Urologic Cancers, 1990-2013. Eur Urol 71, 437-446.

Eichler, K., Hempel, S., Wilby, J., Myers, L., Bachmann, L.M., Kleijnen, J., 2006. Diagnostic value of systematic biopsy methods in the investigation of prostate cancer: a systematic review. J Urol 175, 1605-1612.

Ellwood-Yen, K., Graeber, T.G., Wongvipat, J., Iruela-Arispe, M.L., Zhang, J., Matusik, R., Thomas, G.V., Sawyers, C.L., 2003. Myc-driven murine prostate cancer shares molecular features with human prostate tumors. Cancer Cell 4, 223-238.

Epstein, J.I., Amin, M.B., Reuter, V.E., Humphrey, P.A., 2017. Contemporary Gleason Grading of Prostatic Carcinoma: An Update With Discussion on Practical Issues to Implement the 2014 International Society of Urological Pathology (ISUP) Consensus Conference on Gleason Grading of Prostatic Carcinoma. Am J Surg Pathol 41, e1-e7.

Epstein, J.I., Egevad, L., Amin, M.B., Delahunt, B., Srigley, J.R., Humphrey, P.A., Grading, C., 2016. The 2014 International Society of Urological Pathology (ISUP) Consensus Conference on Gleason Grading of Prostatic Carcinoma: Definition of Grading Patterns and Proposal for a New Grading System. Am J Surg Pathol 40, 244-252.

Epstein, J.I., Egevad, L., Humphrey, P.A., Montironi, R., Members of the ISUP Immunohistochemistry in Diagnostic Urologic Pathology Group, 2014. Best practices recommendations in the application of immunohistochemistry in the prostate: report from the International Society of Urologic Pathology consensus conference. Am J Surg Pathol 38, e6-e19.

Fang, Y., Yu, X., Liu, Y., Kriegel, A.J., Heng, Y., Xu, X., Liang, M., Ding, X., 2013. miR-29c is downregulated in renal interstitial fibrosis in humans and rats and restored by HIF-alpha activation. Am J Physiol Renal Physiol 304, F1274-1282.

Fantini, D., Glaser, A.P., Rimar, K.J., Wang, Y., Schipma, M., Varghese, N., Rademaker, A., Behdad, A., Yellapa, A., Yu, Y., Sze, C.C., Wang, L., Zhao, Z., Crawford, S.E., Hu, D., Licht, J.D., Collings, C.K., Bartom, E., Theodorescu, D., Shilatifard, A., Meeks, J.J., 2018. A Carcinogen-induced mouse model recapitulates the molecular alterations of human muscle invasive bladder cancer. Oncogene 37, 1911-1925.

Fellous, A., Earley, R.L., Silvestre, F., 2019. The Kdm/Kmt gene families in the self-fertilizing mangrove rivulus fish, Kryptolebias marmoratus, suggest involvement of histone methylation machinery in development and reproduction. Gene 687, 173-187.

Feng, X., Zhang, L., Tu, W., Cang, S., 2019. Frequency, incidence and survival outcomes of clear cell renal cell carcinoma in the United States from 1973 to 2014: A SEER-based analysis. Medicine (Baltimore) 98, e16684.

Ferlay, J., Colombet, M., Soerjomataram, I., Mathers, C., Parkin, D.M., Pineros, M., Znaor, A., Bray, F., 2019. Estimating the global cancer incidence and mortality in 2018: GLOBOCAN sources and methods. Int J Cancer 144, 1941-1953.

Ferlay, J., Soerjomataram, I., Dikshit, R., Eser, S., Mathers, C., Rebelo, M., Parkin, D.M., Forman, D., Bray, F., 2015. Cancer incidence and mortality worldwide: sources, methods and major patterns in GLOBOCAN 2012. Int J Cancer 136, E359-386.

Ferlay, J., Soerjomataram, I., Ervik, M., Dikshit, R., Eser, S., Mathers, C., Rebelo, M., Parkin, D.M., Forman, D., Bray, F. GLOBOCAN 2012 v1.0, Cancer Incidence and Mortality Worldwide: IARC CancerBase No. 11 [Internet]. Lyon, France: International Agency for Research on Cancer; 2013. Available from: http://globocan.iarc.fr, accessed on 04/12/2017.

Ferlay, J., Steliarova-Foucher, E., Lortet-Tieulent, J., Rosso, S., Coebergh, J.W., Comber, H., Forman, D., Bray, F., 2013. Cancer incidence and mortality patterns in Europe: estimates for 40 countries in 2012. Eur J Cancer 49, 1374-1403.

Filipas, D., Spix, C., Schulz-Lampel, D., Michaelis, J., Hohenfellner, R., Roth, S., Thüroff, J.W., 2003. Screening for renal cell carcinoma using ultrasonography: a feasibility study. BJU International 91, 595-599.

Fine, S.W., Al-Ahmadie, H.A., Chen, Y.B., Gopalan, A., Tickoo, S.K., Reuter, V.E., 2018. Comedonecrosis Revisited: Strong Association With Intraductal Carcinoma of the Prostate. Am J Surg Pathol 42, 1036-1041.

Fong, D., Spizzo, G., Mitterer, M., Seeber, A., Steurer, M., Gastl, G., Brosch, I., Moser, P., 2012. Low Expression of Junctional Adhesion Molecule A Is Associated with Metastasis and Poor Survival in Pancreatic Cancer. Annals of Surgical Oncology 19, 4330-4336.

Fonseca-Alves, C.E., Kobayashi, P.E., Laufer-Amorim, R., 2018a. Evaluation of NKX3.1 and C-MYC expression in canine prostatic cancer. Res Vet Sci 118, 365-370.

Fonseca-Alves, C.E., Kobayashi, P.E., Rivera Calderon, L.G., Felisbino, S.L., Rinaldi, J.C., Drigo, S.A., Rogatto, S.R., Laufer-Amorim, R., 2018b. Immunohistochemical panel to characterize canine prostate

carcinomas according to aberrant p63 expression. PLoS One 13, e0199173.

Fonseca-Alves, C.E., Rodrigues, M.M., de Moura, V.M., Rogatto, S.R., Laufer-Amorim, R., 2013. Alterations of C-MYC, NKX3.1, and E-cadherin expression in canine prostate carcinogenesis. Microsc Res Tech 76, 1250-1256.

Fossati, N., Willemse, P.M., Van den Broeck, T., van den Bergh, R.C.N., Yuan, C.Y., Briers, E., Bellmunt, J., Bolla, M., Cornford, P., De Santis, M., MacPepple, E., Henry, A.M., Mason, M.D., Matveev, V.B., van der Poel, H.G., van der Kwast, T.H., Rouviere, O., Schoots, I.G., Wiegel, T., Lam, T.B., Mottet, N., Joniau, S., 2017. The Benefits and Harms of Different Extents of Lymph Node Dissection During Radical Prostatectomy for Prostate Cancer: A Systematic Review. Eur Urol 72, 84-109.

Frazier, K.S., Seely, J.C., Hard, G.C., Betton, G., Burnett, R., Nakatsuji, S., Nishikawa, A., Durchfeld-Meyer, B., Bube, A., 2012. Proliferative and nonproliferative lesions of the rat and mouse urinary system. Toxicol Pathol 40, 14S-86S.

Frenette, G., Dube, J.Y., Lacoste, D., Tremblay, R.R., 1987. Radioimmunoassay in Blood-Plasma of Arginine Esterase - the Major Secretory Product of Dog Prostate. Prostate 10, 145-152.

Fresno Vara, J.A., Casado, E., de Castro, J., Cejas, P., Belda-Iniesta, C., Gonzalez-Baron, M., 2004. PI3K/Akt signalling pathway and cancer. Cancer Treat Rev 30, 193-204.

Fu, L., Minton, D.R., Zhang, T., Nanus, D.M., Gudas, L.J., 2015. Genome-Wide Profiling of TRACK Kidneys Shows Similarity to the Human ccRCC Transcriptome. Mol Cancer Res 13, 870-878.

Fu, L., Wang, G., Shevchuk, M.M., Nanus, D.M., Gudas, L.J., 2011. Generation of a mouse model of Von Hippel-Lindau kidney disease leading to renal cancers by expression of a constitutively active mutant of HIF1alpha. Cancer Res 71, 6848-6856.

Fulkerson, C.M., Dhawan, D., Ratliff, T.L., Hahn, N.M., Knapp, D.W., 2017. Naturally Occurring Canine Invasive Urinary Bladder Cancer: A Complementary Animal Model to Improve the Success Rate in Human Clinical Trials of New Cancer Drugs. Int J Genomics 2017, 6589529.

Fulkerson, C.M., Knapp, D.W., 2015. Management of transitional cell carcinoma of the urinary bladder in dogs: a review. Vet J 205, 217-225.

Futterer, J.J., Briganti, A., De Visschere, P., Emberton, M., Giannarini, G., Kirkham, A., Taneja, S.S., Thoeny, H., Villeirs, G., Villers, A., 2015. Can Clinically Significant Prostate Cancer Be Detected with Multiparametric Magnetic Resonance Imaging? A Systematic Review of the Literature. Eur Urol 68, 1045-1053.

Gakis, G., Witjes, J.A., Comperat, E., Cowan, N.C., De Santis, M., Lebret, T., Ribal, M.J., Sherif, A.M., 2013. EAU Guidelines on Primary Urethral Carcinoma. European Urology 64, 823-830.

Gallardo, F., Mogas, T., Baro, T., Rabanal, R., Morote, J., Abal, M., Reventos, J., Lloreta, J., 2007. Expression of androgen, oestrogen alpha and beta, and progesterone receptors in the canine prostate: differences between

normal, inflamed, hyperplastic and neoplastic glands. J Comp Pathol 136, 1-8.

Gandaglia, G., Albers, P., Abrahamsson, P.A., Briganti, A., Catto, J.W.F., Chapple, C.R., Montorsi, F., Mottet, N., Roobol, M.J., Sonksen, J., Wirth, M., van Poppel, H., 2019. Structured Population-based Prostate-specific Antigen Screening for Prostate Cancer: The European Association of Urology Position in 2019. Eur Urol 76, 142-150.

Gandaglia, G., Briganti, A., Fossati, N., Salonia, A., Mottrie, A., Catto, J., Montorsi, F., 2016. The Problem Is Not What to Do with Indolent and Harmless Prostate Cancer-The Problem Is How to Avoid Finding These Cancers. Eur Urol 70, 547-548.

Gao, X., Chen, Y., Chen, M., Wang, S., Wen, X., Zhang, S., 2018. Identification of key candidate genes and biological pathways in bladder cancer. PeerJ 6, e6036.

Geissler, K., Fornara, P., Lautenschlager, C., Holzhausen, H.J., Seliger, B., Riemann, D., 2015. Immune signature of tumor infiltrating immune cells in renal cancer. Oncoimmunology 4, e985082.

Gelman, I.H., 2016. How the TRAMP Model Revolutionized the Study of Prostate Cancer Progression. Cancer Res 76, 6137-6139.

Ghali, F., Patel, S.H., Derweesh, I.H., 2019. Current Status of Immunotherapy for Localized and Locally Advanced Renal Cell Carcinoma. J Oncol 2019, 7309205.

Giannico, G.A., Ross, H.M., Lotan, T., Epstein, J.I., 2013. Aberrant expression of p63 in adenocarcinoma of the prostate: a radical prostatectomy study. Am J Surg Pathol 37, 1401-1406.

Gingrich, J.R., Greenberg, N.M., 1996. A transgenic mouse prostate cancer model. Toxicol Pathol 24, 502-504.

Giri, V.N., Beebe-Dimmer, J.L., 2016. Familial prostate cancer. Semin Oncol 43, 560-565.

Giri, V.N., Knudsen, K.E., Kelly, W.K., Abida, W., Andriole, G.L., Bangma, C.H., Bekelman, J.E., Benson, M.C., Blanco, A., Burnett, A., Catalona, W.J., Cooney, K.A., Cooperberg, M., Crawford, D.E., Den, R.B., Dicker, A.P., Eggener, S., Fleshner, N., Freedman, M.L., Hamdy, F.C., Hoffman-Censits, J., Hurwitz, M.D., Hyatt, C., Isaacs, W.B., Kane, C.J., Kantoff, P., Karnes, R.J., Karsh, L.I., Klein, E.A., Lin, D.W., Loughlin, K.R., Lu-Yao, G., Malkowicz, S.B., Mann, M.J., Mark, J.R., McCue, P.A., Miner, M.M., Morgan, T., Moul, J.W., Myers, R.E., Nielsen, S.M., Obeid, E., Pavlovich, C.P., Peiper, S.C., Penson, D.F., Petrylak, D., Pettaway, C.A., Pilarski, R., Pinto, P.A., Poage, W., Raj, G.V., Rebbeck, T.R., Robson, M.E., Rosenberg, M.T., Sandler, H., Sartor, O., Schaeffer, E., Schwartz, G.F., Shahin, M.S., Shore, N.D., Shuch, B., Soule, H.R., Tomlins, S.A., Trabulsi, E.J., Uzzo, R., Vander Griend, D.J., Walsh, P.C., Weil, C.J., Wender, R., Gomella, L.G., 2018. Role of Genetic Testing for Inherited Prostate Cancer Risk: Philadelphia Prostate Cancer Consensus Conference 2017. J Clin Oncol 36, 414-424.

Gleason, D.F., 1966. Classification of prostatic carcinomas. Cancer Chemother Rep 50, 125-128.

Gnarra, J.R., Tory, K., Weng, Y., Schmidt, L., Wei, M.H., Li, H., Latif, F., Liu, S., Chen, F., Duh, F.M., et al., 1994. Mutations of the VHL tumour suppressor gene in renal carcinoma. Nat Genet 7, 85-90.

Gnarra, J.R., Ward, J.M., Porter, F.D., Wagner, J.R., Devor, D.E., Grinberg, A., Emmert-Buck, M.R., Westphal, H., Klausner, R.D., Linehan, W.M., 1997. Defective placental vasculogenesis causes embryonic lethality in VHL-deficient mice. Proc Natl Acad Sci U S A 94, 9102-9107.

Gobello, C., Castex, G., Corrada, Y., 2002. Serum and seminal markers in the diagnosis of disorders of the genital tract of the dog: a mini-review. Theriogenology 57, 1285-1291.

Gokden, N., Nappi, O., Swanson, P.E., Pfeifer, J.D., Vollmer, R.T., Wick, M.R., Humphrey, P.A., 2000. Renal cell carcinoma with rhabdoid features. Am J Surg Pathol 24, 1329-1338.

Golos, A., Jesionek-Kupnicka, D., Gil, L., Braun, M., Komarnicki, M., Robak, T., Wierzbowska, A., 2019. The Expression of the SLIT-ROBO Family in Adult Patients with Acute Myeloid Leukemia. Arch Immunol Ther Ex 67, 109-123.

Gopalakrishna, A., Fantony, J.J., Longo, T.A., Owusu, R., Foo, W.C., Dash, R., Denton, B.T., Inman, B.A., 2017. Anticipatory Positive Urine Tests for Bladder Cancer. Ann Surg Oncol 24, 1747-1753.

Gopalakrishna, A., Longo, T.A., Fantony, J.J., Owusu, R., Foo, W.C., Dash, R., Inman, B.A., 2016. The diagnostic accuracy of urine-based tests for bladder cancer varies greatly by patient. BMC Urol 16, 30.

Gordan, J.D., Bertout, J.A., Hu, C.J., Diehl, J.A., Simon, M.C., 2007. HIF-2alpha promotes hypoxic cell proliferation by enhancing c-myc transcriptional activity. Cancer Cell 11, 335-347.

Gotte, M., Mohr, C., Koo, C.Y., Stock, C., Vaske, A.K., Viola, M., Ibrahim, S.A., Peddibhotla, S., Teng, Y.H., Low, J.Y., Ebnet, K., Kiesel, L., Yip, G.W., 2010. miR-145-dependent targeting of junctional adhesion molecule A and modulation of fascin expression are associated with reduced breast cancer cell motility and invasiveness. Oncogene 29, 6569-6580.

Grabowska, M.M., DeGraff, D.J., Yu, X., Jin, R.J., Chen, Z., Borowsky, A.D., Matusik, R.J., 2014. Mouse models of prostate cancer: picking the best model for the question. Cancer Metastasis Rev 33, 377-397.

Graham, T.A., Weaver, C., Mao, F., Kimelman, D., Xu, W., 2000. Crystal structure of a beta-catenin/Tcf complex. Cell 103, 885-896.

Grignon, D.J., 2009. The current classification of urothelial neoplasms. Mod Pathol 22 Suppl 2, S60-69.

Gudas, L.J., Fu, L., Minton, D.R., Mongan, N.P., Nanus, D.M., 2014. The role of HIF1alpha in renal cell carcinoma tumorigenesis. J Mol Med (Berl) 92, 825-836.

Gul, A., Rini, B.I., 2019. Adjuvant therapy in renal cell carcinoma. Cancer 125, 2935-2944.

Guo, A., Liu, A., Teng, X., 2016. The pathology of urinary bladder lesions with an inverted growth pattern. Chin J Cancer Res 28, 107-121.

Guo, Y., Mao, S., Zhang, A., Zhang, J., Wang, L., Wang, R., Zhang, W., Zhang, Z., Wu, Y., Cao, X., Yang, B., Yao, X., 2019. Survival Significance of Patients

With Low Prostate-Specific Antigen and High-Grade Prostate Cancer After Radical Prostatectomy, External Beam Radiotherapy, or External Beam Radiotherapy With Brachytherapy. Front Oncol 9, 638.

Gurel, B., Iwata, T., Koh, C.M., Jenkins, R.B., Lan, F., Van Dang, C., Hicks, J.L., Morgan, J., Cornish, T.C., Sutcliffe, S., Isaacs, W.B., Luo, J., De Marzo, A.M., 2008. Nuclear MYC protein overexpression is an early alteration in human prostate carcinogenesis. Mod Pathol 21, 1156-1167.

Gutwein, P., Schramme, A., Voss, B., Abdel-Bakky, M.S., Doberstein, K., Ludwig, A., Altevogt, P., Hansmann, M.L., Moch, H., Kristiansen, G., Pfeilschifter, J., 2009. Downregulation of junctional adhesion molecule-A is involved in the progression of clear cell renal cell carcinoma. Biochem Biophys Res Commun 380, 387-391.

Haase, V.H., Glickman, J.N., Socolovsky, M., Jaenisch, R., 2001. Vascular tumors in livers with targeted inactivation of the von Hippel-Lindau tumor suppressor. Proc Natl Acad Sci U S A 98, 1583-1588.

Hackman, G., Taari, K., Tammela, T.L., Matikainen, M., Kouri, M., Joensuu, T., Luukkaala, T., Salonen, A., Isotalo, T., Petas, A., Hendolin, N., Bostrom, P.J., Aaltomaa, S., Lehtoranta, K., Hellstrom, P., Riikonen, J., Korpela, M., Minn, H., Kellokumpu-Lehtinen, P.L., Pukkala, E., Hemminki, A., FinnProstate, G., 2019. Randomised Trial of Adjuvant Radiotherapy Following Radical Prostatectomy Versus Radical Prostatectomy Alone in Prostate Cancer Patients with Positive Margins or Extracapsular Extension. Eur Urol.

Hadaschik, B.A., Black, P.C., Sea, J.C., Metwalli, A.R., Fazli, L., Dinney, C.P., Gleave, M.E., So, A.I., 2007. A validated mouse model for orthotopic bladder cancer using transurethral tumour inoculation and bioluminescence imaging. BJU Int 100, 1377-1384.

Hamdy, F.C., Donovan, J.L., Lane, J.A., Mason, M., Metcalfe, C., Holding, P., Davis, M., Peters, T.J., Turner, E.L., Martin, R.M., Oxley, J., Robinson, M., Staffurth, J., Walsh, E., Bollina, P., Catto, J., Doble, A., Doherty, A., Gillatt, D., Kockelbergh, R., Kynaston, H., Paul, A., Powell, P., Prescott, S., Rosario, D.J., Rowe, E., Neal, D.E., Protec, T.S.G., 2016. 10-Year Outcomes after Monitoring, Surgery, or Radiotherapy for Localized Prostate Cancer. N Engl J Med 375, 1415-1424.

Hameed, O., Humphrey, P.A., 2005. Immunohistochemistry in diagnostic surgical pathology of the prostate. Seminars in Diagnostic Pathology 22, 88-104.

Hammarsten, P., Josefsson, A., Thysell, E., Lundholm, M., Hagglof, C., Iglesias-Gato, D., Flores-Morales, A., Stattin, P., Egevad, L., Granfors, T., Wikstrom, P., Bergh, A., 2019. Immunoreactivity for prostate specific antigen and Ki67 differentiates subgroups of prostate cancer related to outcome. Mod Pathol.

Han, M., Xu, W., Cheng, P., Jin, H., Wang, X., 2017. Histone demethylase lysine demethylase 5B in development and cancer. Oncotarget 8, 8980-8991.

Han, R.F., Pan, J.G., 2006. Can intravesical bacillus Calmette-Guerin reduce recurrence in patients with superficial bladder cancer? A meta-analysis of randomized trials. Urology 67, 1216-1223.

Hanazono, K., Fukumoto, S., Endo, Y., Ueno, H., Kadosawa, T., Uchide, T., 2014. Ultrasonographic findings related to prognosis in canine transitional cell carcinoma. Vet Radiol Ultrasound 55, 79-84.

Hanazono, K., Nishimori, T., Fukumoto, S., Kawamura, Y., Endo, Y., Kadosawa, T., Uchide, T., 2016. Immunohistochemical expression of p63, Ki67 and beta-catenin in canine transitional cell carcinoma and polypoid cystitis of the urinary bladder. Vet Comp Oncol 14, 263-269.

Hankey, B.F., Myers, M.H., 1987. Black-White Differences in Bladder-Cancer Patient Survival. J Chron Dis 40, 65-73.

Hansel, D.E., Amin, M.B., Comperat, E., Cote, R.J., Knuchel, R., Montironi, R., Reuter, V.E., Soloway, M.S., Umar, S.A., Van der Kwast, T.H., 2013. A contemporary update on pathology standards for bladder cancer: transurethral resection and radical cystectomy specimens. Eur Urol 63, 321-332.

Hara, R., Jo, Y., Fujii, T., Kondo, N., Yokoyoma, T., Miyaji, Y., Nagai, A., 2008. Optimal approach for prostate cancer detection as initial biopsy: prospective randomized study comparing transperineal versus transrectal systematic 12-core biopsy. Urology 71, 191-195.

Harik, L.R., Merino, C., Coindre, J.M., Amin, M.B., Pedeutour, F., Weiss, S.W., 2006. Pseudosarcomatous myofibroblastic proliferations of the bladder: a clinicopathologic study of 42 cases. Am J Surg Pathol 30, 787-794.

Hayami, S., Yoshimatsu, M., Veerakumarasivam, A., Unoki, M., Iwai, Y., Tsunoda, T., Field, H.I., Kelly, J.D., Neal, D.E., Yamaue, H., Ponder, B.A., Nakamura, Y., Hamamoto, R., 2010. Overexpression of the JmjC histone demethylase KDM5B in human carcinogenesis: involvement in the proliferation of cancer cells through the E2F/RB pathway. Mol Cancer 9, 59.

He, H., Han, C., Hao, L., Zang, G., 2016. ImmunoCyt test compared to cytology in the diagnosis of bladder cancer: A meta-analysis. Oncol Lett 12, 83-88.

He, Z., Kosinska, W., Zhao, Z.L., Wu, X.R., Guttenplan, J.B., 2012. Tissue-specific mutagenesis by N-butyl-N-(4-hydroxybutyl)nitrosamine as the basis for urothelial carcinogenesis. Mutat Res 742, 92-95.

Henriet, E., Sala, M., Abou Hammoud, A., Tuariihionoa, A., Di Martino, J., Ros, M., Saltel, F., 2018. Multitasking discoidin domain receptors are involved in several and specific hallmarks of cancer. Cell Adh Migr 12, 363-377.

Henry, C.J., Flesner, B.K., Bechtel, S.A., Bryan, J.N., Tate, D.J., Selting, K.A., Lattimer, J.C., Bryan, M.E., Grubb, L., Hausheer, F., 2018. Clinical Evaluation of Tavocept to Decrease Diuresis Time and Volume in Dogs with Bladder Cancer Receiving Cisplatin. J Vet Intern Med 32, 370-376.

Henry, C.J., McCaw, D.L., Turnquist, S.E., Tyler, J.W., Bravo, L., Sheafor, S., Straw, R.C., Dernell, W.S., Madewell, B.R., Jorgensen, L., Scott, M.A., Higginbotham, M.L., Chun, R., 2003a. Clinical evaluation of mitoxantrone and piroxicam in a canine model of human invasive urinary bladder carcinoma. Clin Cancer Res 9, 906-911.

Henry, C.J., Tyler, J.W., McEntee, M.C., Stokol, T., Rogers, K.S., Chun, R., Garrett, L.D., McCaw, D.L., Higginbotham, M.L., Flessland, K.A., Stokes, P.K., 2003b. Evaluation of a bladder tumor antigen test as a screening test for transitional cell carcinoma of the lower urinary tract in dogs. Am J Vet Res 64, 1017-1020.

Hidayat, K., Du, X., Zou, S.Y., Shi, B.M., 2017. Blood pressure and kidney cancer risk: meta-analysis of prospective studies. J Hypertens 35, 1333-1344.

Higgins, D.F., Kimura, K., Bernhardt, W.M., Shrimanker, N., Akai, Y., Hohenstein, B., Saito, Y., Johnson, R.S., Kretzler, M., Cohen, C.D., Eckardt, K.U., Iwano, M., Haase, V.H., 2007. Hypoxia promotes fibrogenesis in vivo via HIF-1 stimulation of epithelial-to-mesenchymal transition. J Clin Invest 117, 3810-3820.

Hjelmborg, J.B., Scheike, T., Holst, K., Skytthe, A., Penney, K.L., Graff, R.E., Pukkala, E., Christensen, K., Adami, H.O., Holm, N.V., Nuttall, E., Hansen, S., Hartman, M., Czene, K., Harris, J.R., Kaprio, J., Mucci, L.A., 2014. The heritability of prostate cancer in the Nordic Twin Study of Cancer. Cancer Epidemiol Biomarkers Prev 23, 2303-2310.

Hoang, L.L., Tacha, D., Bremer, R.E., Haas, T.S., Cheng, L., 2015. Uroplakin II (UPII), GATA3, and p40 are Highly Sensitive Markers for the Differential Diagnosis of Invasive Urothelial Carcinoma. Appl Immunohistochem Mol Morphol 23, 711-716.

Hodges, K.B., Lopez-Beltran, A., Emerson, R.E., Montironi, R., Cheng, L., 2010. Clinical utility of immunohistochemistry in the diagnoses of urinary bladder neoplasia. Appl Immunohistochem Mol Morphol 18, 401-410.

Hodgson, A., Xu, B., Satkunasivam, R., Downes, M.R., 2018. Tumour front inflammation and necrosis are independent prognostic predictors in high-grade urothelial carcinoma of the bladder. J Clin Pathol 71, 154-160.

Hoeppner, M.P., Lundquist, A., Pirun, M., Meadows, J.R., Zamani, N., Johnson, J., Sundström, G., Cook, A., FitzGerald. M.G., Swofford, R., Mauceli, E., Moghadam, B.T., Greka, A., Alföldi, J., Abouelleil, A., Aftuck, L., Bessette, D., Berlin, A., Brown, A., Gearin, G., Lui, A., Macdonald, J.P., Priest, M., Shea, T., Turner-Maier, J., Zimmer, A., Lander, E.S., di Palma, F., Lindblad-Toh, K., Grabherr, M.G., 2014. An improved canine genome and a comprehensive catalogue of coding genes and non-coding transcripts. PLoS One 9, e91172.

Holthoff, E.R., Byrum, S.D., Mackintosh, S.G., Kelly, T., Tackett, A.J., Quick, C.M., Post, S.R., 2017. Vulvar squamous cell carcinoma aggressiveness is associated with differential expression of collagen and STAT1. Clin Proteomics 14, 40.

Hotta, K., Sho, M., Fujimoto, K., Shimada, K., Yamato, I., Anai, S., Harada, H., Tsujikawa, K., Konishi, N., Shinohara, N., Nakajima, Y., 2015. Clinical significance and therapeutic potential of prostate cancer antigen-1/ALKBH3 in human renal cell carcinoma. Oncol Rep 34, 648-654.

Hou, T., Zhou, L., Wang, L., Kazobinka, G., Zhang, X., Chen, Z., 2017. CLCA4 inhibits bladder cancer cell proliferation, migration, and invasion by suppressing the PI3K/AKT pathway. Oncotarget 8, 93001-93013.

Hou, W., Ji, Z., 2018. Generation of autochthonous mouse models of clear cell renal cell carcinoma: mouse models of renal cell carcinoma. Exp Mol Med 50, 30.

Hu, X., Shao, Y.X., Wang, Y., Yang, Z.Q., Yang, W.X., Li, X., 2019. Partial nephrectomy versus ablative therapies for cT1a renal masses: A Systematic Review and meta-analysis. Eur J Surg Oncol 45, 1527-1535.

Hu, X., Stern, H.M., Ge, L., O'Brien, C., Haydu, L., Honchell, C.D., Haverty, P.M., Peters, B.A., Wu, T.D., Amler, L.C., Chant, J., Stokoe, D., Lackner, M.R., Cavet, G., 2009. Genetic alterations and oncogenic pathways associated with breast cancer subtypes. Mol Cancer Res 7, 511-522.

Huang, Y., Li, G., Wang, K., Mu, Z., Xie, Q., Qu, H., Lv, H., Hu, B., 2018. Collagen Type VI Alpha 3 Chain Promotes Epithelial-Mesenchymal Transition in Bladder Cancer Cells via Transforming Growth Factor beta (TGF-beta)/Smad Pathway. Med Sci Monit 24, 5346-5354.

Hughes, D.F., Biggart, J.D., Hayes, D., 1991. Pseudosarcomatous lesions of the urinary bladder. Histopathology 18, 67-71.

Humphrey, P.A., Moch, H., Cubilla, A.L., Ulbright, T.M., Reuter, V.E., 2016. The 2016 WHO Classification of Tumours of the Urinary System and Male Genital Organs-Part B: Prostate and Bladder Tumours. Eur Urol 70, 106-119.

Hunt, J.D., van der Hel, O.L., McMillan, G.P., Boffetta, P., Brennan, P., 2005. Renal cell carcinoma in relation to cigarette smoking: meta-analysis of 24 studies. Int J Cancer 114, 101-108.

Hur, H., Ham, I.H., Lee, D., Jin, H., Aguilera, K.Y., Oh, H.J., Han, S.U., Kwon, J.E., Kim, Y.B., Ding, K., Brekken, R.A., 2017. Discoidin domain receptor 1 activity drives an aggressive phenotype in gastric carcinoma. BMC Cancer 17, 87.

Iizuka, M., Susa, T., Takahashi, Y., Tamamori-Adachi, M., Kajitani, T., Okinaga, H., Fukusato, T., Okazaki, T., 2013. Histone acetyltransferase Hbo1 destabilizes estrogen receptor alpha by ubiquitination and modulates proliferation of breast cancers. Cancer Sci 104, 1647-1655.

Iizuka, M., Takahashi, Y., Mizzen, C.A., Cook, R.G., Fujita, M., Allis, C.D., Frierson, H.F., Jr., Fukusato, T., Smith, M.M., 2009. Histone acetyltransferase Hbo1: catalytic activity, cellular abundance, and links to primary cancers. Gene 436, 108-114.

Ikeda, S., Hansel, D.E., Kurzrock, R., 2015. Beyond conventional chemotherapy: Emerging molecular targeted and immunotherapy strategies in urothelial carcinoma. Cancer Treat Rev 41, 699-706.

Ikegami, H., Iwasaki, H., Ohjimi, Y., Takeuchi, T., Ariyoshi, A., Kikuchi, M., 2000. Sarcomatoid carcinoma of the urinary bladder: a clinicopathologic and immunohistochemical analysis of 14 patients. Hum Pathol 31, 332-340.

Inamura, K., 2018. Prostatic cancers: understanding their molecular pathology and the 2016 WHO classification. Oncotarget 9, 14723-14737.

Inoue, A., Maeda, S., Kinoshita, R., Tsuboi, M., Yonezawa, T., Matsuki, N., 2017. Density of tumor-infiltrating granzyme B-positive cells predicts favorable prognosis in dogs with transitional cell carcinoma. Vet Immunol Immunopathol 190, 53-56.

Isfoss, B.L., 2011. The sensitivity of fluorescent-light cystoscopy for the detection of carcinoma in situ (CIS) of the bladder: a meta-analysis with comments on gold standard. BJU Int 108, 1703-1707.

Ittmann, M., Huang, J., Radaelli, E., Martin, P., Signoretti, S., Sullivan, R., Simons, B.W., Ward, J.M., Robinson, B.D., Chu, G.C., Loda, M., Thomas, G., Borowsky, A., Cardiff, R.D., 2013. Animal models of human prostate cancer: the consensus report of the New York meeting of the Mouse Models of Human Cancers Consortium Prostate Pathology Committee. Cancer Res 73, 2718-2736.

Iwata, T., Schultz, D., Hicks, J., Hubbard, G.K., Mutton, L.N., Lotan, T.L., Bethel, C., Lotz, M.T., Yegnasubramanian, S., Nelson, W.G., Dang, C.V., Xu, M., Anele, U., Koh, C.M., Bieberich, C.J., De Marzo, A.M., 2010. MYC overexpression induces prostatic intraepithelial neoplasia and loss of Nkx3.1 in mouse luminal epithelial cells. PLoS One 5, e9427.

Iyer, G., Al-Ahmadie, H., Schultz, N., Hanrahan, A.J., Ostrovnaya, I., Balar, A.V., Kim, P.H., Lin, O., Weinhold, N., Sander, C., Zabor, E.C., Janakiraman, M., Garcia-Grossman, I.R., Heguy, A., Viale, A., Bochner, B.H., Reuter, V.E., Bajorin, D.F., Milowsky, M.I., Taylor, B.S., Solit, D.B., 2013. Prevalence and co-occurrence of actionable genomic alterations in high-grade bladder cancer. J Clin Oncol 31, 3133-3140.

Jagannathan, V., Drögemüller, C., Leeb, T.; Dog Biomedical Variant Database Consortium (DBVDC), 2019. A comprehensive biomedical variant catalogue based on whole genome sequences of 582 dogs and eight wolves. Anim Genet 50, 695-704.

Janardhan, A., Kathera, C., Darsi, A., Ali, W., He, L., Yang, Y., Luo, L., Guo, Z., 2018. Prominent role of histone lysine demethylases in cancer epigenetics and therapy. Oncotarget 9, 34429-34448.

Jeffus, S.K., Gehlot, A., Holthoff, E., Stone, R., Spencer, H., Kelly, T., Post, S.R., Quick, C.M., 2015. A fibromyxoid stromal response is associated with an infiltrative tumor morphology, perineural invasion, and lymph node metastasis in squamous cell carcinoma of the vulva. Am J Surg Pathol 39, 1226-1233.

Jeon, M.J., Lim, S., You, M.H., Park, Y., Song, D.E., Sim, S., Kim, T.Y., Shong, Y.K., Kim, W.B., Kim, W.G., 2019. The role of Slit2 as a tumor suppressor in thyroid cancer. Mol Cell Endocrinol 483, 87-96.

Jiang, Q., Xie, M., He, M., Yan, F., Chen, M., Xu, S., Zhang, X., Shen, P., 2019. PITX2 methylation: a novel and effective biomarker for monitoring biochemical recurrence risk of prostate cancer. Medicine (Baltimore) 98, e13820.

Jiao, J., Wang, S.Y., Qiao, R., Vivanco, I., Watson, P.A., Sawyers, C.L., Wu, H., 2007. Murine cell lines derived from Pten null prostate cancer show the critical role of PTEN in hormone refractory prostate cancer development. Cancer Research 67, 6083-6091.

Jing, H., Song, J., Zheng, J., 2018. Discoidin domain receptor 1: New star in cancer-targeted therapy and its complex role in breast carcinoma. Oncol Lett 15, 3403-3408.

Jockers, R., Delagrange, P., Dubocovich, M.L., Markus, R.P., Renault, N., Tosini, G., Cecon, E., Zlotos, D.P., 2016. Update on melatonin receptors: IUPHAR Review 20. Br J Pharmacol 173, 2702-2725.

John, B.A., Said, N., 2017. Insights from animal models of bladder cancer: recent advances, challenges, and opportunities. Oncotarget 8, 57766-57781.

Jones, T.D., Wang, M., Eble, J.N., MacLennan, G.T., Lopez-Beltran, A., Zhang, S., Cocco, A., Cheng, L., 2005. Molecular evidence supporting field effect in urothelial carcinogenesis. Clin Cancer Res 11, 6512-6519.

Joung, J.W., Oh, H.K., Lee, S.J., Kim, Y.A., Jung, H.J., 2018. Significance of Intratumoral Fibrosis in Clear Cell Renal Cell Carcinoma. J Pathol Transl Med 52, 323-330.

Jung, E.J., Lee, H.J., Kwak, C., Ku, J.H., Moon, K.C., 2009. Young age is independent prognostic factor for cancer-specific survival of low-stage clear cell renal cell carcinoma. Urology 73, 137-141.

Kachrilas, S., Dellis, A., Papatsoris, A., Avgeris, S., Anastasiou, D., Gavriil, A., Horti, M., Tseleni Balafouta, S., Livadas, K., Stravopodis, D.J., Alivizatos, G., Voutsinas, G.E., Deliveliotis, C., 2019. PI3K/AKT pathway genetic alterations and dysregulation of expression in bladder cancer. J BUON 24, 329-337.

Kaelin, W.G., Jr., 2007. The von Hippel-Lindau tumor suppressor protein and clear cell renal carcinoma. Clin Cancer Res 13, 680s-684s.

Kanemoto, K., Fukuta, K., Kawai, N., Tozawa, K., Ochiai, M., Okamoto, K., Ohnami, S., Sakamoto, H., Yoshida, T., Kanai, Y., Katoh, M., Yasui, T., Kohri, K., Kakizoe, T., Nakagama, H., 2016. Genomic Landscape of Experimental Bladder Cancer in Rodents and Its Application to Human Bladder Cancer: Gene Amplification and Potential Overexpression of Cyp2a5/CYP2A6 Are Associated with the Invasive Phenotype. PLoS One 11, e0167374.

Kaplan-Lefko, P.J., Chen, T.M., Ittmann, M.M., Barrios, R.J., Ayala, G.E., Huss, W.J., Maddison, L.A., Foster, B.A., Greenberg, N.M., 2003. Pathobiology of autochthonous prostate cancer in a pre-clinical transgenic mouse model. Prostate 55, 219-237.

Kassouf, W., Traboulsi, S.L., Schmitz-Drager, B., Palou, J., Witjes, J.A., van Rhijn, B.W., Grossman, H.B., Kiemeney, L.A., Goebell, P.J., Kamat, A.M., 2016. Follow-up in non-muscle-invasive bladder cancer-International Bladder Cancer Network recommendations. Urol Oncol 34, 460-468.

Kauffman, E.C., Robinson, B.D., Downes, M., Marcinkiewicz, K., Vourganti, S., Scherr, D.S., Gudas, L.J., Mongan, N.P., 2013. Estrogen receptor-beta expression and pharmacological targeting in bladder cancer. Oncol Rep 30, 131-138.

Kaufmann, O., Volmerig, J., Dietel, M., 2000. Uroplakin III is a highly specific and moderately sensitive immunohistochemical marker for primary and metastatic urothelial carcinomas. Am J Clin Pathol 113, 683-687.

Ke, X.S., Qu, Y., Rostad, K., Li, W.C., Lin, B., Halvorsen, O.J., Haukaas, S.A., Jonassen, I., Petersen, K., Goldfinger, N., Rotter, V., Akslen, L.A., Oyan, A.M., Kalland, K.H., 2009. Genome-wide profiling of histone h3 lysine 4

and lysine 27 trimethylation reveals an epigenetic signature in prostate carcinogenesis. PLoS One 4, e4687.

Keating, N.L., O'Malley, A.J., Freedland, S.J., Smith, M.R., 2013. Does comorbidity influence the risk of myocardial infarction or diabetes during androgen-deprivation therapy for prostate cancer? Eur Urol 64, 159-166.

Keller, J.M., Schade, G.R., Ives, K., Cheng, X., Rosol, T.J., Piert, M., Siddiqui, J., Roberts, W.W., Keller, E.T., 2013. A novel canine model for prostate cancer. Prostate 73, 952-959.

Kennedy, P.C., Cullen, J.M., Edwards, J.F., Goldschmidt, M.H., Larsen, S., Munson, L., Nielsen, S. H., 1998. Histological Classification of Tumors of the Genital System of Domestic Animals. Second Series. Volume IV. Armed Forces Institute of Pathology in cooperation with the American Registry of Pathology and WHO Collaborating Center for Worldwide Reference on Comparative Oncology. Washington DC.

Kern, W.H., 1984. The Grade and Pathologic Stage of Bladder-Cancer. Cancer 53, 1185-1189.

Kido, L.A., de Almeida Lamas, C., Marostica, M.R., Jr., Cagnon, V.H.A., 2019. Transgenic Adenocarcinoma of the Mouse Prostate (TRAMP) model: A good alternative to study PCa progression and chemoprevention approaches. Life Sci 217, 141-147.

Kim, J., Roh, M., Doubinskaia, I., Algarroba, G.N., Eltoum, I.E., Abdulkadir, S.A., 2012. A mouse model of heterogeneous, c-MYC-initiated prostate cancer with loss of Pten and p53. Oncogene 31, 322-332.

Kim, M., Kim, J.H., Baek, S.J., Kim, S.Y., Kim, Y.S., 2016. Specific expression and methylation of SLIT1, SLIT2, SLIT3, and miR-218 in gastric cancer subtypes. Int J Oncol 48, 2497-2507.

Klein, E.A., Cooperberg, M.R., Magi-Galluzzi, C., Simko, J.P., Falzarano, S.M., Maddala, T., Chan, J.M., Li, J., Cowan, J.E., Tsiatis, A.C., Cherbavaz, D.B., Pelham, R.J., Tenggara-Hunter, I., Baehner, F.L., Knezevic, D., Febbo, P.G., Shak, S., Kattan, M.W., Lee, M., Carroll, P.R., 2014. A 17-gene assay to predict prostate cancer aggressiveness in the context of Gleason grade heterogeneity, tumor multifocality, and biopsy undersampling. Eur Urol 66, 550-560.

Kleymenova, E., Everitt, J.I., Pluta, L., Portis, M., Gnarra, J.R., Walker, C.L., 2004. Susceptibility to vascular neoplasms but no increased susceptibility to renal carcinogenesis in Vhl knockout mice. Carcinogenesis 25, 309-315.

Klisic, A., Kavaric, N., Bjelakovic, B., Soldatovic, I., Martinovic, M., Kotur-Stevuljevic, J., 2017. The Association Between Retinol-Binding Protein 4 and Cardiovascular Risk Score is Mediated by Waist Circumference in Overweight/Obese Adolescent Girls. Acta Clin Croat 56, 92-98.

Kluth, L.A., Xylinas, E., Crivelli, J.J., Passoni, N., Comploj, E., Pycha, A., Chrystal, J., Sun, M., Karakiewicz, P.I., Gontero, P., Lotan, Y., Chun, F.K., Fisch, M., Scherr, D.S., Shariat, S.F., 2013. Obesity is associated with worse outcomes in patients with T1 high grade urothelial carcinoma of the bladder. J Urol 190, 480-486.

Knapp, D.W., Glickman, N.W., Denicola, D.B., Bonney, P.L., Lin, T.L., Glickman, L.T., 2000. Naturally-occurring canine transitional cell carcinoma of the urinary bladder A relevant model of human invasive bladder cancer. Urol Oncol 5, 47-59.

Knapp, D.W., Henry, C.J., Widmer, W.R., Tan, K.M., Moore, G.E., Ramos-Vara, J.A., Lucroy, M.D., Greenberg, C.B., Greene, S.N., Abbo, A.H., Hanson, P.D., Alva, R., Bonney, P.L., 2013. Randomized trial of cisplatin versus firocoxib versus cisplatin/firocoxib in dogs with transitional cell carcinoma of the urinary bladder. J Vet Intern Med 27, 126-133.

Knapp, D.W., Ramos-Vara, J.A., Moore, G.E., Dhawan, D., Bonney, P.L., Young, K.E., 2014. Urinary bladder cancer in dogs, a naturally occurring model for cancer biology and drug development. ILAR J 55, 100-118.

Knapp, D.W., Ruple-Czerniak, A., Ramos-Vara, J.A., Naughton, J.F., Fulkerson, C.M., Honkisz, S.I., 2016. A Nonselective Cyclooxygenase Inhibitor Enhances the Activity of Vinblastine in a Naturally-Occurring Canine Model of Invasive Urothelial Carcinoma. Bladder Cancer 2, 241-250.

Knijnenburg, T.A., Wang, L.H., Zimmermann, M.T., Chambwe, N., Gao, G.F., Cherniack, A.D., Fan, H.H., Shen, H., Way, G.P., Greene, C.S., Liu, Y.X., Akbani, R., Feng, B., Donehower, L.A., Miller, C., Shen, Y., Karimi, M., Chen, H.R., Kim, P., Jia, P.L., Shinbrot, E., Zhang, S.J., Liu, J.F., Hu, H., Bailey, M.H., Yau, C., Wolf, D., Zhao, Z.M., Weinstein, J.N., Li, L., Ding, L., Mills, G.B., Laird, P.W., Wheeler, D.A., Shmulevich, I., Monnat, R.J., Xiao, Y.H., Wang, C., Network, C.G.A.R., 2018. Genomic and Molecular Landscape of DNA Damage Repair Deficiency across The Cancer Genome Atlas. Cell Reports 23, 239-+.

Knox, M.K., Cowan, N.C., Rivers-Bowerman, M.D., Turney, B.W., 2008. Evaluation of multidetector computed tomography urography and ultrasonography for diagnosing bladder cancer. Clin Radiol 63, 1317-1325.

Kobayashi, S., Fujii, Y., Koga, F., Yokoyama, M., Ishioka, J., Matsuoka, Y., Numao, N., Saito, K., Masuda, H., Kihara, K., 2014. Impact of bladder neck involvement on progression in patients with primary non-muscle invasive bladder cancer: A prospective validation study. Urol Oncol-Semin Ori 32.

Kobayashi, T., Owczarek, T.B., McKiernan, J.M., Abate-Shen, C., 2015. Modelling bladder cancer in mice: opportunities and challenges. Nat Rev Cancer 15, 42-54.

Koga, F., Kawakami, S., Fujii, Y., Saito, K., Ohtsuka, Y., Iwai, A., Ando, N., Takizawa, T., Kageyama, Y., Kihara, K., 2003. Impaired p63 expression associates with poor prognosis and uroplakin III expression in invasive urothelial carcinoma of the bladder. Clin Cancer Res 9, 5501-5507.

Koh, C.M., Bieberich, C.J., Dang, C.V., Nelson, W.G., Yegnasubramanian, S., De Marzo, A.M., 2010. MYC and Prostate Cancer. Genes Cancer 1, 617-628.

Kolodziej, A., Krajewski, W., Matuszewski, M., Tupikowski, K., 2016. Review of current optical diagnostic techniques for non-muscle-invasive bladder cancer. Cent European J Urol 69, 150-156.

Kong, D.B., Chen, F., Sima, N., 2017a. Focal adhesion kinases crucially regulate TGFbeta-induced migration and invasion of bladder cancer cells via Src kinase and E-cadherin. Onco Targets Ther 10, 1783-1792.

Kong, K.H., Oh, H.J., Lim, B.J., Kim, M., Han, K.H., Choi, Y.H., Kwon, K., Nam, B.Y., Park, K.S., Park, J.T., Han, S.H., Yoo, T.H., Lee, S., Kim, S.J., Kang, D.H., Choi, K.B., Eremina, V., Quaggin, S.E., Ryu, D.R., Kang, S.W., 2017b. Selective tubular activation of hypoxia-inducible factor-2alpha has dual effects on renal fibrosis. Sci Rep 7, 11351.

Korkolopoulou, P., Levidou, G., Trigka, E.A., Prekete, N., Karlou, M., Thymara, I., Sakellariou, S., Fragkou, P., Isaiadis, D., Pavlopoulos, P., Patsouris, E., Saetta, A.A., 2012. A comprehensive immunohistochemical and molecular approach to the PI3K/AKT/mTOR (phosphoinositide 3-kinase/v-akt murine thymoma viral oncogene/mammalian target of rapamycin) pathway in bladder urothelial carcinoma. BJU Int 110, E1237-1248.

Koti, M., Xu, A.S., Ren, K.Y.M., Visram, K., Ren, R., Berman, D.M., Siemens, D.R., 2017. Tertiary Lymphoid Structures Associate with Tumour Stage in Urothelial Bladder Cancer. Bladder Cancer 3, 259-267.

Krafft, U., Reis, H., Ingenwerth, M., Kovalszky, I., Becker, M., Niedworok, C., Darr, C., Nyirady, P., Hadaschik, B., Szarvas, T., 2018. Nuclear Localization of Robo is Associated with Better Survival in Bladder Cancer. Pathol Oncol Res.

Krazinski, B.E., Kiewisz, J., Sliwinska-Jewsiewicka, A., Kowalczyk, A.E., Grzegrzolka, J., Godlewski, J., Kwiatkowski, P., Dziegiel, P., Kmiec, Z., 2019. Altered Expression of DDR1 in Clear Cell Renal Cell Carcinoma Correlates With miR-199a/b-5p and Patients' Outcome. Cancer Genomics Proteomics 16, 179-193.

Kudryavtseva, A.V., Nyushko, K.M., Zaretsky, A.R., Shagin, D.A., Alekseev, B.Y., Kaprin, A.D., Snezhkina, A.V., 2017. Deregulation of RBP4 and RBP7 Genes in Clear Cell Renal Cell Carcinoma. Asian J Pharm 11, S183-S186.

Kunju, L.P., Mehra, R., Snyder, M., Shah, R.B., 2006. Prostate-specific antigen, high-molecular-weight cytokeratin (clone 34betaE12), and/or p63: an optimal immunohistochemical panel to distinguish poorly differentiated prostate adenocarcinoma from urothelial carcinoma. Am J Clin Pathol 125, 675-681.

Lachmann, S., Jevons, A., De Rycker, M., Casamassima, A., Radtke, S., Collazos, A., Parker, P.J., 2011. Regulatory domain selectivity in the cell-type specific PKN-dependence of cell migration. PLoS One 6, e21732.

Lai, C.L., van den Ham, R., van Leenders, G., van der Lugt, J., Mol, J.A., Teske, E., 2008a. Histopathological and immunohistochemical characterization of canine prostate cancer. Prostate 68, 477-488.

Lai, C.L., van den Ham, R., van Leenders, G., van der Lugt, J., Teske, E., 2008b. Comparative characterization of the canine normal prostate in intact and castrated animals. Prostate 68, 498-507.

Lamy, P., Nordentoft, I., Birkenkamp-Demtroder, K., Thomsen, M.B., Villesen, P., Vang, S., Hedegaard, J., Borre, M., Jensen, J.B., Hoyer, S., Pedersen, J.S., Orntoft, T.F., Dyrskjot, L., 2016. Paired Exome Analysis Reveals

Clonal Evolution and Potential Therapeutic Targets in Urothelial Carcinoma. Cancer Res 76, 5894-5906.

Langner, C., Hutterer, G., Chromecki, T., Leibl, S., Rehak, P., Zigeuner, R., 2006. Tumor necrosis as prognostic indicator in transitional cell carcinoma of the upper urinary tract. J Urol 176, 910-913; discussion 913-914.

Laufer-Amorim, R., Fonseca-Alves, C.E., Villacis, R.A.R., Linde, S.A.D., Carvalho, M., Larsen, S.J., Marchi, F.A., Rogatto, S.R., 2019. Comprehensive Genomic Profiling of Androgen-Receptor-Negative Canine Prostate Cancer. Int J Mol Sci 20.

Lazaro, M., Gallardo, E., Domenech, M., Pinto, A., Gonzalez-del-Alba, A., Del Alba, A.G., Puente, J., Fernandez, O., Font, A., Lainez, N., Vazquez, S., 2016. SEOM Clinical Guideline for treatment of muscle-invasive and metastatic urothelial bladder cancer (2016). Clin Transl Oncol 18, 1197-1205.

Leav, I., Schelling, K.H., Adams, J.Y., Merk, F.B., Alroy, J., 2001a. Role of canine basal cells in postnatal prostatic development, induction of hyperplasia, and sex hormone-stimulated growth; and the ductal origin of carcinoma. Prostate 48, 210-224.

Lee, C.T., Dunn, R.L., Williams, C., Underwood, W., 3rd, 2006. Racial disparity in bladder cancer: trends in tumor presentation at diagnosis. J Urol 176, 927-933.

Lee, K., Choi, S., Choi, H., Lee, Y., 2016. Clinical experience of MRI in two dogs with muscle-invasive transitional cell carcinoma of the urinary bladder. J Vet Med Sci 78, 1351-1354.

Lee, K.H., Hong, S., Kang, M., Jeong, C.W., Ku, J.H., Kim, H.H., Kwak, C., 2018. Histone demethylase KDM7A controls androgen receptor activity and tumor growth in prostate cancer. Int J Cancer 143, 2849-2861.

Lee, S.E., Hong, S.K., Han, B.K., Yu, J.H., Han, J.H., Jeong, S.J., Byun, S.S., Park, Y.H., Choe, G., 2007. Prognostic significance of tumor necrosis in primary transitional cell carcinoma of upper urinary tract. Jpn J Clin Oncol 37, 49-55.

Lehmann, J., Suttmann, H., Albers, P., Volkmer, B., Gschwend, J.E., Fechner, G., Spahn, M., Heidenreich, A., Odenthal, A., Seif, C., Nurnberg, N., Wulfing, C., Greb, C., Kalble, T., Grimm, M.O., Fieseler, C.F., Krege, S., Retz, M., Schulte-Baukloh, H., Gerber, M., Hack, M., Kamradt, J., Stockle, M., 2009. Surgery for metastatic urothelial carcinoma with curative intent: the German experience (AUO AB 30/05). Eur Urol 55, 1293-1299.

Lerner, S.P., Liu, H., Wu, M.F., Thomas, Y.K., Witjes, J.A., 2012. Fluorescence and white light cystoscopy for detection of carcinoma in situ of the urinary bladder. Urol Oncol 30, 285-289.

LeRoy, B.E., Lech, M.E., 2004. Prostatic carcinoma causing urethral obstruction and obstipation in a cat. J Feline Med Surg 6, 397-400.

Leroy, B.E., Northrup, N., 2009. Prostate cancer in dogs: comparative and clinical aspects. Vet J 180, 149-162.

Li, F., Ji, J.P., Xu, Y., Liu, R.L., 2019a. Identification a novel set of 6 differential expressed genes in prostate cancer that can potentially predict

biochemical recurrence after curative surgery. Clin Transl Oncol 21, 1067-1075.

Li, J., Wan, X., Qiang, W., Li, T., Huang, W., Huang, S., Wu, D., Li, Y., 2015a. MiR-29a suppresses prostate cell proliferation and induces apoptosis via KDM5B protein regulation. Int J Clin Exp Med 8, 5329-5339.

Li, J., Zhou, C., Wang, G., Wang, S., Ni, S., Ye, M., Zhang, J., 2018. Promoter hypermethylation of SLIT2 is a risk factor and potential diagnostic biomarker for nasopharyngeal carcinoma. Gene 644, 74-79.

Li, L., Wang, J., Gao, L., Gong, L., 2015b. Expression of paxillin in laryngeal squamous cell carcinoma and its prognostic value. Int J Clin Exp Pathol 8, 9232-9239.

Li, W., Cheng, Y., Cheng, Y., Ren, H., Han, N., 2014. Clinical efficacy of radical nephrectomy versus nephron-sparing surgery on localized renal cell carcinoma. Eur J Med Res 19, 58.

Li, W., Zhao, Y., Fu, P., 2017. Hypoxia Induced Factor in Chronic Kidney Disease: Friend or Foe? Front Med (Lausanne) 4, 259.

Li, Y., Sun, Y., Yang, Q., Wu, J., Xiong, Z., Li, S., Jin, T., 2019b. Variants in COL6A3 gene influence susceptibility to esophageal cancer in the Chinese population. Cancer Genet 238, 23-30.

Lin, F.Y., Lin, C.W., Yang, S.F., Lee, W.J., Lin, Y.W., Lee, L.M., Chang, J.L., Weng, W.C., Lin, C.H., Chien, M.H., 2015a. Interactions between environmental factors and melatonin receptor type 1A polymorphism in relation to oral cancer susceptibility and clinicopathologic development. PLoS One 10, e0121677.

Lin, J., Zahm, S.H., Shriver, C.D., Purdue, M., McGlynn, K.A., Zhu, K., 2015b. Survival among Black and White patients with renal cell carcinoma in an equal-access health care system. Cancer Causes Control 26, 1019-1026.

Lin, J.H., Zhao, H., Sun, T.T., 1995. A tissue-specific promoter that can drive a foreign gene to express in the suprabasal urothelial cells of transgenic mice. Proc Natl Acad Sci U S A 92, 679-683.

Lin, Y.W., Wang, S.S., Wen, Y.C., Tung, M.C., Lee, L.M., Yang, S.F., Chien, M.H., 2017. Genetic Variations of Melatonin Receptor Type 1A are Associated with the Clinicopathologic Development of Urothelial Cell Carcinoma. Int J Med Sci 14, 1130-1135.

Lindblad-Toh, K., Wade, C.M., Mikkelsen, T.S., Karlsson, E.K., Jaffe, D.B., Kamal, M., Clamp, M., Chang, J.L., Kulbokas, E.J. 3rd, Zody, M.C., Mauceli, E., Xie, X., Breen, M., Wayne, R.K., Ostrander, E.A., Ponting, C.P., Galibert, F., Smith, D.R., DeJong, P.J., Kirkness, E., Alvarez, P., Biagi, T., Brockman, W., Butler, J., Chin, C.W., Cook, A., Cuff, J., Daly, M.J., DeCaprio, D., Gnerre, S., Grabherr, M., Kellis, M., Kleber, M., Bardeleben, C., Goodstadt, L., Heger, A., Hitte, C., Kim, L., Koepfli, K.P., Parker, H.G., Pollinger, J.P., Searle, S.M., Sutter, N.B., Thomas, R., Webber, C., Baldwin, J., Abebe, A., Abouelleil, A., Aftuck, L., Ait-Zahra, M., Aldredge, T., Allen, N., An, P., Anderson, S., Antoine, C., Arachchi, H., Aslam, A., Ayotte, L., Bachantsang, P., Barry, A., Bayul, T., Benamara, M., Berlin, A., Bessette, D., Blitshteyn, B., Bloom, T., Blye, J., Boguslavskiy, L., Bonnet, C., Boukhgalter, B., Brown, A., Cahill, P., Calixte, N., Camarata, J.,

Cheshatsang, Y., Chu, J., Citroen, M., Collymore, A., Cooke, P., Dawoe, T., Daza, R., Decktor, K., DeGray, S., Dhargay, N., Dooley, K., Dooley, K., Dorje, P., Dorjee, K., Dorris, L., Duffey, N., Dupes, A., Egbiremolen, O., Elong, R., Falk, J., Farina, A., Faro, S., Ferguson, D., Ferreira, P., Fisher, S., FitzGerald, M., Foley, K., Foley, C., Franke, A., Friedrich, D., Gage, D., Garber, M., Gearin, G., Giannoukos, G., Goode, T., Goyette, A., Graham, J., Grandbois, E., Gyaltsen, K., Hafez, N., Hagopian, D., Hagos, B., Hall, J., Healy, C., Hegarty, R., Honan, T., Horn, A., Houde, N., Hughes, L., Hunnicutt, L., Husby, M., Jester, B., Jones, C., Kamat, A., Kanga, B., Kells, C., Khazanovich, D., Kieu, A.C., Kisner, P., Kumar, M., Lance, K., Landers, T., Lara, M., Lee, W., Leger, J.P., Lennon, N., Leuper, L., LeVine, S., Liu, J., Liu, X., Lokyitsang, Y., Lokyitsang, T., Lui, A., Macdonald, J., Major, J., Marabella, R., Maru, K., Matthews, C., McDonough, S., Mehta, T., Meldrim, J., Melnikov, A., Meneus, L., Mihalev, A., Mihova, T., Miller, K., Mittelman, R., Mlenga, V., Mulrain, L., Munson, G., Navidi, A., Naylor, J., Nguyen, T., Nguyen, N., Nguyen, C., Nguyen, T., Nicol, R., Norbu, N., Norbu, C., Novod, N., Nyima, T., Olandt, P., O'Neill, B., O'Neill, K., Osman, S., Oyono, L., Patti, C., Perrin, D., Phunkhang, P., Pierre, F., Priest, M., Rachupka, A., Raghuraman, S., Rameau, R., Ray, V., Raymond, C., Rege, F., Rise, C., Rogers, J., Rogov, P., Sahalie, J., Settipalli, S., Sharpe, T., Shea, T., Sheehan, M., Sherpa, N., Shi, J., Shih, D., Sloan, J., Smith, C., Sparrow, T., Stalker, J., Stange-Thomann, N., Stavropoulos, S., Stone, C., Stone, S., Sykes, S., Tchuinga, P., Tenzing, P., Tesfaye, S., Thoulutsang, D., Thoulutsang, Y., Topham, K., Topping, I., Tsamla, T., Vassiliev, H., Venkataraman, V., Vo, A., Wangchuk, T., Wangdi, T., Weiand, M., Wilkinson, J., Wilson, A., Yadav, S., Yang, S., Yang, X., Young, G., Yu, Q., Zainoun, J., Zembek, L., Zimmer, A., Lander, E.S., 2005 Genome sequence, comparative analysis and haplotype structure of the domestic dog. Nature 438, 803-19.

Liu, B.C., Tang, T.T., Lv, L.L., Lan, H.Y., 2018a. Renal tubule injury: a driving force toward chronic kidney disease. Kidney Int 93, 568-579.

Liu, J., Wei, Q., Guo, C., Dong, G., Liu, Y., Tang, C., Dong, Z., 2017. Hypoxia, HIF, and Associated Signaling Networks in Chronic Kidney Disease. Int J Mol Sci 18.

Liu, L., Li, W., Geng, S., Fang, Y., Sun, Z., Hu, H., Liang, Z., Yan, Z., 2016. Slit2 and Robo1 expression as biomarkers for assessing prognosis in brain glioma patients. Surg Oncol 25, 405-410.

Liu, W., Li, L., Ye, H., Tao, H., He, H., 2018b. Role of COL6A3 in colorectal cancer. Oncol Rep 39, 2527-2536.

Ljungberg, B., Albiges, L., Abu-Ghanem, Y., Bensalah, K., Dabestani, S., Fernandez-Pello, S., Giles, R.H., Hofmann, F., Hora, M., Kuczyk, M.A., Kuusk, T., Lam, T.B., Marconi, L., Merseburger, A.S., Powles, T., Staehler, M., Tahbaz, R., Volpe, A., Bex, A., 2019. European Association of Urology Guidelines on Renal Cell Carcinoma: The 2019 Update. Eur Urol 75, 799-810.

Ljungberg, B., Campbell, S.C., Choi, H.Y., Jacqmin, D., Lee, J.E., Weikert, S., Kiemeney, L.A., 2011. The epidemiology of renal cell carcinoma. Eur Urol 60, 615-621.

Loginov, V.I., Pronina, I.V., Burdennyi, A.M., Pereyaslova, E.A., Braga, E.A., Kazubskaya, T.P., Kushlinskii, N.E., 2017. Role of Methylation in the Regulation of Apoptosis Genes APAF1, DAPK1, and BCL2 in Breast Cancer. B Exp Biol Med+ 162, 797-800.

Lopez-Beltran, A., Cheng, L., Mazzucchelli, R., Bianconi, M., Blanca, A., Scarpelli, M., Montironi, R., 2008. Morphological and molecular profiles and pathways in bladder neoplasms. Anticancer Res 28, 2893-2900.

Loukov, D., Naidoo, A., Puchta, A., Marin, J.L., Bowdish, D.M., 2016. Tumor necrosis factor drives increased splenic monopoiesis in old mice. J Leukoc Biol 100, 121-129.

Lowe, D., Fletcher, C.D., Gower, R.L., 1984. Tumour-associated eosinophilia in the bladder. J Clin Pathol 37, 500-502.

Lu, P.J., Sundquist, K., Baeckstrom, D., Poulsom, R., Hanby, A., Meier-Ewert, S., Jones, T., Mitchell, M., Pitha-Rowe, P., Freemont, P., Taylor-Papadimitriou, J., 1999. A novel gene (PLU-1) containing highly conserved putative DNA/chromatin binding motifs is specifically up-regulated in breast cancer. J Biol Chem 274, 15633-15645.

Lu, Z., Yeh, T.K., Wang, J., Chen, L., Lyness, G., Xin, Y., Wientjes, M.G., Bergdall, V., Couto, G., Alvarez-Berger, F., Kosarek, C.E., Au, J.L., 2011. Paclitaxel gelatin nanoparticles for intravesical bladder cancer therapy. J Urol 185, 1478-1483.

Luo, R., Zhang, W., Zhao, C., Zhang, Y., Wu, H., Jin, J., Zhang, W., Grenz, A., Eltzschig, H.K., Tao, L., Kellems, R.E., Xia, Y., 2015. Elevated Endothelial Hypoxia-Inducible Factor-1alpha Contributes to Glomerular Injury and Promotes Hypertensive Chronic Kidney Disease. Hypertension 66, 75-84.

Lynch, H.T., Kosoko-Lasaki, O., Leslie, S.W., Rendell, M., Shaw, T., Snyder, C., D'Amico, A.V., Buxbaum, S., Isaacs, W.B., Loeb, S., Moul, J.W., Powell, I., 2016. Screening for familial and hereditary prostate cancer. Int J Cancer 138, 2579-2591.

Macleod, L.C., Hotaling, J.M., Wright, J.L., Davenport, M.T., Gore, J.L., Harper, J., White, E., 2013. Risk factors for renal cell carcinoma in the VITAL study. J Urol 190, 1657-1661.

Madeb, R., Messing, E.M., 2004. Gender, racial and age differences in bladder cancer incidence and mortality. Urol Oncol-Semin Ori 22, 86-92.

Maeda, S., Tomiyasu, H., Tsuboi, M., Inoue, A., Ishihara, G., Uchikai, T., Chambers, J.K., Uchida, K., Yonezawa, T., Matsuki, N., 2018. Comprehensive gene expression analysis of canine invasive urothelial bladder carcinoma by RNA-Seq. BMC Cancer 18, 472.

Mahadevia, P.S., Alexander, J.E., Rojas-Corona, R., Koss, L.G., 1989. Pseudosarcomatous stromal reaction in primary and metastatic urothelial carcinoma. A source of diagnostic difficulty. Am J Surg Pathol 13, 782-790.

Majewski, T., Yao, H., Bondaruk, J., Chung, W., Lee, S., Lee, J.G., Zhang, S., Cogdell, D., Yang, G., Choi, W., Dinney, C., Grossman, H.B., Logothetis, C., Scherer, S.E., Guo, C.C., Zhang, L., Wei, P., Weinstein, J.N., Issa, J.P., Baggerly, K., McConkey, D.J., Czerniak, B., 2019. Whole-Organ Genomic Characterization of Mucosal Field Effects Initiating Bladder Carcinogenesis. Cell Rep 26, 2241-2256 e2244.

Malmstrom, P.U., Sylvester, R.J., Crawford, D.E., Friedrich, M., Krege, S., Rintala, E., Solsona, E., Di Stasi, S.M., Witjes, J.A., 2009. An individual patient data meta-analysis of the long-term outcome of randomised studies comparing intravesical mitomycin C versus bacillus Calmette-Guerin for non-muscle-invasive bladder cancer. Eur Urol 56, 247-256.

Mantonakis, E., Giaginis, C., Pikoulis, E., Felekouras, E., Patsouris, E., Liakakos, T., Papalampros, E., Theocharis, S., 2017. FAK, Src and p-Paxillin expression is decreased in liver metastasis of colorectal carcinoma patients. J BUON 22, 1097-1106.

Mantovani, A., Allavena, P., Sica, A., Balkwill, F., 2008. Cancer-related inflammation. Nature 454, 436-444.

Marcos-Gragera, R., Mallone, S., Kiemeney, L.A., Vilardell, L., Malats, N., Allory, Y., Sant, M., Group, E.-W., 2015. Urinary tract cancer survival in Europe 1999-2007: Results of the population-based study EUROCARE-5. Eur J Cancer 51, 2217-2230.

Martin-Padura, I., Lostaglio, S., Schneemann, M., Williams, L., Romano, M., Fruscella, P., Panzeri, C., Stoppacciaro, A., Ruco, L., Villa, A., Simmons, D., Dejana, E., 1998. Junctional adhesion molecule, a novel member of the immunoglobulin superfamily that distributes at intercellular junctions and modulates monocyte transmigration. J Cell Biol 142, 117-127.

Martinez Chanza, N., Tripathi, A., Harshman, L.C., 2019. Adjuvant Therapy Options in Renal Cell Carcinoma: Where Do We Stand? Curr Treat Options Oncol 20, 44.

Marvel, S.J., Seguin, B., Dailey, D.D., Thamm, D.H., 2017. Clinical outcome of partial cystectomy for transitional cell carcinoma of the canine bladder. Veterinary and Comparative Oncology 15, 1417-1427.

Mathur, M., Kim, C.M., Munro, S.A., Rudina, S.S., Sawyer, E.M., Smolke, C.D., 2019. Programmable mutually exclusive alternative splicing for generating RNA and protein diversity. Nat Commun 10, 2673.

Matsumoto, K., Satoh, T., Irie, A., Ishii, J., Kuwao, S., Iwamura, M., Baba, S., 2008. Loss expression of uroplakin III is associated with clinicopathologic features of aggressive bladder cancer. Urology 72, 444-449.

McGrath, M., Michaud, D.S., De Vivo, I., 2006. Hormonal and reproductive factors and the risk of bladder cancer in women. Am J Epidemiol 163, 236-244.

McSherry, E.A., McGee, S.F., Jirstrom, K., Doyle, E.M., Brennan, D.J., Landberg, G., Dervan, P.A., Hopkins, A.M., Gallagher, W.M., 2009. JAM-A expression positively correlates with poor prognosis in breast cancer patients. Int J Cancer 125, 1343-1351.

Megquier, K,, Genereux, D.P., Hekman, J., Swofford, R., Turner-Maier, J., Johnson, J., Alonso, J., Li, X., Morrill, K., Anguish, L.J., Koltookian, M., Logan, B., Sharp, C.R., Ferrer, L., Lindblad-Toh, K., Meyers-Wallen, V.N., Hoffman, A., Karlsson, E.K., 2019. BarkBase: Epigenomic Annotation of Canine Genomes. Genes (Basel) 10, pii: E433.

Meng, Z., Liu, Y., Wang, J., Fan, H., Fang, H., Li, S., Yuan, L., Liu, C., Peng, Y., Zhao, W., Wang, L., Li, J., Feng, J., 2019. Histone demethylase KDM7A is required for stem cell maintenance and apoptosis inhibition in breast cancer. J Cell Physiol.

Mengual, L., Burset, M., Ars, E., Lozano, J.J., Villavicencio, H., Ribal, M.J., Alcaraz, A., 2009. DNA microarray expression profiling of bladder cancer allows identification of noninvasive diagnostic markers. J Urol 182, 741-748.

Messer, J.S., Chew, D.J., McLoughlin, M.A., 2005. Cystoscopy: techniques and clinical applications. Clin Tech Small Anim Pract 20, 52-64.

Mestrinho, L.A., Pissarra, H., Faisca, P.B., Braganca, M., Peleteiro, M.C., Niza, M.M., 2015. p63 and E-cadherin Expression in Canine Oral Squamous Cell Carcinoma. Vet Pathol 52, 614-620.

Meuten, D.J., Everitt, J., Inskeep, W., Jacobs, R.M., Peleteiro, M., Thompson, K.G. 2004. Histological Classification of Tumors of the Urinary System of Domestic Animals. Washington, DC: World Health Organization International Histological Classification of Tumors of Domestic Animals, Second Series Volume XI, Armed Forces Institute of Pathology, American Registry of Pathology.

Meuten D.J. and Meuten T.L.K. Tumors of the Urinary System. In Tumors of Domestic Animals, 5th ed.; Meuten, D.J., Ed.; Wiley Blackwell: Ames, IA, USA, 2016; p. 632-688.

Meuten, D.J., Moore, F.M., George, J.W., 2016. Mitotic Count and the Field of View Area: Time to Standardize. Vet Pathol 53, 7-9.

Mhawech, P., Uchida, T., Pelte, M.F., 2002. Immunohistochemical profile of high-grade urothelial bladder carcinoma and prostate adenocarcinoma. Hum Pathol 33, 1136-1140.

Mihatsch, M.J., Rist, M., Romppanen, T., Rutishauser, G., 1979. Prognostic significance of peritumoural inflammation in invasive urothelial bladder carcinoma. Urol Res 7, 97-102.

Minato, A., Fujimoto, N., Kubo, T., 2017. Squamous Differentiation Predicts Poor Response to Cisplatin-Based Chemotherapy and Unfavorable Prognosis in Urothelial Carcinoma of the Urinary Bladder. Clin Genitourin Cancer 15, e1063-e1067.

Minton, D.R., Fu, L., Chen, Q., Robinson, B.D., Gross, S.S., Nanus, D.M., Gudas, L.J., 2015. Analyses of the transcriptome and metabolome demonstrate that HIF1alpha mediates altered tumor metabolism in clear cell renal cell carcinoma. PLoS One 10, e0120649.

Miotto, B., Struhl, K., 2010. HBO1 histone acetylase activity is essential for DNA replication licensing and inhibited by Geminin. Mol Cell 37, 57-66.

Mitchell, T.J., Rossi, S.H., Klatte, T., Stewart, G.D., 2018. Genomics and clinical correlates of renal cell carcinoma. World J Urol 36, 1899-1911.

Miyamoto, H., Yao, J.L., Chaux, A., Zheng, Y., Hsu, I., Izumi, K., Chang, C., Messing, E.M., Netto, G.J., Yeh, S., 2012. Expression of androgen and oestrogen receptors and its prognostic significance in urothelial neoplasm of the urinary bladder. BJU Int 109, 1716-1726.

Mizuma, Y., Watanabe, Y., Ozasa, K., Hayashi, K., Kawai, K., 2002. Validity of sonographic screening for the detection of abdominal cancers. J Clin Ultrasound 30, 408-415.

Moch, H., Cubilla, A.L., Humphrey, P.A., Reuter, V.E., Ulbright, T.M., 2016. The 2016 WHO Classification of Tumours of the Urinary System and Male Genital Organs-Part A: Renal, Penile, and Testicular Tumours. Eur Urol 70, 93-105.

Mohamed, G., Talima, S., Li, L., Wei, W., Rudzki, Z., Allam, R.M., Simmons, W., Tao, Q., Murray, P.G., 2019. Low Expression and Promoter Hypermethylation of the Tumour Suppressor SLIT2, are Associated with Adverse Patient Outcomes in Diffuse Large B Cell Lymphoma. Pathol Oncol Res 25, 1223-1231.

Mohammed, S.I., Craig, B.A., Mutsaers, A.J., Glickman, N.W., Snyder, P.W., deGortari, A.E., Schlittler, D.L., Coffman, K.T., Bonney, P.L., Knapp, D.W., 2003. Effects of the cyclooxygenase inhibitor, piroxicam, in combination with chemotherapy on tumor response, apoptosis, and angiogenesis in a canine model of human invasive urinary bladder cancer. Molecular Cancer Therapeutics 2, 183-188.

Morrissey, J.J., Mobley, J., Figenshau, R.S., Vetter, J., Bhayani, S., Kharasch, E.D., 2015. Urine aquaporin 1 and perilipin 2 differentiate renal carcinomas from other imaged renal masses and bladder and prostate cancer. Mayo Clin Proc 90, 35-42.

Mottet, N., Bellmunt, J., Bolla, M., Briers, E., Cumberbatch, M.G., De Santis, M., Fossati, N., Gross, T., Henry, A.M., Joniau, S., Lam, T.B., Mason, M.D., Matveev, V.B., Moldovan, P.C., van den Bergh, R.C.N., Van den Broeck, T., van der Poel, H.G., van der Kwast, T.H., Rouviere, O., Schoots, I.G., Wiegel, T., Cornford, P., 2017. EAU-ESTRO-SIOG Guidelines on Prostate Cancer. Part 1: Screening, Diagnosis, and Local Treatment with Curative Intent. Eur Urol 71, 618-629.

Motzer, R.J., Hutson, T.E., Tomczak, P., Michaelson, M.D., Bukowski, R.M., Oudard, S., Negrier, S., Szczylik, C., Pili, R., Bjarnason, G.A., Garcia-del-Muro, X., Sosman, J.A., Solska, E., Wilding, G., Thompson, J.A., Kim, S.T., Chen, I., Huang, X., Figlin, R.A., 2009. Overall survival and updated results for sunitinib compared with interferon alfa in patients with metastatic renal cell carcinoma. J Clin Oncol 27, 3584-3590.

Mukai, H., 2003. The structure and function of PKN, a protein kinase having a catalytic domain homologous to that of PKC. J Biochem 133, 17-27.

Mungan, N.A., Aben, K.K.H., Schoenberg, M.P., Visser, O., Coebergh, J.W.W., Witjes, J.A., Kiemeney, L.A.L.M., 2000. Gender differences in stage-adjusted bladder cancer survival. Urology 55, 876-880.

Murray, S.K., Young, R.H., Scully, R.E., 2003. Unusual epithelial and stromal changes in myoinvasive endometrioid adenocarcinoma: a study of their

frequency, associated diagnostic problems, and prognostic significance. Int J Gynecol Pathol 22, 324-333.

Mutsaers, A.J., Widmer, W.R., Knapp, D.W., 2003. Canine transitional cell carcinoma. J Vet Intern Med 17, 136-144.

Naik, M.U., Naik, T.U., Suckow, A.T., Duncan, M.K., Naik, U.P., 2008. Attenuation of junctional adhesion molecule-A is a contributing factor for breast cancer cell invasion. Cancer Res 68, 2194-2203.

Nakamura, E., Kozaki, K., Tsuda, H., Suzuki, E., Pimkhaokham, A., Yamamoto, G., Irie, T., Tachikawa, T., Amagasa, T., Inazawa, J., Imoto, I., 2008. Frequent silencing of a putative tumor suppressor gene melatonin receptor 1 A (MTNR1A) in oral squamous-cell carcinoma. Cancer Sci 99, 1390-1400.

Nam, G.E., Cho, K.H., Han, K., Kim, C.M., Han, B., Cho, S.J., Jung, S.J., Kwon, Y., Kim, Y.H., Kim, D.H., Kim, S.M., Choi, Y.S., Roh, Y.K., Park, Y.G., 2019. Obesity, abdominal obesity and subsequent risk of kidney cancer: a cohort study of 23.3 million East Asians. Br J Cancer 121, 271-277.

Narita, S., Nara, T., Sato, H., Koizumi, A., Huang, M., Inoue, T., Habuchi, T., 2019. Research Evidence on High-Fat Diet-Induced Prostate Cancer Development and Progression. J Clin Med 8.

Nesbit, C.E., Tersak, J.M., Prochownik, E.V., 1999. MYC oncogenes and human neoplastic disease. Oncogene 18, 3004-3016.

Neves, J.B., Cullen, D., Grant, L., Walkden, M., Bandula, S., Patki, P., Barod, R., Mumtaz, F., Aitchison, M., Pizzo, E., Ranieri, V., Williams, N., Wildgoose, W., Gurusamy, K., Emberton, M., Bex, A., Tran, M.G.B., 2019. Protocol for a feasibility study of a cohort embedded randomised controlled trial comparing NEphron Sparing Treatment (NEST) for small renal masses. BMJ Open 9, e030965.

Nguyen, O.N., Grimm, C., Schneider, L.S., Chao, Y.K., Atzberger, C., Bartel, K., Watermann, A., Ulrich, M., Mayr, D., Wahl-Schott, C., Biel, M., Vollmar, A.M., 2017. Two-Pore Channel Function Is Crucial for the Migration of Invasive Cancer Cells. Cancer Res 77, 1427-1438.

Niederhauser, B.D., Kawashima, A., King, B.F., Takahashi, N., 2013. Utility of gadolinium-enhanced MR urography in detection of bladder carcinoma. Eur J Radiol 82, 472-477.

Nielsen, S.M., Rhodes, L., Blanco, I., Chung, W.K., Eng, C., Maher, E.R., Richard, S., Giles, R.H., 2016. Von Hippel-Lindau Disease: Genetics and Role of Genetic Counseling in a Multiple Neoplasia Syndrome. J Clin Oncol 34, 2172-2181.

Nikula, K.J., Benjamin, S.A., Angleton, G.M., Lee, A.C., 1989. Transitional cell carcinomas of the urinary tract in a colony of beagle dogs. Vet Pathol 26, 455-461.

Nilsson, E.M., Laursen, K.B., Whitchurch, J., McWilliam, A., Odum, N., Persson, J.L., Heery, D.M., Gudas, L.J., Mongan, N.P., 2015. MiR137 is an androgen regulated repressor of an extended network of transcriptional coregulators. Oncotarget 6, 35710-35725.

Nissen, N.I., Karsdal, M., Willumsen, N., 2019. Collagens and Cancer associated fibroblasts in the reactive stroma and its relation to Cancer biology. J Exp Clin Cancer Res 38, 115.

Nordquist, L., Friederich-Persson, M., Fasching, A., Liss, P., Shoji, K., Nangaku, M., Hansell, P., Palm, F., 2015. Activation of hypoxia-inducible factors prevents diabetic nephropathy. J Am Soc Nephrol 26, 328-338.

Nordstrom, T., Vickers, A., Assel, M., Lilja, H., Gronberg, H., Eklund, M., 2015. Comparison Between the Four-kallikrein Panel and Prostate Health Index for Predicting Prostate Cancer. Eur Urol 68, 139-146.

Norris, A.M., Laing, E.J., Valli, V.E., Withrow, S.J., Macy, D.W., Ogilvie, G.K., Tomlinson, J., McCaw, D., Pidgeon, G., Jacobs, R.M., 1992. Canine bladder and urethral tumors: a retrospective study of 115 cases (1980-1985). J Vet Intern Med 6, 145-153.

Noy, N., Li, L., Abola, M.V., Berger, N.A., 2015. Is retinol binding protein 4 a link between adiposity and cancer? Horm Mol Biol Clin I 23, 39-46.

Nyberg, M., Hugosson, J., Wiklund, P., Sjoberg, D., Wilderang, U., Carlsson, S.V., Carlsson, S., Stranne, J., Steineck, G., Haglind, E., Bjartell, A., group, L., 2018. Functional and Oncologic Outcomes Between Open and Robotic Radical Prostatectomy at 24-month Follow-up in the Swedish LAPPRO Trial. Eur Urol Oncol 1, 353-360.

Obradovich, J., Walshaw, R., Goullaud, E., 1987. The influence of castration on the development of prostatic carcinoma in the dog. 43 cases (1978-1985). J Vet Intern Med 1, 183-187.

Offermann, A., Hupe, M.C., Sailer, V., Merseburger, A.S., Perner, S., 2019. The new ISUP 2014/WHO 2016 prostate cancer grade group system: first resume 5 years after introduction and systemic review of the literature. World J Urol.

Offersen, B.V., Knap, M.M., Marcussen, N., Horsman, M.R., Hamilton-Dutoit, S., Overgaard, J., 2002. Intense inflammation in bladder carcinoma is associated with angiogenesis and indicates good prognosis. Br J Cancer 87, 1422-1430.

Oh, W.J., Chung, A.M., Kim, J.S., Han, J.H., Hong, S.H., Lee, J.Y., Choi, Y.J., 2016. Differential Immunohistochemical Profiles for Distinguishing Prostate Carcinoma and Urothelial Carcinoma. J Pathol Transl Med 50, 345-354.

Okajima, E., Hiramatsu, T., Hirao, K., Ijuin, M., Hirao, Y., Babaya, K., Ikuma, S., Ohara, S., Shiomi, T., Hijioka, T., Ohishi, H., 1981. Urinary bladder tumors induced by N-butyl-N-(4-hydroxybutyl)nitrosamine in dogs. Cancer Res 41, 1958-1966.

Ord, J.J., Agrawal, S., Thamboo, T.P., Roberts, I., Campo, L., Turley, H., Han, C., Fawcett, D.W., Kulkarni, R.P., Cranston, D., Harris, A.L., 2007. An investigation into the prognostic significance of necrosis and hypoxia in high grade and invasive bladder cancer. J Urol 178, 677-682.

Osawa, T., Muramatsu, M., Wang, F., Tsuchida, R., Kodama, T., Minami, T., Shibuya, M., 2011. Increased expression of histone demethylase JHDM1D under nutrient starvation suppresses tumor growth via down-regulating angiogenesis. Proc Natl Acad Sci U S A 108, 20725-20729.

Owen, L.N. 1980. World Health Organization. Veterinary Public Health Unit & WHO Collaborating Center for Comparative Oncology. TNM Classification of Tumors in Domestic Animals/ edited by L.N. Owen. World Health Organization.

Pagliarulo, V., Bracarda, S., Eisenberger, M.A., Mottet, N., Schroder, F.H., Sternberg, C.N., Studer, U.E., 2012. Contemporary role of androgen deprivation therapy for prostate cancer. Eur Urol 61, 11-25.

Palmeira, C., Oliveira, P.A., Lameiras, C., Amaro, T., Silva, V.M., Lopes, C., Santos, L., 2010. Biological similarities between murine chemical-induced and natural human bladder carcinogenesis. Oncol Lett 1, 373-377.

Palmieri, C., Grieco, V., 2015. Proposal of Gleason-like grading system of canine prostate carcinoma in veterinary pathology practice. Res Vet Sci 103, 11-15.

Park, J., Scherer, P.E., 2012. Adipocyte-derived endotrophin promotes malignant tumor progression. J Clin Invest 122, 4243-4256.

Park, J.C., Gandhi, N.M., Carducci, M.A., Eisenberger, M.A., Baras, A.S., Netto, G.J., Liu, J.J., Drake, C.G., Schoenberg, M.P., Bivalacqua, T.J., Hahn, N.M., 2016a. A Retrospective Analysis of the Effect on Survival of Time from Diagnosis to Neoadjuvant Chemotherapy to Cystectomy for Muscle Invasive Bladder Cancer. J Urol 195, 880-885.

Park, S.Y., Park, J.W., Chun, Y.S., 2016b. Jumonji histone demethylases as emerging therapeutic targets. Pharmacol Res 105, 146-151.

Parker, D.C., Folpe, A.L., Bell, J., Oliva, E., Young, R.H., Cohen, C., Amin, M.B., 2003. Potential utility of uroplakin III, thrombomodulin, high molecular weight cytokeratin, and cytokeratin 20 in noninvasive, invasive, and metastatic urothelial (transitional cell) carcinomas. Am J Surg Pathol 27, 1-10.

Parker, W.R., Wang, R., He, C., Wood, D.P., Jr., 2011. Five year expanded prostate cancer index composite-based quality of life outcomes after prostatectomy for localized prostate cancer. BJU Int 107, 585-590.

Passerotti, C.C., Srougi, M., Bomfim, A.C., Martins, J.R., Leite, K.R., Dos Reis, S.T., Sampaio, L.O., Ortiz, V., Dietrich, C.P., Nader, H.B., 2011. Testing for urinary hyaluronate improves detection and grading of transitional cell carcinoma. Urol Oncol 29, 710-715.

Patai, A.V., Valcz, G., Hollosi, P., Kalmar, A., Peterfia, B., Patai, A., Wichmann, B., Spisak, S., Bartak, B.K., Leiszter, K., Toth, K., Sipos, F., Kovalszky, I., Peter, Z., Miheller, P., Tulassay, Z., Molnar, B., 2015. Comprehensive DNA Methylation Analysis Reveals a Common Ten-Gene Methylation Signature in Colorectal Adenomas and Carcinomas. PLoS One 10, e0133836.

Patrick, D.J., Fitzgerald, S.D., Sesterhenn, I.A., Davis, C.J., Kiupel, M., 2006. Classification of canine urinary bladder urothelial tumours based on the World Health Organization/International Society of Urological Pathology consensus classification. J Comp Pathol 135, 190-199.

Patronek, G.J., Waters, D.J., Glickman, L.T., 1997. Comparative longevity of pet dogs and humans: implications for gerontology research. J Gerontol A Biol Sci Med Sci 52, B171-178.

Pearson, J.M., Banerjee, S.S., Haboubi, N.Y., 1989. Two cases of pseudosarcomatous invasive transitional cell carcinoma of the urinary

bladder mimicking malignant fibrous histiocytoma. Histopathology 15, 93-96.

Pecoraro, A., Palumbo, C., Knipper, S., Mistretta, F.A., Tian, Z., Shariat, S.F., Saad, F., Briganti, A., Fiori, C., Porpiglia, F., Karakiewicz, P.I., 2019. In Patients with Nonmetastatic pT1b Kidney Cancer Cryoablation Predisposes to Higher Cancer Specific Mortality Relative to Partial Nephrectomy. J Urol 202, 1120-1126..

Pettersson, A., Gerke, T., Penney, K.L., Lis, R.T., Stack, E.C., Pertega-Gomes, N., Zadra, G., Tyekucheva, S., Giovannucci, E.L., Mucci, L.A., Loda, M., 2018. MYC Overexpression at the Protein and mRNA Level and Cancer Outcomes among Men Treated with Radical Prostatectomy for Prostate Cancer. Cancer Epidemiol Biomarkers Prev 27, 201-207.

Pham, T.T., Lee, E.S., Kong, S.Y., Kim, J., Kim, S.Y., Joo, J., Yoon, K.A., Park, B., 2019. Night-shift work, circadian and melatonin pathway related genes and their interaction on breast cancer risk: evidence from a case-control study in Korean women. Sci Rep 9, 10982.

Pienta, K.J., Esper, P.S., 1993. Risk factors for prostate cancer. Ann Intern Med 118, 793-803.

Pierorazio, P.M., Walsh, P.C., Partin, A.W., Epstein, J.I., 2013. Prognostic Gleason grade grouping: data based on the modified Gleason scoring system. BJU Int 111, 753-760.

Pinto, A.P., Signorello, L.B., Crum, C.P., Harlow, B.L., Abrao, F., Villa, L.L., 1999. Squamous cell carcinoma of the vulva in Brazil: prognostic importance of host and viral variables. Gynecol Oncol 74, 61-67.

Pitt, S.J., Funnell, T.M., Sitsapesan, M., Venturi, E., Rietdorf, K., Ruas, M., Ganesan, A., Gosain, R., Churchill, G.C., Zhu, M.X., Parrington, J., Galione, A., Sitsapesan, R., 2010. TPC2 is a novel NAADP-sensitive Ca2+ release channel, operating as a dual sensor of luminal pH and Ca2+. J Biol Chem 285, 35039-35046.

Platt, F.M., Hurst, C.D., Taylor, C.F., Gregory, W.M., Harnden, P., Knowles, M.A., 2009. Spectrum of phosphatidylinositol 3-kinase pathway gene alterations in bladder cancer. Clin Cancer Res 15, 6008-6017.

Poirier, V.J., Forrest, L.J., Adams, W.M., Vail, D.M., 2004. Piroxicam, mitoxantrone, and coarse fraction radiotherapy for the treatment of transitional cell carcinoma of the bladder in 10 dogs: a pilot study. J Am Anim Hosp Assoc 40, 131-136.

Pong, W.W., Walker, J., Wylie, T., Magrini, V., Luo, J., Emnett, R.J., Choi, J., Cooper, M.L., Griffith, M., Griffith, O.L., Rubin, J.B., Fuller, G.N., Piwnica-Worms, D., Feng, X., Hambardzumyan, D., DiPersio, J.F., Mardis, E.R., Gutmann, D.H., 2013. F11R is a novel monocyte prognostic biomarker for malignant glioma. PLoS One 8, e77571.

Ponten, F., Jirstrom, K., Uhlen, M., 2008. The Human Protein Atlas--a tool for pathology. J Pathol 216, 387-393.

Popov, H., Donev, I.S., Ghenev, P., 2018. Quantitative Analysis of Tumor-associated Tissue Eosinophilia in Recurring Bladder Cancer. Cureus 10, e3279.

Prizment, A.E., Anderson, K.E., Harlow, B.L., Folsom, A.R., 2007. Reproductive risk factors for incident bladder cancer: Iowa Women's Health Study. Int J Cancer 120, 1093-1098.

Qiao, J., Fang, C.Y., Chen, S.X., Wang, X.Q., Cui, S.J., Liu, X.H., Jiang, Y.H., Wang, J., Zhang, Y., Yang, P.Y., Liu, F., 2015. Stroma derived COL6A3 is a potential prognosis marker of colorectal carcinoma revealed by quantitative proteomics. Oncotarget 6, 29929-29946.

Qin, F., Zhang, H., Ma, L., Liu, X., Dai, K., Li, W., Gu, F., Fu, L., Ma, Y., 2015. Low Expression of Slit2 and Robo1 is Associated with Poor Prognosis and Brain-specific Metastasis of Breast Cancer Patients. Sci Rep 5, 14430.

Qu, X., Huang, X., Wu, L., Huang, G., Ping, X., Yan, W., 2011. Comparison of virtual cystoscopy and ultrasonography for bladder cancer detection: a meta-analysis. Eur J Radiol 80, 188-197.

Quadro, L., Blaner, W.S., Salchow, D.J., Vogel, S., Piantedosi, R., Gouras, P., Freeman, S., Cosma, M.P., Colantuoni, V., Gottesman, M.E., 1999. Impaired retinal function and vitamin A availability in mice lacking retinol-binding protein. EMBO J 18, 4633-4644.

Quinn, M., Babb, P., 2002. Patterns and trends in prostate cancer incidence, survival, prevalence and mortality. Part I: international comparisons. BJU Int 90, 162-173.

Ramos-Vara, J.A., Miller, M.A., Boucher, M., Roudabush, A., Johnson, G.C., 2003. Immunohistochemical detection of uroplakin III, cytokeratin 7, and cytokeratin 20 in canine urothelial tumors. Vet Pathol 40, 55-62.

Ramsey, S.A., Xu, T., Goodall, C., Rhodes, A.C., Kashyap, A., He, J., Bracha, S., 2017. Cross-species analysis of the canine and human bladder cancer transcriptome and exome. Genes Chromosomes Cancer 56, 328-343.

Raven, P.A., D'Costa, N.M., Moskalev, I., Tan, Z., Frees, S., Chavez-Munoz, C., So, A.I., 2018. Development of a murine intravesical orthotopic human bladder cancer (mio-hBC) model. Am J Clin Exp Urol 6, 245-259.

Ravicini, S., Baines, S.J., Taylor, A., Amores-Fuster, I., Mason, S.L., Treggiari, E., 2018. Outcome and prognostic factors in medically treated canine prostatic carcinomas: A multi-institutional study. Vet Comp Oncol 16, 450-458.

Rawla, P., 2019. Epidemiology of Prostate Cancer. World J Oncol 10, 63-89.

Rebbeck, T.R., Devesa, S.S., Chang, B.L., Bunker, C.H., Cheng, I., Cooney, K., Eeles, R., Fernandez, P., Giri, V.N., Gueye, S.M., Haiman, C.A., Henderson, B.E., Heyns, C.F., Hu, J.J., Ingles, S.A., Isaacs, W., Jalloh, M., John, E.M., Kibel, A.S., Kidd, L.R., Layne, P., Leach, R.J., Neslund-Dudas, C., Okobia, M.N., Ostrander, E.A., Park, J.Y., Patrick, A.L., Phelan, C.M., Ragin, C., Roberts, R.A., Rybicki, B.A., Stanford, J.L., Strom, S., Thompson, I.M., Witte, J., Xu, J., Yeboah, E., Hsing, A.W., Zeigler-Johnson, C.M., 2013. Global patterns of prostate cancer incidence, aggressiveness, and mortality in men of african descent. Prostate Cancer 2013, 560857.

Reis, L.O., Ferreira, F., Almeida, M., Ferreira, U., 2011. Urethral carcinoma: critical view on contemporary consecutive series. Medical Oncology 28, 1405-1410.

Reiter, R.J., 2004. Mechanisms of cancer inhibition by melatonin. J Pineal Res 37, 213-214.

Richard, P.O., Jewett, M.A., Bhatt, J.R., Kachura, J.R., Evans, A.J., Zlotta, A.R., Hermanns, T., Juvet, T., Finelli, A., 2015. Renal Tumor Biopsy for Small Renal Masses: A Single-center 13-year Experience. Eur Urol 68, 1007-1013.

Richardsen, E., Andersen, S., Al-Saad, S., Rakaee, M., Nordby, Y., Pedersen, M.I., Ness, N., Grindstad, T., Movik, I., Donnem, T., Bremnes, R., Busund, L.T., 2017. Evaluation of the proliferation marker Ki-67 in a large prostatectomy cohort. PLoS One 12, e0186852.

Richters, A., Aben, K.K.H., Kiemeney, L., 2019. The global burden of urinary bladder cancer: an update. World J Urol.

Riester, M., Werner, L., Bellmunt, J., Selvarajah, S., Guancial, E.A., Weir, B.A., Stack, E.C., Park, R.S., O'Brien, R., Schutz, F.A., Choueiri, T.K., Signoretti, S., Lloreta, J., Marchionni, L., Gallardo, E., Rojo, F., Garcia, D.I., Chekaluk, Y., Kwiatkowski, D.J., Bochner, B.H., Hahn, W.C., Ligon, A.H., Barletta, J.A., Loda, M., Berman, D.M., Kantoff, P.W., Michor, F., Rosenberg, J.E., 2014. Integrative analysis of 1q23.3 copy-number gain in metastatic urothelial carcinoma. Clin Cancer Res 20, 1873-1883.

Ringuette-Goulet, C., Bolduc, S., Pouliot, F., 2018. Modeling human bladder cancer. World J Urol 36, 1759-1766.

Rivera-Calderon, L.G., Fonseca-Alves, C.E., Kobayashi, P.E., Carvalho, M., Drigo, S.A., de Oliveira Vasconcelos, R., Laufer-Amorim, R., 2016. Alterations in PTEN, MDM2, TP53 and AR protein and gene expression are associated with canine prostate carcinogenesis. Res Vet Sci 106, 56-61.

Ro, J.Y., el-Naggar, A.K., Amin, M.B., Sahin, A.A., Ordonez, N.G., Ayala, A.G., 1993. Pseudosarcomatous fibromyxoid tumor of the urinary bladder and prostate: immunohistochemical, ultrastructural, and DNA flow cytometric analyses of nine cases. Hum Pathol 24, 1203-1210.

Robinson, M.D., McCarthy, D.J., Smyth, G.K., 2010. edgeR: a Bioconductor package for differential expression analysis of digital gene expression data. Bioinformatics 26, 139-140.

Rodor, J., Pan, Q., Blencowe, B.J., Eyras, E., Caceres, J.F., 2016. The RNA-binding profile of Acinus, a peripheral component of the exon junction complex, reveals its role in splicing regulation. RNA 22, 1411-1426.

Romanucci, M., Frattone, L., Ciccarelli, A., Bongiovanni, L., Malatesta, D., Benazzi, C., Brachelente, C., Della Salda, L., 2016. Immunohistochemical expression of heat shock proteins, p63 and androgen receptor in benign prostatic hyperplasia and prostatic carcinoma in the dog. Vet Comp Oncol 14, 337-349.

Roperch, J.P., Grandchamp, B., Desgrandchamps, F., Mongiat-Artus, P., Ravery, V., Ouzaid, I., Roupret, M., Phe, V., Ciofu, C., Tubach, F., Cussenot, O., Incitti, R., 2016. Promoter hypermethylation of HS3ST2, SEPTIN9 and SLIT2 combined with FGFR3 mutations as a sensitive/specific urinary assay for diagnosis and surveillance in patients with low or high-risk non-muscle-invasive bladder cancer. BMC Cancer 16, 704.

Ross, J.S., Wang, K., Al-Rohil, R.N., Nazeer, T., Sheehan, C.E., Otto, G.A., He, J., Palmer, G., Yelensky, R., Lipson, D., Ali, S., Balasubramanian, S., Curran, J.A., Garcia, L., Mahoney, K., Downing, S.R., Hawryluk, M., Miller, V.A., Stephens, P.J., 2014. Advanced urothelial carcinoma: next-generation sequencing reveals diverse genomic alterations and targets of therapy. Mod Pathol 27, 271-280.

Rossi, S.H., Klatte, T., Usher-Smith, J., Stewart, G.D., 2018. Epidemiology and screening for renal cancer. World J Urol 36, 1341-1353.

Rusyn, I., Chiu, W.A., Lash, L.H., Kromhout, H., Hansen, J., Guyton, K.Z., 2014. Trichloroethylene: Mechanistic, epidemiologic and other supporting evidence of carcinogenic hazard. Pharmacol Ther 141, 55-68.

Saad, A.M., Gad, M.M., Al-Husseini, M.J., Ruhban, I.A., Sonbol, M.B., Ho, T.H., 2019. Trends in Renal-Cell Carcinoma Incidence and Mortality in the United States in the Last 2 Decades: A SEER-Based Study. Clin Genitourin Cancer 17, 46-57 e45.

Saeki, K., Fujita, A., Fujita, N., Nakagawa, T., Nishimura, R., 2015. Total cystectomy and subsequent urinary diversion to the prepuce or vagina in dogs with transitional cell carcinoma of the trigone area: A report of 10 cases (2005-2011). Can Vet J 56, 73-80.

Samaratunga, H., Fairweather, P., Purdie, D., 2005. Significance of stromal reaction patterns in invasive urothelial carcinoma. Am J Clin Pathol 123, 851-857.

Samaratunga, H., Gianduzzo, T., Delahunt, B., 2014. The ISUP system of staging, grading and classification of renal cell neoplasia. J Kidney Cancer VHL 1, 26-39.

Sanfrancesco, J., McKenney, J.K., Leivo, M.Z., Gupta, S., Elson, P., Hansel, D.E., 2016. Sarcomatoid Urothelial Carcinoma of the Bladder: Analysis of 28 Cases With Emphasis on Clinicopathologic Features and Markers of Epithelial-to-Mesenchymal Transition. Arch Pathol Lab Med 140, 543-551.

Sato, Y., Yoshizato, T., Shiraishi, Y., Maekawa, S., Okuno, Y., Kamura, T., Shimamura, T., Sato-Otsubo, A., Nagae, G., Suzuki, H., Nagata, Y., Yoshida, K., Kon, A., Suzuki, Y., Chiba, K., Tanaka, H., Niida, A., Fujimoto, A., Tsunoda, T., Morikawa, T., Maeda, D., Kume, H., Sugano, S., Fukayama, M., Aburatani, H., Sanada, M., Miyano, S., Homma, Y., Ogawa, S., 2013. Integrated molecular analysis of clear-cell renal cell carcinoma. Nat Genet 45, 860-867.

Schmidt, L.S., Linehan, W.M., 2017. A mouse model of renal cell carcinoma. Nat Med 23, 802-803.

Sciarra, A., De Matteis, A., Mariotti, G., Voria, G., Lucera, R., Di Silverio, F., 2004. Histopathological aspects of transitional cell carcinoma of the bladder: Analysis of 20 years experience. International Journal of Urology 11, 467-475.

Scott, C.S., Jinot, J., 2011. Trichloroethylene and cancer: systematic and quantitative review of epidemiologic evidence for identifying hazards. Int J Environ Res Public Health 8, 4238-4272.

Shah, R.B., 2009. Current perspectives on the Gleason grading of prostate cancer. Arch Pathol Lab Med 133, 1810-1816.

Shanks, J.H., Iczkowski, K.A., 2009. Divergent differentiation in urothelial carcinoma and other bladder cancer subtypes with selected mimics. Histopathology 54, 885-900.

Shapiro, S.G., Raghunath, S., Williams, C., Motsinger-Reif, A.A., Cullen, J.M., Liu, T., Albertson, D., Ruvolo, M., Bergstrom Lucas, A., Jin, J., Knapp, D.W., Schiffman, J.D., Breen, M., 2015. Canine urothelial carcinoma: genomically aberrant and comparatively relevant. Chromosome Res 23, 311-331.

Shariat, S.F., Karakiewicz, P.I., Ashfaq, R., Lerner, S.P., Palapattu, G.S., Cote, R.J., Sagalowsky, A.I., Lotan, Y., 2008. Multiple biomarkers improve prediction of bladder cancer recurrence and mortality in patients undergoing cystectomy. Cancer 112, 315-325.

Sharma, R., 2019. The burden of prostate cancer is associated with human development index: evidence from 87 countries, 1990-2016. EPMA J 10, 137-152.

Shen, S.S., Smith, C.L., Hsieh, J.T., Yu, J., Kim, I.Y., Jian, W., Sonpavde, G., Ayala, G.E., Younes, M., Lerner, S.P., 2006. Expression of estrogen receptors-alpha and -beta in bladder cancer cell lines and human bladder tumor tissue. Cancer 106, 2610-2616.

Shi, R.L., Qu, N., Liao, T., Wang, Y.L., Wang, Y., Sun, G.H., Ji, Q.H., 2016. Expression, clinical significance and mechanism of Slit2 in papillary thyroid cancer. Int J Oncol 48, 2055-2062.

Shimada, K., Nakamura, M., Anai, S., De Velasco, M., Tanaka, M., Tsujikawa, K., Ouji, Y., Konishi, N., 2009. A novel human AlkB homologue, ALKBH8, contributes to human bladder cancer progression. Cancer Res 69, 3157-3164.

Shivakumar, M., Lee, Y., Bang, L., Garg, T., Sohn, K.A., Kim, D., 2017. Identification of epigenetic interactions between miRNA and DNA methylation associated with gene expression as potential prognostic markers in bladder cancer. BMC Med Genomics 10, 30.

Sho, S., Court, C.M., Winograd, P., Russell, M.M., Tomlinson, J.S., 2017. A prognostic mutation panel for predicting cancer recurrence in stages II and III colorectal cancer. Journal of Surgical Oncology 116, 996-1004.

Shroff, E.H., Eberlin, L.S., Dang, V.M., Gouw, A.M., Gabay, M., Adam, S.J., Bellovin, D.I., Tran, P.T., Philbrick, W.M., Garcia-Ocana, A., Casey, S.C., Li, Y., Dang, C.V., Zare, R.N., Felsher, D.W., 2015. MYC oncogene overexpression drives renal cell carcinoma in a mouse model through glutamine metabolism. Proc Natl Acad Sci U S A 112, 6539-6544.

Shu, S., Wang, Y., Zheng, M., Liu, Z., Cai, J., Tang, C., Dong, Z., 2019. Hypoxia and Hypoxia-Inducible Factors in Kidney Injury and Repair. Cells 8.

Shu, Y., Iijima, T., Sun, W., Kano, J., Ishiyama, T., Okubo, C., Anami, Y., Tanaka, R., Fukai, S., Noguchi, M., 2006. The ACIN1 gene is hypermethylated in early stage lung adenocarcinoma. J Thorac Oncol 1, 160-167.

Signoretti, S., Waltregny, D., Dilks, J., Isaac, B., Lin, D., Garraway, L., Yang, A., Montironi, R., McKeon, F., Loda, M., 2000. p63 is a prostate basal cell

marker and is required for prostate development. Am J Pathol 157, 1769-1775.

Sledge, D.G., Patrick, D.J., Fitzgerald, S.D., Xie, Y., Kiupel, M., 2015. Differences in expression of uroplakin III, cytokeratin 7, and cyclooxygenase-2 in canine proliferative urothelial lesions of the urinary bladder. Vet Pathol 52, 74-82.

Snezhkina, A.V., Krasnov, G.S., Zaretsky, A.R., Zhavoronkov, A., Nyushko, K.M., Moskalev, A.A., Karpova, I.Y., Afremova, A.I., Lipatova, A.V., Kochetkov, D.V., Fedorova, M.S., Volchenko, N.N., Sadritdinova, A.F., Melnikova, N.V., Sidorov, D.V., Popov, A.Y., Kalinin, D.V., Kaprin, A.D., Alekseev, B.Y., Dmitriev, A.A., Kudryavtseva, A.V., 2016. Differential expression of alternatively spliced transcripts related to energy metabolism in colorectal cancer. BMC Genomics 17, 1011.

Soave, A., John, L.M., Dahlem, R., Minner, S., Engel, O., Schmidt, S., Kluth, L.A., Fisch, M., Rink, M., 2015. The Impact of Tumor Diameter and Tumor Necrosis on Oncologic Outcomes in Patients With Urothelial Carcinoma of the Bladder Treated With Radical Cystectomy. Urology 86, 92-98.

Sommer, B.C., Dhawan, D., Ratliff, T.L., Knapp, D.W., 2018. Naturally-Occurring Canine Invasive Urothelial Carcinoma: A Model for Emerging Therapies. Bladder Cancer 4, 149-159.

Song, N., Kim, K., Shin, A., Park, J.W., Chang, H.J., Shi, J., Cai, Q., Kim, D.Y., Zheng, W., Oh, J.H., 2018. Colorectal cancer susceptibility loci and influence on survival. Genes Chromosomes Cancer 57, 630-637.

Sorenmo, K.U., Goldschmidt, M.H., Shofer, F.S., Goldkamp, C., Ferracone, J., 2004. Evaluation of cyclooxygenase-1 and cyclooxygenase-2 expression and the effect of cyclooxygenase inhibitors in canine prostatic carcinoma. Vet Comp Oncol 2, 13-23.

Sreedharan, S., Petros, J.A., Master, V.A., Ogan, K., Pattaras, J.G., Roberts, D.L., Lian, F., Arnold, R.S., 2014. Aquaporin-1 protein levels elevated in fresh urine of renal cell carcinoma patients: potential use for screening and classification of incidental renal lesions. Dis Markers 2014, 135649.

Srinivasan, M., Parwani, A.V., 2011. Diagnostic utility of p63/P501S double sequential immunohistochemical staining in differentiating urothelial carcinoma from prostate carcinoma. Diagn Pathol 6, 67.

Stabile, A., Giganti, F., Rosenkrantz, A.B., Taneja, S.S., Villeirs, G., Gill, I.S., Allen, C., Emberton, M., Moore, C.M., Kasivisvanathan, V., 2019. Multiparametric MRI for prostate cancer diagnosis: current status and future directions. Nat Rev Urol.

Stamey, T.A., Yang, N., Hay, A.R., McNeal, J.E., Freiha, F.S., Redwine, E., 1987. Prostate-specific antigen as a serum marker for adenocarcinoma of the prostate. N Engl J Med 317, 909-916.

Stefansson, O.A., Hermanowicz, S., van der Horst, J., Hilmarsdottir, H., Staszczak, Z., Jonasson, J.G., Tryggvadottir, L., Gudjonsson, T., Sigurdsson, S., 2017. CpG promoter methylation of the ALKBH3 alkylation repair gene in breast cancer. BMC Cancer 17, 469.

Stephenson, A.J., Scardino, P.T., Eastham, J.A., Bianco, F.J., Jr., Dotan, Z.A., Fearn, P.A., Kattan, M.W., 2006. Preoperative nomogram predicting the

10-year probability of prostate cancer recurrence after radical prostatectomy. J Natl Cancer Inst 98, 715-717.

Stephenson, W.T., Holmes, F.F., Noble, M.J., Gerald, K.B., 1990. Analysis of bladder carcinoma by subsite. Cystoscopic location may have prognostic value. Cancer 66, 1630-1635.

Su, S.C., Ho, Y.C., Liu, Y.F., Reiter, R.J., Chou, C.H., Yeh, C.M., Lee, H.L., Chung, W.H., Hsieh, M.J., Yang, S.F., 2017. Association of melatonin membrane receptor 1A/1B gene polymorphisms with the occurrence and metastasis of hepatocellular carcinoma. Oncotarget 8, 85655-85669.

Sui, W., RoyChoudhury, A., Wenske, S., Decastro, G.J., McKiernan, J.M., Anderson, C.B., 2017. Outcomes and Prognostic Factors of Primary Urethral Cancer. Urology 100, 180-186.

Sun, F., Baez-Diaz, C., Sanchez-Margallo, F.M., 2017. Canine prostate models in preclinical studies of minimally invasive interventions: part I, canine prostate anatomy and prostate cancer models. Transl Androl Urol 6, 538-546.

Sun, W., Yue, J., 2018. TPC2 mediates autophagy progression and extracellular vesicle secretion in cancer cells. Exp Cell Res 370, 478-489.

Svatek, R.S., Clinton, T.N., Wilson, C.A., Kamat, A.M., Grossman, H.B., Dinney, C.P., Shah, J.B., 2014. Intravesical Tumor Involvement of the Trigone Is Associated With Nodal Metastasis in Patients Undergoing Radical Cystectomy. Urology 84, 1147-1151.

Swartz, M.A., Porter, M.P., Lin, D.W., Weiss, N.S., 2006. Incidence of primary urethral carcinoma in the United States. Urology 68, 1164-1168.

Sylvester, R.J., Oosterlinck, W., van der Meijden, A.P., 2004. A single immediate postoperative instillation of chemotherapy decreases the risk of recurrence in patients with stage Ta T1 bladder cancer: a meta-analysis of published results of randomized clinical trials. J Urol 171, 2186-2190, quiz 2435.

Sylvester, R.J., van der Meijden, A.P., Oosterlinck, W., Witjes, J.A., Bouffioux, C., Denis, L., Newling, D.W., Kurth, K., 2006. Predicting recurrence and progression in individual patients with stage Ta T1 bladder cancer using EORTC risk tables: a combined analysis of 2596 patients from seven EORTC trials. Eur Urol 49, 466-465; discussion 475-467.

Szigetvari, N.M., Dhawan, D., Ramos-Vara, J.A., Leamon, C.P., Klein, P.J., Ruple, A.A., Heng, H.G., Pugh, M.R., Rao, S., Vlahov, I.R., Deshuillers, P.L., Low, P.S., Fourez, L.M., Cournoyer, A.M., Knapp, D.W., 2018. Phase I/II clinical trial of the targeted chemotherapeutic drug, folate-tubulysin, in dogs with naturally-occurring invasive urothelial carcinoma. Oncotarget 9, 37042-37053.

Taccoen, X., Valeri, A., Descotes, J.L., Morin, V., Stindel, E., Doucet, L., Joulin, V., Bocqueraz, F., Coulange, C., Rambeaud, J.J., Fournier, G., Mejean, A., Oncology Committee of the Association Francaise, d.U., 2007. Renal cell carcinoma in adults 40 years old or less: young age is an independent prognostic factor for cancer-specific survival. Eur Urol 51, 980-987.

Taitt, H.E., 2018. Global Trends and Prostate Cancer: A Review of Incidence, Detection, and Mortality as Influenced by Race, Ethnicity, and Geographic Location. Am J Mens Health 12, 1807-1823.

Talmadge, J.E., Singh, R.K., Fidler, I.J., Raz, A., 2007. Murine models to evaluate novel and conventional therapeutic strategies for cancer. Am J Pathol 170, 793-804.

Tan, G.H., Nason, G., Ajib, K., Woon, D.T.S., Herrera-Caceres, J., Alhunaidi, O., Perlis, N., 2019. Smarter screening for prostate cancer. World J Urol 37, 991-999.

Tan, W.S., Rodney, S., Lamb, B., Feneley, M., Kelly, J., 2016. Management of non-muscle invasive bladder cancer: A comprehensive analysis of guidelines from the United States, Europe and Asia. Cancer Treat Rev 47, 22-31.

Tang, S.W., Chang, W.H., Su, Y.C., Chen, Y.C., Lai, Y.H., Wu, P.T., Hsu, C.I., Lin, W.C., Lai, M.K., Lin, J.Y., 2009. MYC pathway is activated in clear cell renal cell carcinoma and essential for proliferation of clear cell renal cell carcinoma cells. Cancer Lett 273, 35-43.

Tasaki, M., Shimada, K., Kimura, H., Tsujikawa, K., Konishi, N., 2011. ALKBH3, a human AlkB homologue, contributes to cell survival in human non-small-cell lung cancer. Br J Cancer 104, 700-706.

Tavora, F., Epstein, J.I., 2009. Urothelial carcinoma with abundant myxoid stroma. Hum Pathol 40, 1391-1398.

Terada, T., 2013. Inverted variant of urothelial carcinoma of the urinary bladder: a report of three cases and a proposal for a new clinicopathologic entity. Int J Clin Exp Patho 6, 766-770.

Teske, E., Naan, E.C., van Dijk, E.M., Van Garderen, E., Schalken, J.A., 2002. Canine prostate carcinoma: epidemiological evidence of an increased risk in castrated dogs. Mol Cell Endocrinol 197, 251-255.

Thaiwong, T., Sledge, D.G., Collins-Webb, A., Kiupel, M., 2018. Immunohistochemical Characterization of Canine Oral Papillary Squamous Cell Carcinoma. Vet Pathol 55, 224-232.

Thompson, R.H., Atwell, T., Schmit, G., Lohse, C.M., Kurup, A.N., Weisbrod, A., Psutka, S.P., Stewart, S.B., Callstrom, M.R., Cheville, J.C., Boorjian, S.A., Leibovich, B.C., 2015. Comparison of partial nephrectomy and percutaneous ablation for cT1 renal masses. Eur Urol 67, 252-259.

Thompson, S.J., Sargsyan, A., Lee, S.A., Yuen, J.J., Cai, J., Smalling, R., Ghyselinck, N., Mark, M., Blaner, W.S., Graham, T.E., 2017. Hepatocytes Are the Principal Source of Circulating RBP4 in Mice. Diabetes 66, 58-63.

Thorsen, K., Sorensen, K.D., Brems-Eskildsen, A.S., Modin, C., Gaustadnes, M., Hein, A.M., Kruhoffer, M., Laurberg, S., Borre, M., Wang, K., Brunak, S., Krainer, A.R., Torring, N., Dyrskjot, L., Andersen, C.L., Orntoft, T.F., 2008. Alternative splicing in colon, bladder, and prostate cancer identified by exon array analysis. Mol Cell Proteomics 7, 1214-1224.

Tian, W., Guner, G., Miyamoto, H., Cimino-Mathews, A., Gonzalez-Roibon, N., Argani, P., Li, X., Sharma, R., Subhawong, A.P., Rezaei, K., Bivalacqua, T.J., Epstein, J.I., Bishop, J.A., Netto, G.J., 2015. Utility of uroplakin II expression as a marker of urothelial carcinoma. Hum Pathol 46, 58-64.

Tomlins, S.A., Bjartell, A., Chinnaiyan, A.M., Jenster, G., Nam, R.K., Rubin, M.A., Schalken, J.A., 2009. ETS gene fusions in prostate cancer: from discovery to daily clinical practice. Eur Urol 56, 275-286.

Tosoian, J.J., Mamawala, M., Epstein, J.I., Landis, P., Wolf, S., Trock, B.J., Carter, H.B., 2015. Intermediate and Longer-Term Outcomes From a Prospective Active-Surveillance Program for Favorable-Risk Prostate Cancer. J Clin Oncol 33, 3379-3385.

Tourinho-Barbosa, R., Srougi, V., Nunes-Silva, I., Baghdadi, M., Rembeyo, G., Eiffel, S.S., Barret, E., Rozet, F., Galiano, M., Cathelineau, X., Sanchez-Salas, R., 2018. Biochemical recurrence after radical prostatectomy: what does it mean? Int Braz J Urol 44, 14-21.

Tracey, E., Watt, H., Currow, D., Young, J., Armstrong, B., 2014. Investigation of poorer bladder cancer survival in women in NSW, Australia: a data linkage study. Bju International 113, 437-448.

Tsukada, Y., Ishitani, T., Nakayama, K.I., 2010. KDM7 is a dual demethylase for histone H3 Lys 9 and Lys 27 and functions in brain development. Genes Dev 24, 432-437.

Turner, N., Lambros, M.B., Horlings, H.M., Pearson, A., Sharpe, R., Natrajan, R., Geyer, F.C., van Kouwenhove, M., Kreike, B., Mackay, A., Ashworth, A., van de Vijver, M.J., Reis-Filho, J.S., 2010. Integrative molecular profiling of triple negative breast cancers identifies amplicon drivers and potential therapeutic targets. Oncogene 29, 2013-2023.

Tuygun, C., Kankaya, D., Imamoglu, A., Sertcelik, A., Zengin, K., Oktay, M., Sertcelik, N., 2011. Sex-specific hormone receptors in urothelial carcinomas of the human urinary bladder: a comparative analysis of clinicopathological features and survival outcomes according to receptor expression. Urol Oncol 29, 43-51.

Udager, A.M., Mehra, R., 2016. Morphologic, Molecular, and Taxonomic Evolution of Renal Cell Carcinoma: A Conceptual Perspective With Emphasis on Updates to the 2016 World Health Organization Classification. Arch Pathol Lab Med 140, 1026-1037.

Uhlen, M., Fagerberg, L., Hallstrom, B.M., Lindskog, C., Oksvold, P., Mardinoglu, A., Sivertsson, A., Kampf, C., Sjostedt, E., Asplund, A., Olsson, I., Edlund, K., Lundberg, E., Navani, S., Szigyarto, C.A., Odeberg, J., Djureinovic, D., Takanen, J.O., Hober, S., Alm, T., Edqvist, P.H., Berling, H., Tegel, H., Mulder, J., Rockberg, J., Nilsson, P., Schwenk, J.M., Hamsten, M., von Feilitzen, K., Forsberg, M., Persson, L., Johansson, F., Zwahlen, M., von Heijne, G., Nielsen, J., Ponten, F., 2015. Tissue-based map of the human proteome. Science 347.

Urquidi, V., Netherton, M., Gomes-Giacoia, E., Serie, D.J., Eckel-Passow, J., Rosser, C.J., Goodison, S., 2016. A microRNA biomarker panel for the non-invasive detection of bladder cancer. Oncotarget 7, 86290-86299.

Valli, V.E., Norris, A., Jacobs, R.M., Laing, E., Withrow, S., Macy, D., Tomlinson, J., McCaw, D., Ogilvie, G.K., Pidgeon, G., et al., 1995. Pathology of canine bladder and urethral cancer and correlation with tumour progression and survival. J Comp Pathol 113, 113-130.

Van Rechem, C., Black, J.C., Boukhali, M., Aryee, M.J., Graslund, S., Haas, W., Benes, C.H., Whetstine, J.R., 2015. Lysine demethylase KDM4A associates with translation machinery and regulates protein synthesis. Cancer Discov 5, 255-263.

Vasconcelos-Nobrega, C., Colaco, A., Lopes, C., Oliveira, P.A., 2012. Review: BBN as an urothelial carcinogen. In Vivo 26, 727-739.

Vasilakaki, T., Koulia, K., Tsavari, A., Arkoumani, E., Liaropoulos, D., Manoloudaki, K., Pavlis, A., Stamatiou, K., 2014. Pseudosarcomatous myofibroblastic proliferation of the urinary bladder: a rare entity. Urology 83, 1409-1411.

Vedder, M.M., de Bekker-Grob, E.W., Lilja, H.G., Vickers, A.J., van Leenders, G.J.L.H., Steyerberg, E.W., Roobol, M.J., 2014. The Added Value of Percentage of Free to Total Prostate-specific Antigen, PCA3, and a Kallikrein Panel to the ERSPC Risk Calculator for Prostate Cancer in Prescreened Men. European Urology 66, 1109-1115.

Venkadakrishnan, V.B., DePriest, A.D., Kumari, S., Senapati, D., Ben-Salem, S., Su, Y., Mudduluru, G., Hu, Q., Cortes, E., Pop, E., Mohler, J.L., Azabdaftari, G., Attwood, K., Shah, R.B., Jamieson, C., Dehm, S.M., Magi-Galluzzi, C., Klein, E., Sharifi, N., Liu, S., Heemers, H.V., 2019. Protein Kinase N1 control of androgen-responsive serum response factor action provides rationale for novel prostate cancer treatment strategy. Oncogene 38, 4496-4511.

Verep, S., Erdem, S., Ozluk, Y., Kilicaslan, I., Sanli, O., Ozcan, F., 2019. The pathological upgrading after radical prostatectomy in low-risk prostate cancer patients who are eligible for active surveillance: How safe is it to depend on bioptic pathology? Prostate 79, 1523-1529.

Verma, S., Rajesh, A., Prasad, S.R., Gaitonde, K., Lall, C.G., Mouraviev, V., Aeron, G., Bracken, R.B., Sandrasegaran, K., 2012. Urinary bladder cancer: role of MR imaging. Radiographics 32, 371-387.

Vickers, A.J., Cronin, A.M., Roobol, M.J., Savage, C.J., Peltola, M., Pettersson, K., Scardino, P.T., Schroder, F.H., Lilja, H., 2010. A four-kallikrein panel predicts prostate cancer in men with recent screening: data from the European Randomized Study of Screening for Prostate Cancer, Rotterdam. Clin Cancer Res 16, 3232-3239.

Vilaseca, A., Guglielmetti, G., Vertosick, E.A., Sjoberg, D.D., Grasso, A., Benfante, N.E., Nguyen, D.P., Corradi, R.B., Coleman, J., Russo, P., Vickers, A.J., Touijer, K.A., 2019. Value of Partial Nephrectomy for Renal Cortical Tumors of cT2 or Greater Stage: A Risk-benefit Analysis of Renal Function Preservation Versus Increased Postoperative Morbidity. Eur Urol Oncol.

Wagner, S., Maibaum, D., Pich, A., Nolte, I., Murua Escobar, H., 2015. Verification of a canine PSMA (FolH1) antibody. Anticancer Res 35, 145-148.

Walker, M., Breider, M., 1987. Intraoperative Radiotherapy of Canine Bladder-Cancer. Vet Radiology 28, 200-204.

Walker, S.M., Knight, L.A., McCavigan, A.M., Logan, G.E., Berge, V., Sherif, A., Pandha, H., Warren, A.Y., Davidson, C., Uprichard, A., Blayney, J.K.,

Price, B., Jellema, G.L., Steele, C.J., Svindland, A., McDade, S.S., Eden, C.G., Foster, C., Mills, I.G., Neal, D.E., Mason, M.D., Kay, E.W., Waugh, D.J., Harkin, D.P., Watson, R.W., Clarke, N.W., Kennedy, R.D., 2017. Molecular Subgroup of Primary Prostate Cancer Presenting with Metastatic Biology. Eur Urol 72, 509-518.

Walsh, P.C., 2017. The Search for the Missing Heritability of Prostate Cancer. Eur Urol 72, 657-659.

Wang, B., Wu, S., Zeng, H., Liu, Z., Dong, W., He, W., Chen, X., Dong, X., Zheng, L., Lin, T., Huang, J., 2015. CD103+ Tumor Infiltrating Lymphocytes Predict a Favorable Prognosis in Urothelial Cell Carcinoma of the Bladder. J Urol 194, 556-562.

Wang, C.Y., Xu, Z.B., Wang, J.P., Jiao, Y., Zhang, B., 2017a. Rb deficiency accelerates progression of carcinoma of the urinary bladder in vivo and in vitro through inhibiting autophagy and apoptosis. Int J Oncol 50, 1221-1232.

Wang, D.D., Zhao, Y.M., Wang, L., Ren, G., Wang, F., Xia, Z.G., Wang, X.L., Zhang, T., Pan, Q., Dai, Z., Chen, J.P., Dai, H.Y., Zhang, W., He, H.W., Zhou, J.M., Tang, G.Y., Zhou, J., Fan, J., Tang, Z.Y., 2011. Preoperative serum retinol-binding protein 4 is associated with the prognosis of patients with hepatocellular carcinoma after curative resection. J Cancer Res Clin Oncol 137, 651-658.

Wang, F., Wu, D., Fu, H., He, F., Xu, C., Zhou, J., Li, D., Li, G., Xu, J., Wu, Q., Chen, J., Su, L., Wang, W., Zhang, S., 2017b. Cofilin 1 promotes bladder cancer and is regulated by TCF7L2. Oncotarget 8, 92043-92054.

Wang, M.C., Valenzuela, L.A., Murphy, G.P., Chu, T.M., 1979. Purification of a Human-Prostate Specific Antigen. Invest Urol 17, 159-163.

Wang, S.I., Parsons, R., Ittmann, M., 1998. Homozygous deletion of the PTEN tumor suppressor gene in a subset of prostate adenocarcinomas. Clin Cancer Res 4, 811-815.

Warde, P., Mason, M., Ding, K., Kirkbride, P., Brundage, M., Cowan, R., Gospodarowicz, M., Sanders, K., Kostashuk, E., Swanson, G., Barber, J., Hiltz, A., Parmar, M.K., Sathya, J., Anderson, J., Hayter, C., Hetherington, J., Sydes, M.R., Parulekar, W., investigators, N.C.P.M.U.P., 2011. Combined androgen deprivation therapy and radiation therapy for locally advanced prostate cancer: a randomised, phase 3 trial. Lancet 378, 2104-2111.

Warren, A.Y., Harrison, D., 2018. WHO/ISUP classification, grading and pathological staging of renal cell carcinoma: standards and controversies. World J Urol 36, 1913-1926.

Waters, D.J., Sakr, W.A., Hayden, D.W., Lang, C.M., McKinney, L., Murphy, G.P., Radinsky, R., Ramoner, R., Richardson, R.C., Tindall, D.J., 1998. Workgroup 4: spontaneous prostate carcinoma in dogs and nonhuman primates. Prostate 36, 64-67.

Weinreb, J.C., Barentsz, J.O., Choyke, P.L., Cornud, F., Haider, M.A., Macura, K.J., Margolis, D., Schnall, M.D., Shtern, F., Tempany, C.M., Thoeny, H.C., Verma, S., 2016. PI-RADS Prostate Imaging - Reporting and Data System: 2015, Version 2. Eur Urol 69, 16-40.

Wernli, K.J., Rutter, C.M., Dachman, A.H., Zafar, H.M., 2013. Suspected extracolonic neoplasms detected on CT colonography: literature review and possible outcomes. Acad Radiol 20, 667-674.

West, K.A., Zhang, H., Brown, M.C., Nikolopoulos, S.N., Riedy, M.C., Horwitz, A.F., Turner, C.E., 2001. The LD4 motif of paxillin regulates cell spreading and motility through an interaction with paxillin kinase linker (PKL). J Cell Biol 154, 161-176.

Widmark, A., Klepp, O., Solberg, A., Damber, J.-E., Angelsen, A., Fransson, P., Lund, J.-Å., Tasdemir, I., Hoyer, M., Wiklund, F., Fosså, S.D., 2009. Endocrine treatment, with or without radiotherapy, in locally advanced prostate cancer (SPCG-7/SFUO-3): an open randomised phase III trial. The Lancet 373, 301-308.

Williamson, S.R., Lopez-Beltran, A., MacLennan, G.T., Montironi, R., Cheng, L., 2013. Unique clinicopathologic and molecular characteristics of urinary bladder tumors in children and young adults. Urol Oncol 31, 414-426.

Wolf, K., Kayacelebi, H., Urhausen, C., Piechotta, M., Mischke, R., Kramer, S., Einspanier, A., Oei, C.H., Gunzel-Apel, A., 2012. Testicular steroids, prolactin, relaxin and prostate gland markers in peripheral blood and seminal plasma of normal dogs and dogs with prostatic hyperplasia. Reprod Domest Anim 47 Suppl 6, 243-246.

Wu, Z., Wang, S., Jiang, F., Li, Q., Wang, C., Wang, H., Zhang, W., Xue, P., Wang, S.L., 2017. Mass spectrometric detection combined with bioinformatic analysis identified possible protein markers and key pathways associated with bladder cancer. Gene 626, 407-413.

Xiang, J., Hu, Q., Qin, Y., Ji, S., Xu, W., Liu, W., Shi, S., Liang, C., Liu, J., Meng, Q., Liang, D., Ni, Q., Xu, J., Zhang, B., Yu, X., 2018. TCF7L2 positively regulates aerobic glycolysis via the EGLN2/HIF-1alpha axis and indicates prognosis in pancreatic cancer. Cell Death Dis 9, 321.

Xiang, Y., Zhu, Z., Han, G., Ye, X., Xu, B., Peng, Z., Ma, Y., Yu, Y., Lin, H., Chen, A.P., Chen, C.D., 2007. JARID1B is a histone H3 lysine 4 demethylase up-regulated in prostate cancer. Proc Natl Acad Sci U S A 104, 19226-19231.

Xiao, G.Q., Rashid, H., 2015. Bladder Neck Urothelial Carcinoma: A Urinary Bladder Subsite Carcinoma With Distinct Clinicopathology. Int J Surg Pathol 23, 517-523.

Xie, X., Rui, W., He, W., Shao, Y., Sun, F., Zhou, W., Wu, Y., Zhu, Y., 2017. Discoidin domain receptor 1 activity drives an aggressive phenotype in bladder cancer. Am J Transl Res 9, 2500-2507.

Xu, C., Lin, C., Xu, Z., Feng, S., Zheng, Y., 2019. Tumor Enucleation vs. Partial Nephrectomy for T1 Renal Cell Carcinoma: A Systematic Review and Meta-Analysis. Front Oncol 9, 473.

Xylinas, E., Rink, M., Robinson, B.D., Lotan, Y., Babjuk, M., Brisuda, A., Green, D.A., Kluth, L.A., Pycha, A., Fradet, Y., Faison, T., Lee, R.K., Karakiewicz, P.I., Zerbib, M., Scherr, D.S., Shariat, S.F., 2013. Impact of histological variants on oncological outcomes of patients with urothelial carcinoma of the bladder treated with radical cystectomy. Eur J Cancer 49, 1889-1897.

Yabuta, S., Shidoji, Y., 2019. Cytoplasmic translocation of nuclear LSD1 (KDM1A) in human hepatoma cells is induced by its inhibitors. Hepat Oncol 6, HEP13.

Yagata, H., Harigaya, K., Suzuki, M., Nagashima, T., Hashimoto, H., Ishii, G., Miyazaki, M., Nakajima, N., Mikata, A., 2003. Comedonecrosis is an unfavorable marker in node-negative invasive breast carcinoma. Pathol Int 53, 501-506.

Yang, Y., Hu, L., Wang, P., Hou, H., Lin, Y., Liu, Y., Li, Z., Gong, R., Feng, X., Zhou, L., Zhang, W., Dong, Y., Yang, H., Lin, H., Wang, Y., Chen, C.D., Xu, Y., 2010. Structural insights into a dual-specificity histone demethylase ceKDM7A from Caenorhabditis elegans. Cell Res 20, 886-898.

Yano, H., Mazaki, Y., Kurokawa, K., Hanks, S.K., Matsuda, M., Sabe, H., 2004. Roles played by a subset of integrin signaling molecules in cadherin-based cell-cell adhesion. J Cell Biol 166, 283-295.

Yee, D.S., Ishill, N.M., Lowrance, W.T., Herr, H.W., Elkin, E.B., 2011. Ethnic differences in bladder cancer survival. Urology 78, 544-549.

Yen, T.Y., Bowen, S., Yen, R., Piryatinska, A., Macher, B.A., Timpe, L.C., 2017. Glycoproteins in Claudin-Low Breast Cancer Cell Lines Have a Unique Expression Profile. J Proteome Res 16, 1391-1400.

Young, R.H., Wick, M.R., Mills, S.E., 1988. Sarcomatoid carcinoma of the urinary bladder. A clinicopathologic analysis of 12 cases and review of the literature. Am J Clin Pathol 90, 653-661.

Yuan, L., Shu, B., Chen, L., Qian, K., Wang, Y., Qian, G., Zhu, Y., Cao, X., Xie, C., Xiao, Y., Wang, X., 2017. Overexpression of COL3A1 confers a poor prognosis in human bladder cancer identified by co-expression analysis. Oncotarget 8, 70508-70520.

Yuan, W., Zhou, L., Chen, J.H., Wu, J.Y., Rao, Y., Ornitz, D.M., 1999. The mouse SLIT family: secreted ligands for ROBO expressed in patterns that suggest a role in morphogenesis and axon guidance. Dev Biol 212, 290-306.

Zepeda-Orozco, D., Wen, H.M., Hamilton, B.A., Raikwar, N.S., Thomas, C.P., 2017. EGF regulation of proximal tubule cell proliferation and VEGF-A secretion. Physiol Rep 5.

Zhai, Q.J., Black, J., Ayala, A.G., Ro, J.Y., 2007. Histologic variants of infiltrating urothelial carcinoma. Arch Pathol Lab Med 131, 1244-1256.

Zhang, H., Gao, P., Fukuda, R., Kumar, G., Krishnamachary, B., Zeller, K.I., Dang, C.V., Semenza, G.L., 2007. HIF-1 inhibits mitochondrial biogenesis and cellular respiration in VHL-deficient renal cell carcinoma by repression of C-MYC activity. Cancer Cell 11, 407-420.

Zhang, L., Zha, Z., Qu, W., Zhao, H., Yuan, J., Feng, Y., Wu, B., 2018a. Tumor necrosis as a prognostic variable for the clinical outcome in patients with renal cell carcinoma: a systematic review and meta-analysis. BMC Cancer 18, 870.

Zhang, M.L., Rosenthal, D.L., VandenBussche, C.J., 2016. The cytomorphological features of low-grade urothelial neoplasms vary by specimen type. Cancer Cytopathol 124, 552-564.

Zhang, N., Li, D., Shao, J., Wang, X., 2015. Animal models for bladder cancer: The model establishment and evaluation (Review). Oncol Lett 9, 1515-1519.

Zhang, Y., Fang, L., Zang, Y., Xu, Z., 2018b. Identification of Core Genes and Key Pathways via Integrated Analysis of Gene Expression and DNA Methylation Profiles in Bladder Cancer. Med Sci Monit 24, 3024-3033.

Zhao, E., Li, L., Zhang, W., Wang, W., Chan, Y., You, B., Li, X., 2019. Comprehensive characterization of immune- and inflammation-associated biomarkers based on multi-omics integration in kidney renal clear cell carcinoma. J Transl Med 17, 177.

Zheng, T., Wang, A., Hu, D., Wang, Y., 2017. Molecular mechanisms of breast cancer metastasis by gene expression profile analysis. Mol Med Rep 16, 4671-4677.

Zhou, M., Netto, G.J. and Epstein, J.I.: Uropathology: Elsevier Saunders; 2012.

Zhu, H., Chen, H., Wang, J., Zhou, L., Liu, S., 2019. Collagen stiffness promoted non-muscle-invasive bladder cancer progression to muscle-invasive bladder cancer. Onco Targets Ther 12, 3441-3457.

Zietman, A.L., DeSilvio, M.L., Slater, J.D., Rossi, C.J., Jr., Miller, D.W., Adams, J.A., Shipley, W.U., 2005. Comparison of conventional-dose vs high-dose conformal radiation therapy in clinically localized adenocarcinoma of the prostate: a randomized controlled trial. JAMA 294, 1233-1239.

Zigeuner, R., Shariat, S.F., Margulis, V., Karakiewicz, P.I., Roscigno, M., Weizer, A., Kikuchi, E., Remzi, M., Raman, J.D., Bolenz, C., Bensalah, K., Capitanio, U., Koppie, T.M., Kassouf, W., Sircar, K., Patard, J.J., Fernandez, M.I., Wood, C.G., Montorsi, F., Strobel, P., Wheat, J.C., Haitel, A., Oya, M., Guo, C.C., Ng, C., Chade, D.C., Sagalowsky, A., Langner, C., 2010. Tumour necrosis is an indicator of aggressive biology in patients with urothelial carcinoma of the upper urinary tract. Eur Urol 57, 575-581.

12. Appendix

Commands for canine UC analysis by RNAseq

To trim files for low quality reads and adapters

```
#!/bin/bash
trim_galore -q 30 --paired 14_r1.fastq.gz 14_r2.fastq.gz;
trim_galore -q 30 --paired 15_r1.fastq.gz 15_r2.fastq.gz
trim_galore -q 30 --paired 17_r1.fastq.gz 17_r2.fastq.gz
trim_galore -q 30 --paired 18_r1.fastq.gz 18_r2.fastq.gz
trim_galore -q 30 --paired 19_r1.fastq.gz 19_r2.fastq.gz
trim_galore -q 30 --paired 21_r1.fastq.gz 21_r2.fastq.gz
trim_galore -q 30 --paired 24_r1.fastq.gz 24_r2.fastq.gz
trim_galore -q 30 --paired 25_r1.fastq.gz 25_r2.fastq.gz
trim_galore -q 30 --paired 26_r1.fastq.gz 26_r2.fastq.gz
trim_galore -q 30 --paired 33_r1.fastq.gz 33_r2.fastq.gz
trim_galore -q 30 --paired 34_r1.fastq.gz 34_r2.fastq.gz
trim_galore -q 30 --paired 47_r1.fastq.gz 47_r2.fastq.gz
```

STAR alignment

```
#!/bin/bash
STAR --genomeDir /media/svznpm/Data/canine/starindex/ --sjdbGTFfile /media/svznpm/Data/canine/starindex/genes.gtf --runThreadN 3 --outFilterMismatchNmax 1 --outSAMtype BAM SortedByCoordinate --chimSegmentMin 20 --chimOutType WithinBAM --outBAMcompression 10 --readFilesIn 14_r1_val_1.fq.gz 14_r2_val_2.fq.gz --readFilesCommand zcat --readFilesCommand zcat --outFileNamePrefix 14star;
STAR --genomeDir /media/svznpm/Data/canine/starindex/ --sjdbGTFfile /media/svznpm/Data/canine/starindex/genes.gtf --runThreadN 3 --outFilterMismatchNmax 1 --outSAMtype BAM SortedByCoordinate --chimSegmentMin 20 --chimOutType WithinBAM --outBAMcompression 10 --readFilesIn 15_r1_val_1.fq.gz 15_r2_val_2.fq.gz --readFilesCommand zcat --outFileNamePrefix 15star;
STAR --genomeDir /media/svznpm/Data/canine/starindex/ --sjdbGTFfile /media/svznpm/Data/canine/starindex/genes.gtf --runThreadN 3 --outFilterMismatchNmax 1 --outSAMtype BAM SortedByCoordinate --chimSegmentMin 20 --chimOutType WithinBAM --outBAMcompression 10 --readFilesIn 17_r1_val_1.fq.gz 17_r2_val_2.fq.gz --readFilesCommand zcat --outFileNamePrefix 17star;
STAR --genomeDir /media/svznpm/Data/canine/starindex/ --sjdbGTFfile /media/svznpm/Data/canine/starindex/genes.gtf --runThreadN 3 --outFilterMismatchNmax 1 --outSAMtype BAM SortedByCoordinate --chimSegmentMin 20 --chimOutType WithinBAM --outBAMcompression 10 --
```

```
readFilesIn 18_r1_val_1.fq.gz 18_r2_val_2.fq.gz --readFilesCommand zcat --outFileNamePrefix 18star;
STAR --genomeDir /media/svznpm/Data/canine/starindex/ --sjdbGTFfile /media/svznpm/Data/canine/starindex/genes.gtf --runThreadN 3 --outFilterMismatchNmax 1 --outSAMtype BAM SortedByCoordinate --chimSegmentMin 20 --chimOutType WithinBAM --outBAMcompression 10 --readFilesIn 19_r1_val_1.fq.gz 19_r2_val_2.fq.gz --readFilesCommand zcat --outFileNamePrefix 19star;
STAR --genomeDir /media/svznpm/Data/canine/starindex/ --sjdbGTFfile /media/svznpm/Data/canine/starindex/genes.gtf --runThreadN 3 --outFilterMismatchNmax 1 --outSAMtype BAM SortedByCoordinate --chimSegmentMin 20 --chimOutType WithinBAM --outBAMcompression 10 --readFilesIn 21_r1_val_1.fq.gz 21_r2_val_2.fq.gz --readFilesCommand zcat --outFileNamePrefix 21star;
STAR --genomeDir /media/svznpm/Data/canine/starindex/ --sjdbGTFfile /media/svznpm/Data/canine/starindex/genes.gtf --runThreadN 3 --outFilterMismatchNmax 1 --outSAMtype BAM SortedByCoordinate --chimSegmentMin 20 --chimOutType WithinBAM --outBAMcompression 10 --readFilesIn 24_r1_val_1.fq.gz 24_r2_val_2.fq.gz --readFilesCommand zcat --outFileNamePrefix 24star;
STAR --genomeDir /media/svznpm/Data/canine/starindex/ --sjdbGTFfile /media/svznpm/Data/canine/starindex/genes.gtf --runThreadN 3 --outFilterMismatchNmax 1 --outSAMtype BAM SortedByCoordinate --chimSegmentMin 20 --chimOutType WithinBAM --outBAMcompression 10 --readFilesIn 25_r1_val_1.fq.gz 25_r2_val_2.fq.gz --readFilesCommand zcat --outFileNamePrefix 25star;
STAR --genomeDir /media/svznpm/Data/canine/starindex/ --sjdbGTFfile /media/svznpm/Data/canine/starindex/genes.gtf --runThreadN 3 --outFilterMismatchNmax 1 --outSAMtype BAM SortedByCoordinate --chimSegmentMin 20 --chimOutType WithinBAM --outBAMcompression 10 --readFilesIn 26_r1_val_1.fq.gz 26_r2_val_2.fq.gz --readFilesCommand zcat --outFileNamePrefix 26star;
STAR --genomeDir /media/svznpm/Data/canine/starindex/ --sjdbGTFfile /media/svznpm/Data/canine/starindex/genes.gtf --runThreadN 3 --outFilterMismatchNmax 1 --outSAMtype BAM SortedByCoordinate --chimSegmentMin 20 --chimOutType WithinBAM --outBAMcompression 10 --readFilesIn 33_r1_val_1.fq.gz 33_r2_val_2.fq.gz --readFilesCommand zcat --outFileNamePrefix 33star;
STAR --genomeDir /media/svznpm/Data/canine/starindex/ --sjdbGTFfile /media/svznpm/Data/canine/starindex/genes.gtf --runThreadN 3 --outFilterMismatchNmax 1 --outSAMtype BAM SortedByCoordinate --chimSegmentMin 20 --chimOutType WithinBAM --outBAMcompression 10 --readFilesIn 34_r1_val_1.fq.gz 34_r2_val_2.fq.gz --readFilesCommand zcat --outFileNamePrefix 34star;
```

STAR --genomeDir /media/svznpm/Data/canine/starindex/ --sjdbGTFfile /media/svznpm/Data/canine/starindex/genes.gtf --runThreadN 3 --outFilterMismatchNmax 1 --outSAMtype BAM SortedByCoordinate --chimSegmentMin 20 --chimOutType WithinBAM --outBAMcompression 10 --readFilesIn 47_r1_val_1.fq.gz 47_r2_val_2.fq.gz --readFilesCommand zcat --outFileNamePrefix 47star;

To quantify gene expression using HTSeq

```
#!/bin/bash
for f in *.bam; do htseq-count -f bam --mode=union ${f} /media/svznpm/Data/canine/starindex/genes.gtf > ${f}.star.htseq.counts.txt; done
```

To index Bam files

```
#!/bin/bash
for f in *.bam;  do samtools index ${f} ${f}.bai; done
```

To unzip files for rMATS trimming

```
#!/bin/bash
for FILE in *.fq.gz
do
gunzip "${FILE}" done
```

Trim reads to uniform length for rMATs splicing analysis

```
#!/bin/bash
python trimFastq.py 14_r1_val_1.fq 74_14_r1_val_1.fq 74;
python trimFastq.py 14_r2_val_2.fq 74_14_r2_val_2.fq 74;
python trimFastq.py 15_r1_val_1.fq 74_15_r1_val_1.fq 74;
python trimFastq.py 15_r2_val_2.fq 74_15_r2_val_2.fq 74;
python trimFastq.py 17_r1_val_1.fq 74_17_r1_val_1.fq 74;
python trimFastq.py 17_r2_val_2.fq 74_17_r2_val_2.fq 74;
python trimFastq.py 18_r1_val_1.fq 74_18_r1_val_1.fq 74;
python trimFastq.py 18_r2_val_2.fq 74_18_r2_val_2.fq 74;
python trimFastq.py 19_r1_val_1.fq 74_19_r1_val_1.fq 74;
python trimFastq.py 19_r2_val_2.fq 74_19_r2_val_2.fq 74;
python trimFastq.py 21_r1_val_1.fq 74_21_r1_val_1.fq 74;
python trimFastq.py 21_r2_val_2.fq 74_21_r2_val_2.fq 74;
python trimFastq.py 24_r1_val_1.fq 74_24_r1_val_1.fq 74;
python trimFastq.py 24_r2_val_2.fq 74_24_r2_val_2.fq 74;
python trimFastq.py 25_r1_val_1.fq 74_25_r1_val_1.fq 74;
python trimFastq.py 25_r2_val_2.fq 74_25_r2_val_2.fq 74;
python trimFastq.py 26_r1_val_1.fq 74_26_r1_val_1.fq 74;
python trimFastq.py 26_r2_val_2.fq 74_26_r2_val_2.fq 74;
python trimFastq.py 33_r1_val_1.fq 74_33_r1_val_1.fq 74;
```

```
python trimFastq.py 33_r2_val_2.fq 74_33_r2_val_2.fq 74;
python trimFastq.py 34_r1_val_1.fq 74_34_r1_val_1.fq 74;
python trimFastq.py 34_r2_val_2.fq 74_34_r2_val_2.fq 74;
python trimFastq.py 47_r1_val_1.fq 74_47_r1_val_1.fq 74;
python trimFastq.py 47_r2_val_2.fq 74_47_r2_val_2.fq 74;
```

rMATs Splicing Analysis

```
python RNASeq-MATS.py -s1 /media/svznpm/Data/canine_bladder/GC_NM_6402_FFPE_TCC/trimgalore/74_15_r1_val_1.fq:/media/svznpm/Data/canine_bladder/GC_NM_6402_FFPE_TCC/trimgalore/74_15_r2_val_2.fq,/media/svznpm/Data/canine_bladder/GC_NM_6402_FFPE_TCC/trimgalore/74_18_r1_val_1.fq:/media/svznpm/Data/canine_bladder/GC_NM_6402_FFPE_TCC/trimgalore/74_18_r2_val_2.fq,/media/svznpm/Data/canine_bladder/GC_NM_6402_FFPE_TCC/trimgalore/74_33_r1_val_1.fq:/media/svznpm/Data/canine_bladder/GC_NM_6402_FFPE_TCC/trimgalore/74_33_r2_val_2.fq -s2 /media/svznpm/Data/canine_bladder/GC_NM_6402_FFPE_TCC/trimgalore/74_14_r1_val_1.fq:/media/svznpm/Data/canine_bladder/GC_NM_6402_FFPE_TCC/trimgalore/74_14_r2_val_2.fq,/media/svznpm/Data/canine_bladder/GC_NM_6402_FFPE_TCC/trimgalore/74_17_r1_val_1.fq:/media/svznpm/Data/canine_bladder/GC_NM_6402_FFPE_TCC/trimgalore/74_17_r2_val_2.fq,/media/svznpm/Data/canine_bladder/GC_NM_6402_FFPE_TCC/trimgalore/74_34_r1_val_1.fq:/media/svznpm/Data/canine_bladder/GC_NM_6402_FFPE_TCC/trimgalore/74_34_r2_val_2.fq -gtf /media/svznpm/Data/canine/starindex/genes.gtf -bi /media/svznpm/Data/canine/starindex/ -t paired -len 74 -novelSS 1 -o /media/svznpm/Data/canine_bladder/rmats_output/NT18-33-15_T17-34-14
```